Energy Storage Strategies

Comparative analysis of short term storage systems for low quality heat in Dutch dwellings

Delft University of Technology
Faculty of Architecture
Department Architectural Engineering and Technology

Graduation Report Martin van Meijeren
30-10-2013

Author	Martin van Meijeren MSc Architectural Engineering + Technology (AE+T) *Student number 1376101*	martinvanm@gmail.com
First mentor	Prof. ir. P.G. Luscuere *AE+T: section Building Services*	P.G.Luscuere@tudelft.nl
Second mentor	Dr. ir. W.H. van der Spoel *AE+T: section Building Physics*	W.H.vanderSpoel@tudelft.nl
External examiner	Ir. R. Binnekamp *Real Estate and Housing: section Corporate Real Estate Management*	

Preface

Dear reader,

This report includes my graduation work conducted in the master Architectural Engineering and Technology at Delft University of Technology. The thesis aims, in accordance with the context of the Green Building Innovation studio, to investigate how the built environment can be more sustainable.

The research focused on the reduction of primary energy consumption of a dwelling using low temperature heat storage. The majority of this study was carried out on an energy system level, which provided me more insight in parameters that influence a dwellings heat demand, but also in heat pump technology and latent thermal energy storage.

The process of my graduation research is reflected in this report, starting with a broad literature study to energy storage technologies in order to deal with introduction of renewable energy resources. This is followed by theory on the exergy approach and on heat pump energy systems, which is necessary for a proper understanding of the guidelines for development of different control strategies for a heat pump combined with energy storage. After description of the two models that were developed to assess the energetic potential of short term energy storage, finally the results and conclusions are presented.

I would like to thank several contributors to my work for their ideas and help in defining and shaping the issues that were investigated in this thesis. First of all my two mentors Peter Luscuere and Wim van der Spoel for their valuable ideas, support and guidance during my graduation.

I am also grateful for the support of Techniplan Adviseurs, Dick van der Kooij and Rychard de Jong in particular.

Finally, I would like to express my gratitude to Itai Cohen, Panagiotis Papanastasis, Sabine Jansen, Bert van Dorp and Werner van Westering for their insightful comments and advice on my work.

Martin van Meijeren,

Delft, October 2013

Abstract

This report describes the development of energy storage strategies for short term Thermal Energy Storage in residential buildings with an air-source heat pump. Short term TES allows advanced integration of renewables because the associated mismatch between demand and availability is solved. It also enables electrical load management.

The aim of the research was to develop control strategies which define a control sequence of heat pump operations with the purpose of minimization of primary energy input for space heating. This is achieved by more frequent utilization of free, low quality energy input. Exergy principles were used to assess the quality of energy. More free input will minimize the amount of work (high quality input) that is additionally required for the heat pump to generate the heating energy. In a conventional heat pump energy system, the installation is controlled without notion of exergetic optimal operation. This reference control strategy was compared to three optimization control strategies that were developed in this research, in combination with different storage capacities. The most advanced optimization strategy involves Greedy Optimal Control. This strategy defines optimal control of the installation based on estimates of future heat loads and future conditions for generation.

First, a numerical MATLAB model was constructed in order to explore and compare the *energetic* potential of the strategies. This model showed that the optimization strategies result in significant primary energy saving when applied to large storage volumes that can only be realized within dwellings with latent TES. In latent TES, the high storage density during the phase change allows more compact storage. Secondly, the most potential storage configurations were translated into six use cases. The performance in terms of energy and exergy of these uses cases in combination with the most optimal control strategy (according to the MATLAB outcomes) was further simulated in a detailed TRNSYS model, and compared with the conventional control strategy. The aim of this model was to assess the influence of dynamic behavior of the storage medium, heating emission system and temperature control on the performance of both strategies. The model also included transient simulation of latent storage (macroencapsulated hydrated salt modules in a TES tank). The best duration for low temperature heat storage (for the considered capacities) turns out to be 24 hours ahead. This study has shown that the control strategy that optimizes operation and storage according to exergy principles, results in maximum 10% reduction of primary energy consumption for space heating compared to the reference situation.

Keywords: variability renewable energy resources; short term thermal energy storage; predictive control strategies; exergy analysis; phase change material; heat pump; primary energy consumption; electrical load management;

Table of contents

1 Introduction

Because of the inevitable depletion of fossil fuels which are currently the major energy sources, the world nowadays tries to replace these resources by renewables. Although at a small rate of growth, the share of renewable resources in the total energy resource mix is increasing (IEA 2008). The main challenge in substituting fossil fuels by renewable resources concerns energy supply reliability. This is especially relevant in the case of electricity demand and generation, but also for lower quality energy demands e.g. heat (IEC, 2010).

Renewable resources, e.g. wind or solar power, do not provide energy at a constant rate: they are fundamentally intermittent. Some resources do have a good measure of periodicity. Solar, wind or natural heat and cold do have roughly daily cycles, most biomass is only available during specific seasons. Their availability is highly affected by changes in weather conditions on short and long time scale: renewables don't have an "on"-button. One moment their availability is abundant, a few minutes later it may not be available anymore. Considering renewables-based generation both on grid- and pro-sumer scale, energy demand and supply can be matched by two means:

Demand-side management - involves actions in order to adjust the demand to the availability of supply. It controls the on-off button of the energy demand. This is called load shifting, were energy needs are shifted from times with large overall demand to periods of lower needs or abundant supply. Demand-side management encourages users to shift their electricity consumption towards periods of energy surplus from renewables, e.g. by introducing time-of-day electricity pricing, a key aspect of the future smart grid. Users can temporary lower or extend their consumption or use local short term storage. Better mutual exchange of energy in small/large networks is another way of demand control.

Short and long term storage - storage systems can also establish the demand-supply match, by storing renewable energy when it is available for later use. This is called time shifting, or peak leveling. By using storage, daily demand fluctuations could be balanced but also seasonal fluctuations, which are especially relevant in building space heating. Peak leveling reduces the installed generation power. Short term storage can solve grid power quality problems introduced by renewable electricity.

Besides transport and industry, buildings account for almost one-third of the global final energy consumption. Space and water heating and cooling together are estimated to account for approximately half of the buildings energy consumption (IEA, 2011). This heating and cooling mainly demands "low quality" energy, due to its associated temperatures. If we want to meet this energy demand without using high quality fossil resources (e.g. by using heat pumps instead of gas boilers), we are dependent on low quality variable renewables like biomass, solar energy, ground(water) or

natural (ambient) heat and cold. Recent developments in low temperature emission systems in low energy buildings support this integration.

Besides active solar thermal and CHP, heat pumps provide a mature and efficient technology to take advantage of renewable energy for space and water heating and cooling. Heat pumps will significantly increase their share in space and water heating, according to the heating and cooling roadmap of International Energy Agency (IEA 2011). From circa 800 mln. installed heat pumps today it will reach 3.500 mln. by 2050.

Availability of solar energy, and thus energy contained by ambient air, means that the quality of this energy fluctuates with outside conditions (i.e. quality of these resources can be closer to- or further away from the quality required for space heating). Energy storage combined with a smart control strategy for heat generation could benefit from this variability in quality, which could improve the performance of an energy system with a heat pump. This study aims to develop energy storage control strategies that could improve utilization of natural heat of ambient air within residential buildings. Before the energetic potential of these strategies were investigated using resp. an explorative model and a detailed simulation model, a broader review of different storage technologies and their characteristics was performed.

2 Definition and scope

2.1 Problem statement

Most renewables do have an intermittent nature, causing a mismatch in time between demand and supply.

Currently, the low-quality heating and cooling demand in the built environment is met with high quality energy resources e.g. gas or electricity. Although alternative – renewable, low quality - energy sources are readily available, our dependency on fossil fuels is only increasing. Besides active solar thermal and Combined Heat and Power, heat pumps provide a mature and efficient technology for an increased contribution of renewables. The International Energy Agency expects that the application of heat pumps for domestic space and water heating will rapidly increase (IEA, 2011). Currently, ground source heat pumps are most common, but air-source heat pumps are a potential competitive variant. Air-source heat pumps allow for more easy installation and do not need underground heat exchangers, which reduces investment costs.

Natural and renewable resources (e.g. desirable ambient air temperatures or sun) are intermittent. This means energy is not always available, or could not always be produced efficiently, immediately at the moment of demand.

2.2 Objective

The goal of this graduation project is to assess the energetic potential of short term energy storage in meeting the low temperature heat demand in a residential building with an air-source heat pump.

The hypothesis is that storage for a short term could shift peak loads to moments of supply surplus, which could improve the performance of an air source heat pump, and in general support the integration of intermittent renewables in the power grid. The investigated storage systems should reduce the high quality energy consumption necessary to meet the heat demand.

Boundary conditions

- short term storage: maximum of one week;
- three annual heat demands of resp. passiv-haus standards, a new built dwelling and a dwelling according to standards several years ago, i.e. 15 kWh m^2, 25 kWh m^2 and 35 kWh m^2 will be assessed. TRNSYS model only involves characteristics for a new built dwelling;
- for simplification reasons, no PV or solar thermal collectors will be included in the models. Optimization of HW or electricity consumption for appliances would be interesting but is left out of the scope of this research which will solely focus on space heating demand;
- generation system: combi air-source heat pump, calculated with theoretical COP performance

within the MATLAB model, real performance in the TRNSYS model;

- focus on performance in Dutch climate, although results might be valid in many other countries.

2.3 Research questions

Main research question

What could be the energetic consequences of short term storage of low quality heat applied in a contemporary Dutch dwelling with an air-source heat pump?

Sub research questions

1. Which technologies for storage of energy in different energy forms can be distinguished?

2. How could available solutions for thermal energy storage be integrated in an energy system design for a typical Dutch residential building?

3. How could the selected storage options adjust the daily heat demand profile in such a way that the heating energy can be generated with a minimum amount of work? (strategy development)

4. What is the effect of the developed storage strategies on the total (primary) energy consumption and installed system power that is necessary to meet the heat load?

5. How does the most optimal strategy perform in terms of energy and exergy when dynamic effects of storage medium and emission system are taken in account?

2.4 Approach and methodology

This research aimed for development and assessment of an energy system and associated control strategy for a residential building. The theory from the literature study functioned as design input in the development of the energy system, of control optimization strategies and of the latent thermal storage system.

The schematic in Figure 2-1 shows the methodical subdivision of the process which is briefly described below. This line of approach is also reflected in the structure of this report. In chapters 3, 4 and part of chapter 5 outcomes of literature study are presented. Chapters 5 and 6 show the development and results of the energy system and storage control strategies. Chapter 6 also includes the MATLAB comparative analysis which leads to use cases that were analyzed more into detail in chapter 7.

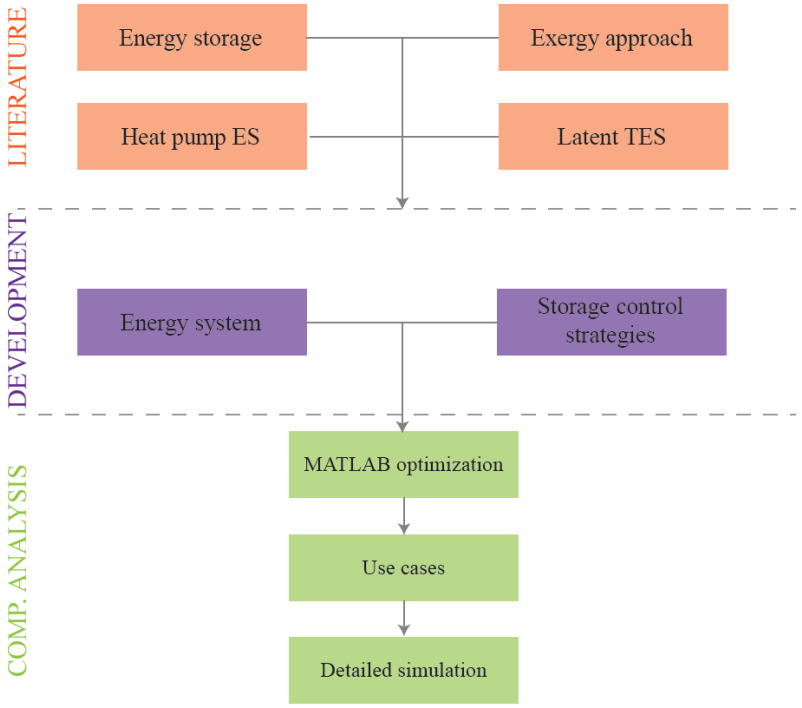

Figure 2-1: Methodical approach

Literature study

1. Issue of demand supply mismatch and storage technologies available, state of the art.

2. Exergy principles – quality of energy.

3. Air-source heat pumps.

- performance state of the art heat pumps;
- application in dwellings (energy system analysis);
- heat demand in dwellings (ventilation/occupancy/appliances).

3. Advanced study low temperature storage options.

- theory and previous research outcomes;
- commercial applications;
- basic heat and mass transfer theory.

Strategy and system development

- development of different control strategies which aim for increased utilization of ambient heat;
- development of an energy system that takes into account exergy principles;
- development and design of (latent) thermal energy storage options.

Comparative analysis

Calculation software – Comparison has been done in two stepped coarse-to-fine approach. First, a simplified model is developed in MATLAB, in order to compare different storage strategies. Most potential use cases are translated to a more complex model in TRNSYS V17, in which a first attempt of assessment of the energetic performance of the storage strategies within a complete energy system is performed, including dynamic effects of storage and emission.

Analysis framework – An input- output approach is used, in which the energy and exergy balance of each component of the energy system in TRNSYS are assessed. This analysis includes the following system components: conversion, storage, distribution, emission.

Exergy principles- Exergy analysis reveals thermodynamic losses that would not be revealed in energy analysis.

Sensitivity analysis - Possible consequences of change in input variables different from expectation (e.g. different installed power or heat demand) on the system and output will be investigated within the MATLAB optimization. This will give insight in the impact of building characteristics and other design variables.

2.4.1 Relevance

Societal relevance - Well-designed thermal energy storage systems can reduce the primary energy consumption while maintaining high comfort level in a building. The application of air-source heat pumps within residential buildings is foreseen to increase. Contemporary air-source heat pumps are cheaper than ground-source heat pumps but less efficient. Compared to conventional gas-fuelled energy generators, heat pumps are associated with lower CO2 emission and make use of scarce (fossil) energy resources into a smaller degree. The exergy approach could help to slow down/minimize the current depletion of fossil fuel resources as well, because it enables more advanced utilization of renewables (in this case low-quality energy contained by ambient air). Quality levels of the space heating demand (low-temperature emission systems will become the standard) can be met with energy with similar quality levels.

Scientific relevance - This study investigates how integrated short term energy storage could help to meet a dwellings heat demand with minimum amount of work. Exergy analysis is applied in order to give new insights. A variable renewable energy resource is used, while indoor comfort level should be maintained. PCM investigations emphasis on cooling applications in offices, while it is also interesting to investigate if the low temperature heat demand in dwellings typologies (showing more diverse charge-discharge cycles) could also benefit from active heat accumulation.

3 (Thermal) Energy Storage

The previously outlined broader issue of demand supply mismatch that accompanies the introduction of renewables, gave reason for a literature study on energy storage technologies that can be distinguished in order to solve this mismatch. This chapter aims to provide an overview of technologies and methods that are currently available for the storage of energy. Energy storage systems will be discussed according to the form in which the energy is stored (Figure 3-1).

Every type of energy could theoretically be transformed into every other form of energy. These conversions also take place when energy of a certain form e.g. solar radiation or thermal energy is converted in another form for storage to be finally converted to the energy form useful for the end-user (e.g. electricity or heat). Storage of energy in the built environment is limited to the forms of mechanical, electric, chemical and thermal energy.

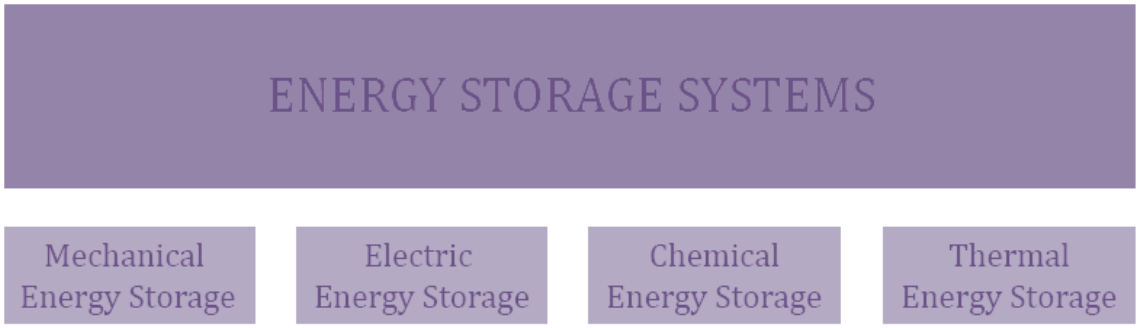

Figure 3-1: Classification of forms of energy storage in the built environment

Energy storage systems can be characterized and compared on a few general criteria:

Storage capacity - Amount of energy that is storable in the storage system in watt-hour, which is the energy equivalent of working at a power of 1W (3.600J) for 1 hour (Farret, 2006).

Energy density - Amount of energy that can be stored per unit volume in MJ/m^3. The energy density is important considering required volume or space.

Cycle efficiency and power - For systems that aim at storing and regenerating high-quality energy (electricity or gas), cycle efficiencies and installed power are indicated. It gives the electrical efficiency, i.e. the percentage of power input that is available after withdrawal.

Storage duration - Storage duration is determined by requirements on energy density (for long or medium term needs) and power density (for short or very short term needs) (Farret, 2006). Following intervals will be used to categorize storage methods according to duration and function:

- Transient (microseconds-seconds). Very short term: Power quality (grid), compensate for voltage sacks, back-up systems, system reliability during fault management.

- Short term (minutes-few hours). Load following/leveling: stores renewable energy surplus to cover load during short term load peaks, smoothes renewable energy deficits, backup.
- Medium term (several hours-days). Stores renewable energy for compensation of weather-based changes: daily fluctuations.
- Long term (weeks to months). Stores renewable energy for compensation of seasonal fluctuations, includes large power storage systems.
- Timeless. Time has no influence on the quantity and quality of the stored energy.

Droste-Franke introduced the energy-to-power ratio in order to classify systems according to energy supply duration. This E2P is simply derived by dividing the installed capacity in kWh by the peak power in kW (Droste-Franke, et al., 2012). Short-term storage systems have an E2P ratio smaller than 0,25h. This means they can fulfill a very large number of charge/discharge cycles per day. Medium-term storage systems with E2P ratios of 1-10h can supply energy for several hours. They do have a limited number of full cycles up to two per day. Long-term storage systems do have an E2P ratio varying from 50-500h, with a small number of storage cycles per year.

3.1 Mechanical energy

Mechanical storage utilizes the energy that can be stored in the motion and/or the position of a buffer medium (e.g. water or air) or object. This involves changes in the motion of mass, kinetic energy, and changes in potential energy. All technologies of storage in mechanical energy do have grid electric energy as input. During the storing process the electricity is converted to mechanical energy and vice versa at moments of demand.

3.1.1 Pumped-Hydro storage (PHS)

Storage duration	medium-long
Storage capacity	~ GWh
Energy density	3 [MJ m-3] (300m)
Cycle efficiency	70-85 [%]
Power	100-1.000 [MW]

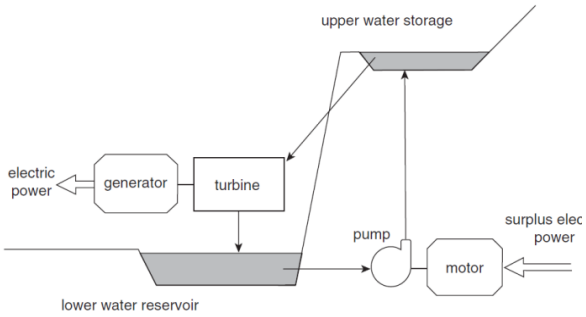

Figure 3-2: PHS (Farret, 2006)

Pumped hydroelectric storage is a method to store potential energy from height differences in water levels. This storage method already exists for a long time and its principle is well-known. As can be seen in Figure 3-2, a PHS system consists of two reservoirs located at different elevations. During periods with a low electricity demand, water is pumped from the lower reservoir to the upper one using excess generation capacity. During peak hours, the water is released back into the low reservoir through a turbine, generating electricity. Discharge times range from several hours to days.

Figure 3-3: Reservoir Energie-eiland KEMA-Lievense (Van Velzen, 2010)

The amount of energy stored is proportional to the volume of the water storage and the height difference between the two reservoirs. Approximately 70-85% of the electrical energy that is used to pump the water into the elevated reservoir can be regained. Losses occur due to evaporation from the exposed water surface in both reservoirs and (small) conversion losses.

PHS is the most mature technology for large power capacity storage at a relatively high efficiency. Other advantages are the installations practically unlimited cycle stability and long lifetime. However,

its construction time is a large drawback, as well as the environmental damage from constructing reservoirs. PHS is mainly used for energy management in high-power applications. By the introduction of a time shift, load variations on the power grid can be flattened which prevents the need for peaking power plants. It is also used for power quality control and as a power reserve. PHS is considered to be an interesting storage technology for wind variability applications. In order to level renewable power variations, the PHS should be able to provide power to the grid within minutes.

The approximately 250 PHS plants worldwide do have a cumulative capacity of over 120 GW, which is 99% of the world-wide installed electrical storage capacity (IEC, 2011). Still, this represents only 3% of the global power generation capacity. More capacity is installed at a rate of circa 5 GW per year. Despite the lack of appropriate geography, two Dutch plants were proposed in the eighties: an "energy-island" in the North Sea (KEMA, 20 GWh) and the "OPAC" (Royal Haskoning, 9 GWh). Both concepts should provide back-up storage for large wind farms. Although technically feasible, their realization was questioned due to high investment costs (Van Velzen, 2010).

3.1.2 Compressed air energy storage (CAES)

Storage duration	medium-long
Storage capacity	~ GWh
Energy density	8-15 [MJ m-3]
Cycle efficiency	40-50 [%]
Power	50-300 [MW]

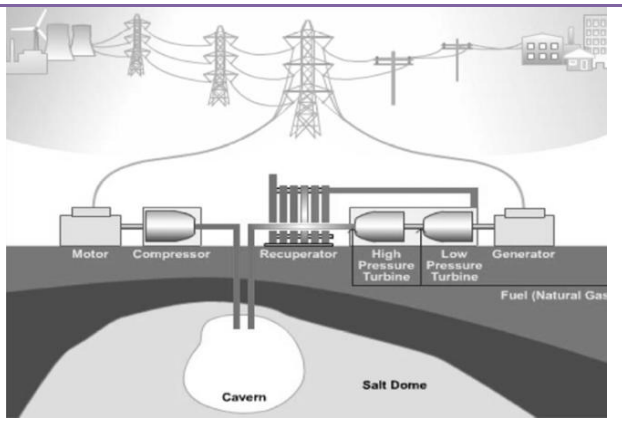

Figure 3-4: Schematic of Compressed Air storage (Hadjipaschalis, 2009)

The principle of Compressed air energy storage is comparable with pumping up a bicycle tire. The work required to do so increases as the pressure rises. If the valve is opened, the gas stored in the tire is released. This shows that energy can be stored by making use of the elastic properties of gases. The amount of energy stored (in a fixed volume) is determined by pressure and temperature.

Compressed air energy storage systems use existing underground sites (e.g. empty natural gas storage caves or abandoned mines) to store gas under very high pressure at near-ambient temperatures. This process decouples the compression and expansion cycles of a conventional gas turbine, storing electric energy in the form of elastic potential energy of compressed air. See Figure 3-4. During off-peak demand periods, energy is stored by compression (driven by an electric motor) of air into the underground cavity. Upon regeneration of this energy, compressed air is extracted from the underground, heated and then expanded through a high pressure turbine. After being mixed with fuel,

the expanded air is combusted through a low pressure turbine. Both turbines are connected to a generator in order to produce electricity. Generation takes place at peak demand hours or moments when renewable energy is not available.

Worldwide, two CAES plants have been built. The first one was built in Huntorf, Germany, storing air 600 m underground and providing a peak power of 290 MW for 2h. A second, 110 MW-26h CAES installation is located in Alabama, USA, using an old mined salt dome at -450m. Several other plants are under construction. CAES joins the main drawback of PHS: reliance on favorable geography (in this case underground storage area and availability of natural gas) and a low energy density. Capital costs should be spread over large power storage to make this storage method feasible (Chen, et al., 2009). The combustion of fossil fuels at the end of the storage process and the accompanied contaminating emission, makes the technology less attractive.

Together with PHS, CAES is the only technology currently used for large-scale power and high energy storage applications. In order to make it economically attractive, it must be combined with other functions e.g. seasonal storage (Beaudin, et al., 2010). Energy can be stored for days, months or even years. CAES has a smaller impact on the surface environment than PHS. The cycle efficiency of the existing CAES plants is limited to 40-50% because the heat released during the compression step is dissipated by cooling. This is a serious problem from an energy and exergy point of view, since compression to a pressure of 70 atm produces heat of about 1.000K (Huggins, 2010). Advanced Adiabatic CAES is proposed, in which the compression heat is stored in order to pre-heat the air during the expansion process. Although this system is still in a laboratory phase, system efficiencies of 70% seem feasible (Droste-Franke, et al., 2012).

CAES is used to provide reserve power during peak hours (time shift), and for load following due to its frequent and fast start-up/shut-down cycle. This makes CAES is a suitable storage method for mitigation of wind variability according to (Cavallo, 2007).

3.1.3 Flywheel energy storage (FES)

Storage duration	transient-short
Storage capacity	1-30 kWh
Energy density	240-950 [MJ m-3]
Cycle efficiency	85-95 [%]
Power	1 [kW] – 1 [MW]

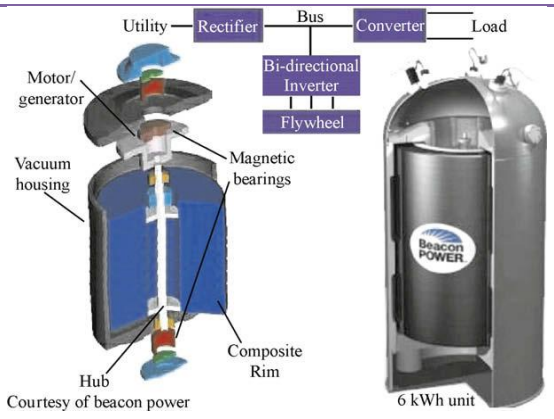

Figure 3-5: Beacon Power 6 kWh flywheel unit (Beacon Power, 2007)

Besides storage of potential energy, like PHS and CAES, it is possible to store kinetic energy by bringing mass in linear or rotational motion. Flywheel storage is a device which contains a flywheel that spins at a high velocity to achieve maximum storage of rotational kinetic energy. The flywheel is accelerated by means of an electric motor, which is used as a generator in the case of discharge. The total energy stored in a flywheel system is proportional to the mass and speed (^2) of the rotating body (rotor). The power rating depends on the motor-generator (Chen, et al., 2009).

Available technologies can be distinguished in slow rotating flywheels with approximately 5.000 revolutions per minute (rpm), medium rotational speeds of 25.000 rpm and fast rotational speeds of a few 100.000 rpm. Increasing the rotational speed does not always mean more energy can be stored. At a certain point, the rotor radius must be reduced to limit the centrifugal forces. For safety reasons, flywheels are constructed of many small pieces, and housed in very robust steel containment.

Flywheels are high power storage devices, which deliver very high power for short periods of time. The number of full charge-discharge cycles is between 10.000-several 100.000 and they can be charged in a matter of minutes, which makes flywheels advantageous over batteries for storage purposes with many cycles (e.g. power quality). Compared to batteries, flywheels require less space (higher power density) and no conditioned space to ensure performance.

Conventional flywheel systems consist of metal rotors and conventional bearings, operating at low speeds. Currently, high performance flywheels made of fiber reinforced plastics (carbon or Kevlar) are under development. The introduction of these materials combined with ultra-low friction bearing assemblies should enable flywheels to store up to 36 MJ for recovery over a period of a few hours, and energy densities over 1000 MJ m^{-3} can be achieved (Huggins, 2010; Ter-Gazarian, 2011; Hadjipaschalis, 2009). If flywheels will ever reach loss-free capacities sufficient for long-term storage of large quantities of electricity, is hard to predict (Vollebrecht, 2012).

The instantaneous efficiency of flywheels typically is 90-95%. Due to losses in bearings and friction of the rotating body, flywheels suffer from a high self-discharge rate between 55% and 100% per day, depending on the product (Beaudin, et al., 2010). Hadjipaschalis mentions even higher losses of 20% of the stored capacity per hour (Hadjipaschalis, 2009). If many charge-discharge cycles are performed per day, this is no problem. For long-term storage however, flywheels are not sufficient (yet). Proper storage periods should maintain within tens of minutes (Chen, et al., 2009). This restrains commercially available flywheels from application in energy management. The technology is mostly applied in local high power/short duration applications, e.g. as a power quality device for electrical power distribution grids or back-up power reserve. Combinations with variable renewable energy sources are just starting, according to (Beaudin, et al., 2010). A 5 kWh, 200 kW flywheel is used to stabilize a wind-hydrogen system supplying 10 off-grid households in Utsira, Norway. Manufacturer UPT demonstrated flywheels for smoothing wind variations, Beacon Power for PV fluctuations.

3.2 Electric energy storage (EES)

Electrical energy is determined by the product of the voltage and quantity of charge that passes through a device. Energy can be stored in the form of electrical energy by two general mechanisms. Capacitors store energy by separating negative and positive electrical charges. The second mechanism concerns storage of electrical energy in magnetic systems. Electric energy storage systems are, like flywheels, most applicable in situations that demand storage of modest amounts of energy under transient conditions i.e. within short periods and at high rates. High power and fast kinetics are required, rather than a large amount of energy to be stored.

3.2.1 Double-layer Capacitor (DLC)

Storage duration	transient
Storage capacity	0-2 kWh
Energy density	20-70 [MJ m-3]
Cycle efficiency	85-98 [%]
Power	0-300 [kW]

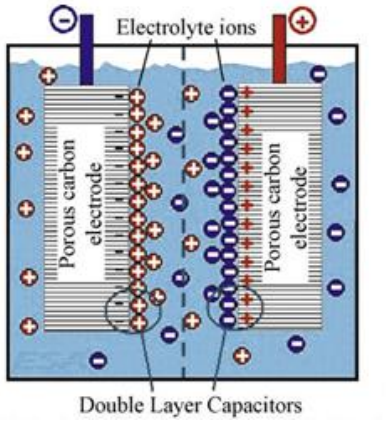

Figure 3-6: Supercapacitor schematic (Chen, 2009)

Electrochemical double-layer capacitors, also called supercapacitors, fill in the gap between well-known small supercapacitors (used for power back-up in electronics e.g. computer memories, cameras) and electrochemical batteries. Supercapacitors combine the characteristics of both, except the presence of a chemical reaction. This increases its cycling capacity. Fast charge-discharge cycling, lifetime over 100.000 cycles at high efficiency and high power make capacitors advantageous over batteries. Instead of an electrochemical reaction, electricity is stored in electric static fields (Figure 3-6).

Major problems of capacitors are short storage durations and high self-discharge losses (5-40% per day). Since these problems are similar to flywheels, their application is also restricted to fast cycling applications requiring very high power such as power quality control, not capable for long term energy storage or large quantities of electrical energy. The typical discharge time of supercapacitors is below 10s. Considering the support of variable renewable energy sources, large supercapacitors can be used for back-up power during short voltage failures or extension of battery life (Beaudin, et al., 2010).

3.2.2 Superconducting Magnetic Energy Storage (SMES)

Storage duration	transient
Storage capacity	0-10 kWh
Energy density	50-70 [MJ m-3]
Cycle efficiency	90-97 [%]
Power	0.1-10 [MW]

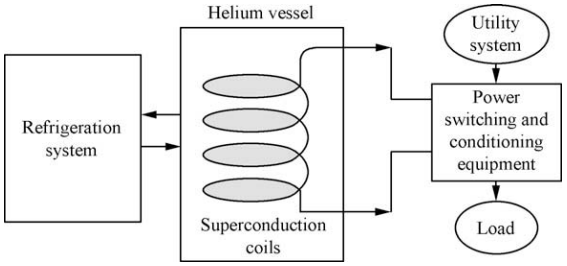

Figure 3-7: SMES system schematic (Chen, 2009)

The energy storage capacities of electromagnets can be much larger than that of similar size capacitors. SMES is the only technology known to store direct current directly (Chen, et al., 2009). Energy is stored in a magnetic field which is created by the flow of direct current in a large coil, see Figure 3-7. The amount of stored energy is determined by the current flowing in the coils. Since losses are proportional to the current squared, superconducting coils are required which have zero resistance. To maintain the conducting material in a state of superconductivity, the coils should be cooled to a very low *critical temperature* below -170℃. This cooling process of "high-temperature" superconducting materials (conventional materials needed a temperature of 4K), uses liquid helium or nitrogen.

Considering the electrical conversion and storage only, superconducting magnetic storage has high storage efficiency. SMES has a fast response time (less than 100ms), but can only generate electricity at rated capacity for a few seconds. Although energy can theoretically be stored indefinitely, the storage time is limited by the energy demand of the refrigeration system. In contrast to batteries, SMES maintains performance after a large number of full discharges ensuring a long lifetime.

A drawback is related to the strong electromagnetic forces associated with large scale storage, which demands underground installation (Huggins, 2010). Underground storage is also necessary in order to reduce infrastructural interventions. To give an example of the size of a SMES system: to store a large load of 5000 MWh, the coil requires a diameter between 150 and 500m (Ibrahim, et al., 2008). SMES for longer term storage applications is currently investigated (IEC, 2010).

SMES is only used for Uninterruptible power supply and power quality control for large industrial customers (Chen, et al., 2009). The technical feasibility of SMES for improvement of the reliability of renewable energies is currently investigated. For most purposes though, flywheels and capacitors form more attractive (especially considering operating temperatures) alternatives for the same niche (Beaudin, et al., 2010).

3.3 Chemical energy storage (CES)

Storage in a chemical carrier or medium can have three basic primary energy forms: chemical energy of organic matter, electric energy (electrochemical) and thermal energy (thermochemical). Chemical energy is energy that is stored in substances as binding energy between atoms, which can be released as kinetic energy during a reaction.

The energy density of biomass-related chemical storage is approximately a 100 times higher than any other forms of energy storage discussed. This gives chemical storage systems a big lead over other storage methods (Semadeni, 2004). Primary storage of energy in chemical form occurs in crude oil, natural gas, coal and biomass. Instead of direct combustion, the chemical resources can be converted into intermediate liquid or gaseous energy carriers called biofuels/secondary fuels (Sorensen, 2007).

In essence, fossil fuels and biomass involve the collection and storage of the sun's (luminous) energy into a chemical form due to photosynthesis (which can be utilized nowadays). On average, 0,3% of the solar energy is stored as carbon compounds in land plants (Semadeni, 2004). In the case of fossil fuels, million years of fossilation approximately doubled the energy density.

3.3.1 Primary chemical energy storage

3.3.1.1 Coal, crude oil

Storage duration	timeless
Energy density	38.000 [MJ m-3]

Coal is a combustible mineral, formed over millions of years through decomposition of plant material. The coal stock is rapidly decreasing. Crude oil, also called petroleum, is a liquid fossil fuel. It has the highest energy density of all fossil fuels. Oil reserves are expected to remain economically exploitable for the next 20 years (Semadeni, 2004).

3.3.1.2 Natural Gas

Storage duration	timeless
Energy density	35 [MJ m-3]

Natural gas is found underground, associated with oil and in coal beds. It is also present as *methane clathrates* under the oceans. Natural gas can be used as a fuel for electricity generation in steam turbines or high temperature gas turbines. It is considered to be the cleanest fossil fuel, because while producing the same amount of heat, 30-45% less CO_2 is emitted than burning oil or coal (Huggins, 2010). Gas consists of methane, MH_4 for over 80%. It is stored in two basic ways: compressed in tanks (liquid state, LNG) or in large underground storage facilities e.g. empty salt caverns. Electricity production by direct combustion of fossil fuels in power plants shows efficiencies of circa 40% using coals, and 60% using gas turbines (Woudstra, 2012).

3.3.1.3 Biomass

Storage duration	timeless
Energy density	1-10.000 [MJ m-3]

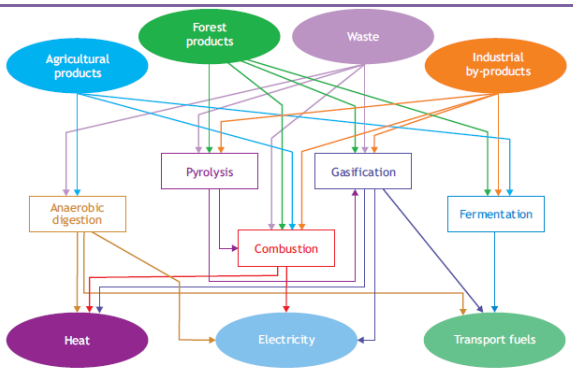

Figure 3-8: Pathways energy conversion from biomass (IEA, 2007)

Primary biomass can be defined as any organic matter available on a renewable basis (Semadeni, 2004). Biomass is considered as an important renewable energy resource for the future. The fact that biomass also contains nutrients and potential raw material for a number of industries, should however be kept in mind. Bio-energy cannot be separated from the production of food, timber industries or organic feedstock dependent industries. In a proper functioning market, the application value of biomass is reflected in its economic value. Higher total economic value can be obtained by separating substances or materials for high quality purposes, e.g. pharmacy (by refinery) and use residues for lower value applications like conversion into electricity or heat, instead of using the entire product for low quality applications. Figure 3-9 shows the economic value pyramid of biomass.

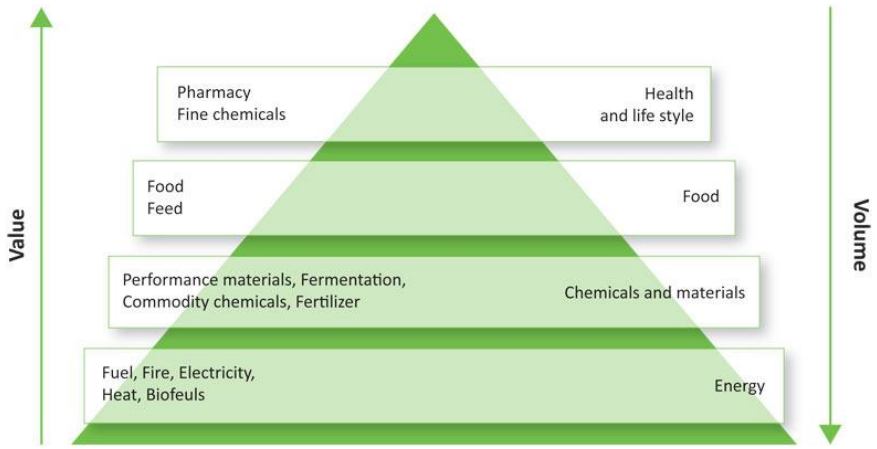

Figure 3-9: Pyramid of the economic value of biomass (source: betaprocess.eu)

A wide range of biomass products, from wood fuel to rapeseed, could be used for generation of heat, electricity and liquid fuels. Waste and residue materials should also be seen as biomass sources. Conversion of chemical energy to thermal energy by combustion of biomass is very common. All bioenergy pathways end up with combustion of a solid, liquid or gaseous biofuel gaining thermal, electric or mechanical energy (Figure 3-8). Direct combustion of solid raw biomass, e.g. woody

residues, for heat production has maximum thermal efficiencies of 50-60%. Raw biomass is bulky and has variable, mostly low energy densities. The emitted gases are polluting (van der Hoeven, 2007; Kammen, 2004). Electricity can be generated via a steam-Rankine cycle combustion. Typical capacities of existing biomass power plants are 1-50 MWe. The conversion efficiency is low (15-20%). Combustion using cogeneration reaches overall fuel efficiencies over 80%. Biomass can also be co-fired with fossil fuels in existing power plants. Fossil substitution up to 20% can be realized while maintaining efficiency (Sorensen, 2007; Sterner, 2009).

3.3.2 Secondary fuels

Most organic material contains a significant amount of water, and therefore it needs conversion into a secondary fuel to get the energy available in an useful way. Transport, distribution and energy storage require treatment of primary biomass to more suitable, secondary carriers e.g. gas or fuels. This conversion increases the energy densities. Some secondary fuels, i.e. biogas and hydrogen, can have both biomass and (renewably generated) electricity as primary energy form. These secondary fuels are a very interesting carrier of future renewable electrical or chemical energy (Woudstra, 2012).

3.3.2.1 Hydrogen

Storage duration	long
Energy density	10 [MJ m-3] (g)

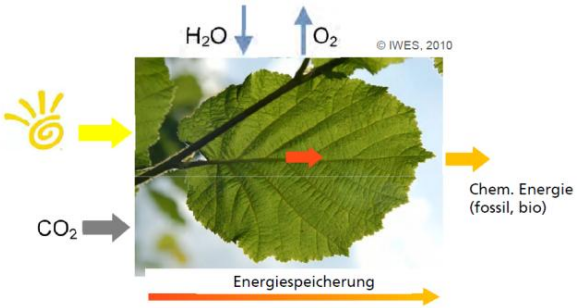

Figure 3-10: Energy storage in nature (Fraunhofer, 2011)

Hydrogen is not a primary energy source. Similar to electricity it is an energy carrier, a fuel with energy stored in its chemical potential. Hydrogen is believed to become a major energy carrier for renewable energy systems (Semadeni, 2004). Hydrogen producing processes are based on photolysis in biological systems, where water is split using solar radiation. Instead of hydrogen, a more complex and more energy-rich molecule (i.e. biomass) is formed by capturing CO_2, see Figure 3-10. Hydrogen can have biomass (chemical energy) or electricity (electrical energy) as primary energy source:

Biomass - Hydrogen can be derived from biomass via a large number of biochemical and thermochemical pathways that are extensively described in (Nath & Das, 2003; Sorensen, 2007). The pyrolysis technology is most potential from techno-economic perspective. Recently, photosynthetic production of hydrogen using microalgae is investigated. In order to grow, microalgae need water with suitable nutrients, CO_2 and light. During anaerobic incubation inside a so called photobiotic reactor, hydrogen released by the microalgae can be induced. Technical issues, e.g. poor volumetric efficiencies and harvesting efficiency make this process costly (Amaro, 2012; Gupta, 2011).

Power - Storage of renewable-based electricity by hydrogen production differs from other energy storage methods because production, storage and use are separated. An electrolyser produces hydrogen and oxygen from water by introduction of an electric current. Renewable electric energy is converted to chemical energy according to reaction 3.1:

$$2H_2O + \text{energy} \rightarrow 2H_2 + O_2. \qquad (3.1)$$

Electrolysis is a relatively new method for hydrogen production, with almost 100% conversion efficiency (Gupta, 2011; Beaudin, et al., 2010). After storage, hydrogen can be converted back into electrical energy by a fuel cell. The principle of a fuel cell is similar to secondary batteries, except the fact that one of the reactants, hydrogen, is externally supplied (Figure 3-11). The redox reactions at both electrodes cause a transfer of ions through the electrolyte, which generates an external current. Fuel cells convert chemical energy to electric energy by inverse electrolysis (reaction 3.1 reversed). A clear overview of available fuel cells/electrolytes is given in (Haeseldonckx & D'haeseleer, 2004).

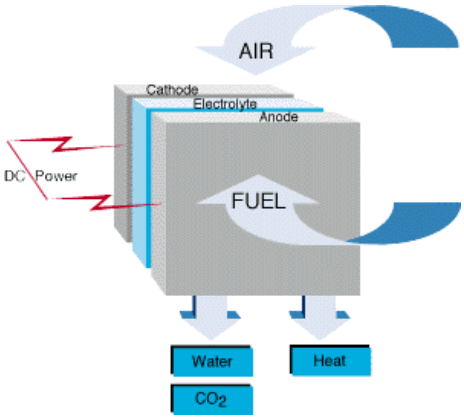

Figure 3-11: Fuel cell principle (Boulanger, 2003)

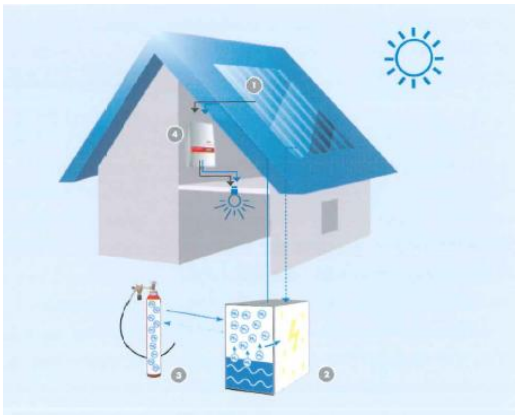

Figure 3-12: Fuel cell-integrated energy system (Sauter, 2012)

In fuel cells, more than 40% of the initial energy is converted into heat. When heat is utilized, the total efficiency increases to 80% (Beaudin, et al., 2010). The lack of hydrogen infrastructure requires expensive on-site hydrogen production. Regenerative fuel cells contain an electrolyser within the cell. Regenerative SO-FC and PEM-FC are developed, with electrical efficiencies up to 60%. Current research focuses on cycle lifetime improvement (Boulanger, 2003). Until now, natural gas is the common fuel for fuel cells because of its easy availability (Haeseldonckx & D'haeseleer, 2004).

Storage of pressurized hydrogen gas in caverns or strong tanks is a common large scale storage method. Losses are neglectable, but energy for compression should be seen as conversion losses. In *liquid* state, almost a 100 times more hydrogen can be stored per weight unit. Much energy is required however to keep hydrogen in liquid state around -253℃, thermal losses sum up to 1-3% daily. Hydrogen storage within a solid-state system is promising but more conceptual. Hydrogen is bound to a metal compound e.g. metal hydrides or carbon. This system stores more hydrogen per unit volume than other storage options, at safe near-ambient temperatures (Boulanger, 2003; Semadeni, 2004).

Applications of a fuel cell for medium term hydrogen storage can be at district level e.g. a small wind power-hydrogen system on an off-grid island (Nakken, et al., 2010). Fuel cells are also available for single family houses (Albus, et al., 2010; Sauter, 2012), in the scale of 1-5 kW_e. Sauter proposes a hydrogen-based fuel cell system for seasonal storage of excess electrical energy generated by PV (Figure 3-12). 1.200 kWh of hydrogen can be stored in a tank. In order to exchange the waste heat associated by the electricity regeneration in winter, the gaseous water that results from the reaction between hydrogen and oxygen is led through a heat exchanger, charging a buffer tank for DHW and space heating. The system is currently tested (Sauter, 2012).

3.3.2.2 Biogas/methane

Storage duration	long
Energy density	5-18 [MJ m-3]

Methane-rich gases can be produced from non-fossil organic matter, e.g. crops, waste and residues. Biogas is the most promising biofuel because it is directly accessible, has good storage stability and can be produced via a variety of paths (Semadeni, 2004). Sterner defines 78 biomass pathways to final energy via multiple production processes, collection and conversion methods (Hoogendoorn, et al., 2008; Sterner, 2009). Main conversion concepts for production of biogas or methane are fermentation and gasification. The Fraunhofer Institute proposes substitution of natural gas by biogas as a storage medium for renewable energy. The substitute gas is bio-methane (CH_4), called Substitute Natural Gas (SNG), which can be produced via three main paths (Specht, et al., 2011)(Sterner, 2011):

Biogas (CH_4+CO_2) to SNG - from "wet" biomass, using anaerobic fermentation.

BioSyngas (raw gas with H_2, CO, CO_2, H_2O and CH_4) to SNG - from "dry" biomass, using gasification.

Power to Gas - from renewables-based electricity, using electrolytic hydrogen production in combination with carbon (di)oxide (industrial residue or waste CO_2 from biogas upgrading).

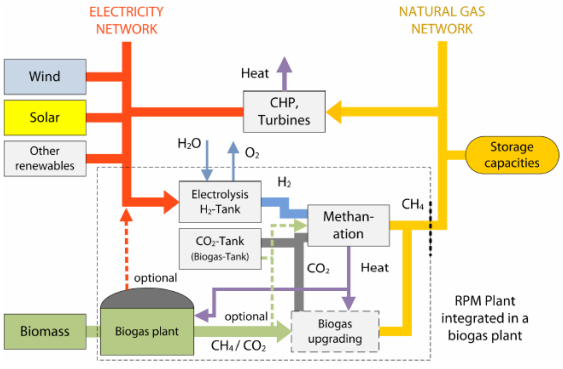

Figure 3-13: Integration of a biogas plant and renewable power (Sterner, 2009)

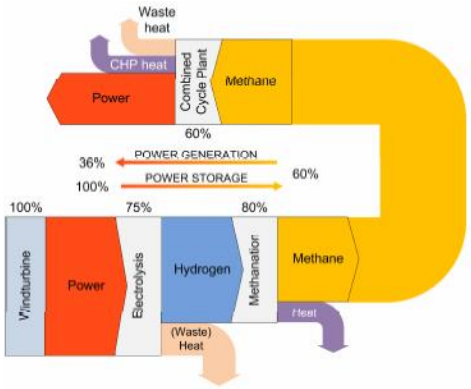

Figure 3-14: Performance of complete storage cycle of power-gas-power (Sterner, 2009)

Combinations of the Fraunhofer concepts are attractive, e.g. waste components from the biogas upgrading could be used as a feedstock for methanation with the hydrogen produced by electrolysis. This can be seen in the schematic in Figure 3-13. The overall electrical efficiency for the Power-to-Gas concept is 36%, overall fuel utilization 85-90% (Sterner, 2010), see Figure 3-14. SNG generation allows for seasonal storage of renewable energy in an existing infrastructure, which is a major advantage over hydrogen- or electricity storage.

Specht illustrates the possibilities of the Power-to-Gas concept as follows: the storage capacity of the German electricity grid is circa 0,04 TWh (storage duration within one hour), whereas the storage capacity of the gas grid is over 200 TWh, allowing storage for months. Biogas needs to be upgraded, removing CO_2, before it can be fed into the grid. Syngas needs cleaning treatment. Depending on the feedstock, thermo-chemically produced biogas can have an energy content of 5-18 MJ m^{-3}. This is lower than pipe-line quality natural gas, so mixing can't be unlimited.

Besides for storage in the gas grid, SNG and biogas can be used in decentralized Combined Heat and Power (*micro-CHP*) or as transportation fuels (Specht, et al., 2011). CHP forms the most preferable application from energy efficiency point of view. Cogeneration plants fuelled with SNG from maize- or grass silage and switchgrass achieve highest electrical efficiencies of 30% and total fuel utilization of 55-60%. Small bio-gas fuelled CHP's that can be integrated in a single family dwelling are available in capacity ranges of 1-5,5 kW_e. During electricity production, waste heat is stored in a buffer tank for DHW and space heating, see Figure 3-15. 85% of the initial energy of the gas is utilized. Similar size fuel cells are commercially available, with electrical efficiencies of 30-40%. The high-temperature gas-fuelled BlueGen Fuel cell achieves 60% electrical efficiency (Albus, et al., 2010; Castell & Margalef, 2010; Sterner, 2009).

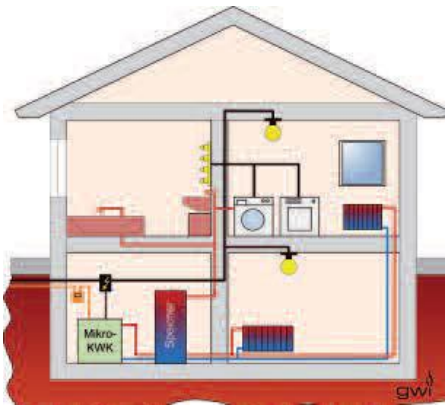

Figure 3-15: uCHP in a single family house system (Albus,2010)

Figure 3-16: BlueGen Fuel cell (Gommans, 2012)

3.3.2.3

3.3.2.4 Liquid bio-fuels

Storage duration	timeless
Energy density	17k - 20k [MJ m-3]

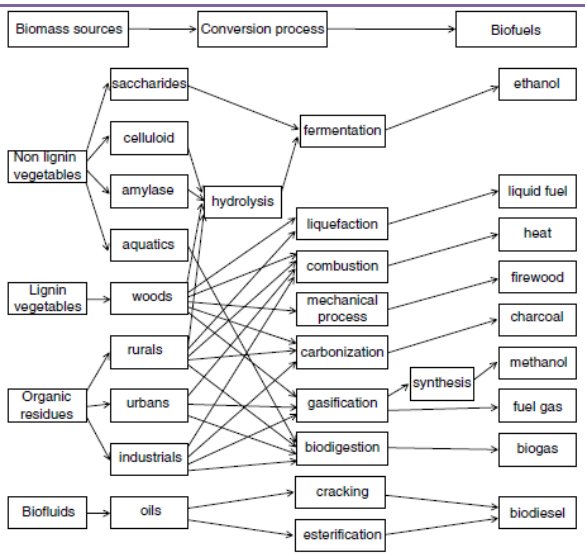

Figure 3-17: Processes for bio-fuel production (Farret,2006)

Bio-fuels are produced via various thermochemical or biochemical processes that convert biomass into more useful intermediate energy forms. Particular interest concerns the conversion of biomass into liquids, since they can replace petroleum based fuels in the transportation sector, but can also be used in CHP plants (Sorensen, 2007; Kammen, 2004). Bio-fuels can be used in existing infrastructure directly. Main processes for biomass to bio-fuel conversion are shown in Figure 3-17. Biomass gasification is the most efficient and economical conversion process of biomass feedstock to high density fuels (synthesis gas) (Farret, 2006). Some biofuels are discussed more detailed in Appendix A.

Based on the impact of feedstock consumption on the global food market and food security (*food vs. fuel dilemma*), fuels can be classified as first, second or third generation bio-fuel (Daroch, et al., 2012). Biomass feedstock containing edible oils, like palm oil, soybeans, rapeseed are considered as first generation feedstock. Vegetable oil is a vital component of human food. Some other feedstock (maize, sugarcane) require large quantities of arable land to grow crops. Secondary feedstocks do not compete the global food market. Examples of non-edible oil crops are Jatropha and tobacco seed.

Agricultural waste, restaurant grease, waste cooking oils and animal fats are also considered second generation feedstock. These feedstocks may not be abundant enough to completely replace current transportation fuels. Therefore a third generation is proposed, which is not related to food production at all. The most promising feedstock in this generation are microalgae. Microalgae combine a high growth rate with good seed oil content, which makes its biomass productivity and oil yield larger than that of first two generations crops. Volumetric efficiencies are still poor, and processing technology is in development stage (Amaro, 2012; Ahmad, et al., 2011).

3.3.3 Secondary batteries

Storage duration	short-medium
Storage capacity	1-1.000 kWh
Energy density	70-1.500 [MJ m-3]
Cycle efficiency	60-95 [%]
Power	0-few [MW]

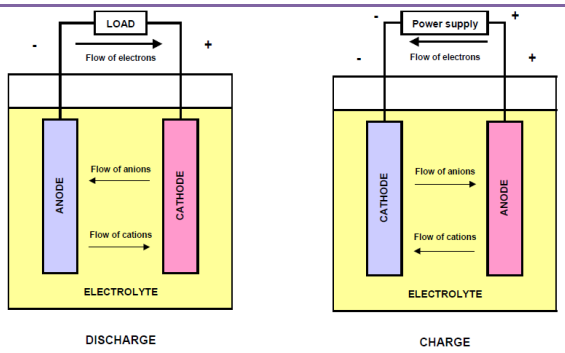

Figure 3-18: Simplification of battery energy storage (Lailler, 2003)

A secondary (or rechargeable) battery converts the chemical energy it contains directly to electric energy by means of an electrochemical redox reaction. This redox reaction involves electron transfer from one material to another through an electric circuit, see Figure 3-18. Self-discharge results from leakage of electrons through the electrolyte (Lailler, 2003).

Besides reduction of storage capacity, a battery system's life-time is significant reduced when it operates under high fluctuations. Various combinations of batteries with high power storage methods that can have many thousands of cycles e.g. flywheels or supercapacitors, have been proposed and tested in autonomous renewable energy systems. These systems have large power fluctuations in generation. Batteries could be used as energy suppliers (low self-discharge, high energy density), whereas flywheels or super-capacitors function best as power suppliers, combining advantages of both systems (Brown & Chvala, 2005; Prodromidis & Coutelieris, 2012; van Voorden, et al., 2007).

Several anode-cathode configurations are discussed in Appendix A – Literature review, including applications and performance. Some batteries contain metals that are environmentally hazardous, or have limited supply reserves. Other Electrical Energy Storage methods also use these metals. With circa 20 year of economical extraction of lead and zinc reserves left, lead-acid and Zi-Br batteries may encounter shortage, see Table 10-1 in Appendix A – Literature review (Beaudin, et al., 2010).

3.3.4 Flow batteries

Storage duration	Medium-long
Storage capacity	1-1.000 MWh
Energy density	70-100 [MJ m^3]
Cycle efficiency	75-85 [%]
Power	0,1-10 [MW]

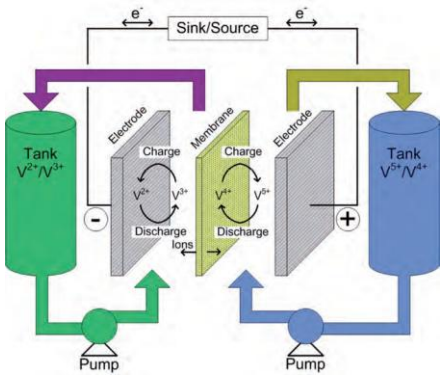

Figure 3-19: Schematic functioning flow battery (IEC, 2011)

Flow batteries are batteries that store energy in one or more electro-active species which are dissolved in liquid electrolytes. At least one of the electrolytes is stored in an external tank and pumped through the reactor that converts chemical energy directly into electricity (Figure 3-19) and vice versa when the battery is recharged. Contrary to secondary batteries, energy is stored in the electrolyte solutions itself. This means that self-discharge is nihil and depth of discharge can be ignored, which makes flow batteries suitable for seasonal energy storage. Power quality and mitigation of variable renewable energy sources are other good applications because of the fast response time and high discharge rate (Chen, et al., 2009). See Appendix A – Literature review.

3.3.5 Chemical reactions

Storage duration	long
Energy density	1.000 [MJ m-3]
Thermal efficiency	20-65 [%]
Operating temperature	-50 - 1.000 [C]

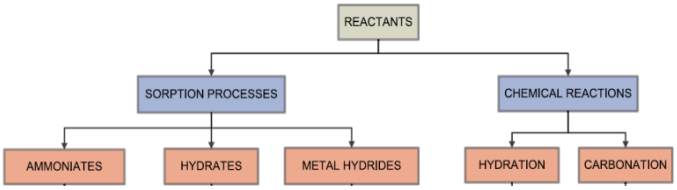

Figure 3-20: Chemisorption materials (Cot-Gores, 2012)

Thermal energy storage involves sensible, latent and thermochemical storage. Thermochemical storage is different from the first two forms since thermal energy is stored in the form of chemical energy. Although additional progress is needed to make the technology commercially available, some breakthroughs were made in two decades of research (Cot-Gores, et al., 2012). Main advantages of thermochemical storage are its high energy density and wide range of operating temperatures. Due to its complexity, thermochemical storage won't compete with sensible and latent forms for short term energy storage. Seasonal storage of waste or solar heat is more potential (Zondag, 2010).

The first main form of thermochemical storage is *fysisorption* storage. In a fysisorption process, water vapor is *adsorbed* by a liquid or a porous solid material called *sorbent* or *sorption material*, which thereby releases heat (discharge). When heat is fed into the system (charge), the water vapor is driven out of the sorption material again. Well known adsorption materials are silica gel and zeolite. This process is used in sorption cooling machines in utility buildings. Gas fuelled adsorption heat pumps could also be used for space heating and DHW.

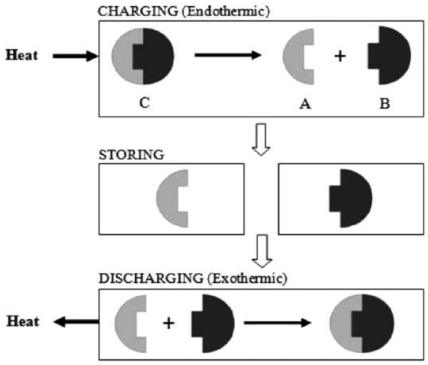

Figure 3-21: Closed thermochemical process (Abedin, 2012)

A slightly different form of sorption storage is *chemisorption*, see Figure 3-20. The storage principle is comparable to fysisorption, but the uptake of vapor results in an actual change in molecular crystalline structure and chemical properties of the sorption material. Chemisorption is based on a reversible reaction, see Figure 3-21. A chemisorption material (C) absorbs and converts thermal energy into two components (A and B) by an endothermic chemical reaction. The two isolated components are stored separately in storage tanks or inside thermochemical systems. When the stored energy is required, A and B are combined and heat is regenerated by the reversed reaction.

Chemisorption materials can be classified as ammoniates, hydrates and metal hydrides (Figure 3-20). These materials have higher energy densities than adsorption materials, but more stability problems are present (Zondag, 2010). Investigations aim to develop material pairs for thermochemical sorption heat pumps, called chemical heat pumps, as alternatives to conventional heat pumps.

Solid-gas systems contain a solid material that absorbs gas. Open systems are more compact and simpler than closed systems. Open systems extract gas from ambient air, and are more suitable for seasonal storage with a low number of cycles. A common solid-gas combination is water vapor with hydrated salt. The heat necessary to make the sorbent (water) gaseous can be obtained from the soil (ground exchanger) or solar thermal (Zondag, 2010). Closed systems are more suitable for heating or cooling in utility or industrial applications, with a large number cycles and higher temperatures. Stability of the chemisorption material is important here, requiring advanced materials. High temperature industrial waste heat can be used. Investigations on solid-gas heat pump systems show low performance which is mainly caused by the poor heat and mass transfer in metal salts (Cot-Gores, et al., 2012). Common chemisorptions materials are ammonia, methanol or ethanol.

3.4 Thermal energy storage (TES)

Thermal energy can be stored in a medium for later use via three main reversible processes shown in Figure 3-22, i.e. by a temperature difference of the medium (sensible), a phase change of the medium (latent) or by a chemical reaction. On a molecular level, the process of energy addition can result in increasing molecular movement (temperature difference), weakening or cracking of molecular bonds (melting or evaporation) and cracking or changing of molecular bonds (reaction) (Zondag, 2010). Thermochemical storage is discussed before. This paragraph deals with storage by physical processes.

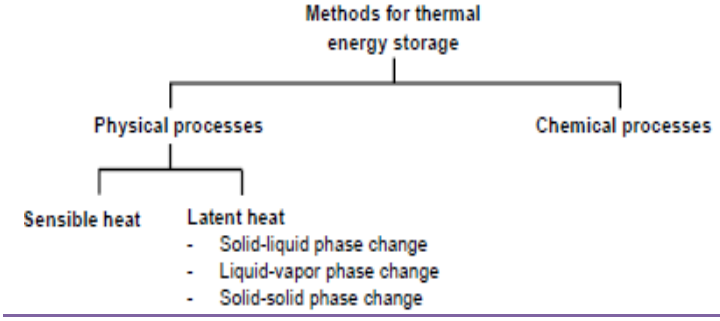

Figure 3-22: Classification of TES methods (Mehling, 2008)

Short- and long term storage of heat and cold can improve climate systems, because it (IEA, 2011):

- improves system efficiency by avoiding partial load operation or operation at other sub-optimal times.
- shifts demand over time to reduce peak load (short term).
- improves renewable energy contribution (utilize daily or seasonal fluctuations).

Storage duration, energy density, insulation values and surface-to-volume ratio are aspects that determine performance of a TES system. All influence the energy losses to thermal energy input ratio. Seasonal storage requires large capacities, what makes reduction of thermal losses a crucial design parameter. Short term, daily energy storage involves volumes that can be installed within a building.

3.4.1 Sensible TES

Storage duration	medium-long
Energy density	< 220 [MJ m-3]
Cycle efficiency	50-90 [%]
Range of operation	as large as possible

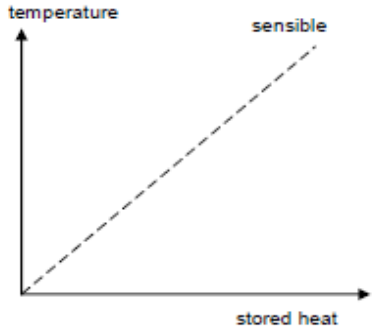

Figure 3-23: Sensible heat storage

Sensible TES systems are simpler in design than latent heat or thermochemical storage systems, but suffer from the disadvantage of a relatively small energy density and disability to store or deliver energy at a constant temperature. The amount of energy *E* stored by heating a material with mass *m* from its initial temperature T_0 to temperature T_1 is (Socaciu, 2011):

$$Q = \int_{T0}^{T1} mc_p \ \mathrm{dT} \qquad (3.2)$$

where c_p is the specific heat capacity of the storage material at constant pressure. From eq. 3.2 can be seen that the amount of sensible heat stored is simply defined by the specific heat capacity of the liquid or solid storage medium, its mass and temperature rise.

3.4.1.1 Underground TES (UTES)

Seasonal thermal storage for three or more months requires great volumes, which is possible in underground thermal energy storage systems (UTES). The temperature of the soil increases with depth. In Holland the increase rate is approximately 31˚C per kilometer depth (SKB, 2011). At depths more shallow than 0,8m below surface, the ground temperature fluctuates daily, following ambient temperatures. Within few meters depth, temperature fluctuations are seasonal. At greater depths, the

prevailing temperature equals the local average annual temperature, increasing with depth because of geothermal heat flux. Higher-enthalpy storage systems, like geothermal boreholes, take advantage of this geothermal heat flux. Lower-enthalpy systems, e.g. horizontal ground heat exchangers take advantage of seasonal temperature variations near to the surface (Dickinson, et al., 2009). In essence, these technologies utilize renewable resources and do not store energy. They will not be further discussed. Open UTES systems use groundwater directly to store energy, closed systems store energy by an exchanger medium. Three general types of UTES can be distinguished (Semadeni, 2004):

Aquifer ATES

Energy density	110-150 [MJ m-3]
Depth	30-150m

Aquifer energy storage is an open UTES system that uses natural water in a saturated, permeable underground layer as direct heat transfer medium. A *doublette* ATES system consists of two separate wells, one for extraction and storage of cold water, one for warm water. During summer, the system uses waste heat from the building (from the cooling process) to charge the warm well. This well can be discharged in winter, while the cold well is charged. This bi-directional system utilizes seasonal fluctuations. ATES systems have high efficiency and can save up to 50% on energy consumption for heating and cooling (NVOE, 2012). Up to several GWh thermal energy can be stored. The energy is stored in one single aquifer, which makes the system area consuming. No groundwater flow is allowed in the aquifer and the systems have several site-specific requirements (Novo & Bayon, 2010).

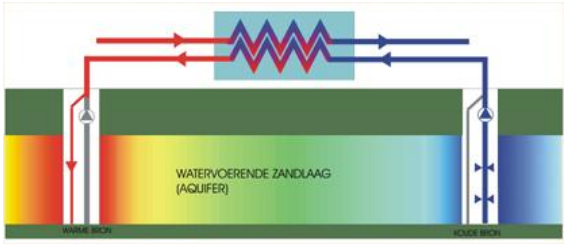

Figure 3-24: Doublette in cooling mode (NVOE, 2012)

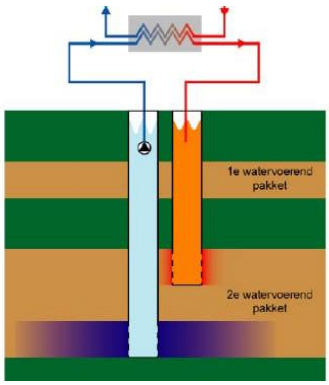

Figure 3-25: Monowell in cooling mode (NVOE)

A *monowell* works similar to doublette ATES but has only one well. The hot and cold storage occurs on top of each other, which makes the system more complex and expensive. It requires less space and is also very efficient. Open ATES systems in Holland store energy at depths between 20 and 80m below surface. Ground water that is extracted from one of the wells, exchanges heat with the buildings water circuit via a heat exchanger. Cold is typically stored at approximately 8˚C during winter, heat is stored at 15˚C during summer. In theory, from every 10 kWh of energy stored in ATES, up to 9 kWh can be regained (IEA, 2011).

In practice, the temperature difference between the hot and cold well is often smaller than designed, decreasing performance of the heat pumps that upgrade the heat/cold to the required temperature level (Koenders, 2007). Due to unbalance between the wells, the soil could structurally cool down or heat up. To prevent this, buildings with a net cooling demand regenerate the soil using dry coolers. Still, 70% of the Dutch ATES systems perform badly, by lack of integrated design, mismanagement, or non-ideal ground compositions (van Wijck, 2012). ATES seasonal storage is economically feasible for more than 50 dwellings or offices with over 2.000 m2 gross floor area.

High temperature UTES has several advantages over low temperature ATES. It eliminates the need for heat upgrading to end-use conditions, e.g. by heat pumps or boilers. In summer waste heat or renewable heat (solar thermal) could be stored for shortage during winter (Drijver, 2012). Several ATES systems for storage of 30-60˚C are operational in Holland. Worldwide, only one open storage system of 70˚C is active, 300m underneath Reichstag Berlin (Semadeni, 2004). Recently, a high-temperature ATES system was completed at the Wageningen University campus, Holland. An aquifer at a depth of 350-450m is charged with solar thermal heat and waste heat from greenhouses. 500 GJ heat can be discharged annually, aimed storage efficiency is 30-50% (NVOE, 2012).

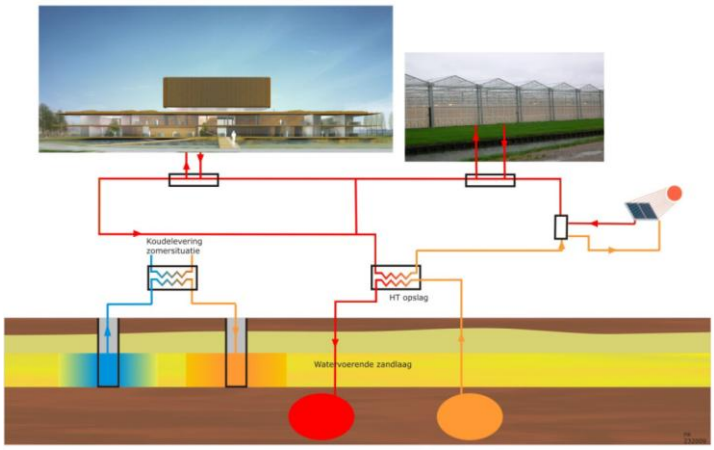

Figure 3-26: LT and HT ATES system NIOO (NVOE, 2013)

Cavern storage CTES

Energy density	150-220 [MJ m-3]
Depth	200-800m

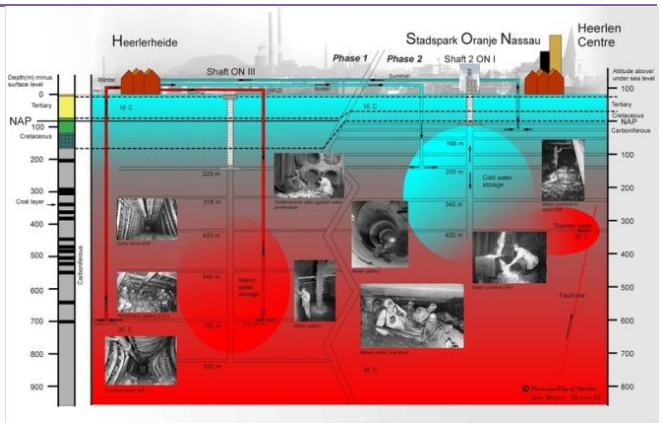

Figure 3-27: CTES in empty mines in Heerlen NL, section (Rooijen, 2010)

Energy storage in caverns uses existing empty man-made underground caverns as storage medium, e.g. abandoned mines filled with ground water. Due to the low thermal conductivity and high specific heat capacity c_p of the granite or rock, relatively large energy quantities can be stored per cubic meter. Closed mines can contain large water quantities of different temperature levels (Semadeni, 2004).

An example of this storage method is CTES system in an abandoned coal mining net in Heerlen. The site contains two warm wells (30˚C) at a depth till -700 m, and two cold wells (16˚C) at circa -250m (see Figure 3-27). The mine water will be pumped up and transported to several local energy plants, where the low quality heat or cold is upgraded to 35-45˚C for heating and 16-18˚C by heat pumps or CHP. The first plant was completed in 2008, and delivers energy to a new built district. Buildings are designed in accordance with the generated temperature levels, with low temperature heating/high temperature cooling emission systems (Roijen & Op 't Veld, 2010).

Borehole BTES

Energy density	50-100 [MJ m-3]
Depth	20-150m

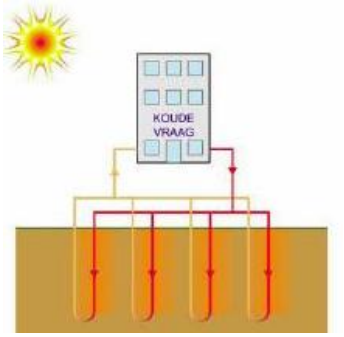

Figure 3-28: BTES, summer modus (heat charging) (NVOE, 2012)

Borehole energy storage uses a closed system with vertical heat exchangers that are inserted deeply into the ground. Thermal energy is transferred to or from the ground by conduction at the piping surface, (dis-)charging the soil (Figure 3-28). The exchanger consists of several U-shaped loops, filled with antifreeze (water-glycol) that has no direct contact with the ground-water. Typically, the heat exchanger loops are placed till a depth of 30-70m deep, where the groundwater temperature is in between 10 and 12˚C (NVOE, 2012). These stable temperatures ensure good heat pump performance (Rosen, 2012). Depending on the soil composition, available space and amount of energy to be stored, the depth and number of closed loops are defined. Vertical heat exchangers can be applied for single dwellings and small offices, but do have longer pay-back times.

3.4.1.2 Water storage

Energy density	220-290 [MJ m-3]

The specific heat of water is higher than that of concrete, aluminum or brick. Main applications are:

Stratified tanks - Short term or buffering (duration maximum one day) of energy for space heating or hot water in individual buildings almost always includes a water buffer tank. Usually, this

is an insulated steel container of 100-200 liters. Buffers for storage of solar thermal heat are often larger (Sorensen, 2007). Maintaining stratification inside tanks greatly improves collector and system efficiency because the medium temperature heat can heat up colder layers. Stability of the stratification is influenced by heat conduction at tank walls, ambient heat loss through the shell and outlet design. Even at large withdrawal flow rates, stratification can be maintained (Semadeni, 2004).

Water (underground) basins - The advantage of the ground as an insulator is exploited in storage of rainwater in a pit under greenhouses. Literature describes several tests of large-scale seasonal storage of high temperature heat from solar collectors in (partially) underground pits. In order to use the area above the pits, expensive structures are required. In gravel-water mixtures this is not needed. A 1.500m^3 gravel-water mixture pit was tested in Steinfurt, providing 325 MWh heat yearly to 42 apartments. Gravel-water pits are more cost-effective than water tanks, but they require 50% larger volumes to store a similar energy quantity (Novo & Bayon, 2010).

Chilled water - TES also includes sensible storage of water below ambient temperatures. Cooling capacity can be stored in chilled water at temperatures of 3,3-5,5˚C. Conversion can involve electrical powered chillers (COP 4,0), or waste or solar heat driven adsorption or absorption chillers with COP's of 0,7-1,2. Chilled water storage can be used in large utility buildings to store night-time, off-peak energy for daytime peak use. Chiller COP's are higher for water storage than for ice, but less energy can be stored per kg water than per kg ice (Dincer & Rosen, 2002).

3.4.1.3 Building thermal mass storage

Energy density	~10 [MJ m-3] (ΔT 5K)

Figure 3-29: Physical processes influenced by thermal mass (Hensen, 2010)

Like for water, the storage or accumulation ability of building thermal mass is determined by the specific heat capacity and mass of the materials. By 1˚C temperature increase of 1kg concrete, 0.88 kJ can be stored (1kg water: 4,19 kJ). Thermal mass influences three physical processes (Figure 3-29):

- transmission losses through the envelope (delayed);
- radiation due to occurring heat gains (delayed);
- adaption of temperature after a change in setpoint e.g. by user (delayed).

In general, buildings with a higher thermal mass can flatten out daily temperature fluctuations better: its thermal inertia is increased. This makes it possible to shift heat or cold supply and extraction from occupation times to more desirable moments (Schrever, 2002). Storage of cold in a more massive building structure during the night could decrease the need for cooling during the day, because the room temperature has a lower start temperature and increases at a slower rate.

When winter and in-between seasons considered as well, it is hard to conclude anything on the effect of a more slow reaction time on consumption. In winter, a higher thermal mass provides a passive way of utilization of external and internal heat gains. Heavy buildings will however require a larger heating power in order to heat up the room within an acceptable time span during a cloudy winter morning. In very light-weight buildings like offices and other utility, cooling and heating demands can occur on the same day during spring or autumn. More thermal mass could be beneficial here. In dwellings or other building typologies that do not allow the heating system to shut down during night, a higher thermal inertia will be even more beneficial (Hensen, et al., 2010).

When passive means are insufficient to reduce or shift the predominant load (heating or cooling), thermo-active building systems could be used. Concrete core activation involves heat exchanger piping integrated in the neutral axis of a floor construction. In contrast to surface-related systems like floor heating or chilled ceilings, concrete core activation utilizes the whole floor construction as thermal storage medium. Concrete core activation limits options for room acoustics improvement and technical flexibility in/on the ceiling (Hausladen, 2004).

3.4.2 Latent TES

Storage duration	medium-long
Energy density	180-300 [MJ m-3]
Cycle efficiency	75-90 [%]
Range of operation	1-3 [K]

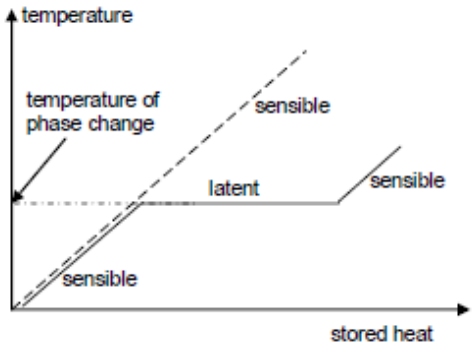

Figure 3-30: Latent heat storage during l/s phase change (Mehling, 2008)

In latent TES, thermal energy is transferred when a substance changes from solid to liquid state. While heat is absorbed during melting or released during solidification, Phase Change Materials (PCM) keep their temperature constant at the melting temperature (or *phase change temperature*).. Because the volume does not change significantly during the phase change (<10%), the energy stored is equal to the enthalpy difference. Upon melting, PCM can have a very high change of enthalpy, thus storing large quantities of heat or cold. Heat required for the phase change is called fusion heat. After phase change, PCM have sensible storage behavior again, as can be seen from Figure 3-30 (Zalba, et al., 2003; Sharma, et al., 2009). For two reasons PCM have potential for short or long term energy storage (Mehling, 2008):

- PCM store and supply large quantities of heat at nearly constant temperature.
- PCM are suited for temperature control since temperature doesn't significantly change during (dis-) charge.

Since the comfortable room temperature range of buildings is limited to approximately 20-24˚C, PCM are considered as the most advanced materials to establish smoothing of temperature fluctuations and load peaks in buildings by increasing its thermal inertia (Hausladen, 2004; Mehling, 2008). Many PCM with suitable phase-change temperatures have been investigated in previous decades, without coming commercial available because their chemical, economical and kinetic performance turned out to be poor (Sharma, et al., 2009; Mehling, 2008).

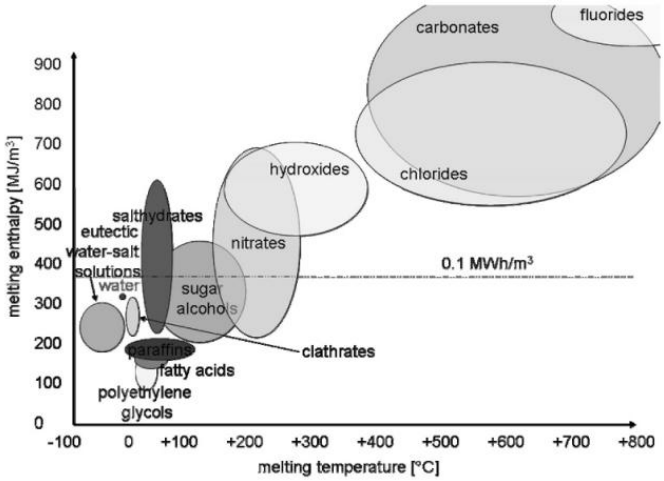

Figure 3-31: Classes of possible PCM and their melting temperatures enthalpy (Cabeza, 2011)

Table 3-1: Comparison PCM (Zalba, et al., 2003)

Organics	**Inorganics**
Advantages	
No corrosives	Greater fusion enthalpy
Low/none undercooling	Rel. good thermal conductivity
Chemical and thermal stability	
Disadvantages	
Lower fusion enthalpy	Undercooling
Low thermal conductivity	Corrosion
Flammability	Phase separation
	Lack thermal stability

Table 3-2: Comparison storage densities

Product	Class	kJ kg-1	Melting T or ΔT in ˚C
Sensible heat			
Water	-	21	ΔT = 5
Concrete	-	5	ΔT = 5
Latent heat of melting (-fusion)			
Water	-	330	0
RT 20	Paraffin	172	22
Climsel C23	Salt hydrate	148	23
Climsel C24	Salt hydrate	108	24
RT 25	Paraffin	131	25
RT 26	Paraffin	232	26
STL 27	Salt hydrate	213	27

Figure 3-31 shows available salt hydrates (inorganics) and paraffin's (organics) with melting temperatures below 100˚C. Main characteristics are described in Table 3-1. In Table 3-2, thermophysical properties of some commercial PCM with melting temperatures within the human comfort range are compared with water and construction materials (after Cabeza 2011). It shows that 35 times more heat can be stored during the phase change of 1 kilogram of RT20 PCM than while heating up 1 kilogram concrete by 5˚C. Below, a short discussion of the main classes of latent heat storage materials will be given:

Cold TES using ice - From Table 3-2 can be seen that its latent heat of fusion is not matched by any other PCM. Producing ice however requires chillers that are inefficient compared to chilled water production or heat pumps, and encounters difficulties (Dincer & Rosen, 2002).

Organic PCM - Organic PCM are discussed most extensively in literature. They are further subdivided into paraffins (alkanes) and non-paraffins. Cycling stability of paraffins is proven. Fatty acids share the advantages of paraffins, but they are more expensive (Sharma, et al., 2009).

Inorganic PCM - Because water-salt solutions consist of two components, they are vulnerable to phase separation which decreases cycle stability. Mixtures and encapsulation are developed to eliminate its disadvantages. The relatively high latent heat of fusion and wide range of different melting temperatures make salt hydrates attractive materials for thermal energy storage (Cabeza, 2011). Salt hydrates are often applied for solar energy storage (higher melting temperatures).

General PCM applications that can be distinguished are: improving building thermal mass (temperature control) or (medium-long term) energy storage with high densities. In the latter, low conductivity values can cause problems because the energy discharge could take too long, while a slow release is an advantage for temperature control (Zalba, et al., 2003).

In utility buildings, PCM improving thermal inertia is of particular interest for heat protection in summer, using melting points between 24 and 26˚C. Active systems using air or water as heat transfer fluid are constructed. The heat transfer fluid is used to control and fasten the charge and discharge of the PCM. The combination of peak load shifting and free cooling could lead up to 50% cooling demand reduction (Zhu & Garett, 2012; Hausladen, 2004).

In residential buildings, PCMs with a melting temperature around 20˚C could damp temperature fluctuations (improving thermal comfort) or divide heat loads over the whole day (lowering the heat demand). A study on passive integration in a single dwelling concluded that a phase change temperature of 1-1,5 ˚C above the rooms setpoint temperature enables maximum energy savings (van der Spoel, 2004). Active systems, e.g. in floor heating systems or inside buffer tanks are also investigated and will be discussed in Chapter 7.1.1. PCM have been often proposed for application in solar domestic hot water systems, where its constant temperature improves collector efficiency.

3.5 Conclusions

In this chapter different energy storage technologies have been classified, that could improve the substitution of fossil fuels by renewable with an intermittent nature. The fossil stock is constantly in a range corresponding to several months of consumption. New technologies will need to meet the same requirements as those of current technologies they substitute. Preferably, their production and utilization should use existing production and conversion processes. In order to illustrate the advantage of fossil fuels over renewable energy storage strategies that are discussed, some energy densities are compared below:

Table 3-3: Energy densities of storage methods

Storage	MJ m-3
Crude oil	38.000
Battery Lead-acid	240
Fuel cell/H2	120
Biogas/syngas	18
SMES	10
CAES (80 bar)	8
PHS (300m)	3

The systematic description showed that there is a wide range of energy storage technologies for different storage needs for different time periods:

Electrical energy storage - EES is urgently needed for intermittent renewable energy supply, and therefore shows a rapid technological development (Beaudin, et al., 2010; Chen, et al., 2009). Technologies that can enhance the reliability and power quality of the grid by storing energy for milliseconds to several hours, are: supercapacitors, SMES flywheels and advanced batteries (NaS, Li-ion). Energy management (load following) by bridging power during several hours, can be provided by batteries (NaS, Li-ion, Me-air) or fuel cells but also PHS and CAES, which all have a fast response and long discharge time over periods of hours. For long term energy storage for weeks or months, PHS, CAES, flow batteries and fuel cells are technically viable. Flow batteries and fuel cells are in far stage of development.

Electricity storage applications range from large scale storage at the generation side and transmission systems, to storage in (mostly off-grid) dwellings. It is also foreseen to play a major role in energy managements in future micro-grids and increased self-consumption of PV electricity in dwellings (IEC, 2010). Using more scarce resources for EES in batteries however, will further impact the availability of certain metals, e.g. for fuel cells (palladium) or Li-ion batteries.

Bio-chemical storage - Secondary fuels such as hydrogen and biogas can store large quantities of electrical or chemical energy with very high densities (Table 3-3). In the case of

hydrogen production, 60-70% of the electricity is lost during conversion to the storage energy form, although the waste heat can be utilized to achieve higher total primary fuel consumption. Overall chain efficiencies of conversion of biomass into power and heat via hydrocarbon secondary fuels e.g. syngas or SNG, are higher. The production of most biomass feedstock occupies a lot of space, so waste or industrial residues form potential alternatives especially for energy supply at local or regional scale. Cleaned bio-gas can be stored and distributed using existing natural gas facilities. Exergy losses and degradation of scarce nutrients are associated disadvantages (Woudstra, 2012). High quality energy demands e.g. transportation fuels and pharmacy might be primary applications of biomass, waste heat could be supply energy for residences (Gommans, 2012).

Thermal energy storage - In contrast to the aforementioned energy storage methods which maintain the high quality of the energy stored (losing energy during conversion though), thermal energy storage involves energy with a low exergetic value. TES is therefore more appropriate for water and space heating and cooling in industrial and domestic buildings. Sensible storage in liquids is most investigated and proven. Its relatively easy realization is a major advantage over electrical storage, and its application can reduce the need for centralized electricity storage (Gommans, 2012). The fact that it is not only used for short term storage for peak shaving, but for seasonal (U)TES of large quantities of renewable and natural energy too, shows its mature state.

Electrical heat pumps are increasingly used to save energy and exploit low-exergy renewables. Because the availability of these resources fluctuates on a daily, weekly and seasonal basis, integration of energy storage for different durations can yield significant savings by storing surplus energy for moments of shortage. This way, despite the intermittent availability, demand can always be met.

A simultaneous development is the growing interest in diurnal thermal energy storage for electrical load management in both new and existing buildings, shifting electrical heating and cooling demands to periods when electricity prices are lower or to periods in which renewable energy is available. In the future smart grid, with electricity prices that vary according to availability, these periods will coincide. The potential of short term storage of heat for load management in residential buildings will be further investigated in this study.

Thermochemical storage is suitable for long term storage only due to its complexity but good cycle stability. Despite many advantages, short term sensible (low temperature) heat storage in water is limited because it needs large volumes in order to achieve adequate capacities. Phase change materials that can absorb and release large quantities of latent heat in a small operating temperature range, allowing more compact short term storage.

4 The exergy approach

4.1 Energy conversion / introduction to the concept

Energy can be stored within systems in various forms. It can also be converted from one form to another form of energy and transferred between systems. This transformation between different energy forms is called conversion. Most relevant energy forms in energy systems in the built environment are defined below (Moran & Shapiro, 2006; Walls, 2009) :

Work

Work done is the work of a force *F* (N) acting over a distance *s* (m), unit Joule:

$$W = Fs \quad (4.1)$$

Work done on an object or *body* can be considered as transfer and storage of energy into that body. It can be stored as kinetic energy (moving object from s1 to s2) or potential energy (moving object vertically from z1 to z2 thus storing gravitational energy). (Moran & Shapiro, 2006) uses the following definition of work:

> *Work is done by a system on its surroundings if the sole effect on everything external to the system could have been the raising of a weight.*

This definition is important for understanding work and exergy. In this example, the work done (force and motion) is clear, in some situations e.g. an electric current from a potential difference across two electrodes of a battery, force and motion are less clear. According to the definition is work though because the effect of the current *could have been* an increase in height of a weight (if the current was supplied to an electric motor).

Heat

Heat *Q* is defined as energy transfer to or from a body (with mass *m* and specific heat capacity *c*) by changing its internal energy *U* and thus its temperature *T*:

$$Q = U_2 - U_1 = mc\,(T_2 - T_1) \quad (4.2)$$

According to the first law of thermodynamics, the total amount of energy is conserved in all conversions and transfers. The first law thus concerns the quantity of energy, calculated by energy balances for a system. Current systems in buildings are designed according to this balance, where quantity energy required should be matched with quantity of energy supplied.

The second law of thermodynamics tells that during a conversion, quality is lost and entropy (disorder) increases. Exergy represents the part of an energy flow which can (still) be completely transformed into any other form of energy. In other words, it represents the potential of a given energy

quantity to perform work: its quality.

Exergy is thus a measure of the *quality* of energy (Moran & Shapiro, 2006):

> *Exergy can be defined as the maximum theoretical work that can be obtained from a quantity of energy or matter by bringing this energy or matter into equilibrium with a reference environment.*

If two objects at temperatures T_1 and T_2 ($T_1>T_2$) are connected, heat will flow spontaneously and irreversibly from object 1 to 2. As T_2 approaches T_1, the rate of heat transfer approaches zero (energy in object 1 is now of little practical interest). This does not mean energy is lost (it is transferred from one system to another), but the second law tells us that quality is lost.

Heat thus can't be completely converted in a high quality energy form. Carnot derived the *Carnot limitation*, which concerns any energy conversion process that involves heat engines. It defines the maximum efficiency that can be obtained from any reversible thermal power cycle that operates between two reservoirs with temperatures T_{hot} and $T_{cold,}$ in degrees Kelvin, see Figure 4-1. Heat Q_H is transferred from the hot reservoir to the system, but not all heat can be converted into work since from the second law is known, a certain amount is rejected to the cold reservoir. The maximum efficiency that can be obtained is called the Carnot efficiency:

$$\eta_{max} = \frac{T_H - T_C}{T_H} = 1 - \frac{T_C}{T_H} \qquad 4.3$$

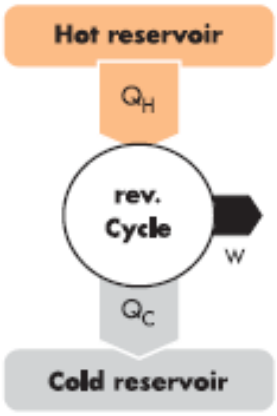

Figure 4-1: A reversible thermal power cyle (e.g. Carnot)

In real (irreversible) cycles, the efficiency will always be lower than Carnot, typically a factor 0,5 because of friction and other losses within the cycle (Woudstra, 2012).

The work obtained from this cycle for a given Q_H and given temperatures is (derived from the first and second law of thermodynamics):

$$W = Q_H \cdot \eta_{max} = Q_H \cdot \left(1 - \frac{T_C}{T_H}\right) \quad 4.4$$

Below, some definitions will be given.

4.2 Important definitions

Reference environment

The reference environment can be described as the surroundings of a system, which can act as an unlimited sink or source. A reference environment:

- is unlimited (source or sink)
- is unchanged by the processes regarded in the system
- is always available

Usually, the ambient air surrounding the building is considered as reference environment. The calculation of the exergy of heat transfer is based on cycle in Figure 4-1 and equations 4.3 and 4.4, but assumes the environment (T_0) to be one of the reservoirs.

General equation of exergy of heat

For both $T>T_0$ (where T is the hot reservoir T_H) and $T<T_0$ (T is T_C), the exergy of heat transfer is calculated by:

$$dEx = dQ_{rev} \left(1 - \frac{T_0}{T}\right) \quad 4.5$$

In the case of $T<T_0$, dQ_{rev} refers to the heat rejected to the cold source and is therefore a negative value.

Exergy factor (also called quality factor)

Substitution of T_0 in equation 3.3 gives the exergy factor of heat:

$$f_{ex} = \frac{Ex_Q}{Q} = 1 - \frac{T_0}{T} \quad 4.6$$

The exergy factor is defined as the exergy content of a system divided by the energy content, or Ex_Q/Q. Temperature T is the temperature of the hot source. Depending on the subject of the exergy calculation, this could be the condenser temperature, supply water temperature, room temperature etc.

4.3 Difference energy and exergy analysis

The essence awareness is that some forms of energy do have a higher quality than other forms of energy. Chemical energy like in fossil fuels (e.g. gas) and electrical energy do have an exergy factor of 1, since in theory they can completely be converted into every other energy form e.g. heat. The other way around, converting heat to electrical energy is difficult and accompanied with large losses (i.e. in quantity and quality). In conversions that do not involve temperature changes (isothermal), the Carnot limitation is not applicable does not determine the maximum efficiencies that can be achieved. Exergy destruction takes place in all conversion processes, and is often not deducible from thermal efficiencies that are commonly used to indicate the performance of a process (Woudstra, 2012).

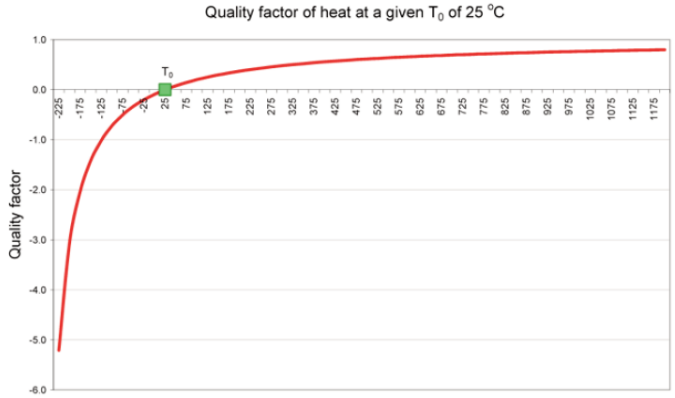

Figure 4-2: Exergy factor as a function of the system temperature divided by reference temperature (25C)

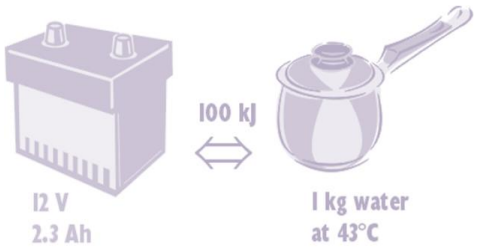

Figure 4-3: Similar quantity, different quality (Ala-Juusela, 2004)

The relevance of a combination between energy and exergy in appreciating quality is illustrated by the example in Figure 4-3. 100 kJ electrical energy stored in a 12V/2.3Ah car-battery is easier to transform into something useful for us, than the same amount of energy stored in 1 kg water of 43°C in an ambient temperature of 20 °C, which is only useful for cleaning dishes. It illustrates the definitions of work and exergy, as stated before. By using exergy analysis, the quality of energy can be quantified.

4.4 Application of exergy in buildings

Currently, all assessments of energy use in buildings are based on quantitative analysis, which could overlook quality destruction. Gas fuelled hot water boilers can have thermal efficiencies of 95%, but there exergy performance is around 10%. Exergy analysis can help designers to choose more efficient energy supply systems (Torio & Schmidt, 2011). Important outcomes using exergy analysis in short:

- more efficient use of fossil fuels (e.g. by avoiding “high efficient” boilers).
- more efficient use of renewables with high thermodynamic potential.
- highlights importance of using low temperature renewable resources available to supply heat demands in buildings.

- low quality, exergy efficient emission systems allow integration of these renewables.

The application of the exergy concept for evaluation of energy conversion systems does include exergy destruction, which indicates the ideal thermodynamic potential of a process (Jansen, et al., 2010). It also provides means for evaluating quantitatively the factors that should be improved to obtain the best theoretical performance (Moran & Shapiro, 2006).

4.5 Low exergy systems in buildings

Since high quality energy such as chemical energy (gas) or electrical energy consist of pure exergy, they should be only used for purposes that require this level of energy quality such as appliances, cooking or lighting. Domestic hot water of 55˚C has a lower quality demand, but it is currently often met with electrical boilers or gas-fuelled combi-boilers, which use high-quality energy input. The same generators are used for space heating and cooling. Space heating and cooling require near ambient temperature water or air, which thus has a very low exergy or potential to be converted for another purpose. Generating this demand by use of high quality energy input involves large quality destruction, although from an energetic perspective nothing seems wrong (e.g. HR-107boilers).

Emission systems for low-temperature heating (or high-temperature cooling) that become the standard in contemporary low energy houses, could be supplied with low exergy resources (Jansen, et al., 2010). Low temperature renewables are abundantly available, e.g. energy contained by solar radiation or ambient air. Adaption demand and supply in terms of quality levels is therefore very relevant (see Figure 4-4), and forms the design guideline in development of the energy system used in this study.

Although a comparison of the improvement of a system that takes into account exergy with conventional energy generators would be interesting, this is not possible within the scope of this graduation. Comparisons of different energy systems using detailed exergy calculations are already available, and show good performance for heat pump systems ((Jansen, et al., 2010; Woudstra, 2012).

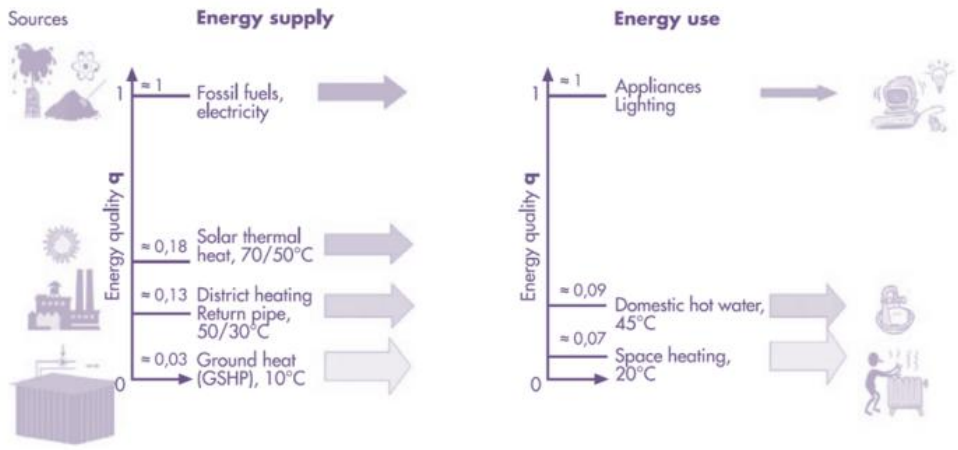

Figure 4-4: Sources and domestic uses of energy with similar quality levels (Torio, 2011)

5 Space heating in dwellings

Considering the associated temperatures, the space heating demand in dwellings can be matched with low quality resources. Heat pumps can deliver this demand by upgrading low-grade heat using a small amount of high quality energy.

5.1 Heat pumps

Heat pumps move thermal energy from a lower to higher temperature medium, in a way similar to (reversed) refrigerators. It consists from a compressor, condenser, expansion valve and evaporator:

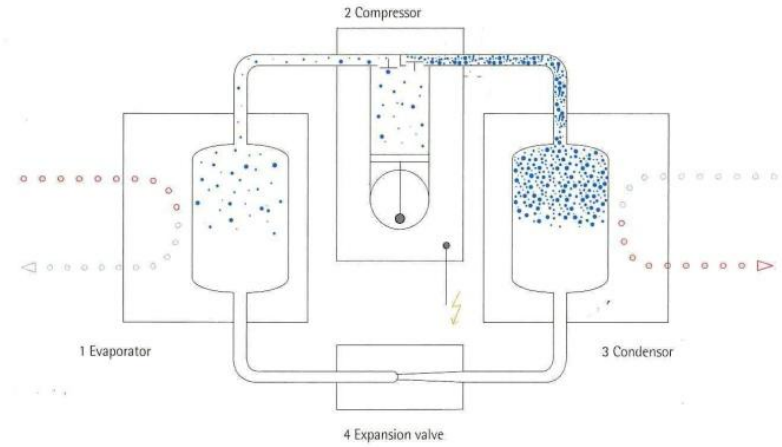

Figure 5-1: Schematic functioning of a heat pump (Hausladen, 2008)

In a Carnot cycle, the system executing the cycle undergoes four reversible processes: two adiabatic, two isothermal. The reversible refrigeration (heat pump cycle) works as follows (see the steps in the figure above):

1: gas expands isothermally (evaporation) at TC while receiving energy QC from the cold reservoir by a heat exchanger.

2: gas is compressed adiabatically until its temperature reaches TH. This process requires compressor electricity (work).

3: gas is compressed isothermally (condensation) at TH while energy QH is exchanged to the hot reservoir.

4: gas expands adiabatically (pressure drop produced by expansion valve) until its temperature is decreased to TC.

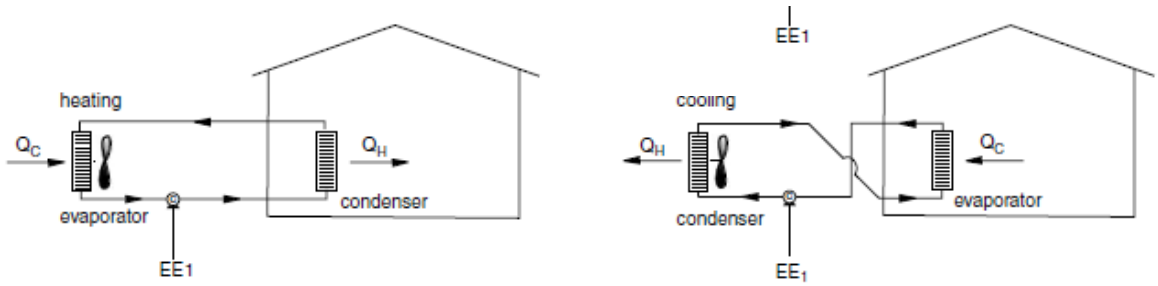

Figure 5-2: Heat pump heating and cooling mode (Farret, 2006)

In heating mode, the useful heat that can be delivered to the room is the sum of heat transferred to the outdoor unit from the surroundings/cold source Q_C and electrical energy required by the compressor EE_1 for operation:

$$Q_H = Q_C + EE_1 \quad 5.1$$

The ratio between the useful energy output to the energy input is presented by the Coefficient of Performance, COP. The COP of an electrical heat pump in heating mode is derived as follows (Farret, 2006):

$$COP_H = \frac{Q_H}{EE_1} \quad 5.2$$

Where,

Q_H = Energy output condenser, kWh_{th}

EE_1 = Energy input compressor, kWh_{el}

The process can be reversed (refrigerator cycle) in order for the machine to work as a cooling machine, following step 3-4-1-2 in Figure 5-1. According to equation 5.1, cooling mode:

$$COP_C = \frac{Q_C}{EE_1} \quad 5.3$$

Where,

Q_C = Energy output evaporator, kWh_{th}

EE_1 = Energy input compressor, kWh_{el}

While the Carnot efficiency concerns the amount of work (electrical input) required per unit heat transfer (equation 4.3 and 4.4), the COP represents the inverse: the heat transfer obtained per unit of work performed by the compressor. Substitution of the Carnot efficiency in equation 5.2 gives:

$$COP_H = \frac{Q_H}{W} = \frac{T_H}{T_H - T_C} \quad 5.4$$

Where,

T_H = Absolute temperature hot source, K

T_C = Absolute temperature cold source, K

In order to determine the actual performance of a system over a complete heating/cooling season, the seasonal performance factor (SPF) is introduced. This is the total electrical energy input that is necessary to produce an amount of useful energy output (ISSO 744, 2009):

$$SPF = \frac{Q_{useful}}{Q_{necessary}} \quad 5.5$$

Where,

Q_{useful} = total useful energy output, MWh_{th}

$Q_{necessary}$ = total energy necessary for the internal and external circuit, MWh_{el}

5.2 Applications of domestic heat pumps

Four modes of implementation of heat pumps in domestic energy systems can be distinguished (ISSO 744, 2009). Which operation mode is most appropriate depends on spatial conditions and the chosen heat source of the heat pump.

Monovalent operation - The heat pump generates the total domestic heat demand. This operation mode is most common for heat pumps with water as a heat source, combined with a storage tank in order to reduce on-off frequency of the heat pump.

Mono-energetic operation (also called bivalent-parallel) - In mono-energetic application, the heat pump is able to generate the average heat demand, which suffices for the major part of the year. An auxiliary electrical heater provides additional heating power during extremely cold occasions. The heat pump and auxiliary heating are operative simultaneously. Air-source heat pumps are often part of a mono-energetic system because of the efficiency drop at low ambient temperatures.

Bivalent operation - In case a conventional generation system, such as gas fuelled boiler, provides auxiliary heating during peak heat demands, one speaks of a bivalent system. In bivalent-alternative systems, the generators only operate alternately. In bivalent semiparallel configuration the generators can work alternately and simultaneously. The heat pump provides the required heating energy down to a defined minimum outside temperature, after which the auxiliary system provides the total energy demand.

For well insulated buildings with small average transmission losses and -heat demands, monovalent or mono-energetic operations are sufficient. Since the case study used in this thesis, meets contemporary insulation standards and contains energy storage, a monovalent heat pump will be investigated.

Because the heat pump needs to cover the heat losses of the dwelling in all situations, its heating power should equal the heat demand at -10 C outside temperature.

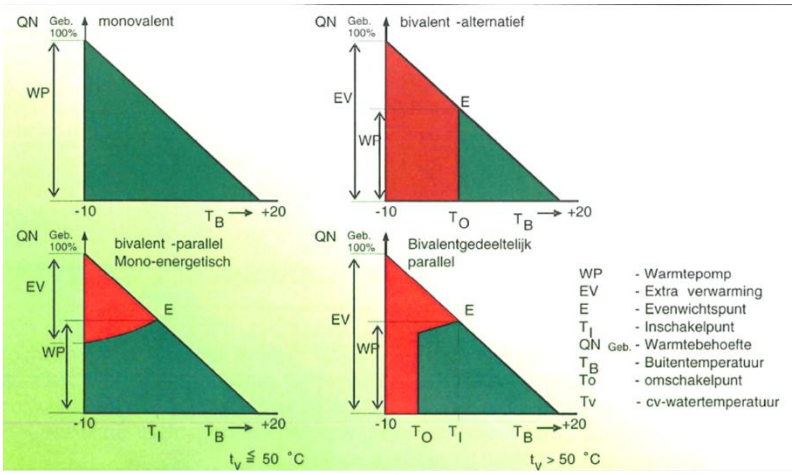

Figure 5-3: Different operation modes for heat pumps (ISSO 744)

5.3 Available heat sources and their characteristics

Despite the cold sensation, a heat source of -10˚C still contains heat. When the temperature of a source is above the absolute minimum (-273,15˚C), heat can be extracted from it. Possible heat sources could be the ground (using horizontal or vertical heat exchangers, or groundwater using ATES), solar, water (surface water or waste water) or air. Characteristics of these heat sources are extensively described in literature (e.g. (Forsen, 2005; Pardo, et al., 2010). The smaller the temperature difference between the heat source and the internal circuit (air or water), the better the COP is.

Although air-source heat pumps can also have exhaust air as heat source, this study investigates ambient air as heat source. Outside air is an easily accessible potential renewable energy resource. The fact that air is subject to large daily and seasonal fluctuations highly influences the COP. Overall COP are still improving, mainly because of advances in components and better overall system integration. Typical efficiencies (SPF) for heat pumps with ground as heat source are higher than for air source heat pumps (see Figure 5-4). This is because the ground is affected in a smaller degree by ambient temperature fluctuations. In order to exploit the ground as heat source, systems of exchanger pipes or boreholes need to be installed, which is increases its installation costs (ca. twice the costs for ASHPs, (Forsen, 2005)).

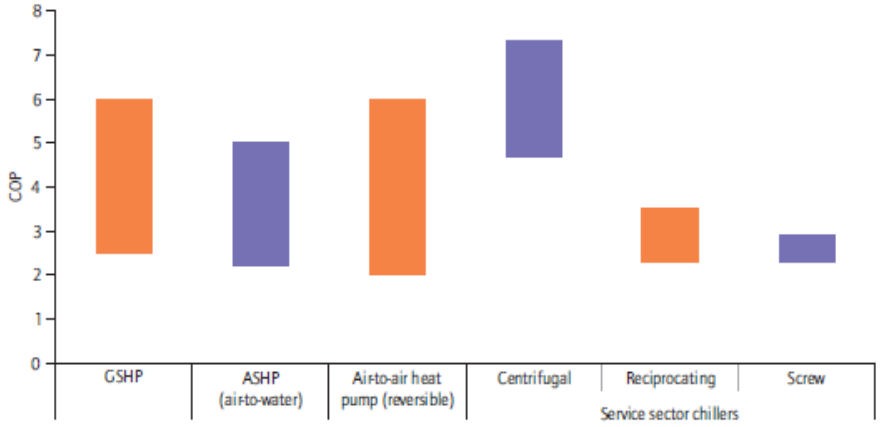

Figure 5-4: Efficiency ranges of different heat pumps (IEA-HPP, 2011)

An air to water heat pump can extract heat from the environment down to temperatures of -25˚C. Typical installed capacities in single family dwellings in Europe are 2-15 kW_{th} (IEA, 2011). Field tests of the SPF of 23 combi air-source heat pumps installed in German houses in 2008 and 2009 have been performed by the IEA (IEA, 2011). Maximum performance factors occurred in transitional seasons, as can be expected. The average two-year SPF is 2,8. Almost all heat pumps were equipped with auxiliary electrical heaters, (6% back-up energy fraction over two years). Average space inlet temperatures were 36,9˚C. Field tests for ground-source heat pumps concluded an average SPF of 4,0.

5.3.1.1 Air-source heat pump types

Air-source heat pumps can be installed in different configurations, since the condenser and evaporator can be separated. All components can be combined in one unit that is situated inside or outside the building, but a dual (or split) configuration is also possible. In this configuration, the condenser is inside the building, whereas the compressor and evaporator are situated in an exterior unit. The refrigerant transfers the generated energy between both components. This solution can be selected when interior space is limited.

Almost all air-to-water heat pump suppliers offer their system for space heating and domestic hot water preparation, so called combi heat pumps. Most heat pumps (e.g. using refrigerants R290 or R410A) can produce exiting water temperatures up to 55℃, although this deteriorates the compressors lifetime and is accompanied with low efficiencies. Selection of another refrigerant that performs better at higher water temperatures is an option, but will again reduce the efficiency at production of relatively low water temperatures. According to Krevel, DHW production with a heat pump is only economically interesting when accompanied with COP above 2,2. A heat pump combined with an auxiliary heater to heat up the last 5-10℃ to 60℃, will not achieve this COP (Krevel, 2001). This thesis will not include such hybrid applications of the heat pump, but focuses on its optimal working range, i.e. for generation of low temperatures or low quality heat.

Alternatives for domestic hot water preparation are air-to-water heatpumpboilers, solar thermal or electrical boilers, the latter is associated with low COP's as well.

5.4 Heat pump systems in residential buildings

5.4.1 Hydraulic circuits

The application of a heat pump requires a system design that is quite different from conventional generation systems. Whereas the installed power of conventional systems (e.g. gas boilers) is large, the heating power of heat pumps is limited by the power of the electrical connection and is dimensioned to meet the critical instantaneous heat demand.

This means that a proper alignment of the emission system to the heat pump becomes crucial. When not properly aligned, the power of the heat pump in practice could turn out to be too small in case of unexpected high transmission losses because of construction defects or in case of an under-dimensioned emission system. Since heat pumps do perform better at lower water temperatures, a certain under-capacity leads to discomfort faster (since design water temperatures are close to minimal required room temperatures by comfort regulations) (ISSO 744, 2009; ISSO 72, 2013).

The following design rules can be adopted in order to ensure energy systems wherein the heat pump performs at its optimum efficiency (Traversari & Oostendorp, 2000; ISSO 744, 2009; Krevel, 2000):

Minimize supply water temperatures – From equation 5.4 follows that the COP is better at small differences between the temperature of the heat source and the required supply water temperature ($T_{hot\ source}$ in this case is the condensation temperature, $T_{cold\ source}$ the temperature at the evaporator). Lower supply and retour temperatures of the emission system will thus lead to a better performance of the heat pump. This makes emission systems that require low temperatures, e.g. floor heating or convectors, preferable over high temperature emission systems such as radiators.

Ensure a minimum flow rate through the condenser - Low flow rates can occur when more and more heating groups are closed because the rooms are comfortable, increasing the resistance of the system. A minimum flow rate over the condenser is required for a good heat transfer from the internal circuit (refrigerant) to the external circuit containing the space heating water. Bad heat transfer can lead to overheating within the condenser causing the heat pump to enter an error mode because of high- or low pressure in the internal circuit.

Reduce on-off cycling of the heat pump - Frequent on-off cycling of the heat pump can occur in case the retour water temperature rises too fast. This is the case in heating groups with a small water content, thus having a small buffering capacity. Changes in heat demand require a fast response of the heat pump. Turning the heat pump on and off reduces the compressors lifetime and the energy efficiency, since it takes a while before a heat pump operates on the maximum COP after it is switched on. In a simple version, heat pumps contain one single speed compressor which can only be switched on and off. Heating capacity of the heat pump can't be adjusted to the demand, so the heat pump simply has to turn off when the demand is met. By using two or more compressors in parallel,

the generation capacity can be adapted to the demand in steps, which reduces the number of on-off cycles. This solution becomes economical in collective or large systems.

In inverter driven heat pumps, the frequency of the compressor can be controlled (see Figure 5-5). In part load situations, the generated energy as well as consumed electricity is reduced by decreasing the compressor frequency. At a lower frequency, the heat pump is able to work with a smaller temperature difference between condenser and evaporator (thus a lower condenser temperature) which enables a good COP during part load operation and a reduction of on-off cycles because the same quantity of heat is generated during a longer period.

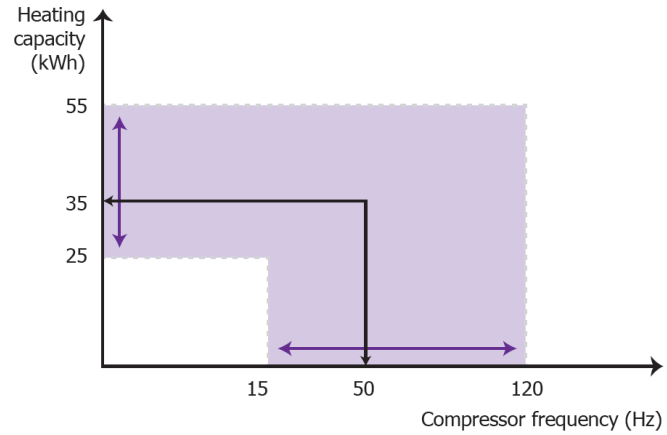

Figure 5-5: Frequency control and heating output heat pump

An alternative way to maintain the number of on-off cycles low, is by increasing the energy system's inertia by the application of heat buffering. This is the driving factor in the design of hydraulic systems in residential buildings because sufficient buffer capacity in the emission system does prevent (too) many on-off cycles and too low flow rates through the condenser. Krevel distinguishes the following possible measures for increasing the inertia of an energy system (Krevel, 2000):

A. Bypass with safety valve (Figure 5-6)

This (conventional) solution always ensures the minimum flow rate over the condenser: even while all heating groups are closed, the bypass duct guarantees the required flow. Besides the energy that is lost by doing this, this circuit won't reduce the on-off cycles of the heat pump. In case all groups are closed, the bypass circuit however, doesn't contain sufficient buffer capacity which will make the retour water to heat up fast.

B. One open heating group (Figure 5-7)

This is the most economical and simple solution, still performing good. By alternately opening one of the heating groups, the minimal flow can be ensured and the heat pump can operate for longer periods. For this system to work properly, the groups should be large enough (containing sufficient quantities of water) so they will not be heated up too fast.

A disadvantage of system B is that rooms will be heated regardless the need/demand for heating, simply because the heat pump has not reached its minimum operation duration yet.

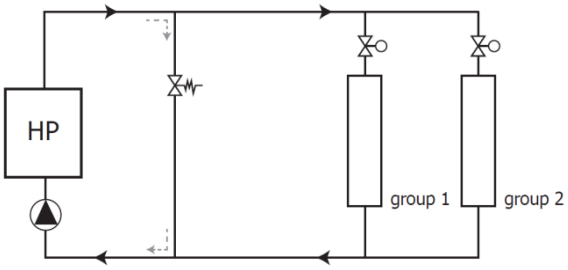

Figure 5-6: A. Bypass with safety valve (HP = Heat Pump)

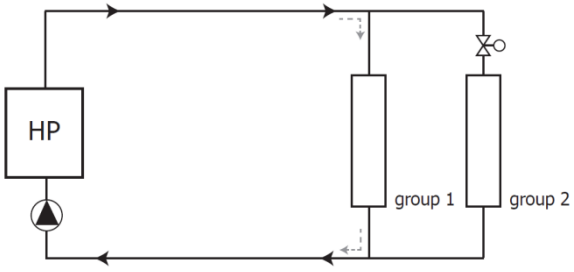

Figure 5-7: B. One open heating group

C. Open manifold (Figure 5-8)

An open manifold (in Dutch: *open verdeler*) hydraulically decouples the generation circuit and the emission circuit. The generation circuit is called primary circuit, the heating groups are called secondary circuit. Both circuits require a circulation pump, in the secondary circuit a frequency controlled pump is common, because these pumps can adjust the flow rate in order to maintain a constant pressure difference over the heating groups. Per circuit, a minimum flow rate is required. Preferably the flow rates are equal. This system does not solve the problem of too little buffer capacity, except when combined with system B.

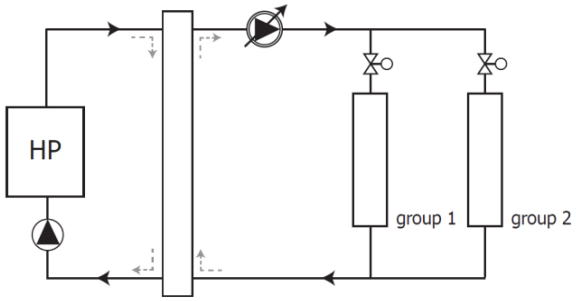

Figure 5-8: C. Open manifold

D. Serial buffer (Figure 5-9)

This solution increases the water content and thus the buffer capacity of the circuit, so it takes longer before the retour water temperature drops too low (reducing on-off cycles). When all heating groups are closed except for one, a minimal flow rate is still guaranteed. Preferably the buffer is placed in the retour of the circuit. When applied on the supply side, the temperature of the water supply to the heating groups would rise too slow. This configuration has the same characteristics as system B, but with a larger buffer capacity. A serial buffer increases the reaction time of the system to changes in heat demand of the groups.

E. Parallel buffer (Figure 5-10)

This solution is more expensive and requires more floor space, but is ideal. Parallel buffers can fulfill the following functions (Traversari & Oostendorp, 2000):

- decouple the primary and secondary circuits (providing more control over the groups);
- smooth operation of heat pump (less temperature fluctuations, less on-off cycles because of large buffer capacity);
- storage of heat over a certain period (in order to profit from energetic or financial favorable circumstances).

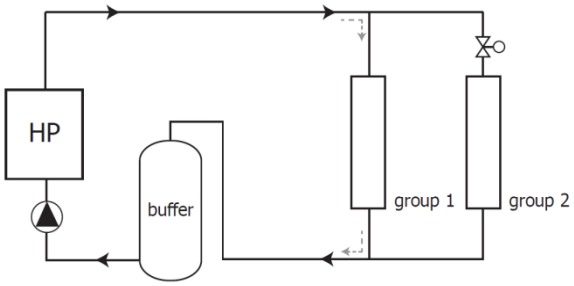

Figure 5-9: D. Serial buffer tank

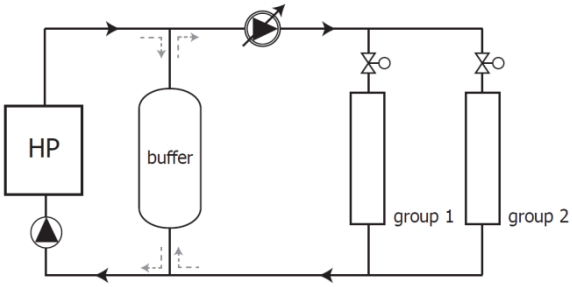

Figure 5-10: E. Parallel buffer

Energy buffers will not only provide more control over the heating groups individually, but it also offers possibilities for load management; generate energy at moments when renewable energy is available. Therefore, hydraulic circuit E will be further investigated.

5.4.2 Combination heat pumps and short term TES

The literature review concluded that thermal energy could improve system efficiency because it helps to avoid partial load operation and operation at suboptimal times from an energy quality (and COP) point of view. This is especially the case with air-source heat pumps. Although their performance is good during transitional seasons with outdoor temperatures close to the room temperature, improvement can be made during winter e.g. by the addition of an energy sink (Candanedo & Athienitis, 2011).

When combined to on-site electricity generation, storage is needed to hold the energy so it can coincide with demands. If the end-use energy form is thermal (heat or cold), it is better (i.e. easier and associated with smaller conversion losses) to store thermal energy for a short term instead of storing electrical energy and converting the electrical energy to heat on demand (Mehling, 2008). Operation of the heat pump during moments with surplus electricity generation will lead to cost reductions.

5.5 Case study

Dwellings provide a more interesting case study for storage systems than utility buildings, because most investigations on (latent) heat storage focuses on cooling purposes in offices, where a larger number of charge-discharge cycles need to be performed at a regular pattern. Dwellings however, are user controlled, meaning that occupancy changes and storage (dis)charge cycles will not necessarily be regular or daily. One of the main goals of this study is to see how this influences the performance of short term storage. By variation of internal gains, (dis)charge strategies and storage media, the interesting case study that residential buildings offer, will be exploited.

5.5.1 Geometrical characteristics

The case study of this research is a reference dwelling, as described by SenterNovem[1]. A terraced house (called "tussenwoning") comprising 124,3m^2 was used in the simulation model. This single family dwelling type represents 50 percent of the Dutch building stock. As can be seen in the figures below, the dwelling consists of two floors and an attic and has a north-south orientation.

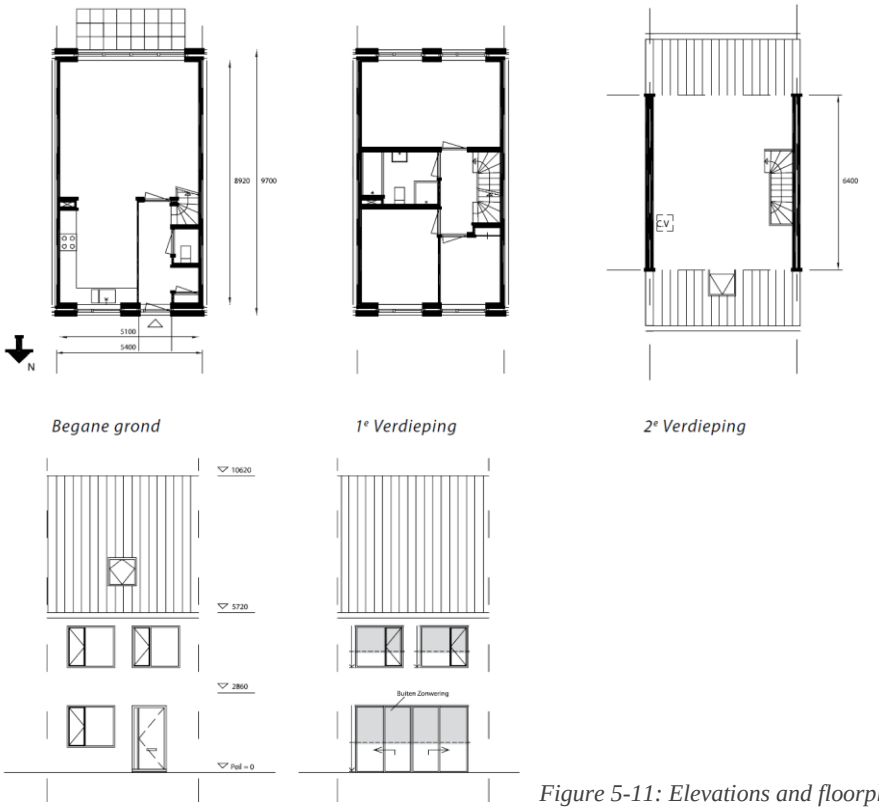

Figure 5-11: Elevations and floorplans of reference dwelling

5.5.2 Setpoint temperatures

In accordance with NEN 7120[2], the heating setpoint temperature is 20 ºC throughout the whole day. The cooling setpoint is chosen two degrees higher than NEN's guideline: 26 ºC.

[1] Referentiewoningen nieuwbouw, Senternovem 2006

[2] NEN 7120 Energieprestatie van gebouwen

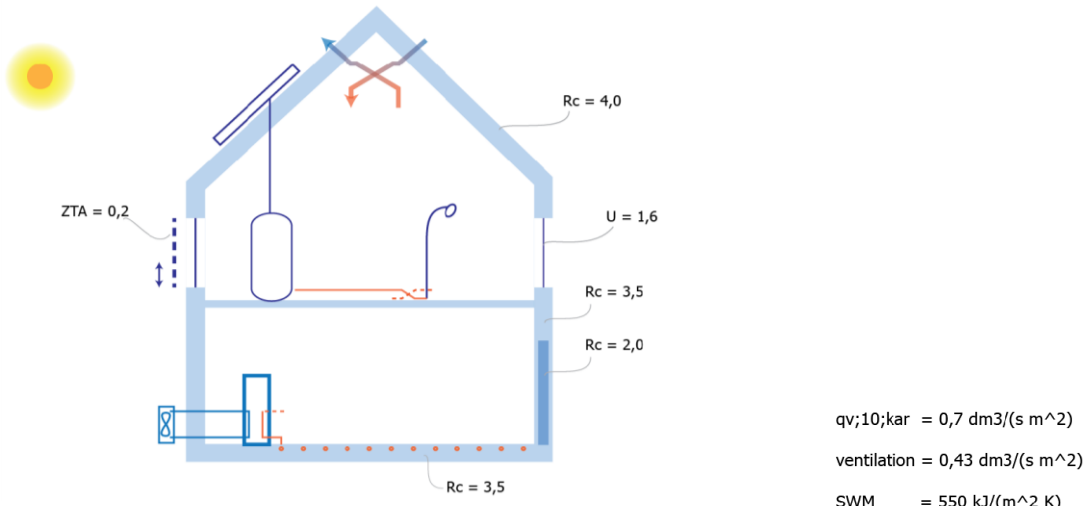

Figure 5-12: Main characteristics of the case study dwelling

Contemporary building standards do require an EPC (Energy Performance Coefficient) of 0.6. The modeled construction was defined in such a way, that this requirement would be met (in accordance with Agentschap NL[3]): Dwellings according to these standards do have an annual heat demand of 20-25 kWh m^{-2} [4]. Appendix B contains detailed information on geometrical and construction data of the case study and typical ventilation and infiltration rates, used for the MATLAB and TRNSYS models.

5.5.3 Internal gains

In accordance with NEN-ISO 13790[5], different internal heat load profiles have been assumed:

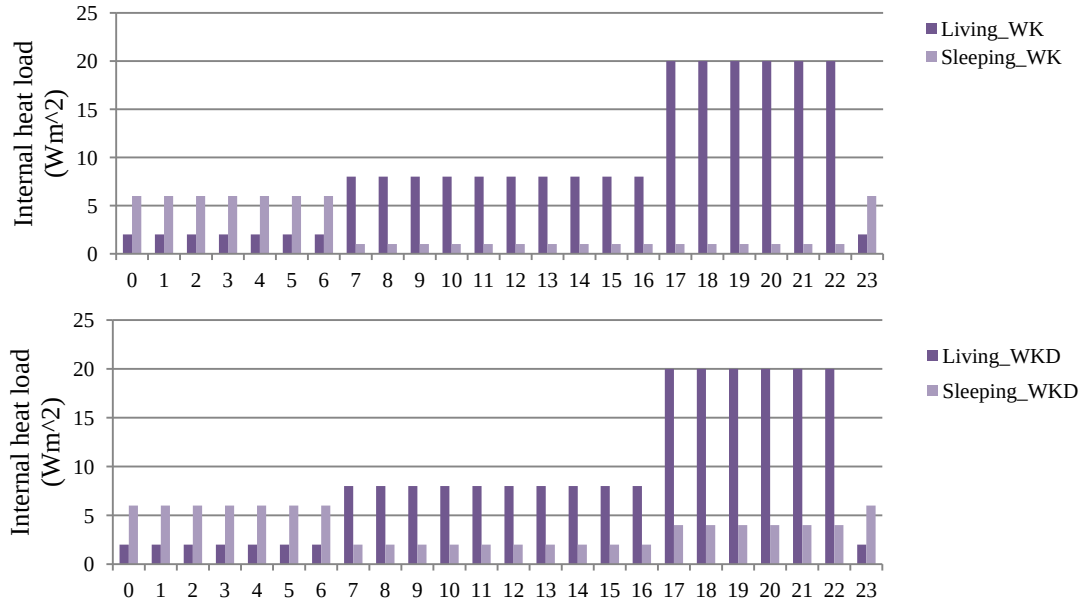

Figure 5-13: Daily profiles of internal gains per zone (occupation and appliances), weekdays (top) and weekends (bottom)

[3] Agentschap NL Referentiewoningen EPC<0,6, 2012

[4] ECN 2010 Referentieraming energie en emissies 2010-2020 Gebouwde Omgeving

[5] NEN-ISO 13790 Energy performance of buildings

5.5.4 Hydraulic circuit / Building services

5.5.4.1 Selected heat pump

The combination of a single speed compressor heat pump with a parallel buffer (circuit E, discussed in subsection 5.4.1) will maintain all benefits of the circuit, because of the decoupled primary and secondary circuit. The application of a buffer will ensure the same effects as a heat pump with an inverter driven compressor (generation can be adapted to the demand, smooth heat pump operation). More buffer content allows for a smaller installed heat pump power, because peaks in instantaneous heat demand can be met with energy from the buffer.

Additional installation area required for a buffer forms a disadvantage in the Dutch residential stock where floor area is expensive. This is the reason for a growing market in (small) inverter driven heat pumps. Still, this thesis will focus on a single-stage heat pump with a buffer because the potential for electrical load management will be explored. Besides, alternative storage mediums e.g. PCM provide the possibility to reduce buffer volumes. The heat pump selected for simulation is the smallest air-to-water heat pump on the market. Performance curves are added in Appendix D – Heat pump data.

5.5.4.2 Emission system

Since low water temperatures at the condenser of a heat pump significantly improve their performance, a low temperature emission system is preferable. A floor heating system with supply temperatures between 25 and 35 ˚C is used in the detailed simulations, and will be discussed later.

5.5.4.3 Water temperature control

The water temperature required from the heat pump, can be defined and controlled via two methods (Traversari & Oostendorp, 2000), as can be seen in the control schematics in Figure 5-14.

Climate curve (stooklijn) - Control on supply temperature, no feedback from room temperature (see Figure 5-14). A climate curve can be seen as a pre-control. It only controls the supply water temperature and therefore disturbances in the system (like internal gains) are not taken into account. Post-control (e.g. by manual- or thermostat controlled valves in the rooms) is required.

Room thermostat - Direct feedback of the room temperature to the energy generator.

In this research, a climate curve is used because it reduces the supply water temperature as soon as outside temperatures rise. As we saw, lower supply temperatures improve the heat pump performance.

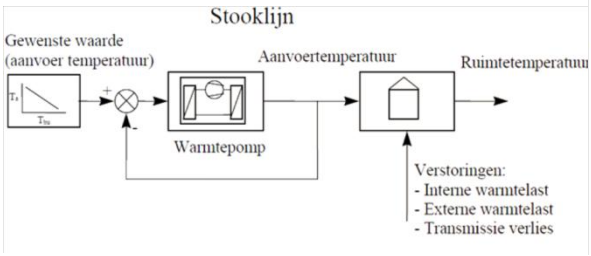

Figure 5-14: Water temperature control: climate curve

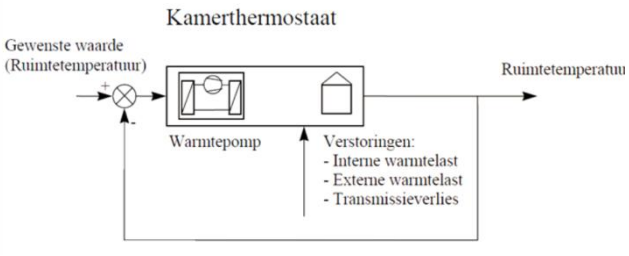

.. and room thermostat (Traversari and Oostendorp, 2000)

6 Exergetic optimization strategies

6.1 MATLAB model

In order to get a quick insight in the course of the heat demand and conditions for energy generation throughout the day, a numerical MATLAB model was constructed. No interpolation is used and the time step of the model is one hour since the weather data used is given per hour.. Time step 1 regards the interval between the entire previous hour (t-1) and the current hour (t), conform standards in (ISSO 32, 2011). In order for the model to have similar conditions as the dynamic simulation in TRNSYS, data (dry bulb temperature, solar radiation, internal gains) from the TRNSYS 17 weather file was used. Below, the most important formulas, definitions and assumptions used in the MATLAB model are discussed.

The instantaneous heat demand is calculated from a simplified linear energy balance of the dwelling. Changes in parameters (like internal heat gains or transmission) do not have an immediate effect on the instantaneous heat demand, but are damped or delayed by the buildings thermal mass (Hausladen & Liedl, 2012; Hensen, et al., 2010). Tent structures do have a damping factor of 1, the factor of extremely heavy buildings goes down to zero. In order to take the effect of thermal mass into account, a conservative damping factor of 0,8 has been applied. The net instantaneous heat demand, P_{dem}, is calculated according to equation 6.1:

$$P_{dem} = P_{trans} + P_{vent} + P_{inf} + P_{sol} + P_{int} \quad [W] \qquad 6.1$$

Where,

P_{trans} = transmission losses through envelope [W]

$$P_{trans} = q_{envelope} * dT$$

where,

$q_{envelope}$ = heat transfer through envelope [W/K] (entry: 78,17 W/K, see Appendix B – Properties of Case study dwelling)

dT = temperature difference $T_{in} - T_{out}$ [K]

P_{vent} = central ventilation losses to heat up air till 20 ˚C, after heat recovery [W]

$$P_{vent} = q_{vent} * c_{air} * dT$$

where,

q_{vent} = ventilation flow rate [kg/s]

c_{air} = specific heat air [kJ/kgK]

dT = temperature difference $T_{in} - T_{after\ heat\ recovery}$ [K]

P_{inf} = infiltration losses [W]

$$P_{inf} = q_{inf} * c_{air} * dT$$

where,

q_{inf} = infiltration flow rate [kg/s]

c_{air} = specific heat air [kJ/kgK]

dT = temperature difference $T_{in} - T_{out}$ [K]

P_{sol} = heat gains by solar radiation [W] (negative entry)

data for P_{sol} is imported from TRNSYS (output SQSOLT: sum of shortwave solar radiation transmitted through windows of all airnodes (not kept 100 % in airnode))

P_{int} = internal heat gains [W] (negative entry)

input for P_{int} is described in paragraph 11.3 Heat gains.

The hourly space heating energy demand, E_{dem_hourly} , is derived by:

$$E_{dem-hourly} = P_{dem} * 3{,}6 \quad [kJ] \qquad 6.2$$

The following assumptions made in the model for the sake of simplification:

- the model is non-continuous, uses a 1-hour time step;
- steady room temperature of 20 ˚C, small effect of the buildings time constant;
- when gains are larger than losses, the heat demand is zero;
- only space heating demand is considered, domestic hot water preparation is not part of this exploration.

Figure 6-1 on the next page, shows the monthly energy balance of the dwelling, resulting from MATLAB, containing all parameters of equation 6.1. The graph shows that transmission losses are the main source for the heat demand. Ventilation losses are marginal due to efficient heat recovery. Solar gains are higher during summer, the peaks are prevented by sunshading. The occurrence of a heat demand during summer is an effect of the simplifications in the model (no dynamic calculation involving room temperature and thermal mass). Because of this, heating and cooling demands can occur on the same day.

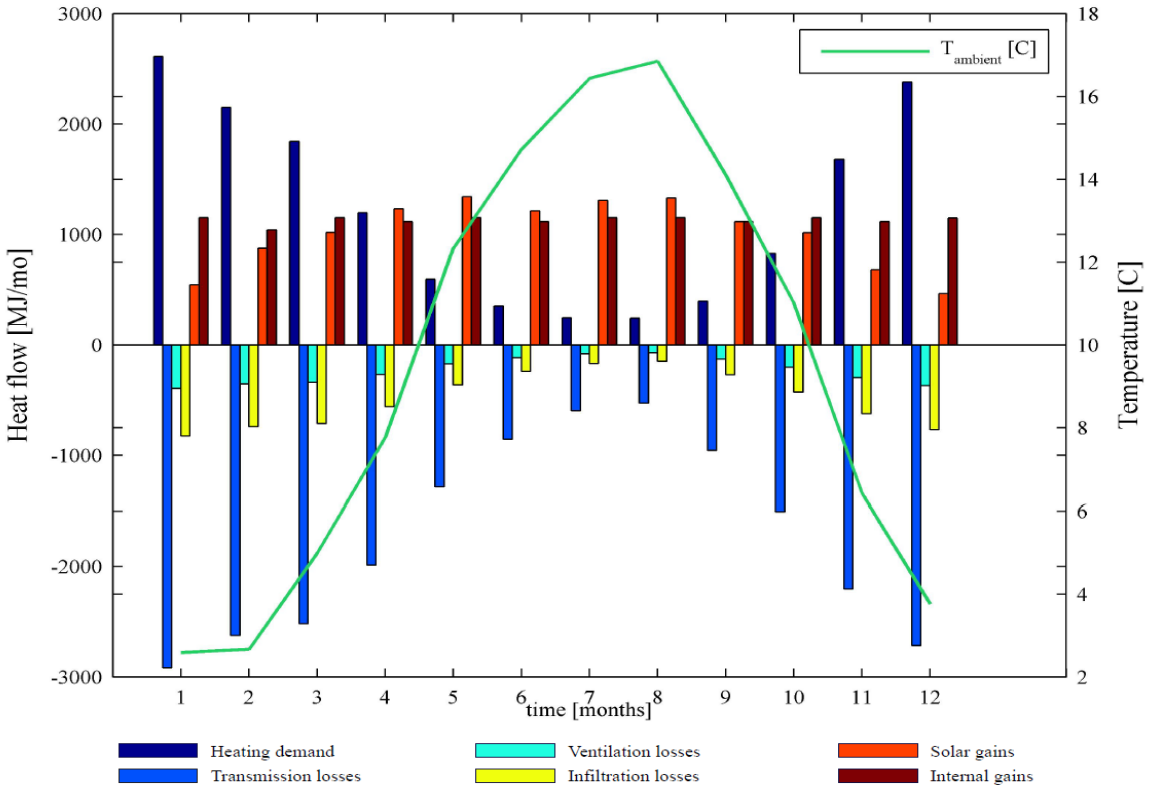

Figure 6-1: Parameters in monthly energy balance of the dwelling

The heating power for energy generation (by the heat pump) is derived from the COP_{CARNOT} from equation 5.4 via two formulas. First, a realistic COP is calculated using the condensation temperature for $T_{hot\ source}$, and the temperature at the evaporator for $T_{cold\ source}$:

$$COP_{real} = \eta_{compressor} * \frac{T_{co}}{T_{co} - T_{ev}} \qquad 6.3$$

Where,

$\eta_{compressor}$ = compressor efficiency [-] (typical 0,4-0,6. 0,5 is used)

T_{co} = temperature internal circuit condenser [K] = $T_{entering\ water}$ – 10 K

$T_{entering\ water}$ required follows from a climate curve;

T_{ev} = temperature internal circuit evaporator [K] = $T_{ambientair}$ – 10 K

Subsequently, the heating power for energy generation P_{gen} can be calculated:

$$P_{gen} = P_{el} * COP_{real} \quad [W] \qquad 6.4$$

Where,

P_{el} = electrical power consumed by heat pump [W] (default: 1 kW, see Appendix D)

Heating energy per hour, E_{gen_hourly} , is derived as follows:

$$E_{gen-hourly} = P_{gen} * 3{,}6 \qquad [kJ] \qquad 6.5$$

The exergy factor is already mentioned before, equation 4.6, and is rewritten for the *energy generation* as follows (absolute temperatures):

$$f_{ex} = 1 - \left(\frac{T_{ambient}}{T_{condenser}}\right) \qquad [-] \qquad 6.6$$

When the exergy factor is mentioned n the remaining part of the report, it concerns the exergy (or quality) of the *generated* energy according to equation 6.6, and not the quality of the resource (ambient air).

6.2 Problem definition

In order to be able to recognize daily patterns in heating energy demand, the course of the load during several days of a typical winter week are plotted in Figure 6-2, superposed:

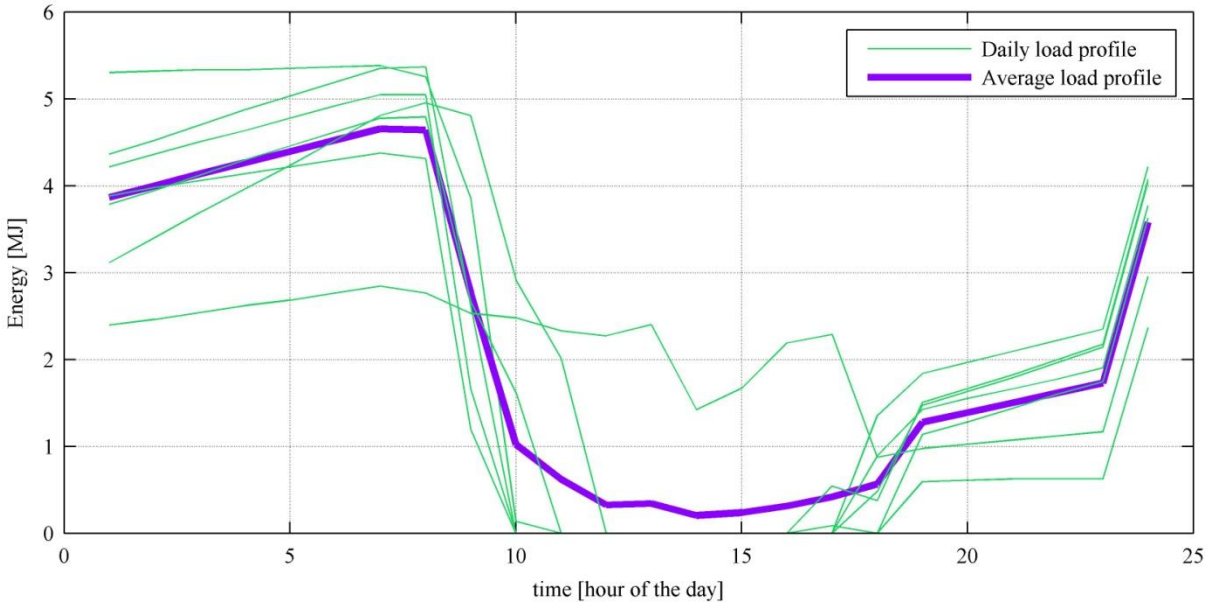

Figure 6-2: Superposed hourly energy demand typical winter week (last week of February)

The major part of the heat demand occurs from 0:00-10:00 AM. After sunset, the heat demand remains low for several hours because of the presence of internal gains (until 24h).

The total heat demand of an exemplary day during this winter week (February 28) is 52,6 MJ. A heat pump could generate this amount of energy within several hours. In conventional systems, the heat pump generates this energy at the moments of the energy demand. Figure 6-3 contains a plot of the exergy factor of February 28 (informs on the amount of work per generated quantity of heat, W/Q), and the amount of work (i.e. electrical input of the heat pump) required to generate a certain amount of heat.

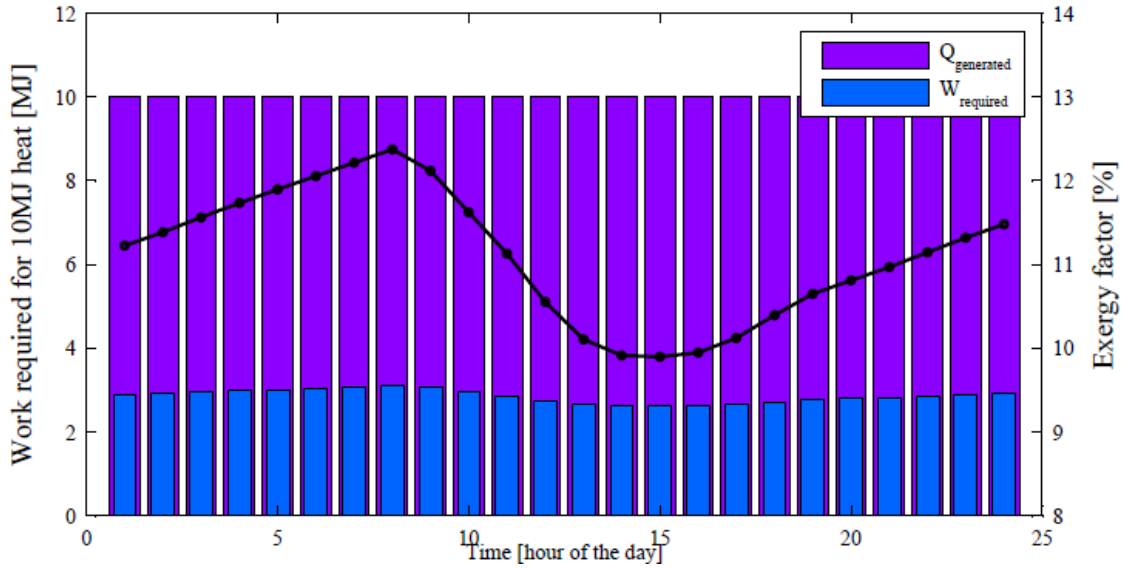

Figure 6-3: Work required in order to produce 10 MJ heat, per hour of February 28 (right axis and line: exergy factor)

As can be seen in the figure, the *maximum* exergy factor coincides with the space heating load peak from 0:00-10:00 AM. This means that more work is required in order to produce the 10 MJ heat than would be necessary around 3 PM (at *minimal* exergy factor).

Single-stage heat pumps have a fixed electrical input. Figure 6-4 shows the amount of heat produced at a continuous 1 kW work input. Again several days are superposed in order to see the daily optimum around 3 PM (maximum heat output, so maximum COP). Maximum COP occurs at the exergy factor's minimum (compare Figure 6-3 with Figure 6-4). When producing energy during these optimal hours, significantly more energy can be produced with the same amount of work than simultaneous with the heat demand during night. In case of February 28, the total daily heat demand can be generated within 4 optimal hours (using 14,4 MJ work) or 5 suboptimal hours (18 MJ work).

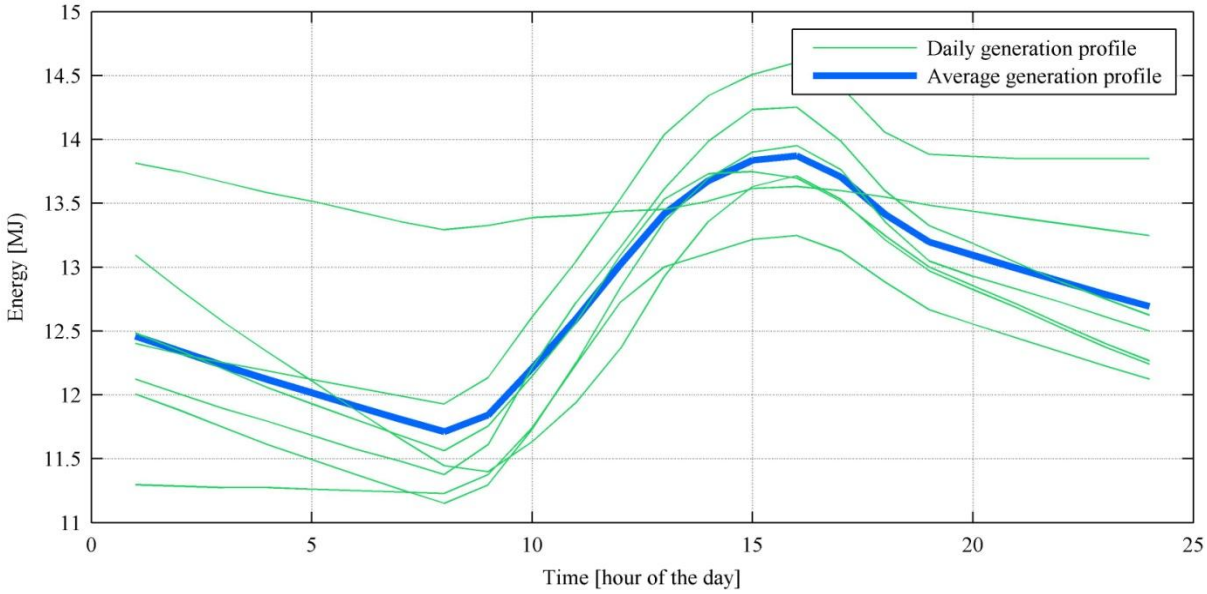

Figure 6-4: Superposed hourly energy generation typical winter week (last week of February)

Figure 6-4 showed that the heat pump is able to produce the daily energy demand with less work when it could operate during optimal conditions (at minimal exergy factors). Rephrased in the spirit of the first chapters of this study: there is a mismatch between availability of energy (with a quality close to the required quality) and the heat load. By introduction of energy storage, the load profile can be adjusted in order to approach the optimal generation profile as much as possible (notice: they can never completely match because then all the heating energy should be generated at the minimal exergy factor). An ideal TES (infinite volume) could completely decouple the demand and generation profile (two separate load profiles are introduced, for demand and supply side of TES, see Figure 6-5).

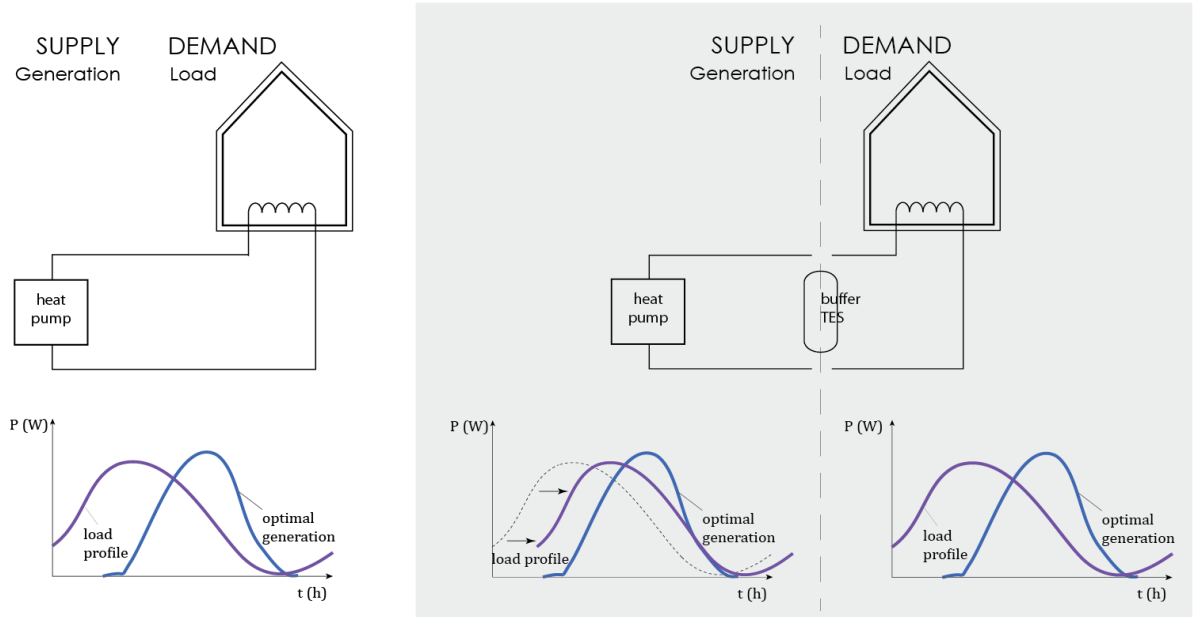

Figure 6-5: Heating load profile conventional situation (left) and in a system using TES (right), introducing two profiles

If a strategy could be developed in which the most optimal hours are used to generate the energy required for a certain future period (e.g. the next day), this could reduce the primary energy consumed. Characteristics of the TES are foreseen to have a big influence on the degree in which the heat load (and generation-) profile can approach the optimal generation profile. The development of an algorithm that can assess the potential gains, considering TES, is discussed below.

The problem at hand can be classified as a linear integer optimization problem, which can be expressed as follows (objective function):

minimize $E_{primary}\ (x)$

subject to $0\ \leq \min x$

$1\ \geq \max x$

$\mathrm{x\ is\ integer}$

$0\ \leq \mathrm{buffercontent}\ \leq \mathrm{upperlimit}$

The primary energy consumed $E_{primary}$ is a function of variable x according to equation 6.7:

$$E_{primary} = \sum_{t+1}^{t+prediction} E_{primary\ per\ hour} * x \qquad 6.7$$

where *x* is a vector containing the hours at which the heat pump should be operative. Therefore, *x* is binary. If the horizon that the algorithm looks into the future is 24 hours, then *x* could look as follows:

$$x = \begin{bmatrix} 0 \\ 0 \\ 1 \\ 1 \\ 0 \\ \vdots \\ 0 \end{bmatrix} \text{ at } t = \begin{bmatrix} 1 \\ 2 \\ 3 \\ 4 \\ 5 \\ \vdots \\ 24 \end{bmatrix}$$

As said before, this optimization problem is linear because all inputs and variables only involve simple addition, subtraction, division and multiplication. The degree of freedom of the solution is integer, because entries of *x* are integer. A linear constraint is given by the capacity of the buffer (buffercontent should not be negative or above the maximum energy content).

In order to solve this optimization problem, a MATLAB model was constructed. The purpose of this explorative study in MATLAB is to derive a buffer (dis)charge strategy that results in a minimal yearly primary energy consumption (see schematic in Figure 6-6). With this model, subsequently a sensitivity analysis can be done, which gives insight in the effect of certain parameters on the primary energy consumption. With the outcomes of that in mind, use cases can be defined in which most influential parameters are varied. These use cases will be calculated with in a more detailed, tentative assessment using a dynamic TRNSYS simulation model.

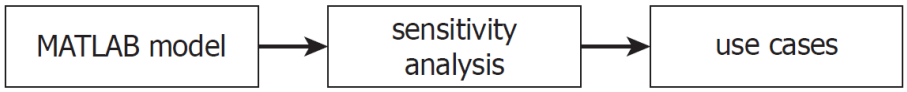

Figure 6-6: Purpose of the MATLAB model within the research

6.3 Optimization strategies

6.3.1 General

Below, some additional important formula's and assumptions will be explained.

Heat losses from the buffer are calculated in a steady state, 1-dimensional manner. Only heat flux by conduction is taken into account, using Fourier's law:

$$q = -\lambda * \frac{dT}{dx} = \lambda * \frac{T_1 - T_2}{d} = h_c * (T_1 - T_2) \quad [W/m^2] \qquad 6.8$$

where,

h_c = heat transfer coefficient, or $\frac{\lambda}{d}$ [W/m^{2}K]

T_1 = T_{water} temperature buffer medium [°C]

T_2 = $T_{surface}$ temperature of buffer envelope [°C] (assumed: equals room temperature)

The total heat flow per time step depends on the envelope area of the storage. In the model, a cylindrical volume is assumed (this makes equation 6.8 a simplification since it describes a flat plate):

$$\dot{Q} = q * A \quad [W] \qquad 6.9$$

Where,

q = heat flow [W/m^2], equation 6.8

A = heat transfer surface, $A = \pi * d * (0{,}5d + h)$ [m^2]

The time an algorithm looks into the future (e.g. in order to predict demand or exergy factor) is given in the parameter *prediction horizon.* Ideal prediction is assumed. In reality, prediction of weather conditions for more than three days becomes uncertain, and prediction of the space heating demand involves complex dynamic parameters, e.g. behavior of the emission system. These effects will be investigated in the TRNSYS model.

Cost per generated kJ$_{th}$, pE$_{gen}$, is given by equation 6.10:

$$pE_{gen} = \frac{pE(t) * E_{el}}{E_{gen}} \quad [€/kJ_{th}] \qquad 6.10$$

Where,

pE(t) = price electricity day-night tariff, contemporary price structure, see Appendix C [€/kJ$_{el}$]

E_{el} = electrical energy consumed [kJ$_{el}$], 3.600 kJ/hr (1 kW)

E_{gen} = generated heating energy [kJ$_{th}$]

An important assumption follows from the fact that the model is a discrete integer model, which makes it impossible to operate the heat pump for less than one hour (the time step). Therefore, all generated energy is supplied to the buffer, and the required heating energy is subtracted from the buffer. After a hour of heat pump operation the new buffer balance, called *buffercontent*, is as follows:

$$buffercontent(t) = buffercontent(t-1) + E_{gen}(t-1:t) - E_{dem}(t-1:t) - E_{losses}(t-1:t) \quad 6.11$$

Where,

buffercontent = useful energy content of the buffer, see definition below [kJ]

E_{gen} = energy generated in the previous hour [kJ]

E_{dem} = energy demand in the previous hour [kJ]

E_{losses} = energy losses in the previous hour [kJ]

If the installation was not operative during the previous time step, the new buffer balance is calculated according to:

$$buffercontent(t) = buffercontent(t-1) - E_{dem}(t-1:t) - E_{losses}(t-1:t) \quad 6.12$$

The output variable *buffercontent* is a measure of the amount of useful energy that the buffer contains. Useful means that the temperature of the water remains at a level in which it can be supplied to a floor heating system. While calculating the buffercontent, the buffer is assumed as fully mixed:

$$Q_{buffercontent} = m * c_{p;water} * (T_{water} - T_{supplymin}) \quad 6.13$$

where,

m = buffer mass [kg] or: $V*\rho_{water}$

$c_{p;water}$ = specific heat water [kJ/kgK]

T_{water} = water temperature, fully mixed

$T_{supplymin}$= minimal supply temperature (defines useful energy) [˚C], 23 ˚C

This means that $Q_{buffercontent}$ becomes zero when the water temperature drops below 23 [˚C] (in a stratified tank, water at the top would still be a few degrees higher). The maximum allowed energy content (hereafter called: *upperlimit*) occurs when T_{water} = 35˚C. This definition is used to maintain the temperatures supplied to the floor within a 25-35 ˚C range, which ensures good heat pump operation.

6.3.2 Strategy A – reference strategy

Strategy A represents the reference control strategy for a heat pump combined with a buffer tank. In this situation, the heat demand is primary withdrawn from the buffer. When the buffer content is too small to provide the heat demand for the next hour, the heat pump is switched on. It is switched off again only when the buffer is completely recharged (has reached its upper limit). This control strategy is common in practice, the reference strategy simulated in TRNSYS is based on this strategy too. Outside conditions do not play a role in the decision making.

The programming block schematic in Figure 6-7 shows which steps are involved in this strategy.

In initial condition, the buffer is fully charged and the heat pump is off. Controllable input variables are:

- buffer volume (maximum energy content = upperlimit)
- buffer height
- insulation grade

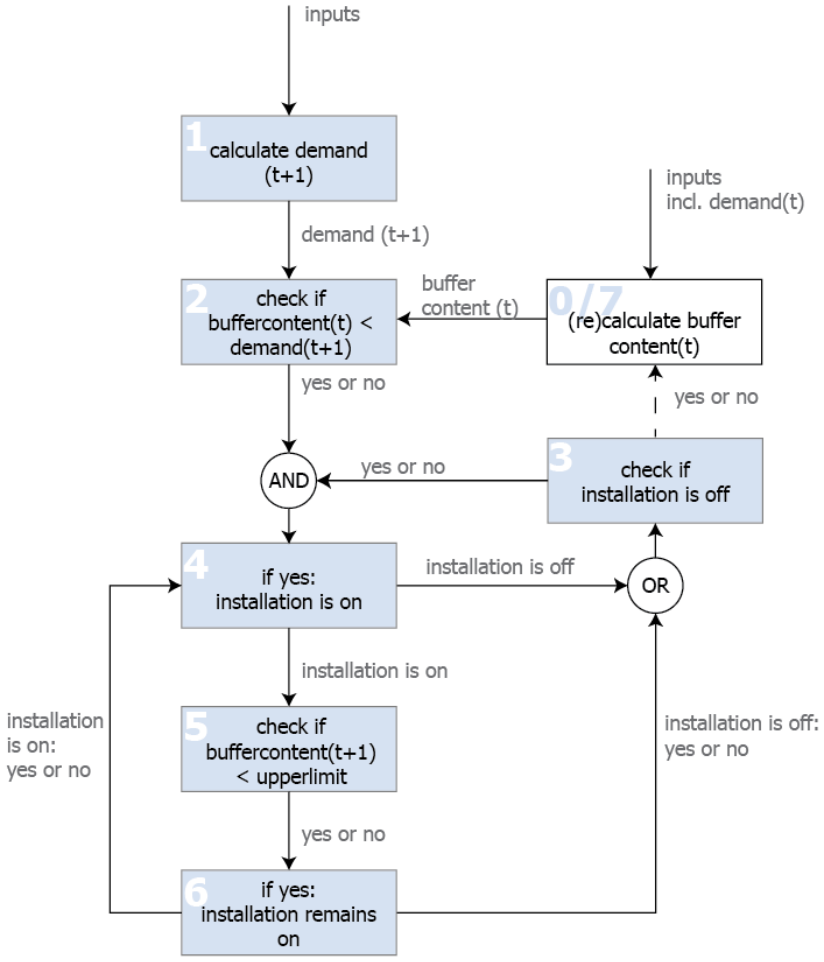

Figure 6-7: Block schematic for control strategy A

6.3.3 Strategy B – Charge storage every day after specified time

Figure 6-4 clearly illustrated that the most optimal energy generation hours are always gathered around the maximum at 15:00h. With this in mind, strategy B was developed. From a certain time onwards, the installation will recharge the buffer. It stops if the buffer is full OR if the buffer contains the sum of the predicted energy demand for the rest of the same day and the next day. The hour after which the charge process starts will be defined by finetuning of the variable *hourstartrecharge*, which will be approximately around 14:00h.

The programming block schematic in Figure 6-8 shows which steps are involved in this strategy.

In initial condition, the buffer is fully charged and the heat pump is off. Controllable input variables are:

- prediction horizon (number of hours on the next day for which the heat demand will be stored on the current day)
- hourstartrecharge (hour at which recharge can start in order to exploit favorable conditions)
- buffer volume (maximum energy content = upperlimit)
- buffer height
- insulation grade

The requested energy in step 2b is the sum of the predicted energy demand for the rest of the current day plus the predicted energy demand for the prediction horizon:

$$requested\ energy(t) = sum\left(E_{dem-hourly}\left(t+1:\ t_{endoftheday}\right)\right) + sum\left(E_{dem-hourly}\left(t_{day2}:t+predictionhorizon\right)\right) \quad 6.14$$

Where,

E_{dem_hourly} = hourly heat demand, see eq. 6.2 [kJ]

$t_{endoftheday}$ = hour of the current day = 24 [h]

t_{day2} = first hour of the next day [h]

predictionhorizon = hours that algorithm looks into future [h]

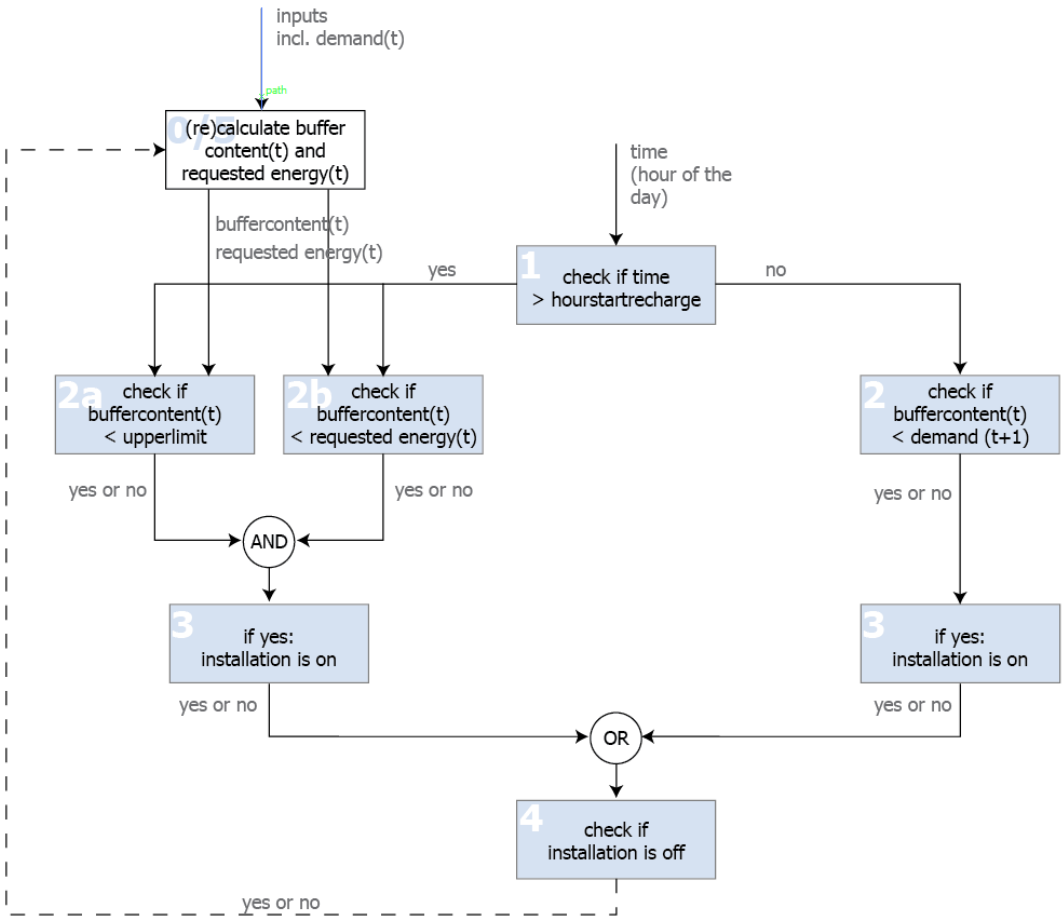

Figure 6-8: Block schematic for control strategy B

6.3.4 Strategy C

A disadvantage of strategy B is that during some days, the buffer will already be filled before the best hours have been reached. Thus, some optimal hours can still be not taken advantage of because the buffer was charged or the demand for the next day was relatively small.

In strategy C, the most optimal hours for operation are selected at the beginning of every day. This decision making moment takes place at the first hour of every day. The parameter *prediction horizon* in this strategy, therefore concerns the time the algorithm looks ahead into the future from the first hour of the current day onwards. The energy that is already generated on the previous day for the current day is subtracted from the total energy demand. The requested energy *per day* is defined as follows:

$$requested\ energy = sum\left(E_{dem-hourly}\left(t_{firsthour}: t + predictionhorizon\right)\right) - buffercontent(t_{firsthour}) \quad 6.15$$

Where,

E_{dem_hourly} = predicted hourly heat demand, see eq. 6.2 [kJ]

$t_{firsthour}$ = first hour of the current day = 1 [h]

predictionhorizon = hours that algorithm looks into future [h]

buffercontent($t_{firsthour}$) = energy content buffer at first hour of current day [kJ]

The programming block schematic in Figure 6-9 shows which steps are involved in this strategy. In initial condition, the buffer is fully charged and the heat pump is off. Controllable input variables are:

- prediction horizon (number of hours ahead for which demand will be stored on the current day)
- buffer volume (maximum energy content = upperlimit)
- buffer height
- insulation grade

Important to note is that the parameter *buffervalue* is non-physical because it is only used for decision making. It doesn't take into account energy losses nor the constraints of the buffer limitations. Including these constraints in the *buffervalue* would make the algorithm too complicated. As can be seen in the block schematic, the decision making and the activation of the installation are decoupled.

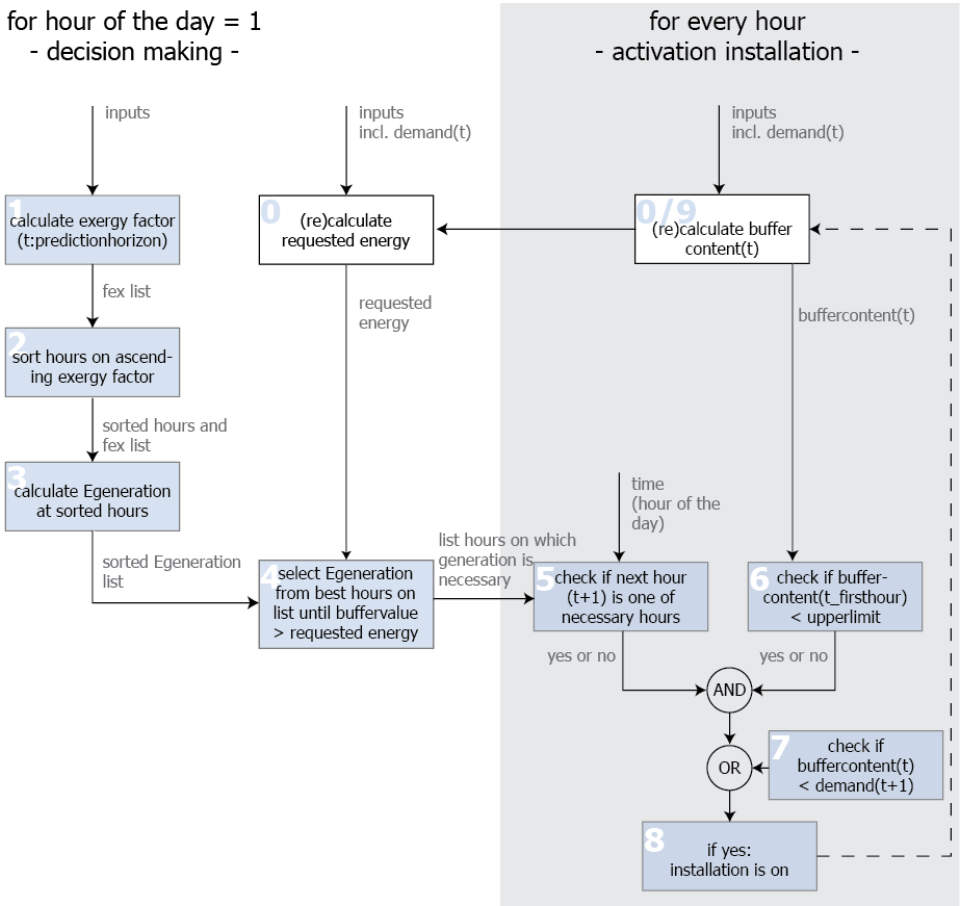

Figure 6-9: Block schematic for control strategy C

6.3.5 Strategy D

Strategy D is a variant of strategy C, and is the most advanced algorithm to solve this optimization problem. The decision making cycle, which in strategy C was performed once every day, is now being performed at every time step. Stated differently: the prediction horizon recedes at every time step. This type of control, wherein *at every time step* the most optimal solution (read: the most optimal hours necessary to operate) within the predictionhorizon is defined, is called Greedy linear integer receding optimal control (Vizvari, 1987).

The requested energy is defined at every time step using the equation below:

$$requested\ energy(t) = sum\left(E_{dem-hourly}\,(t+1:t+predictionhorizon)\right) - (buffercontent(t) - bset) \quad 6.16$$

Where,

E_{dem_hourly} = predicted hourly heat demand, see eq. 6.2 [kJ]

t+1 = starting from the next hour [h]

predictionhorizon = hours that algorithm looks into future [h]

buffercontent(t) = energy content buffer at current hour [kJ]

bset = buffer setpoint, explained below [kJ]

The programming block schematic in Figure 6-10 shows which steps are involved in this strategy. In initial condition, the buffer is fully charged and the heat pump is off. Controllable input variables are:

- prediction horizon (number of hours ahead for which heat demand will be stored)
- buffer volume (maximum energy content = upperlimit)
- bset
- buffer height
- insulation grade

Besides the non-physical parameter *buffervalue,* the buffer setpoint *bset* is introduced. *bset* is a threshold that prevents the algorithm from postponing generation too long because more optimal hours appear when the prediction horizon exceeds. As can be seen in equation 6.16, the difference between the buffercontent and the buffer setpoint is subtracted from the total requested energy (that needs to be generated).

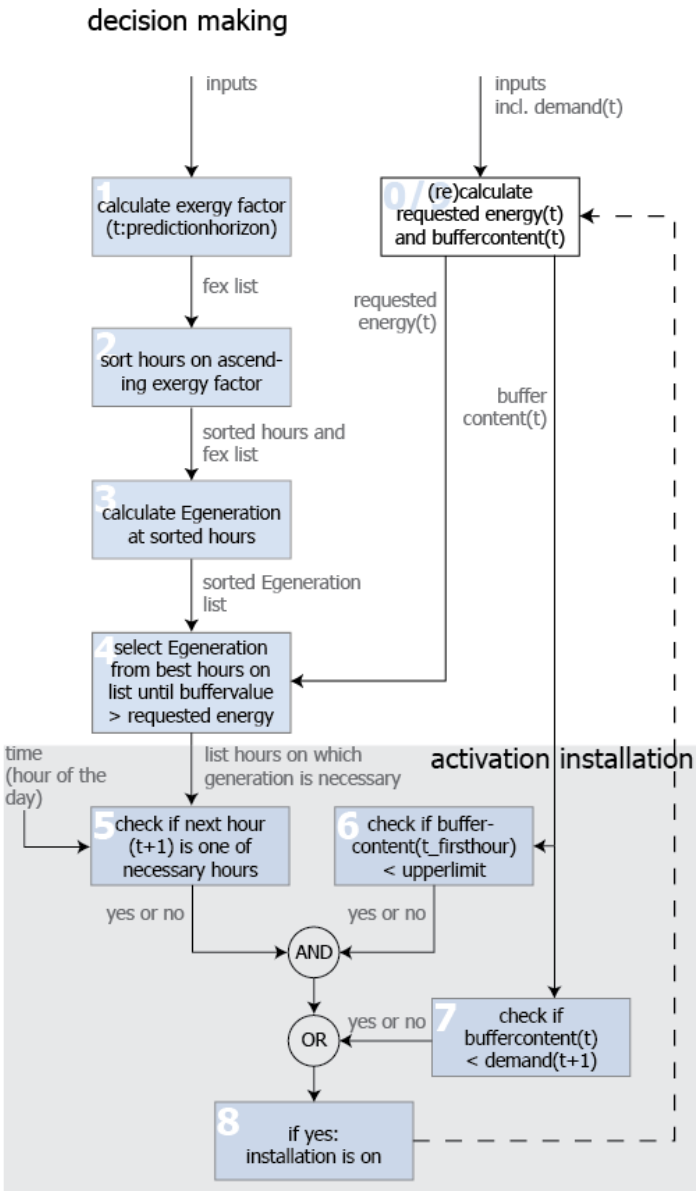

Figure 6-10: Block schematic for control strategy D

When the buffercontent rises above bset (see Figure 6-11), this difference becomes positive and the requested energy is reduced. When buffercontent drops too low, the requested energy will rise and more hours of heat pump operation will be necessary before buffervalue is greater than the requested energy (step 4 of the block schematic). The optimal bset entry is to be defined by finetuning.

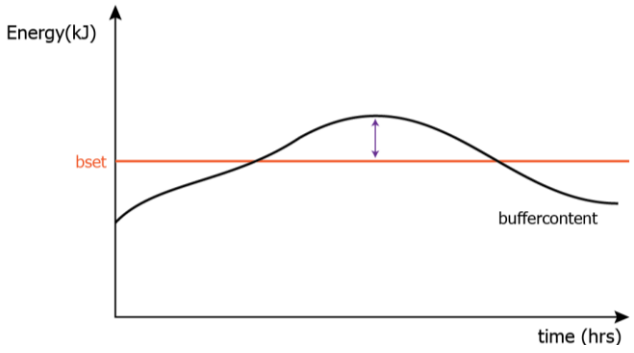

Figure 6-11: Buffersetpoint bset *(difference buffercontent-bset)*

6.4 Calculation cases

In equations 6.3 and 6.4 could be seen that the COP and energy generated by the heat pump do depend on the temperature of the supply water. This temperature derives from a simple climate curve based on the outside temperature, see figure below.

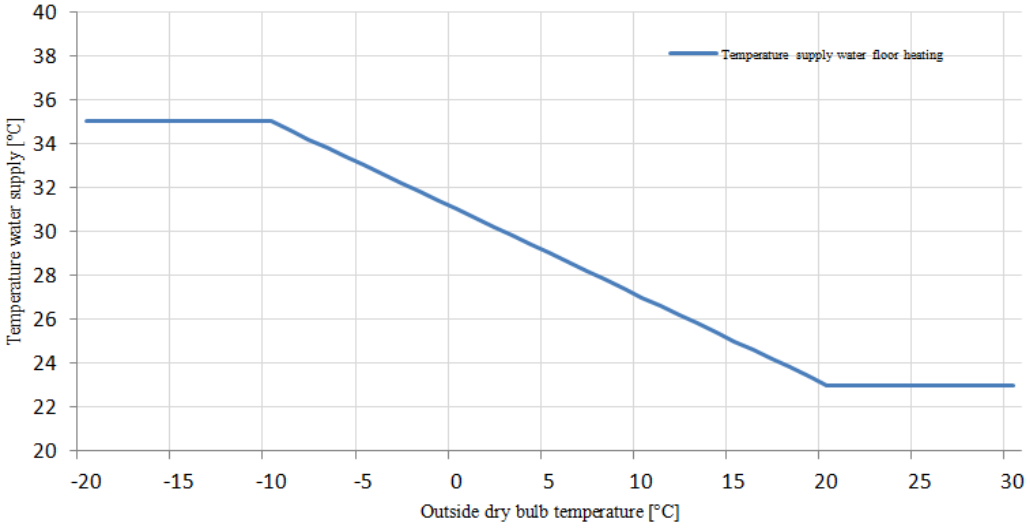

Figure 6-12: Desired temperature water supply

Strategy A uses this climate curve to define which temperature is produced. Since other strategies look ahead into the future, they can't make use of an instantaneous climatecurve, but instead the heat pump should charge the buffer with water that is warm enough to meet supply requirements of the worst case situation during the prediction horizon. This is taken in to account in the calculation of strategies B, C and D.

It can be assumed that the possible energy content of the buffer (defined by the volume and specific heat of the storage medium) is a variable that has a big influence on the approximation of the optimal generation profile. It determines which amount of the daily heating energy load can be stored on forehand. Several buffer volumes ranging from conventional sizes (100-500L water) have been calculated with, as well as volumes that are equivalent with latent heat storage. The latter are based on a rough estimation, using the heat of fusion of a certain amount of PCM (200 kJ/kg, in a 600L tank). The (equivalent) upper limit (useful energy contained when the buffer is at 35 ˚C) is based on a 12 K temperature difference, since the minimal supply temperature is 23 ˚C.

The storage volumes that will be investigated are volumes that could be installed inside typical dwellings. Large sensible energy volumes are also calculated, which are equivalent to latent thermal storage (quick scan calculation). Storage of the same amount of energy in a latent thermal energy storage requires significantly less space than when stored only by sensible storage.

Table 6-1 Calculated storage volumes and associated energy storage capacities

Buffer volume (L)	Buffer volume (kg)	Upperlimit (MJ)
100	100	5
200	200	10
250	250	12,6
500	500	25
1.000	1000	50
1.500 (eq. 600L 30vol% PCM)	1500	75
2.000 (eq. 600L 50vol% PCM)	2000	100

Secondly, the prediction horizon is varied (not relevant for reference strategy A, in case of strategy B only 24h is meaningful). In strategy D, a prediction horizon of 12 hours was calculated as well.

Prediction horizon (hrs)	Strategy B	Strategy C	Strategy D
12		X	X
24	X	X	X
48			X

Other variables were kept constant, their influence has been investigated in the sensitivity analysis eg:

- Electrical power heat pump (kept at 1.0 kW_{el})
- Heat demand of the dwelling
- Allowed temperature between buffer full or empty (kept at $23 < T_{water} < 35$)

A full year calculation (8760 hours) has been performed with the MATLAB model for all four strategies. In order to get insight in how the algorithm works, results for the typical winter week (end February) are discussed. The conditions are plotted in Figure 6-13. The yearly heating energy demand is 14.488 MJ, which is 32,5 kWh/m^2. In order to keep the report compact, the functioning of every strategy is only illustrated for the volumes 500L and 2000L, and the most optimal prediction horizon. For more detailed results, see Appendix C.

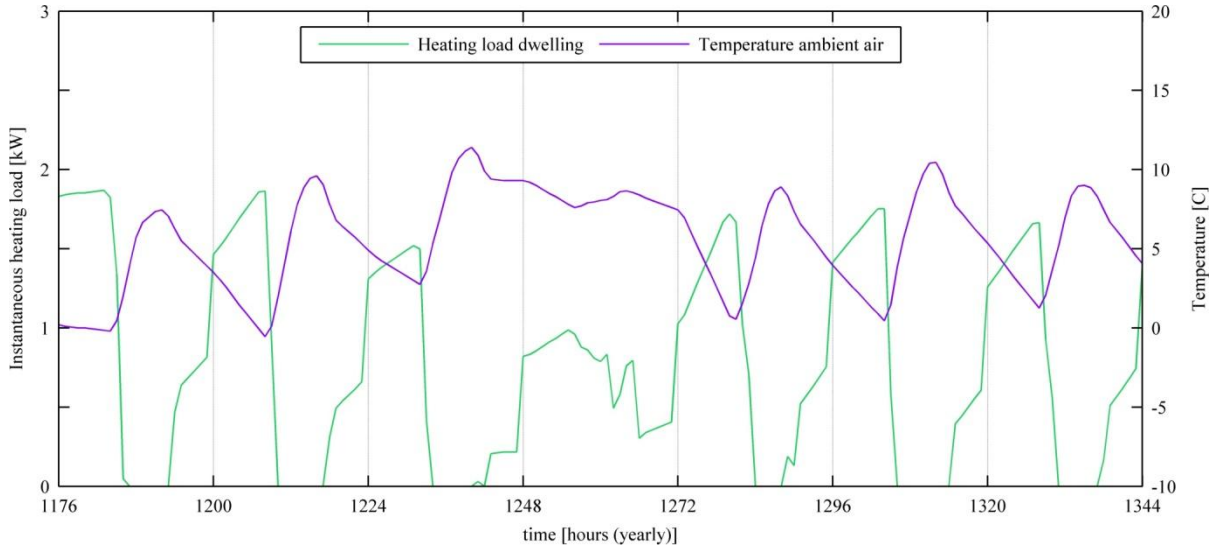

Figure 6-13: Dry bulb ambient air temperature and instantaneous heat load for the typical winter week

6.5 Results

6.5.1 Strategy A

Variables	
Buffer volumes [kg]	500
Buffer upperlimit [MJ]	25

The following figures show the development of the energy content of the small and large buffer volumes during the typical winter week. The large buffer is only (dis-)charged once every two days, whereas the small buffer lasts only one day (or less when the demand is large e.g. in the midweek). Resulting yearly saldi are shown in Table 6-2.

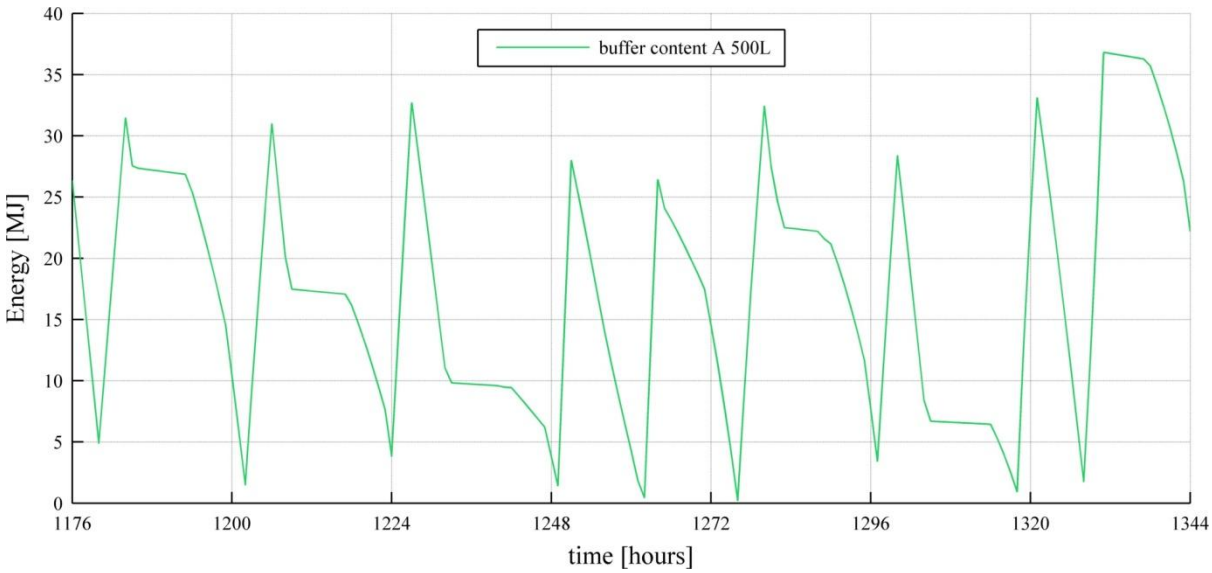

Figure 6-14: Energy content of the buffer

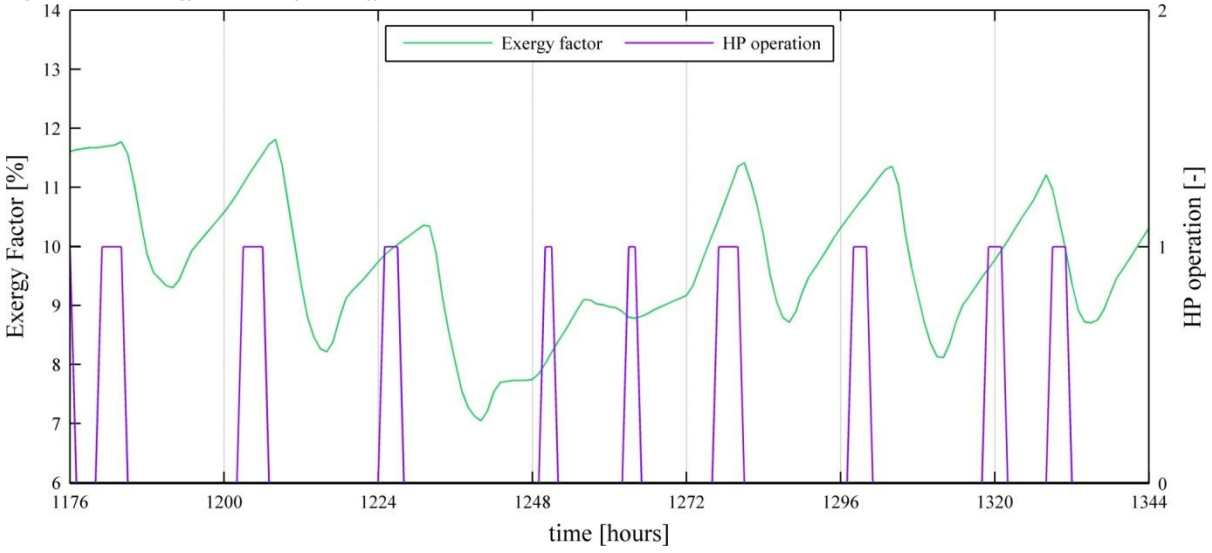

Figure 6-15: Exergy factor and operation pattern of the installation

Variables	
Buffer volumes [kg]	2000
Buffer upperlimit [MJ]	100

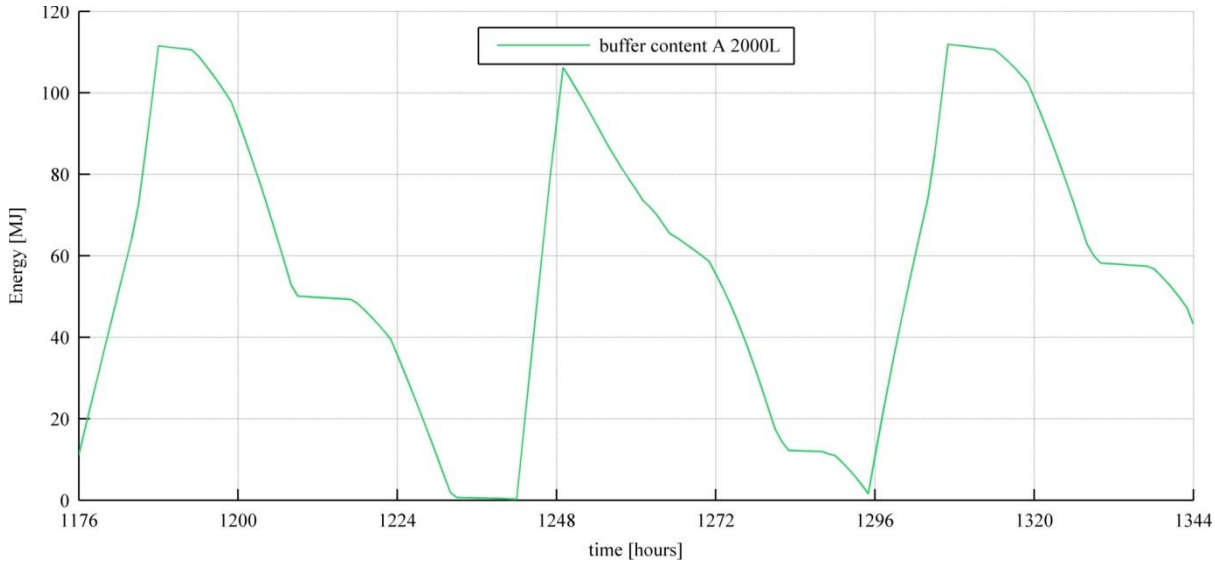

Figure 6-16: Energy content of the buffer

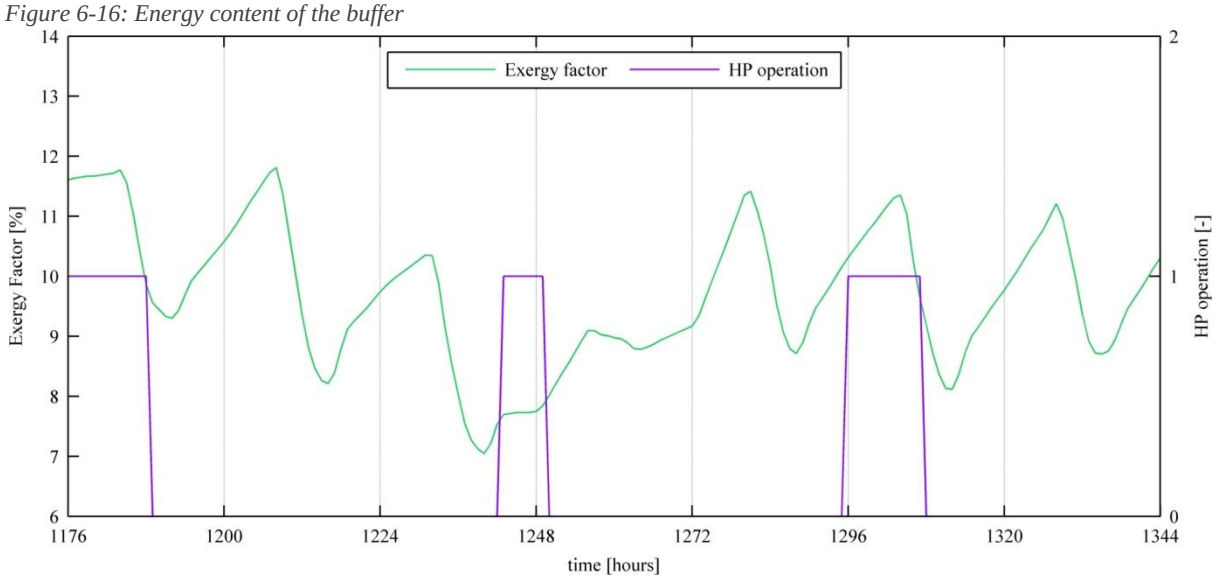

Figure 6-17: Exergy factor and operation pattern of the installation

Table 6-2 – yearly sums strategy A,volumes 500 and 2000 L

Buffer volume [kg]	5e2	2e3
Energy generated [MJ]	14.905	15.304
Work (electrical energy consumed) [MJ]	4.025	4.061
Primary energy consumed [MJ]	10.303	10.396
Hours that installation is on [h]	1.118	1.128
Number of on/off cycles [-]	369	111

6.5.2 Strategy B

Variables	
Buffer volumes [kg]	500
Buffer upperlimit [MJ]	25
Installation starts from	2 PM

The energy content of the small buffer is too small for the algorithm to work properly. It is not possible to store the entire heat demand for the next day in once, which leads to on/off cycling of the installation around the upper and lower limit (saw-tooth pattern in the graph). Figure 6-21 however shows that 2000L is sufficiently large, which enables generation during hours close to the exergy minima (i.e. maximum ambient temperatures) resulting in good heat pump performance.

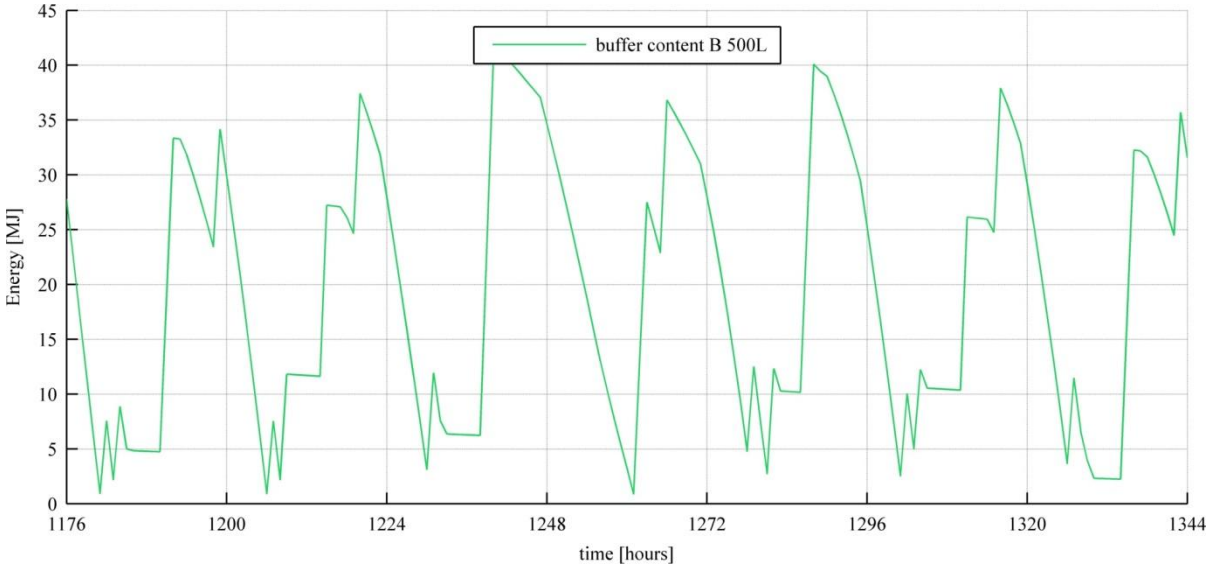

Figure 6-18: Energy content of the buffer

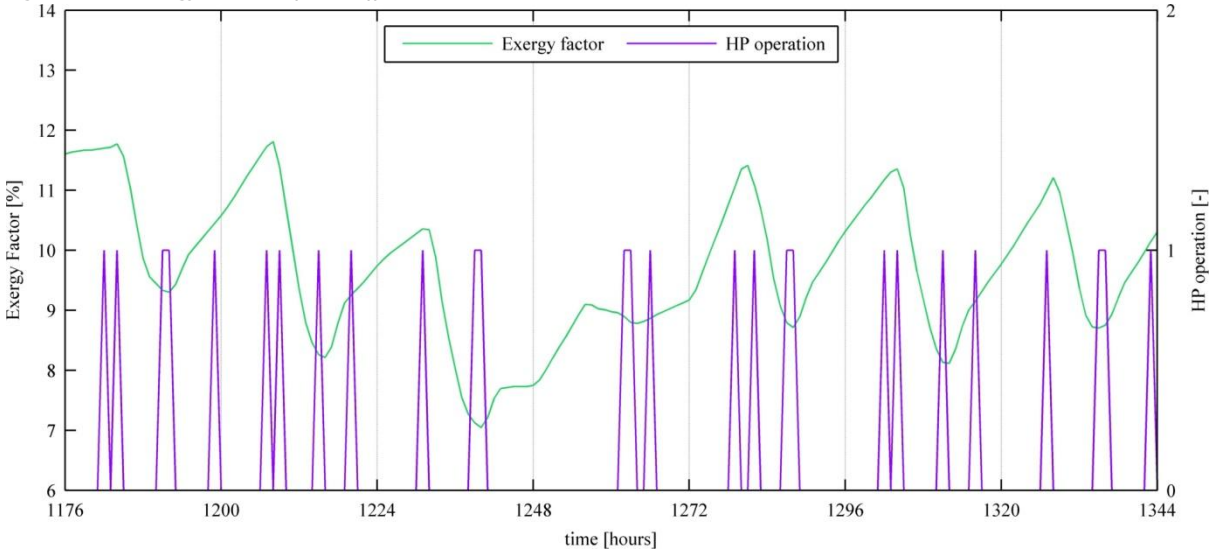

Figure 6-19: Exergy factor and operation pattern of the installation

Variables	
Buffer volumes [kg]	2000
Buffer upperlimit [MJ]	100

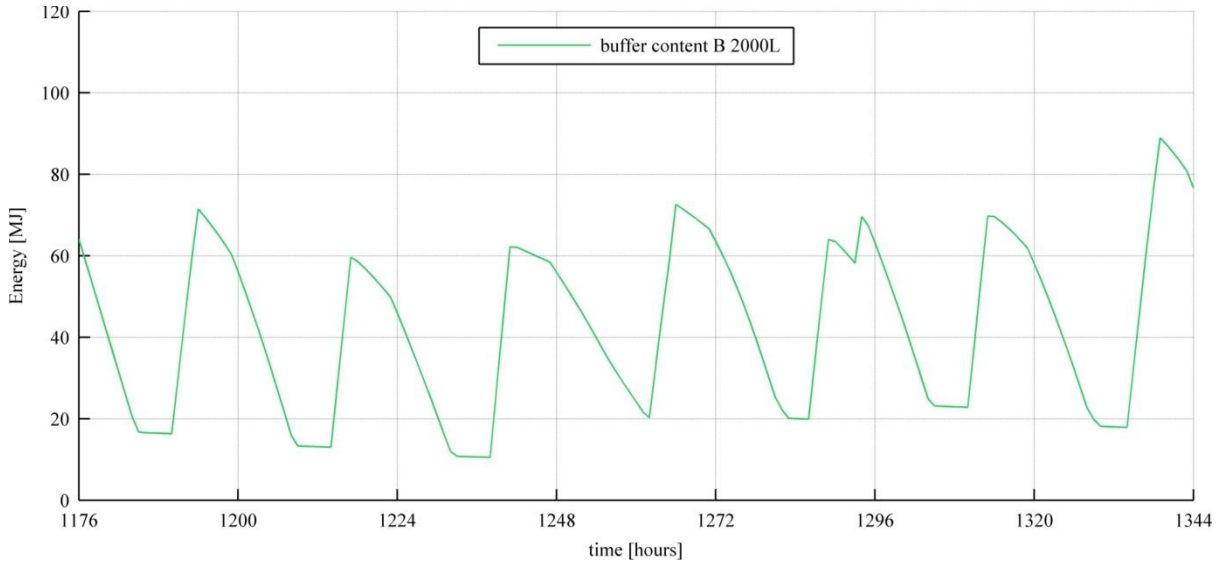

Figure 6-20: Energy content of the buffer

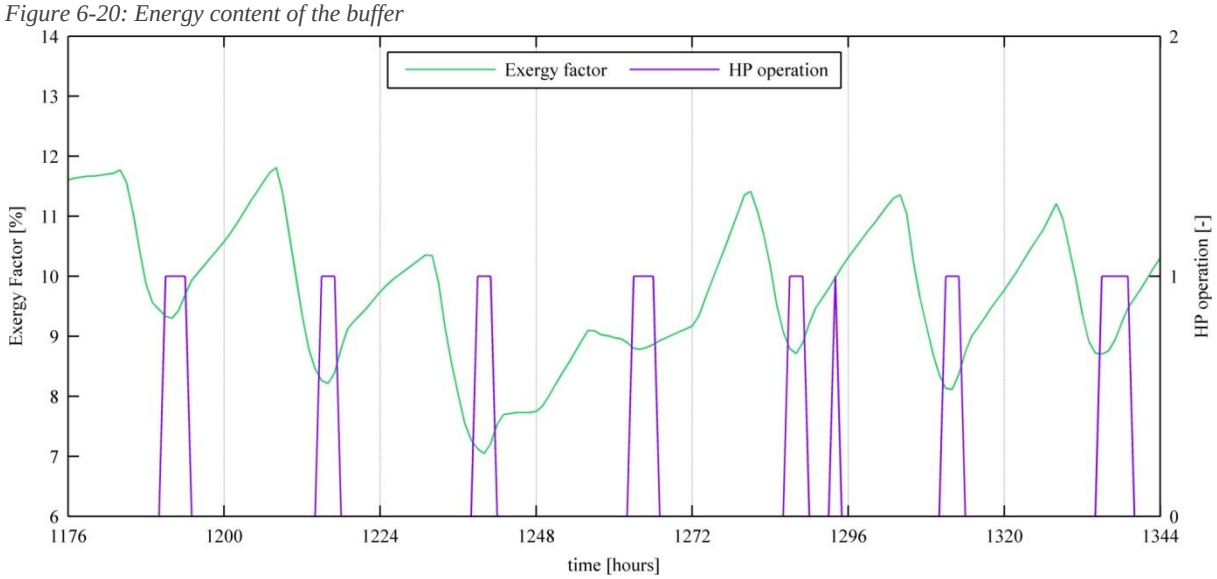

Figure 6-21: Exergy factor and operation pattern of the installation

Table 6-3 – yearly sums strategy B, and savings compared to strategy A (similar volumes)

Buffer volume [kg]	5e2	Reduction [%]	2e3	Reduction [%]
Energy generated [MJ]	14.953	-	15.145	1
Work (electrical en. consumed) [MJ]	3.794	6	3.722	8
Primary energy consumed [MJ]	9.714	6	9.529	8
Hours that installation is on [h]	1.054	6	1.034	8
Number of on/off cycles [-]	818	+122	325	+193

6.5.3 Strategy C

Variables	
Buffer volumes [kg]	500
Buffer upperlimit [MJ]	25
Prediction horizon [hrs]	36 (from 1 AM)

Again, the 500L buffer is too small for the algorithm to work properly. Before the next minimum (trough) exergy factor is reached, the buffer is empty and needs to be recharged at suboptimal hours in order to contains sufficient energy for the coming hours. With a larger volume, one can see that the larger heat demand during midweek is foreseen and generated during optimal hours. At the beginning of the week, generation is delayed too much, and the buffer crosses the lowerlimit early.

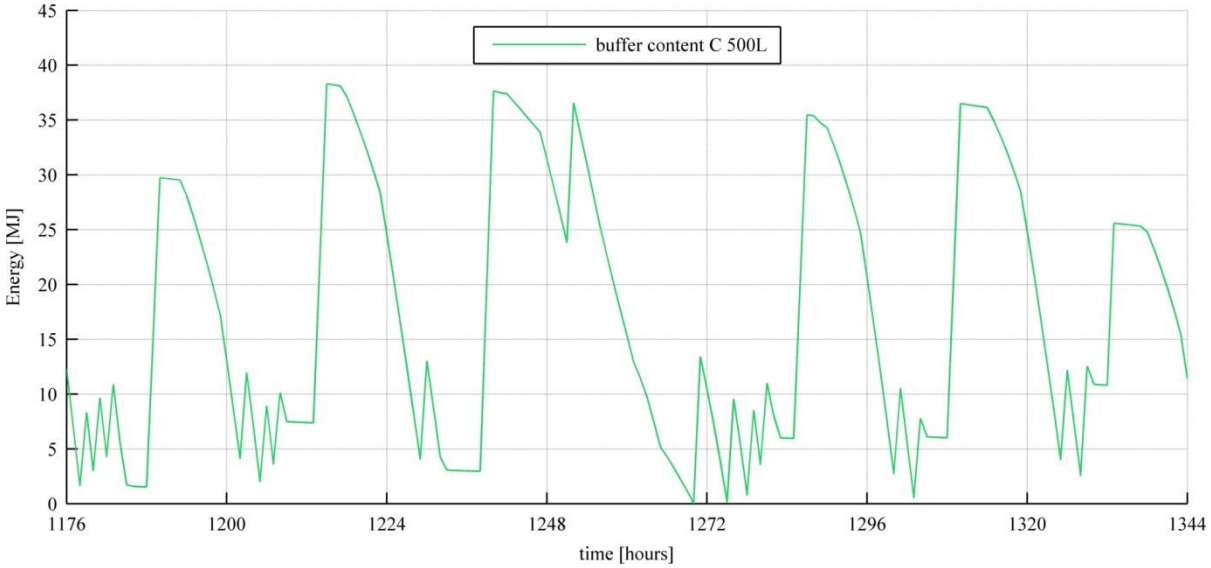

Figure 6-22: Energy content of the buffer

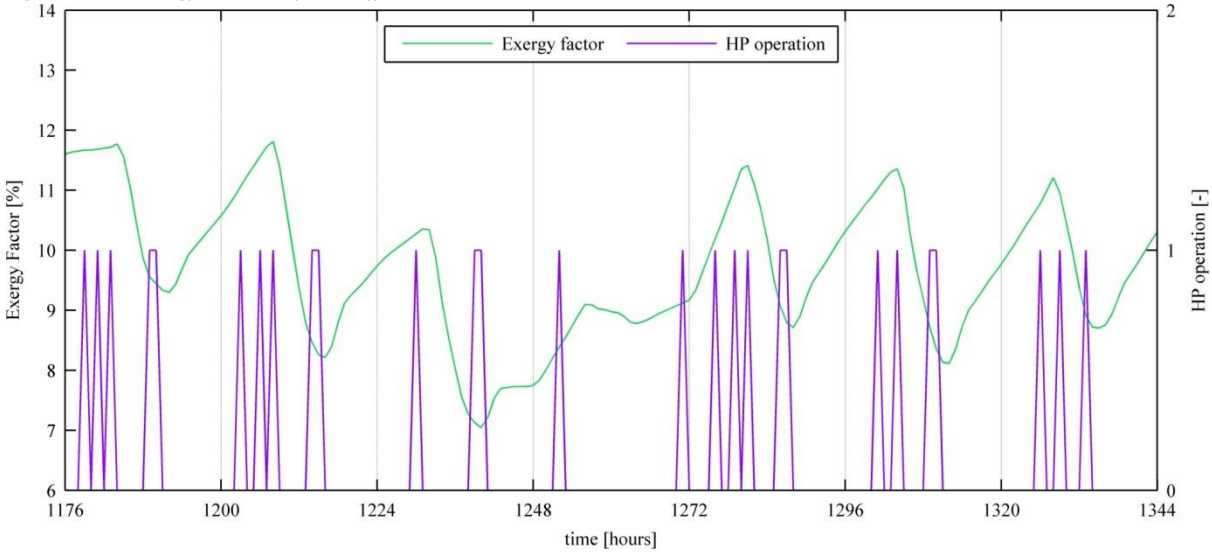

Figure 6-23: Exergy factor and operation pattern of the installation

Variables	
Buffer volumes [kg]	2000
Buffer upperlimit [MJ]	100
Prediction horizon [hrs]	36 (from 1 AM)

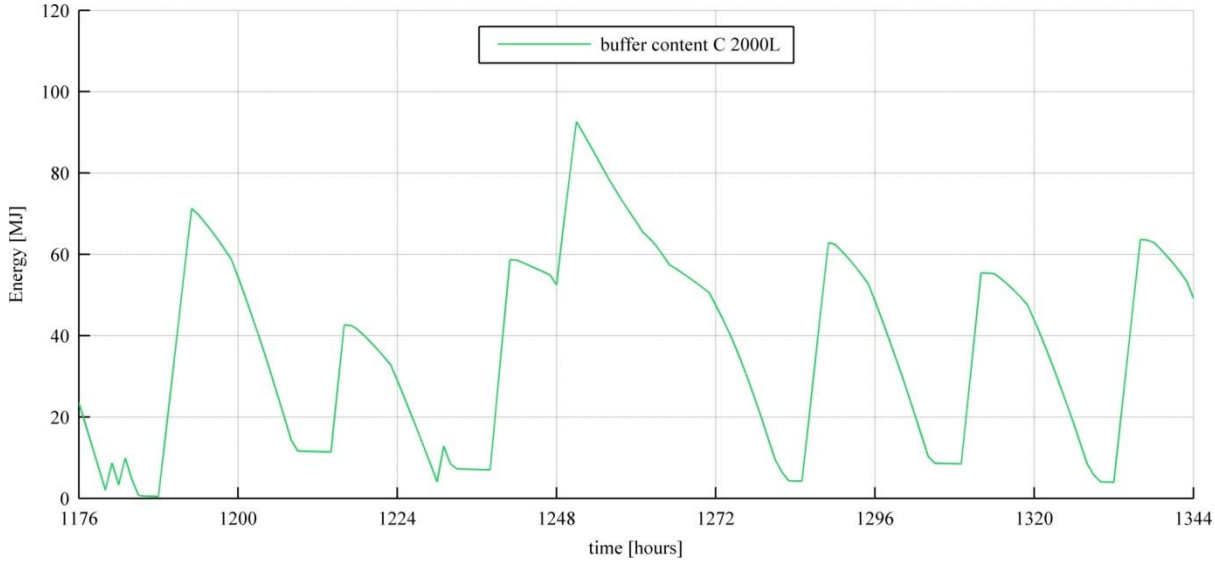

Figure 6-24: Energy content of the buffer

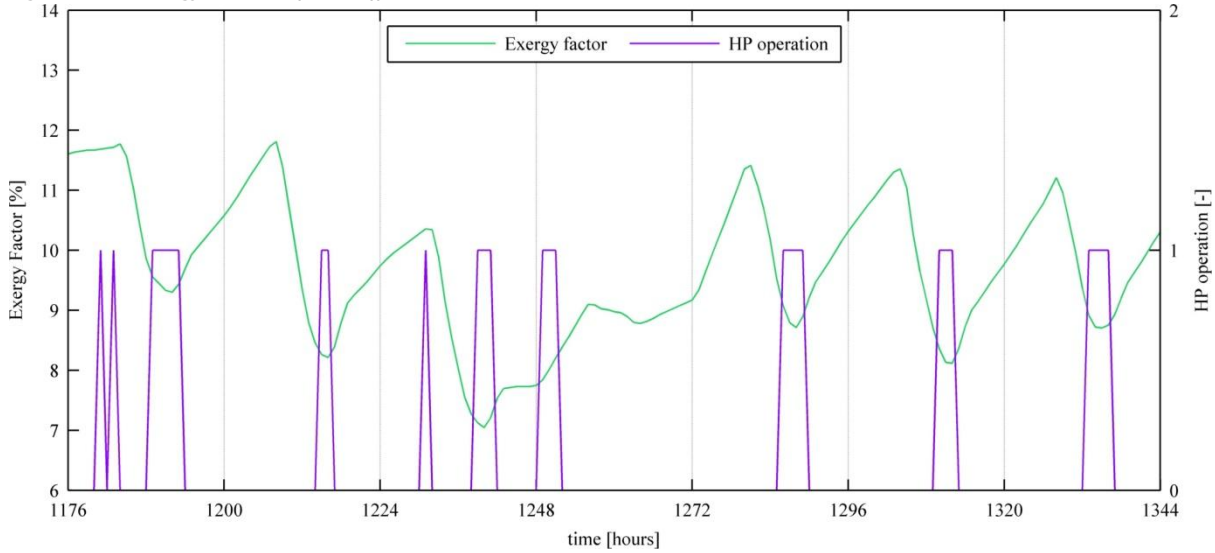

Figure 6-25: Exergy factor and operation pattern of the installation

Table 6-4 – yearly sums strategy C, and savings compared to strategy A (similar volumes)

Buffer volume [kg]	5e2	Reduction [%]	2e3	Reduction [%]
Energy generated [MJ]	14.939	-	15.082	1
Work (electrical en. consumed) [MJ]	3.823	5	3.697	9
Primary energy consumed [MJ]	9.787	5	9.465	9
Hours that installation is on [h]	1.057	5	1.022	9
Number of on/off cycles [-]	836	+134	468	+322

6.5.4 Strategy D

Variables	
Buffer volumes [kg]	500
Buffer upperlimit [MJ]	25
Prediction horizon [hrs]	12

Figure 6-27 illustrates that a short prediction horizon works well for small buffer volumes, although operation at exergy maxima still can't be completely prevented. The 2000L buffer results in a much better controlled operation of the heat pump. During the majority of the week, operation coincides with the exergy minima. The peak heat demand during midweek is foreseen.

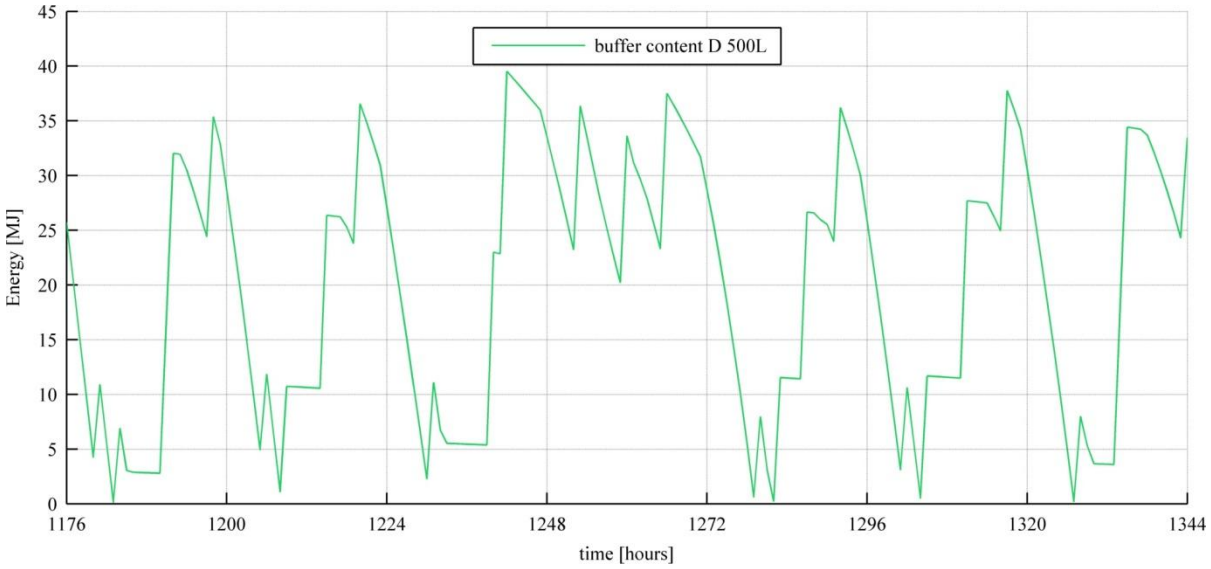

Figure 6-26: Energy content of the buffer

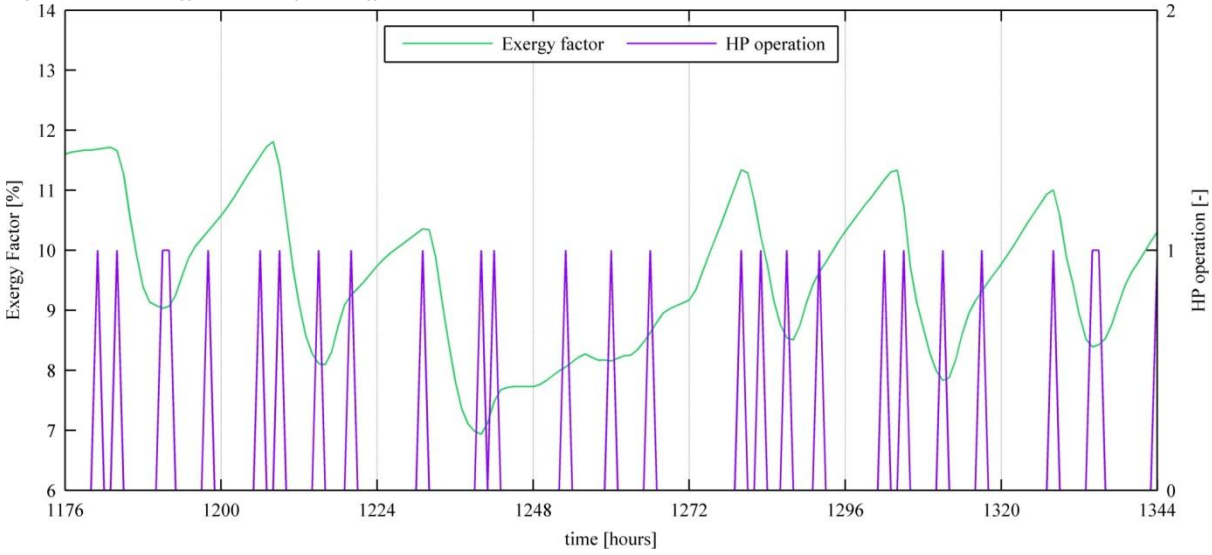

Figure 6-27: Exergy factor and operation pattern of the installation

Variables	
Buffer volumes [kg]	2000
Buffer upperlimit [MJ]	100
Prediction horizon [hrs]	24

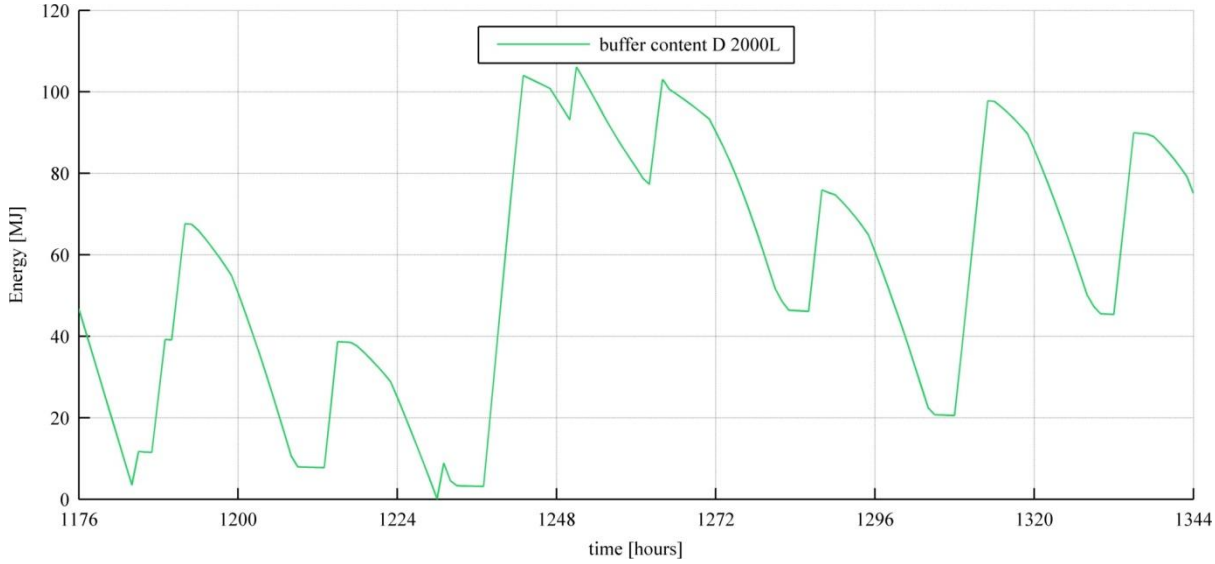

Figure 6-28: Energy content of the buffer

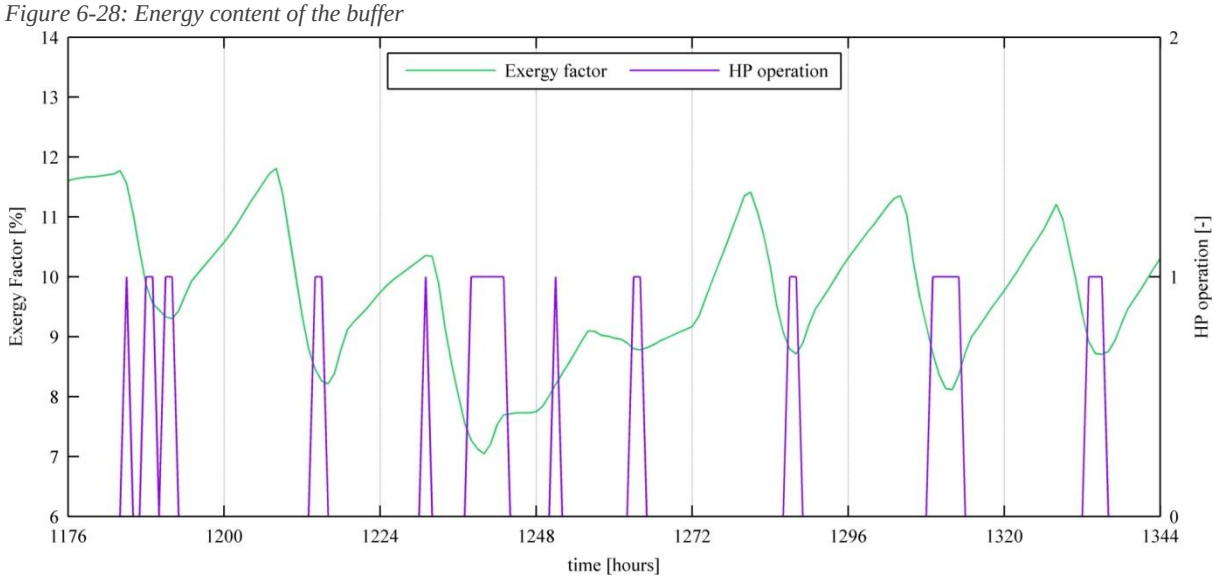

Figure 6-29: Exergy factor and operation pattern of the installation

Table 6-5 – yearly sums strategy D, and savings compared to strategy A (similar volumes)

Buffer volume [kg]	5e2	Reduction [%]	2e3	Reduction [%]
Energy generated [MJ]	14.964	-	15.315	-
Work (electrical en. consumed) [MJ]	3.748	7	3.647	10
Primary energy consumed [MJ]	9.594	7	9.336	10
Hours that installation is on [h]	1.041	7	1.013	10
Number of on/off cycles [-]	861	+133	455	+310

6.5.5 Comparison strategies

The yearly primary energy consumption of the strategies discussed in the previous subsections, are presented altogether in Figure 6-30. Performance for other volumes are also plotted, the numbers can be found in Appendix C. For small volumes, strategy D with a 12 hour receding horizon gives the best results (approximately 800 MJ savings at 500L). Larger buffer volumes enable the storage of the energy demand of one full day, which further increases the savings (a prediction horizon of one day becomes attractive above 75 MJ maximum energy content). Similar differences are found in annual hours of operation (Figure 6-31).

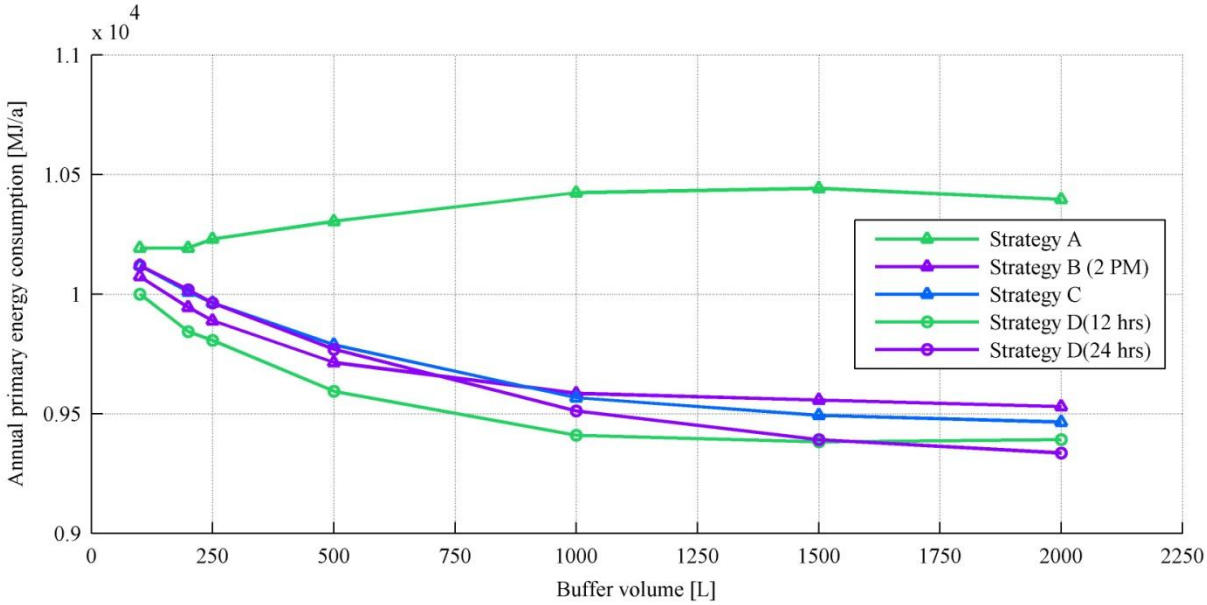

Figure 6-30: Primary energy consumed yearly for every strategy

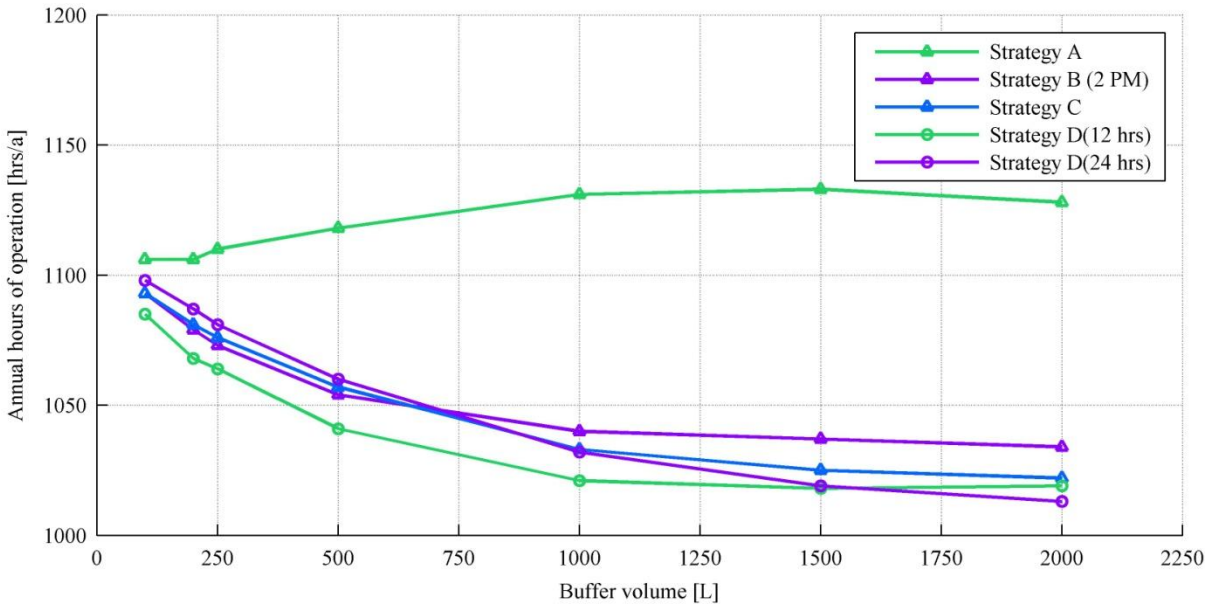

Figure 6-31: Yearly operational hours installation for every strategy

Reference strategy A represents the minimum amount of on/off cycles possible, because the heat pump only switches off after the buffer is completely recharged. The same partly applies to the second strategy (at small volumes it performs like the other strategies because the buffer is empty before the desired hours of operation have been reached). As could also be seen in the exemplary winter week, strategy C and D (24 hr horizon) establish a smoother operation profile for larger buffer volumes because it considers the most optimal suboptimal hours as well.

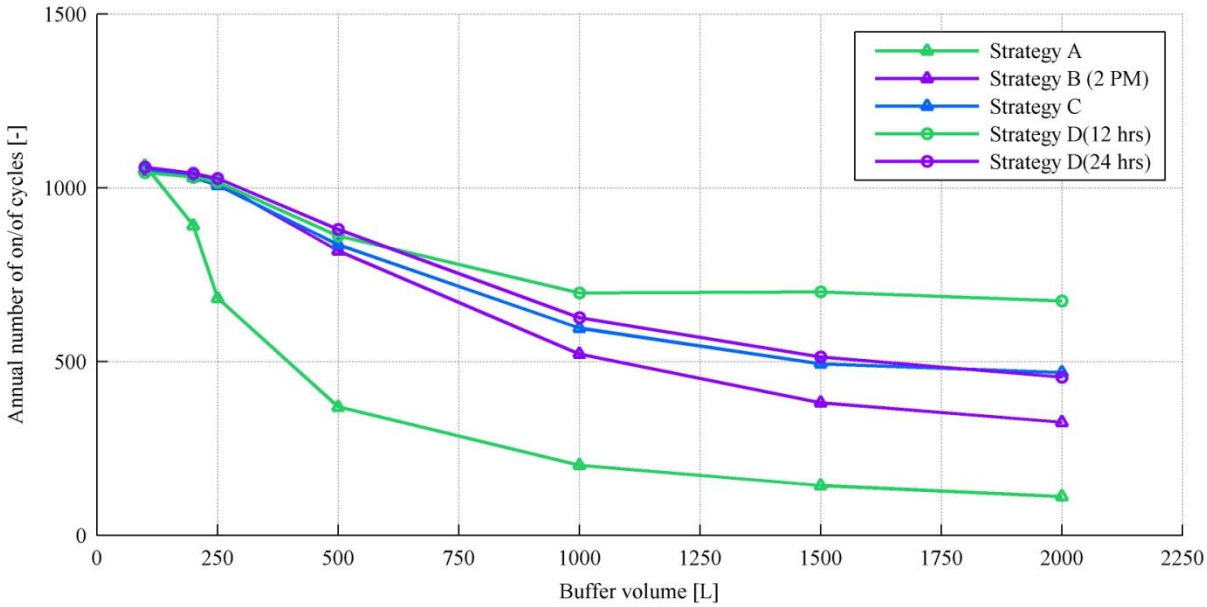

Figure 6-32: Annual number of on/off cycles for every strategy

Finally -although in a small extent-, Figure 6-33 proves that the optimization strategies, despite heat pump operation during hours of high-tarif electricity, reduce the electric energy input in such a degree that *operational* costs are decreased on a yearly basis.

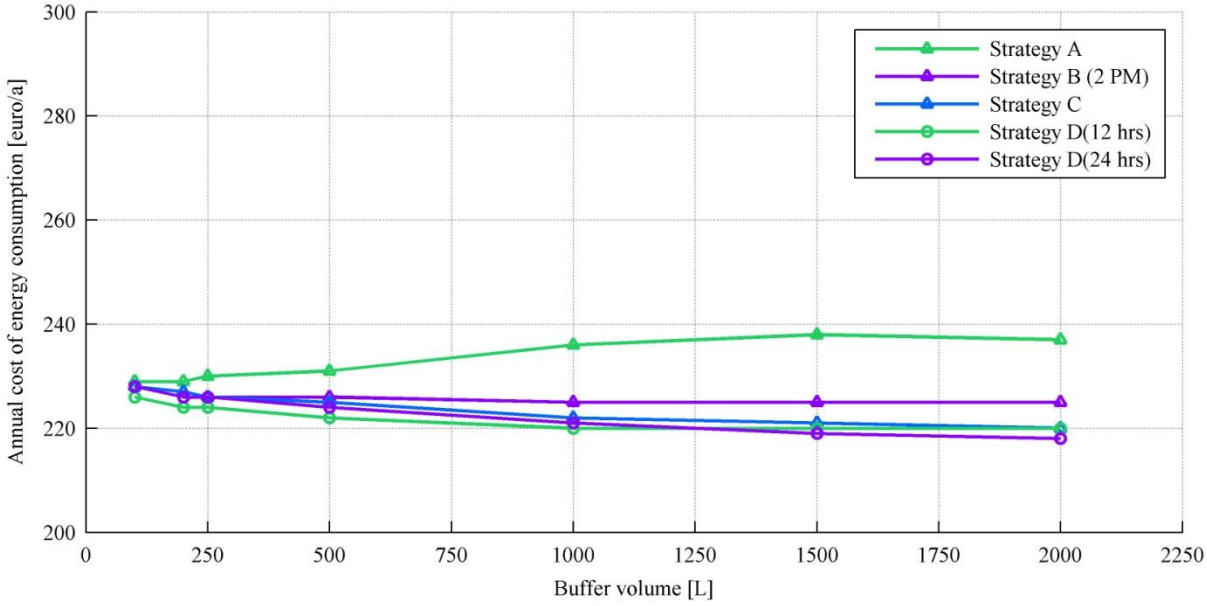

Figure 6-33: Yearly costs of electricity consumption installation for every strategy

6.6 Sensitivity analysis

In this subsection the influence of changes in some important parameters is examined. Although sensitivity analysis is performed for all strategies, this report only contains results for the reference strategy A and strategy D (12 and 24 hr prediction horizon). Parameters in Table 6-6 were varied:

Table 6-6 – Parameters analyzed in sensitivity check

Parameter	Default	Variant 1	Variant 2
Longer prediction horizons [hrs]	C (12), D (12,24)	C (48)	D(48)
Installed power P_{EL} heat pump [kW]	1,0	0,75	1,50
Annual heat demand [MJ/year]	14.488 (32,5 kWh/m²)	10.866 (24 kWh/m²)	7.244 (16 kWh/m²)
Temperature limits buffer [C]	23 -35 (12 K)	29 – 36 (7K)	-
DHW	DHW not considered	DHW	

First, the performance of strategy A and D (2000L buffer) during an extreme winter week (2nd week February) should be mentioned. The associated graphs can be found in subsection 12.1.2. Extreme cold conditions do force strategy D to operate at suboptimal moments (operation during minimum temperatures still avoided). This is the main reason for the large number of on/off cycles compared to strategy A. When comparing the figure below with the average outside temperatures in Figure 6-1, one could see that the algorithm works best during moderate conditions.

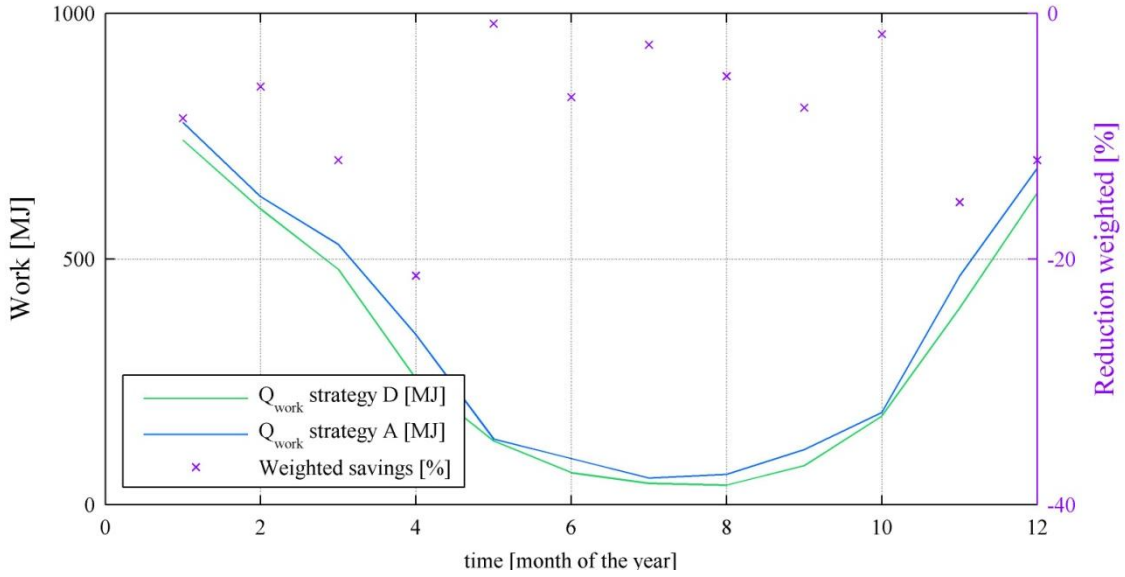

Figure 6-34: Weighted reduction in work consumed, monthly values

Below, the main conclusions per varied parameter will be summarized (details in appendix):

Prediction horizon–Table 12-9 shows that considered volumes and associated energy content, are insufficient for storage more than one day ahead. Longer horizons don't gain additional savings.

Annual heat demand – The optimization strategies perform significantly better at lower heat demands (with the same stored energy more hours of heat demand can be covered).

Temperature limits buffer – This parameter can reduce the potential of the storage strategies to a small extent (a 5 degrees smaller difference leads to 2% less reduction of work/primary energy).

Installed power – A buffer tank allows for a 25% smaller installed power, while still meeting the heat demand. Moreover, the storage strategies maintain relative savings, see Figure 6-35. Obviously, the yearly hours of operation will increase when using a smaller heat pump.

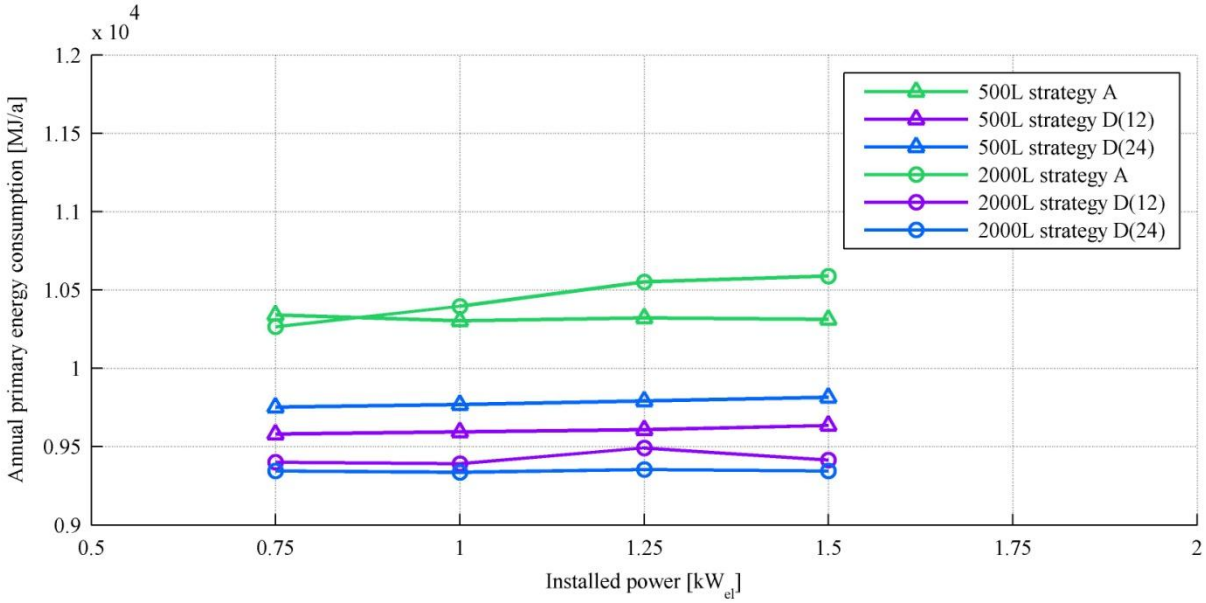

Figure 6-35: Yearly primary energy consumption strategies A and D, for different installed power

DHW production – Although application of the optimization algorithms to the DHW demand results in primary energy savings up to 5% yearly, the performance is negatively influenced by large thermal losses that are associated with storage of hot water in larger buffer volumes.

6.7 Conclusions

Three control strategies have been developed in order to optimize the daily heat load profile (and energy generation accordingly) so that the heat demand (14.488 MJ_{th} per year) is met with a minimum amount of work. The developed strategies can be combined with TES systems of any size and can therefore be applied to optimize storage for different time spans.

This study investigated short term storage in a reference dwelling. Calculations on the performance of the storage strategies were therefore limited to relatively small storage volumes (i.e. storage of small energy quantities). The three optimization strategies were compared to a conventional control strategy, which controls the heat pump without notion of exergetic performance. Yearly calculations show that the strategies seem to yield significant reduction of work (and primary energy) when combined with storage volumes larger than 250 liters sensible heat storage. Especially buffer capacities equivalent to energy quantities that could be stored in latent TES systems, can be regarded with cautious optimism. The control strategy using a Greedy optimization algorithm (strategy D)

shows most promising results. A 12 hour receding horizon performs best for small buffers, combined with large storage capacities an one-day horizon shows best results. The potential in minimization of work becomes visible in the distribution of generation per exergy factor, Figure 6-36 (after doctoral thesis on exergy in the built environment (Jansen, 2013)). Control strategy D shows a shift of the energy generation (and heat load) towards lower exergy factors compared to reference strategy A.

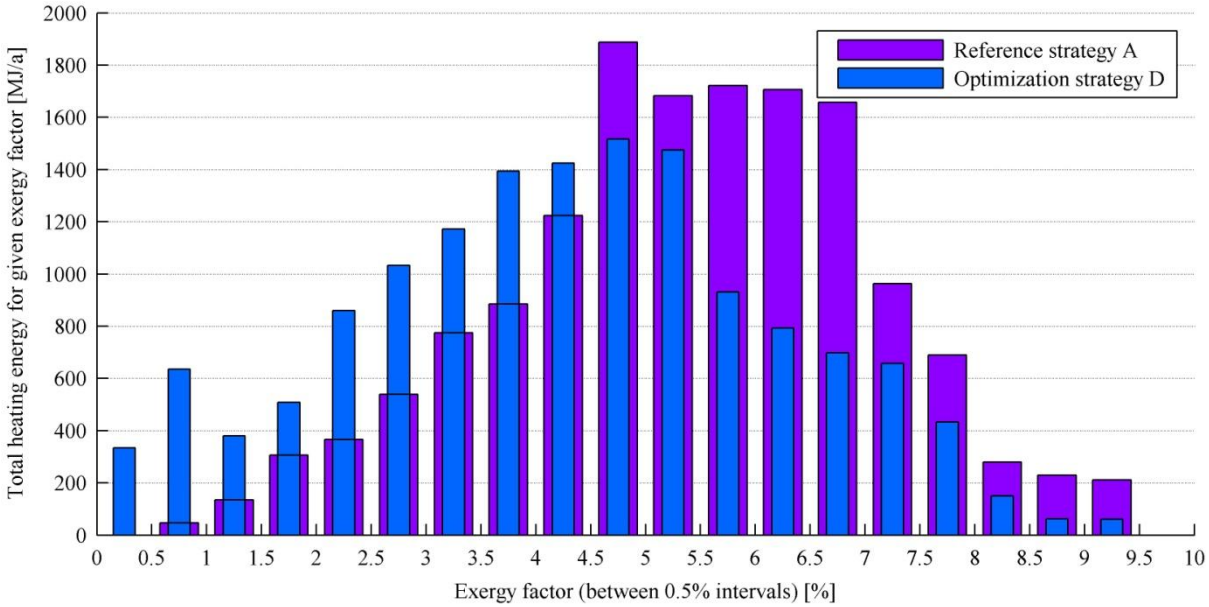

Figure 6-36: Distribution of yearly heating energy per exergy factor of this demand (F_{ex} = 1-T_0/T_{room})

Sensitivity analysis showed that the outcomes should be considered with caution, because of assumptions that had to be done within the non-continuous MATLAB model. Further investigation that considers dynamic effects of some important parameters will reveal if the potential that can be concluded from the MATLAB exploration is justified.

6.7.1 Use cases for further investigation

The reference TRNSYS model will use a control strategy similar to strategy A. From the MATLAB exploration and discussion of the results, follows that strategy D ensures an optimal minimization of work and primary energy consumption. Therefore, this strategy should be further investigated using TRNSYS. From a practical point of view (space limitations in dwellings), a 500 L sensible storage buffer will be investigated. Secondly, it would be interesting to see if a more compact volume of 200L including latent heat storage could have the same performance as the 500L tank (useful energy content both ±25 MJ_{th}). Finally, a storage system with capacities equivalent to 1500 and 2000L water (energy content 75-100 MJ_{th}) will be evaluated, since the MATLAB model showed most potential savings for these capacities. An overview of the use cases following from the MATLAB study:

Storage volume [L]	Eq. useful energy content [MJ]	Storage strategy (prediction horizon 12 + 24 hrs)
200, including PCM	~ 25	Reference A, strategy D
500	~ 25	Reference A, strategy D
600, including PCM	~ 75-100	Reference A, strategy D

7 Assessment dynamic effects storage component and emission system

7.1 Theory on low-temperature heat storage media

7.1.1 Phase Change Material

This paragraph will first discuss the most important properties of PCM more into detail, followed by an overview of different ways of integration of PCM into a real TES system. This introduction is required before the final simulation model is explained. Finally, the simulation results are presented together with conclusions.

7.1.2 Material properties

Phase Change Materials are used for storage of heat with larger energy densities combined with rather small temperature changes. Important to mention is that PCM are engineered, since their properties can be customized by changing the composition. The following properties should be considered for a good latent storage system design (Dincer & Rosen, 2002; Gunther, 2009):

- high latent heat of fusion or phase change enthalpy, Δh
- suitable phase-change temperature, T_{pc}
- good heat transfer.

7.1.2.1 Latent heat of fusion and enthalpy

In sensible storage, a quantity of heat Q is stored by changing the temperature of a storage medium:

$$Q = \int_{Ti}^{T2} m \cdot c_p \cdot \mathrm{dT} \qquad 7.1$$

where T_i is the initial temperature and T_2 the final temperature of the medium with specific heat c_p.

Latent thermal energy storage involves storage of a large amount of heat in the form of latent energy during the phase change of a storage medium (Lane, 1986):

$$Q = m \cdot a_m \cdot \Delta h_m + \int_{Ti}^{Tpc} m \cdot {c_p}^{solid} \cdot \mathrm{dT} + \int_{Tpc}^{T2} m \cdot {c_p}^{liquid} \cdot \mathrm{dT} \qquad 7.2$$

where in the left term of this equation, a_m is the fraction melted and Δh_m the heat of fusion per unit mass. Δh_m is a change in enthalpy during the change of the substance from one state to another. The enthalpy h is a measure of the (internal) energy per unit mass of a substance, expressed in kJ/kg. Table 3-2 contains the heat of fusion of several relevant PCM, showing its advantage over sensible heat storage. PCM with a high latent heat of fusion are preferable, so that a given amount of energy can be stored with a smaller amount of material.

The storage capacity of latent systems is also defined by the sensible heat capacities in solid and liquid state, which are included in resp. the central (c_p^{solid}) and right (c_p^{liquid}) term of equation 7.2. These terms use the normal expression of the enthalpy as a function of $c_p \cdot d$T from eq. 7.2

7.1.2.2 Phase change temperature

The initial literature review showed that PCM are available in a wide spectrum of melting temperatures and compositions. Many PCM show a broadened melting range, meaning that the phase change enthalpy is not attributed to a single temperature but to a transition temperature zone (Mehling, 2008; Gunther, 2009). Only two PCM material classes are available commercially, with melting temperatures relevant for application in the built environment: salt hydrates and paraffin.

For an optimal latent TES unit, the transition zone of the PCM must match the intended operating temperature span of the latent TES unit (i.e. operating temperatures of the heating and cooling systems). Storage units using salt hydrates are limited to the range of 15-65˚C, because their fusion-solidification behavior can't be easily modified (Dincer & Rosen, 2002). Paraffins can be composed with much wider melting temperature ranges.

7.1.2.3 Thermal conductivity

Table 7-1 makes clear that non-organic PCM do have a better thermal conductivity than organic materials i.e. non-metallic liquids (Mehling, 2008). This means that paraffins (organic PCM) do have poorer heat transfer properties. Since PCM store large quantities of heat in a small volume, and that this heat needs to be transferred to the outside of the storage in order to utilize it, low heat transfer coefficients do form a problem associated with latent heat storages.

Table 7-1 Thermal conductivity of different PCM materials (source: Mehling 2008)

PCM class	Thermal conductivity [W/mK]
Organic	0,1 W/mK
Non-organic	0,5 W/mK
PCM-graphite 1	5 W/mK
PCM-graphite 2	25 W/mK

Several measures can be taken in order to improve the heat transfer coefficients of latent heat storage. Enhancement techniques involve addition of fins, insertion of a metal matrix in the PCM, PCM dispersed with high conductivity particles (e.g. graphite) or micro or macro encapsulation within containers with good thermal conductivities (Agyenim, 2009).

7.1.2.4 Real behaviour versus theory

In real applications, the behaviour of PCM deviates from theoretical behaviour. The following effects are described in literature, see Figure 7-1:

Hysteresis – Change from liquid to solid state (melting) occurs at a higher temperature than phase change from liquid to solid (solidification). The degree of hysteresis can be engineered.

Subcooling – The material does not solidify immediately upon cooling below the thermodynamic melting point, but after a temperature well below it is reached. This problem only occurs in salt hydrates, paraffins exhibit little or no subcooling (Dincer & Rosen, 2002). Subcooling can be reduced or prevented by addition of nucleators.

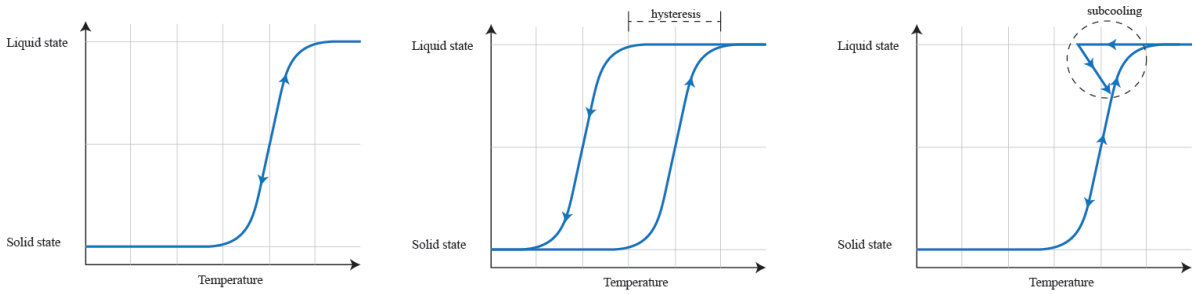

Figure 7-1: Theoretical melting and solidification process (left), hysteresis (center) and subcooling effect (right)(Notenboom DWA, 2013)

7.1.2.5 Selection

Main advantages and disadvantages of hydrated salts and paraffins are summarized in Table 3-1. PCM can be compared according to various thermodynamic, chemical, technical and economical criteria (Dincer & Rosen, 2002). Besides poorer heat transfer properties, paraffins do have lower densities, greater fire hazard, more nuisance potential and higher costs than salt hydrates. Therefore hydrated salts are more attractive for implementation in TES. Another important parameter in the selection of an appropriate PCM material, forms the embodied energy. By taking into account the energy associated with the manufacturing process of PCM and its final disposal, an assessment can be made of the energy reduction achieved during the complete life cycle of the PCM. Salt hydrates have smaller embodied energy than paraffins (de Gracia, 2010).

7.1.3 Design concepts latent heat storage

Considering the rather low conductivity of PCM, storage design plays a key role in improvement of the heat transfer and thus the storage performance. Mehling defines three major principles of latent heat storage (Mehling, 2008).

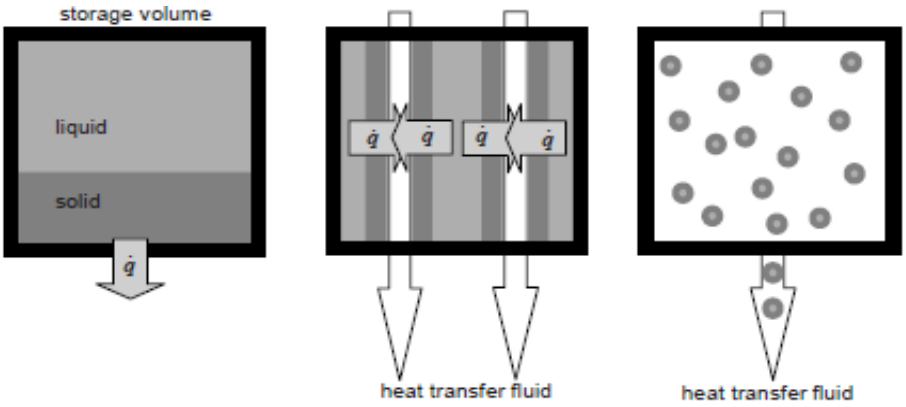

Figure 7-2: Basic latent heat storage design options, heat exchange by heat transfer: on storage surface (left), on large surfaces within storage (center) or by exchanging the storage medium (right). (Mehling, 2008)

7.1.3.1 Heat transfer at the surface of the storage

The storage options were classified according to the way heat is transferred from the storage for final use (i.e. discharging the storage).

In the first option, heat transfer to a fluid occurs on the surface of the heat storage. Active control of the (dis)charging process of the PCM is not possible. Heat transfer can be maximized using a container or surface material with a high thermal conductivity or by increasing the heat exchanger area. This design can be found in passive application of PCM for room temperature control purposes (Mehling, 2008), i.e. increasing thermal inertia instead of active storage. Examples of this storage option is integration of PCM in building materials, e.g. PCM enhanced concrete or wallboards or PCM modules in a floor heating system or cooled ceiling (Baetens, 2010; van der Spoel, 2004).

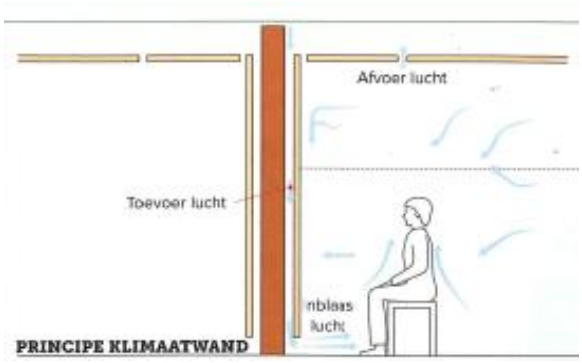

Figure 7-3: Air vented PCM wall panels, Ecofactorij Apeldoorn (Wind, 2012)

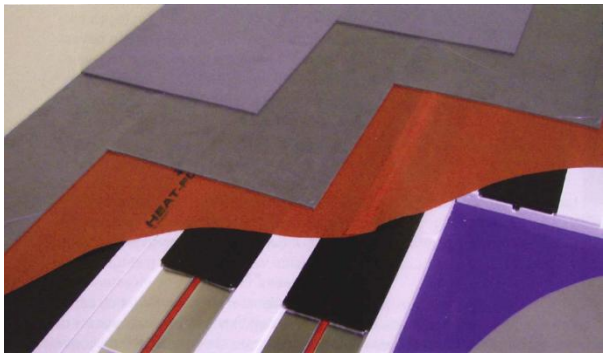

Figure 7-4: PCM lamella's on top of the floor heating piping, Unifloor floor heating system (source: unifloor.nl)

7.1.3.2 Heat transfer on large surfaces within the storage

A very efficient way of increasing heat transfer area, is using internal heat transfer surfaces, which is the second design concept. A heat transfer fluid is required to transport heat in and out of the storage. Heat is transferred by actively moving the heat transfer fluid (forced convection) and not by free convection. This so called *active* heat transfer allows the storage process to be controlled, which makes it a suitable method for storage of heat and cold. By not only exchanging heat at the storage outside surface, less PCM is required to store the same amount of energy (Mehling, 2008; Cabeza, 2011). Three basic types of PCM storages with heat transfer on internal surfaces can be distinguished. They will be discussed according to the most important output variables in storage design: the storage density and (dis)charge power (Heinz & Streicher, 2006).

Heat exchanger – this involves storages that work like any other heat exchanger between two fluids, in this case one side of the heat exchanger contains PCM. The HTF flows through the heat exchanger and exchanges heat with the PCM. Usually, a heat exchanger type storage consist of a storage vessel filled with PCM and an internal heat exchanger (e.g. equally distributed pipes). This configuration results in very high storage densities, up to 95 vol.% PCM. An example is the Ecophit pipe heat exchanger (see Figure 7-5), which is filled with 85 vol.% salt hydrate (NaOAc). In this case

the PCM was dispersed with graphite in order to improve heat transfer (Mehling, 2008). Medrano has experimentally investigated several small water heat exchangers with PCM in one side, and concluded maximum thermal powers and storage densities for a compact heat exchanger and double pipe heat exchangers (Medrano, 2009). Flat plate air to air heat exchangers (e.g. used in airconditioning) with PCM are slightly different from the previous examples. The large number of thin metal fins that are attached are to the heat exchanger in order to increase the heat transfer surface because of low convective heat transfer coefficients on the air side, are now used to enhance heat transfer in the PCM (Heinz & Streicher, 2006; Stritih, 2003). An example of this system is shown in Figure 7-6.

Storages of this type typically achieve high thermal power at the start of the (dis)charge, while the power that can be obtained later highly depends on the heat exchanger design. A disadvantage of this system is that it's envelope and the heat exchanger need to be geometrically adjusted in order to ensure proper heat transfer in all parts of the PCM (more expensive, restricts flexibility in storage design). Besides, integration of PCM with different melting points is relatively difficult.

Figure 7-5: Pipe heat exchanger Ecophit (SGL Technologies)

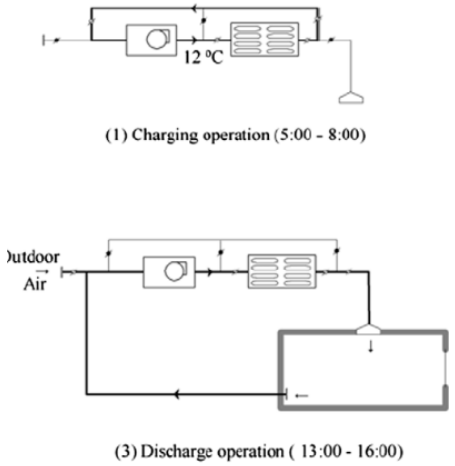

Figure 7-6: HVAC integrated PCM, for peak load shifting and free cooling purposes in an office (Yamaha and Misaki)

Direct contact – In contrast to the heat exchanger type, in a direct contact storage the heat exchange between the heat transfer fluid and the PCM proceeds without a heat exchanger wall (direct contact with the PCM). The absence of thermal resistance of a heat exchanger wall improves the heat transfer. In order to prevent mixing, the PCM should be insoluble in the heat transfer fluid, and the density of the PCM should be sufficiently high for enabling phase segregation. In case of salt hydrates, oil can be the HTF. Since PCM has a higher density than the HTF, the HTF is pumped into the storage from the bottom and exchanges heat with the PCM while it rises (Figure 7-7). Only experimental set-ups reported, e.g. a 1000mm high cylinder using a PCM-oil mixture in (Nomura, 2013). Volume fractions PCM (thus storage densities) similar to that of indirect heat exchangers are possible. Compared to indirect heat exchangers without heat transfer enhancement e.g. fins, direct contact storages can exchange heat more rapidly because of the direct contact. Direct contact systems

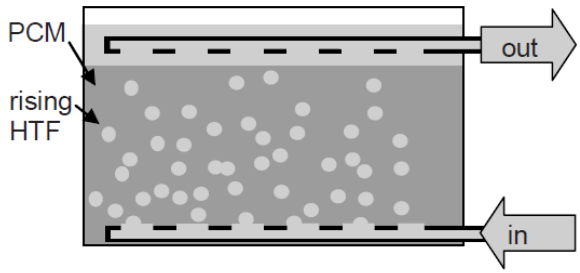

Figure 7-7: Direct contact storage principle (Mehling, 2008)

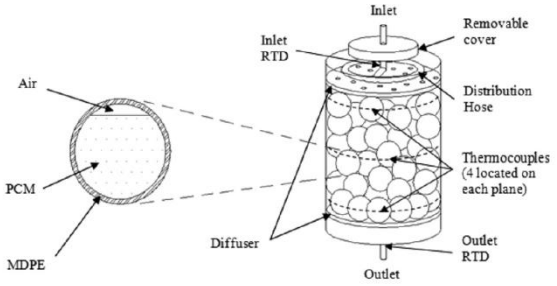

Figure 7-8: PCM nodule and TES system (Amin, 2012)

also have simple structures. A disadvantage is that an extra pump and heat exchanger are required since the HTF can't be directly supplied to the emission system (the HTF coming from the storage might be contaminated with PCM) (Mehling, 2008; Nomura, 2013).

Macroencapsulation (modules) – concerns inclusion of several ml to liters PCM in a macroscopic containment (Mehling, 2008). Because of its corrosive nature, salt hydrates are often macro encapsulated. Modular systems allow for easy integration in buffer tanks and the possibility of using PCM with different melting ranges in one tank (Heinz & Streicher, 2006; Ibanez, et al., 2006). Also, modules are easier to manufacture, and prefabrication allows cheaper series production. In order to guarantee a good heat transfer between the surrounding heat transfer medium (water is most common) and the PCM, the modules should have a high surface area to volume ratio. Different geometries were investigated before, cylindrical and spherical modules are most common and can achieve a good surface area to volume ratio.

Storages with macroencapsulated PCM in combination with air as a heat transfer fluid were investigated, mainly using flat plate modules (better heat transfer). This study however focuses on applications using water as HTF since this is the medium used by the heating emission system. The most common encapsulation in module storages uses spheres. Spherical capsules, also called *nodules*, arrange themselves automatically when filled into a tank. The maximum possible PCM fraction using nodules of similar size, is 74 vol.% (Mehling, 2008). An example is a cylindrical tank filled with 60 spheres of 37mm diameter which equals 40 vol.% PCM (Amin, 2012), see Figure 7-8.

The performance of cylindrical PCM modules within a storage tank was also tested, using PCM fractions of 30 vol.% (Heinz & Streicher, 2006). This experiment tested modules filled with PCM, a salt hydrate – graphite compound showed higher discharge powers than paraffin. The higher conductivity of the compound thus led to shorter discharge times, which is preferable in most applications. The tests were used to validate a TRNSYS model (Puschnig, et al., 2005), in which module diameters were varied. This numerical model confirmed that smaller diameters (higher area to volume fractions) result in better heat exchange. (Cabeza, et al., 2006) describes an experiment including PCM modules in the top of a storage tank only, in order to reheat the water by PCM more

effectively since it compensates thermal losses at the top (storage density is increased only at the top, see Figure 7-9). Different volume fractions ranging from 2 to 6 vol.% PCM were investigated, using different module configurations. Higher PCM fractions resulted in higher storage densities (20-45% more) but were accompanied by higher thermal losses.

Storages using modules do combine latent heat storage with a considerable amount of sensible heat storage, since the fraction of water is typically more than 25 vol.%. Compared to the previous heat exchanger storage types, the storage density of storages with macroencapsulated PCM is thus lower. The discharge power of these systems right after the start of (dis)charge however, is relatively high. (Dis)charge time depends on the heat transfer between the PCM modules and surrounding water.

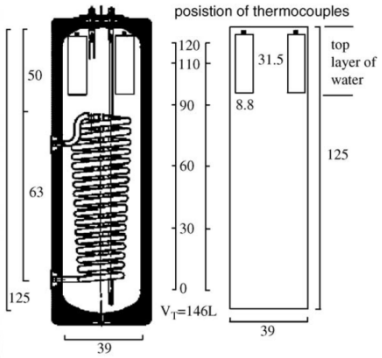

Figure 7-9: Hot water tank and PCM modules (Cabeza, 2006)

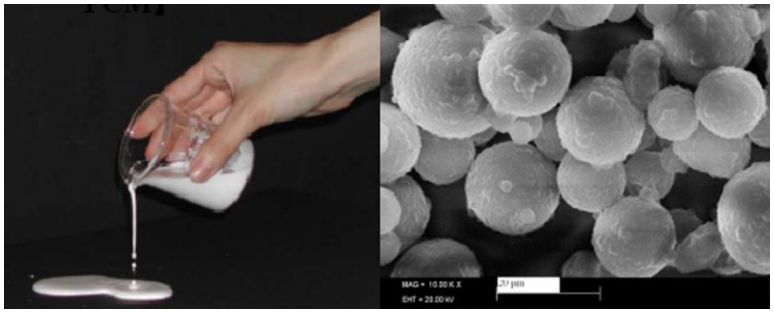

Figure 7-10: PCM slurry and microscopic image of PCM particles (Wang, 2008)

7.1.3.3 Heat transfer by exchanging the storage medium

In the previous storage types, the PCM remained within the storage vessel and heat was exchanged using a heat transfer fluid. This heat transfer however takes time and improvements do complicate the storage design. In the third main storage option, the HTF is the heat storage medium itself. This is possible by encapsulation of PCM in capsules with diameters of just a few μm, called microencapsulation. If these microcapsules are dispersed in water, a pumpable substance is obtained, called *slurry*, see Figure 7-10. The water ensures fluid behavior even when the PCM within the capsules is solidified. Microencapsulation is only possible for paraffin, and has several advantages:

- A slurry will transport more energy at the same volume flow rate and the piping system itself acts as (part) of a storage.
- Large number of small capsules improve the heat transfer (larger heat transfer area).

Although an increase of the concentration of microcapsules will increase the storage density of the slurry, the viscosity will also increase strongly. Slurries with a 40% PCM concentration has been successfully pumped (Heinz & Streicher, 2006), higher concentrations would reduce heat transfer coefficients and increase pressure losses while pumping. Slurry storage can be used for heating and cooling applications, because slurries can be pumped into emission systems, e.g. floor heating or

climate ceilings. (Wang, 2008) describes a cooled ceiling system combined with a slurry storage. Storages using slurries do have a high (dis)charge power because of the increased energy density of the HTF. Associated storage densities compared to the previous design options is typically lower (Mehling, 2008; Heinz & Streicher, 2006).

The design guidelines from literature were translated into several storage layouts that could be implemented in the basic circuit of the case study dwelling. They are included in Appendix E. Only one storage design was selected for further detailed simulation of the different use cases.

7.1.3.4 Storage duration and selected design principle

For short term storage the discharge power normally has to be relatively high in comparison to the storage densities (in long term storage applications this is vice versa) (Heinz & Streicher, 2006; Mehling, 2008). This requires certain conditions concerning PCM module sizes or the thermal conductivity of the PCM material respectively.

For high thermal powers, storage designs with heat transfer on internal surfaces are favorable. Macro-encapsulation and heat exchangers do achieve maximum discharge powers, which make these concepts most potential for further investigation of their performance for short term storage. Besides, these storage systems can be charged and discharged at any moment desired (active heat transfer), which is necessary when combined with the developed storage control strategies.

Direct and indirect heat exchangers can achieve higher storage densities, but macroencapsulation in modules provides slightly higher discharge power, because of the combination of latent and sensible heat storage. Besides, modular systems do provide more design flexibility (different configurations and PCM fractions can be realized easily) and are most interesting from economical point of view. A final advantage of modules over heat exchangers is that their performance can be assessed more easily in numerical models.

7.2 TRNSYS model

7.2.1 Description basic model

In short, TRNSYS (V17) is an energy simulation software that uses a modular system approach. This approach makes it a flexible program, in which new components ("Types") can be integrated..

7.2.1.1 TRNBuild

Dynamic space heating energy demand of the case study was derived from TRNBuild. The TRNBuild preprocessing kernel can be used to construct a multi-zone building (Type 56), which allows detailed simulation of the thermal behavior of multiple thermal zones. The input is described in Appendix B. In order to simulate different occupation patterns and temperature controls, two thermal zones were distinguished: a living (ground floors) and a sleeping zone (two top floors).

7.2.1.2 Exergy calculation

Use cases will be analyzed and compared using dynamic calculations of the energy and exergy demand. A yearly calculation with a 0,1 hour time step is performed for every case. Exergy values are calculated per time step, using ambient air temperatures as reference temperature T_0 (Torio & Schmidt, 2011). The exergy factor of heat at constant temperature is calculated using the simplified approach (Jansen, et al., 2010; Walls, 2009) of equation 7.3. The exergy factor of sensible heat transferred by a flow of matter (e.g. water) can be calculated using the thermodynamic average of T_1 and T_2 in equation 7.4. In order to prevent simulation errors in case $T_2 = T_1$ (e.g. in initial condition), this thermodynamic average was replaced by the numerical average of T_1 and T_2 (eq. 7.5), a simplification that does not introduce big differences in resulting exergy values for small dT. This equation is used to calculate the exergy of inputs and outputs of each energy system component.

$$F_{ex} = 1 - \frac{T_0}{T} \tag{7.3}$$

$$F_{ex}(Q_{sens}, T_2 - T_1) = \left(1 - \frac{T_0}{T_2 - T_1} * ln\frac{T_2}{T_1}\right) \tag{7.4}$$

$$F_{ex}(Q_{sens}, T_2 - T_1) = 1 - \frac{T_0}{\overline{T}} \tag{7.5}$$

7.2.1.3 Simplified model

In order to be able to dimension the building services, a calculation has been performed in TRNSYS without the climate system but with the correct building characteristics. TRNSYS is able to define the ideal heating and cooling power necessary to maintain the room temperature above the heating setpoint and below the cooling setpoint. Since the TRNBuild kernel defines the ideal heating power based on occurring air temperatures instead of operative temperatures, the temperature setpoints were converted as follows:

$$T_{air} = (T_{operative} - 0{,}5 * T_{mean;surface}) * 2 \tag{7.6}$$

The outcomes of the simplified yearly simulation are shown below.

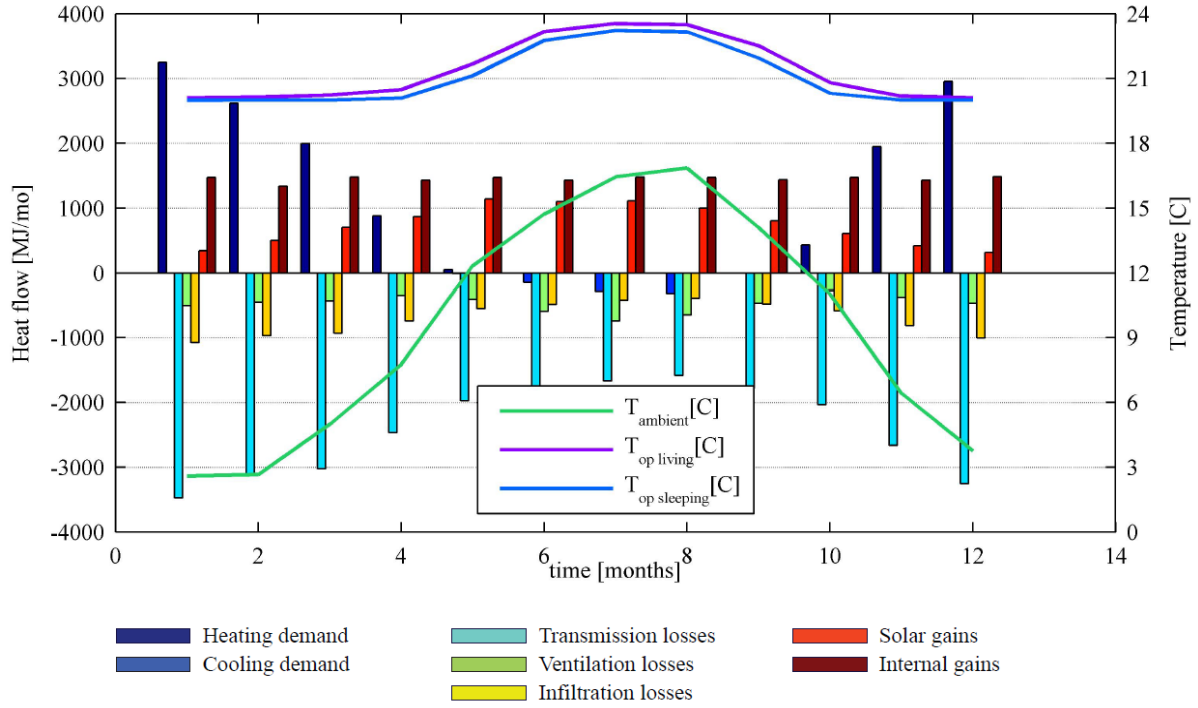

Figure 7-11: Parameters in monthly energy balance of the dwelling, living and sleeping zone together

Cooling demand only occurs from June to August, as can be seen in Figure 7-11, and the loads are not very significant (yearly cooling demand: 764 MJ or 212 kWh). This proves that the cooling case can be taken care of by passive measures. Passive measures used in this model are a bypass control of the heat recovery system, additional natural ventilation above room temperatures of 24 ℃ and sunshading on the South façade. The heat pump could be reversed in order to supply the remaining cooling load. Energy and exergy (simplified calculation) values for the heat demand are summarized below:

Table 7-2 Monthly energy and exergy demand for heating, per zone

Month	Avg Te [C]	QHEAT living [MJ]	Exdem,Q_H living [MJ]	QHEAT sleeping [MJ]	Exdem,Q_H sleeping [MJ]	QHEAT total [MJ]	Exdem,Q_H total [MJ]	F_{EX} (Ex/En) [%]
January	2,6	1.050	71	2.202	141	3.252	212	6,5
February	2,7	823	56	1.791	115	2.614	172	6,6
March	5,0	577	35	1.418	81	1.995	116	5,8
April	7,8	228	13	654	35	881	48	5,4
May	12,3	11	1	41	2	51	3	4,9
June	14,7	0	0	0	0	0	0	0
July	16,4	0	0	0	0	0	0	0
August	16,8	0	0	0	0	0	0	0
September	14,1	0	0	0	0	0	0	0
October	11,0	90	5	342	16	432	20	4,7
November	6,4	575	30	1.400	72	1.948	103	5,3
December	3,8	934	60	2.022	123	2.957	183	6,2
Total	**9,5**	**4.261**	**271**	**9.869**	**584**	**14.129**	**855**	**5,7**
Total [kWh]	**-**	**1.184**	**75**	**2.741**	**162**	**3.925**	**237**	**-**

The living zone has smaller heat demand (23 kWh/m^{2}a) than the sleeping zone (38 kWh/m^{2}a). This difference has two causes. First, the internal gains of the living zone are larger than in the sleeping zone (especially during the evening), and internal gains do have a big impact in well insulated buildings. Secondly, the living zone consists of a large South-orientated glazed façade, which means more solar gains are absorbed compared to the sleeping zone. Instantaneous heat demands are summarized in Table 7-3. The maximum occurring total instantaneous heat demand is 2.9 kW. This means a heat demand of circa 24 W/m^2 net floor space, which is a reasonable value for a well-insulated dwelling.

Table 7-3 Maximum instantaneous heat demands per zone

	Living zone	Sleeping zone	Living + sleeping zone
Heating power [W]	1.689	1.722	2.940
Spec. power [W/m²]	32	24	24

7.2.2 Implementation energy system

7.2.2.1 Hydraulic circuit and temperature control

Subsequently the building services were implemented in the TRNSYS Studio, according to the system described in paragraph 5.5.4 Hydraulic circuit / Building services. The heat pump was simulated using Type 941. This Type simulates a single-stage air-to-water heat pump. Data for the heating capacity and electrical power input depending on the entering air temperatures and entering water temperature need to be supplied. The data supplied is based on manufacturer data described in Appendix D. The final hydraulic circuit is presented in Figure 7-12. The parallel buffer tank divides the circuit in a primary and secondary side (which can decouple the heat demand profile from the emission system on the secondary side from the heat generation profile on the primary side).

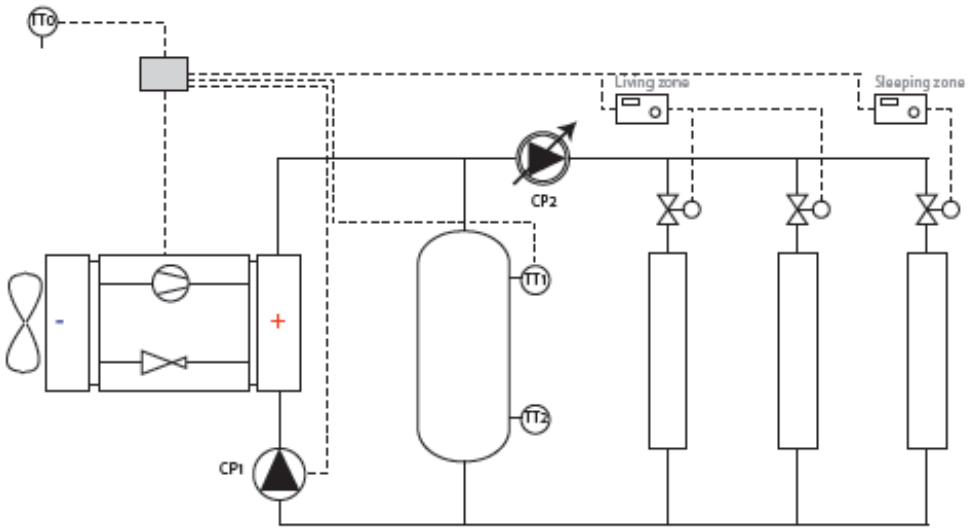

Figure 7-12: Hydraulic circuit, including the control connections to the heat pumps software

Primary circuit - (pre-)control of the heat pump operation depends on the storage control strategy that is simulated:

The conventional, reference strategy A uses an instantaneous climate curve in combination with the measured temperatures TT1 and TT2 in order to define operation of the heat pump. A weather based temperature control on the desired supply water temperature to the floor heating has been implemented. This climate curve is similar to the one used in MATLAB.

Control strategy D selects a sequence of heat pump operations based on an algorithm that aims to minimize the required work input of the energy generation according to prediction of the heat demand for a receding horizon.

Secondary circuit - the flow in secondary circuit (i.e. the actual heat demand) is based on the control variable room temperature (PID), see Figure 7-13 (only proportional/integral actions were activated, the derivative is not necessary for this purpose). This is called post-control, which is similar for all strategies. It is a simplified representation of real systems which include open/closed valves or stepped thermostats with hysteresis for different heating groups.

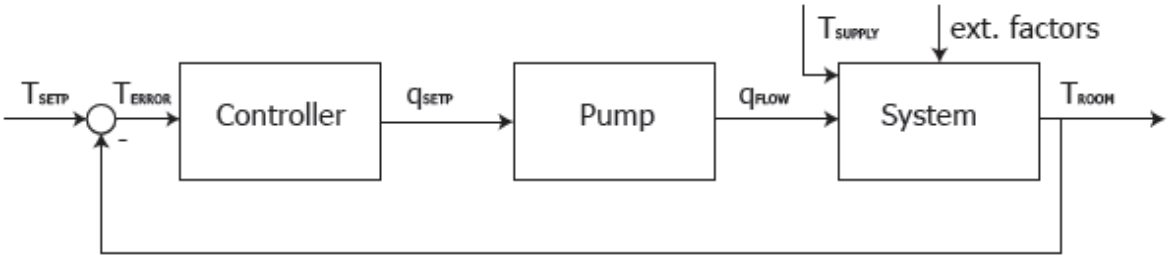

Figure 7-13: Block schematic of control strategy implemented in TRNSYS

7.2.2.2 Stratified storage tank

The storage tank is obviously the crucial component within the energy system, and this component has been simulated using the most detailed tank model in TRNSYS. The standard TRNSYS library only contains a sensible energy storage tank (Type 60), which is used for the simulation of the reference cases (sensible storage only). The number of calculation nodes can be defined, and the degree of stratification is determined by the number of horizontal segments (nodes) calculated (Klein, 2012). Type 60-f allows the height and thermal losses of every layer to be specified separately. Each layer is assumed to be fully mixed, so uniform temperature is assumed within each node.

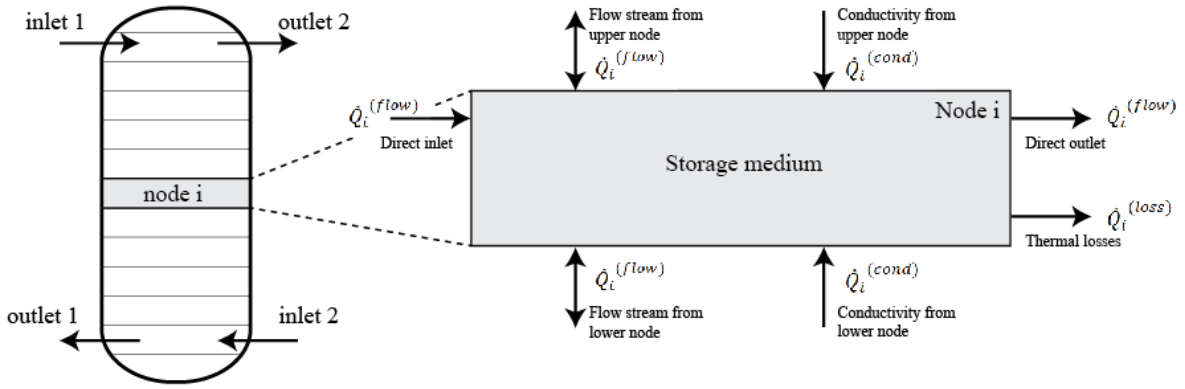

Figure 7-14: Energy balance for each i^{th} storage node (after Bony, 2005)

The energy balance (Figure 7-14) for every storage node is given by equation 7.7 (Klein, 2012):

$$\dot{Q}_i^{(medium)} = \dot{Q}_i^{(flow)} + \dot{Q}_i^{(cond)} + \dot{Q}_i^{(loss)} \qquad 7.7$$

where:

$Q^{(medium)}$ = energy of storage medium in node i

$Q^{(flow)}$ = charged or discharged energy via direct connection (inlet/outlet flow) and/or flow upward / downward within the tank

$Q^{(cond)}$ = thermal conduction to neighboring nodes

$Q^{(loss)}$ = thermal losses to the ambient through tank envelope

The temperature of each node T_i depends on the mass m_i and heat capacity of the storage medium C_p of that node, and is derived from equation 7.7 as follows (Bony, et al., 2005):

$$\dot{Q}_i^{(medium)} = m_i * C_p * \frac{dT_i}{dt} \qquad 7.8$$

A vertical cylindrical storage tank was modeled in the simulations, with 11 temperature levels and two inlets and outlets.

7.2.2.3 Emission system

The simulation of radiant heating or cooling systems integrated in massive constructions, involves the calculation of a multidimensional thermal conduction problem. In order to reduce calculation time, TRNSYS does not use a Finite Element Method to do this, but simplified calculation method developed by Koschenz and Lehmann (Koschenz & Lehmann, 2000). The method is suitable for dynamic calculations, and shows good accordance with FEM modeling according to the TRNSYS documentation (Klein, 2012). A detailed mathematical description can be found in the documentation. This calculation method is integrated within the Multizone building, so the floor heating system could be defined within the TRNBuild kernel.

The dimensions of the emission system that is simulated for the case study dwelling, are defined conform ISSO guidelines. Appendix H elaborates on the sizing of the simulated system.

7.2.3 Strategy A

In MATLAB, heat pump operation was based on energy content (full and empty) calculations for a fully mixed buffer. An approach that is closer to real energy systems could be simulated in TRNSYS. The conventional control of a heat pump combined with TES, reference strategy A in TRNSYS, is based on the common control strategy described in (ISSO 72, 2013). A stratified buffer was calculated, and heat pump operation is based on the water temperatures that are measured at the bottom of the tank (TT1, 20% height) and the top (TT2, 80% height). Since the top temperature is measured at a distance below the outlet, it's temperature will always be a few degrees below supply water temperature. The following operation order is used:

1. When heat demand occurs in the rooms, primary the buffer is discharged.

2. When TT1 drops below the required supply water temperature (conform climate curve), the installation is switched on. The on-off heat pump will slowly heat up the retour water from the floor heating until the required temperature is met. CP2 regulates the flow of the supply water depending on the room temperature (see Figure 7-13).

3. When the heat demand drops, the rest of the generated energy will charge the buffer (exponential effect: the more the heat demand drops, the faster the buffer is charged).

4. The installation is switched off when TT2 exceeds the climate curve temperature.

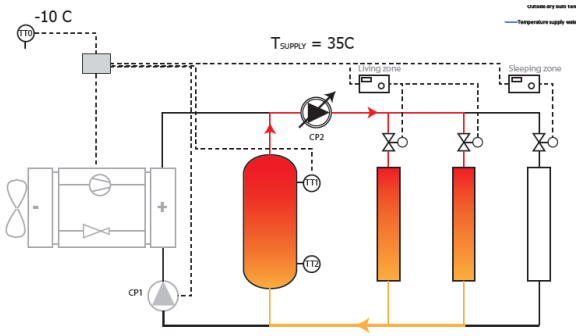

Figure 7-15: Step one: discharge the buffer

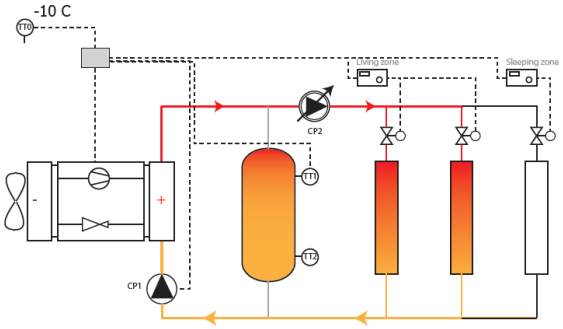

Figure 7-16: Step two: provide heat demand with HP

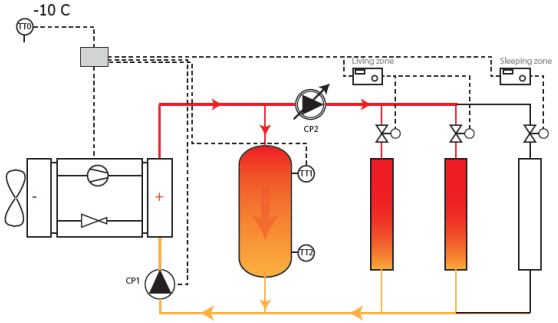

Figure 7-17: Step three: recharge buffer when heat demand in groups decreases

7.2.4 Modelling of optimization strategy D

A connection had to be made between MATLAB and TRNSYS, because the optimization algorithm of strategy D, was written in MATLAB. Calling a MATLAB algorithm during a simulation is possible via Type 155. Prior to every time step, the algorithm defines the optimal control sequence and communicates to TRNSYS whether the heat pump should operate during the next time step.

7.2.4.1 Predictive control strategy

The algorithm that was written for the exergy minimization problem described in subsection 6.3 and was assessed in the hourly-time step MATLAB model, needed some adjustments in order to be used in the transient TRNSYS simulation.

First, the predicted energy generation was adjusted to the performance curves of the modeled air-to-water single stage heat pump (see appendix) instead of the Carnot calculation used in MATLAB. The heating energy output and associated electrical input is calculated based on entering air- and water temperatures. Although dry bulb air temperature can be predicted quite accurate, prediction of the entering water temperature is not possible within the transient simulation.

Since energy is stored for future use, the buffer should have a temperature that is sufficiently high to cover future required supply temperatures. This is necessary for the system to be able to response fast to future room temperature drops (with sufficient heating power). This means that use of an instantaneous climate curve for the water supply temperatures will not suffice. The required water temperature exiting the heat pump (and exiting the buffer) needs to be the maximum supply water temperature resulting from the instantaneous climate curve for the receding prediction horizon (using predicted outside temperatures). See equation 7.9. The entering water temperature of the heat pump (retour buffer) is five degrees lower (temperature difference used by manufacturers).

$$T_{water\ exiting}\ (t) = T_{upperlimit} = \max\left(T_{supply\ climatecurve}(t{:}\ t + predictionhorizon)\right) \quad 7.9$$

$$T_{water\ entering\ HP}(t) = T_{water\ exiting}\ (t) - 5 \quad 7.10$$

This way, the buffer will not be completely charged at all times. Temperature levels in the tank can still be adjusted according to the heat demand that is foreseen, which will increase heat pump efficiency. The upper limit temperature of the buffer (i.e. water temperature at 20% height for which the algorithm assumes the buffer as "full" and further generation is terminated) is equal to $T_{water\ exiting}$. The lower limit temperature (i.e. water temperature at 80% height for which the buffer is assumed "empty" and the algorithm will force heat pump operation in order to be able to supply required energy to the emission system) was also based on the instantaneous climate curve, but with a temperature difference. Since many on/off cycles deteriorate a heat pumps lifetime, a minimum

operation time has been set of 12 minutes (i.e. two TRNSYS time steps), in accordance with ISSO recommendations.

One of the assumptions of the MATLAB model was an ideal prediction of the heat demand, because the heat demand was derived based on relatively simple linear equations. Accurate estimation of future heat demand is crucial because the optimization algorithm bases the sequence of control operations on this prediction. The use of simplified building models in order to predict future heating loads is a method that is successfully used in predictive control strategies (Kummert, et al., 1996; Candanedo & Athienitis, 2011). A building can be seen as a linear system. The indoor temperature is mainly affected by the ambient air temperature, solar gains passing through the envelope, total internal gains for appliances and occupants and heat delivered by the emission system. When the heating power of the floor heating is the variable of interest, the response of this output to different values of the inputs can be analyzed. Outcomes for these variables from the simplified TRNSYS model which was described above, were used to assess the relation between the values of these variables (forcing functions) and the heating power (or: output) that was required in order to maintain the indoor temperature close to the setpoint (see Figure 7-18). Analysis was performed for this relation for every month of the year.

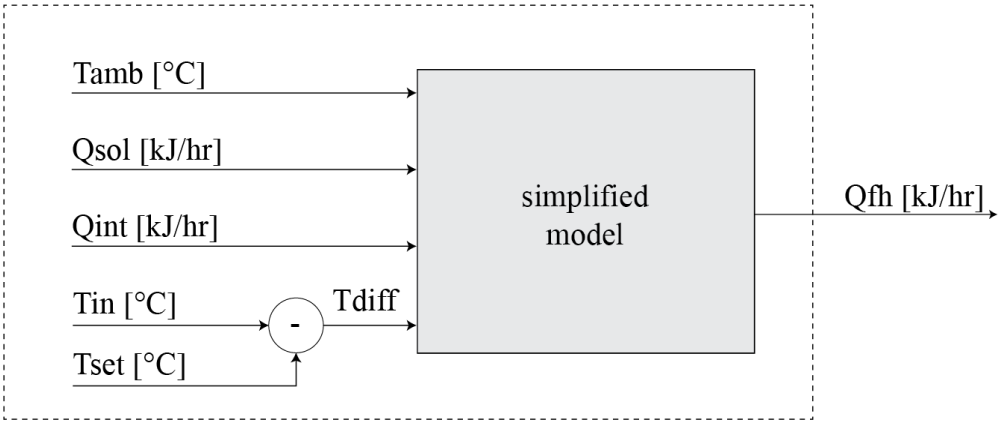

Figure 7-18: Four forcing functions that influence the required heating power

The abovementioned method is used to determine the heating power pattern within the dynamic simulation, based on prediction of the values of relevant input forcing functions (provided by micro-controllers and online weather forecasts in real applications). Although this approach for heat load estimation is proven to be successful according to literature, it will not provide an ideal estimation. The method is based on the assumption of a linear relation between a selection of inputs and the output derived from a simplified model which neglects effects of the time constant that is introduced by the specific emission system (Kummert, et al., 1996).

7.2.5 Modelling of PCM

7.2.5.1 Simulation theory

In the past decade, major progression was made in the transient simulation of PCM within different software. Different Types (simulation components) have been developed for use in TRNSYS, described in (Bony, et al., 2005). In the majority of these models, the enthalpy method (Clauβen 1993) is used to describe PCM behavior, which considers the enthalpy as a continuous and invertible function of temperature, h=h(T). When a storage is modeled involving media that undergo a phase change, the specific heat capacity C_p (and it's specific enthalpy) will thus vary according to temperature T.

For the modellization of PCM in this study, Type 840 was used, which is developed and provided by dr. H. Schranzhofer from the Institute of Thermal Engineering at University of Technology Graz (former Type 240). The model for transient simulation of a PCM storage tank Type840 is well documented in (Heinz & Streicher, 2006; Puschnig, et al., 2005; Schranzhofer, et al., 2006). Experimental validation showed good agreement between the model and real behavior of a sensible heat storage tank and a tank including PCM modules (Bony, et al., 2005; Heinz & Schranzhofer, 2007). Type 840 uses the enthalpy method described before. A precise enthalpy curve can be supplied by an external data file. Hysteresis and subcooling can be included, the types operation is further described in (Heinz & Schranzhofer, 2007). The energy balance calculation of each node is based on the math behind Type 60 sensible storage tank (see Figure 7-14):

$$\dot{Q}_i^{(medium)} = \dot{Q}_i^{(flow)} + \dot{Q}_i^{(cond)} + \dot{Q}_i^{(loss)} + \dot{Q}_i^{(\text{PCM } modules)} \qquad 7.11$$

where additionally,

$Q_i^{(\text{PCM modules})}$ = heat exchange between the storage medium and the built-in PCM modules

The energy balance for each storage node leads to the time evolution of the enthalpy h_i and via the relation h=h(T) also to the nodes temperature T_i (eq. 7.13) :

$$\dot{Q}_i^{(medium)} = m_i * \frac{h_i^{p+1} - h_i^p}{dt} \qquad 7.12$$

$$h_i^{p+1} = h_i^p + \frac{dt}{m_i} * \dot{Q}_i^{(medium)} \qquad 7.13$$

The enthalpy of the new time step *p+1* evolves from the enthalpy from the previous time step *p* via eq. 7.13, where *dt* is the size of the time step.

Type 840 calculates heat transfer between the storage fluid and the PCM modules ($Q_i^{(\text{PCM modules})}$ in eq. 7.11), and heat transfer inside the PCM modules by conduction and the phase change processes. Convection effects in the PCM's liquid phase are not considered. The model allows for the simulation

of three different built-in PCM modules into three user-defined zones. Three different module geometries can be integrated in the tank: spheres, cylinders and plates. PCM properties (conductivity, enthalpy, density, viscosity) as well as geometry (length, diameter, wall thickness) can be adjusted. In case of a spherical geometry, the modules are divided in a 1-dimensional nodal network, while heat transfer in cylinders and plates has to be calculated using a 2-dimensional network. A cylindrical module is thus divided in vertical (nodes) and radial segments which also contain nodes:

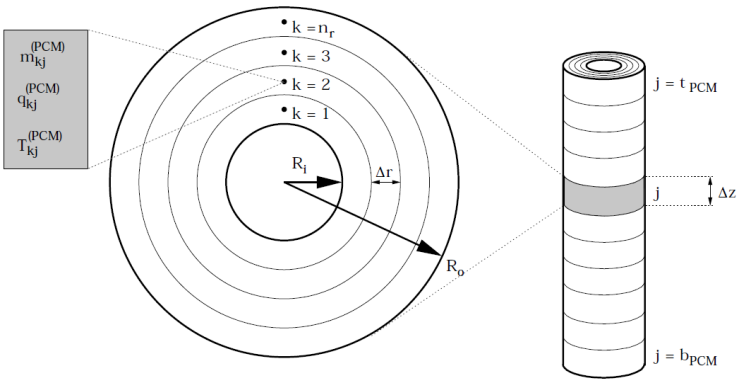

Figure 7-19: Geometry of a hollow cylinder PCM module (inner radius R = zero when module is completely filled).(Puschnig, 2004)

The energy balance of a PCM module for element *ki*, from which h_i^{p+1} can be derived is:

$$m_{ki} * \frac{h_{ki}^{p+1} - h_{ki}^{p}}{dt} = V_{ki} * \lambda^{(PCM)} * \left[\frac{T_{ki+1}^{(PCM)} - 2 * T_{ki}^{(PCM)} + T_{ki+1}^{(PCM)}}{(\Delta z)^2}\right] \qquad 7.14$$

$$+ V_{ki} * \lambda^{(PCM)} * \left[\frac{r_{k+1} * (T_{k+1i}^{(PCM)} - T_{ki}^{(PCM)}) - r_{k*}(T_{ki}^{(PCM)} - T_{k-1i}^{(PCM)}}{r_k + 0{,}5 * (\Delta r)^2}\right]$$

$$- (U * A)_{in}^{(PCM)} * \left[T_{1;i}^{(PCM)} - T_i\right] - (U * A)_{out}^{(PCM)} * \left[T_{nr;i}^{(PCM)} - T_i\right]$$

Where the first two terms in equation 7.14 describe heat conduction to neighboring PCM elements, and the last term concern heat transfer to the storage fluid at the inner and outer segment of the PCM modules (see Figure 7-19). Δz is the height of one node, Δr the radial node depth.

7.2.5.2 Exploration Type 840

A theoretical temperature-enthalpy curve was constructed based on literature values. Lane provided the following thermophysical properties of gelled Glauber's Salt (Lane, 1986).

Gelled Glauber's Salt	Na_2SO_4 . 10 H_2O
Scientific name	Sodium sulfate decahydrate
Melting temperature [C]	31
Thermal conductivity (l) [W/mK]	0,55
Thermal conductivity (s) [W/mK]	0,70
Density [kg/m3]	1.450
Sensible specific heat [kJ/kgK]	3.1
Heat of fusion [kJ/kg]	186

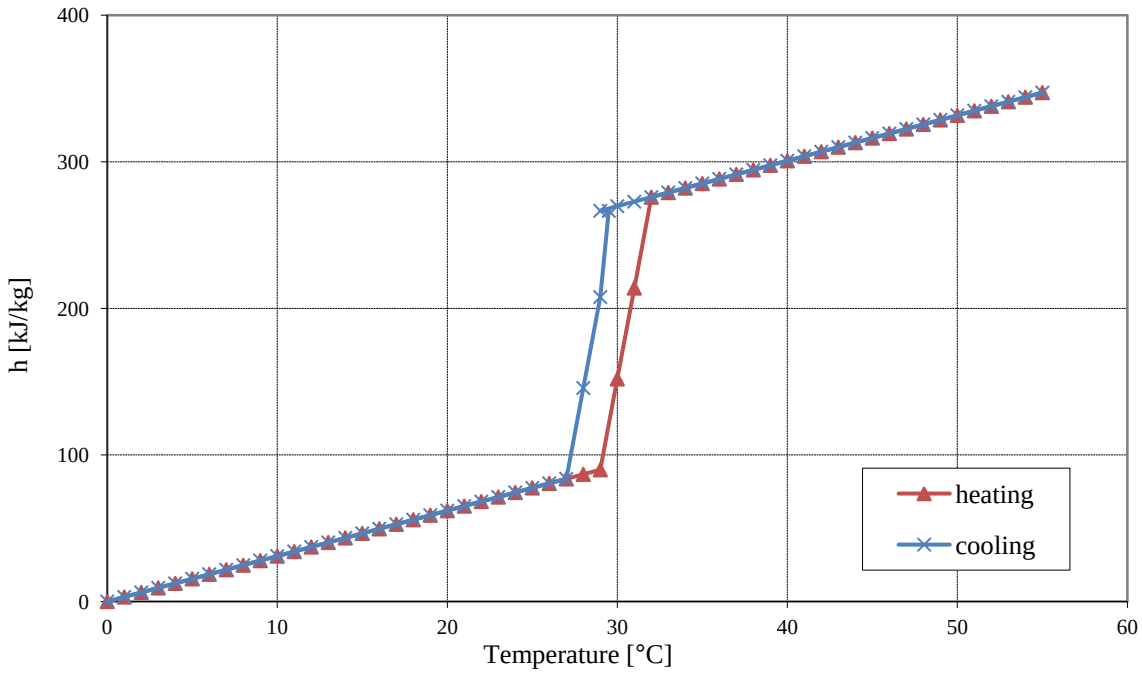

Figure 7-20: Temperature-enthalpy curve for simulated salt hydrate

A melting range (transition zone) of three degrees was introduced, as well as a two degree hysteresis between heating and cooling curve. These are theoretical values in order to include the hysteresis effect in the simulations, literature presents a large variety of hysteresis ranges (Mehling, 2008; Dincer & Rosen, 2002; Zalba, et al., 2003). For the PCM container, properties of PVC were used in accordance with (Heinz & Schranzhofer, 2007).

A short explorative study was performed using the transient PCM storage model Type 840. The goal of this study was the selection of appropriate PCM configurations for use in the final TRNSYS model (use cases including latent thermal storage). The following design recommendations could be distillated from literature on the application of PCM modules in TES (Puschnig, et al., 2005; Cabeza, et al., 2006; Heinz & Streicher, 2006; Ibanez, et al., 2006; Mehling, et al., 2003; Gracia, 2011):

- Modules should be as thin as possible (high surface to volume ratio), to maximize heat transfer between modules and water (power). Typical diameters of 10-100mm were found.
- The container material should have high conductivity values (metallic/PVC).
- A saturation PCM energy density seems to exist (the additional capacity of too large amounts of PCM can't be properly utilized,). Potential energy densities ranges from 5 to 50 Vol%.
- Application in the top layer (25%) of a buffer is a more effective measure of increasing energy density while compensating for heat losses at the top of the tank.

Calculated scenario's are summarized in Table 7-4. The initial temperature of the (whole) store is 35 ˚C, and the discharge process is observed using parameters that are visualized in Figure 7-21.

Table 7-4 – Simulated cylindrical PCM modules integrated in storage tank (and kg's associated per energy density)

Tank volume [m³]	PCM outer diameter [mm]	Height (% of buffer) and CASE	5 vol% - no. of modules	15 vol% - no. of modules	30 vol% - no. of modules	50 vol% - no. of modules
0,2	33	25 (I)	56 (15 kg)	170 (44 kg)	-	-
0,2	33	90 (II)	16	47	94 (87 kg)	-
0,2	53	25 (I)	20	61	-	-
0,2	53	90 (II)	6	17	34	-
0,6	53	25 (I)	41 (44 kg)	122 (131 kg)	-	-
0,6	53	90 (II)	11	34	68 (261 kg)	113 (435 kg)
0,6	73	25 (I)	21	63	-	-
0,6	73	90 (II)	6	17	35	-

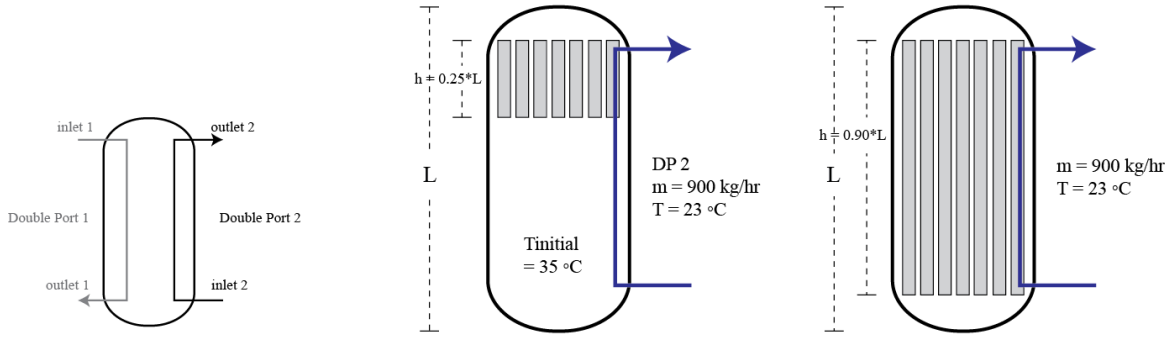

Figure 7-21: Left: double port principle Type 840, centre (case I) and right (Case II): parameters PCM exploration

The in- and outlets in Type 840 consist of double port connections: the in- and outlet on one side of the tank have the same mass balance. In the detailed TRNSYS model, DP2 is solely used to discharge the tank (Figure 7-21), DP1 will be used to charge the tank. Two major cases can be distinguished: CASE I concerns all scenario's with modules of 25% of the storage height, CASE II modules are covering 90% of the tanks height. Exemplary results for 600L, case I and II are shown:

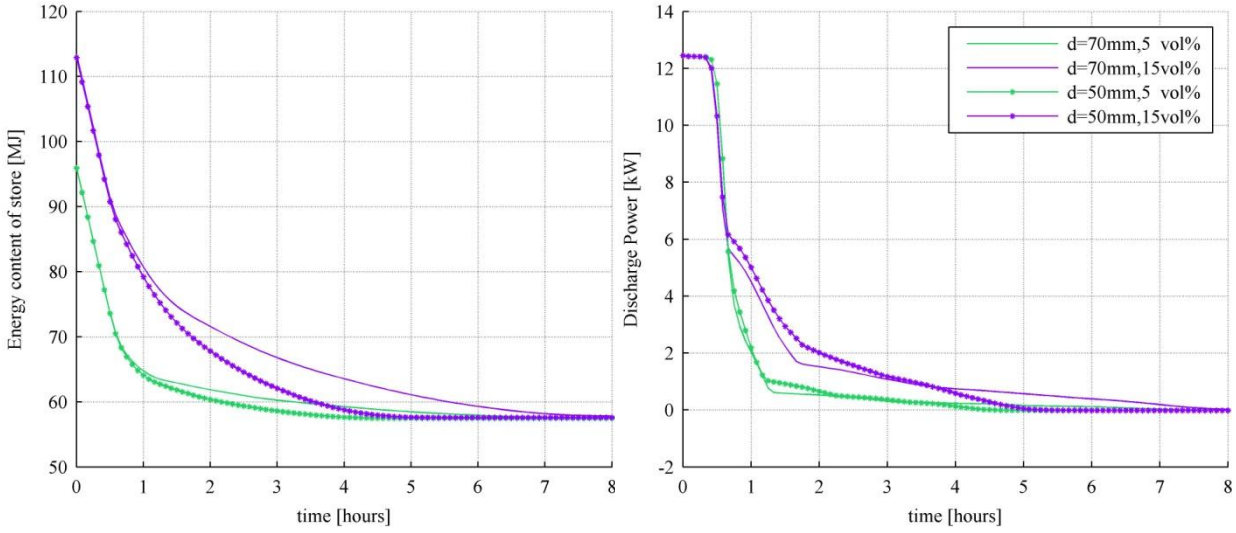

Figure 7-22: Energy content and discharge power of the storage, 600L case I

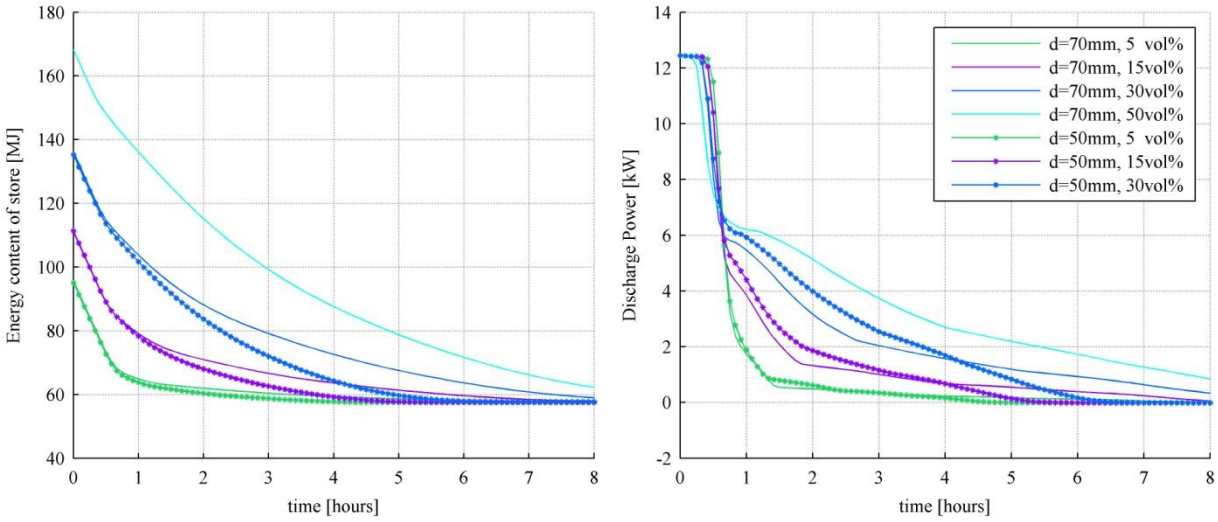

Figure 7-23: Energy content and discharge power of the storage, 600L case II

Main observations are (see additional figures - for 200L as well – in Appendix F):

1) Modules with smaller diameters discharge the same amount of energy faster (note the higher discharge power when phase change is reached after ca. one hour).

2) The influence of the module height can be compared for 5 and 15 Vol% (44 kg PCM): negligible difference in discharge powers between case I and II (it typically takes ca. 15 min less to discharge scenario's of case I). Figure 15-1 shows that for case I the top layer benefits from the latent storage capacity, while case II maintains stratification. Thermal losses of case I (for 8 hours) are 5% lower.

3) Discharge time is within functional limits for all scenario's (peak heat demand lasts 6-8 hours), 5 Vol% (and maybe 15%) might be discharged too fast and makes little difference with water.

With these observations in mind, as well as recommended use cases with latent storage that were concluded from MATLAB, six use cases for the detailed TRNSYS simulation are specified:

Table 7-5 – Further investigated TES options (sensible and latent)

Case	Volume [L]	Length modules [% of h-buffer]	No. of modules	Out diameter [mm]	Energy density [Vol% PCM]	Energy content [MJ]
A1	200	25	170	33	15	18,0
A2	200	90	94	33	30	25,0
B	500	- (sensible only)	-	-	-	~ 25,0
C1	600	25	122	53	15	50,0
C2	600	90	68	53	30	72,0
C3	600	90	113	53	50	108,0

7.3 Results and discussion

7.3.1 Typical winter week

The same typical winter week as in the MATLAB discussion (last week of February) will be used to illustrate the TRNSYS outcomes. In order to limit report size, the results of strategy A and D will be presented for only one use case: Case C3 (0,6 m^3, 50 vol% PCM).

In Figure 7-24, the course of the energy content of the buffer is shown for strategy A. Flows to the floor heating system of the living and sleeping zone are visible too. As soon as the operative temperature drops below the 20˚C setpoint, the floor heating requires heat. Peak heat demand occurs every day around 6AM. First the buffer is discharged, and when it is empty the heat pump starts and supplies heat directly to the floor (bypassing the buffer). As soon as the heat demand decreases, remaining heat produced by the heat pump is used to recharge the buffer.

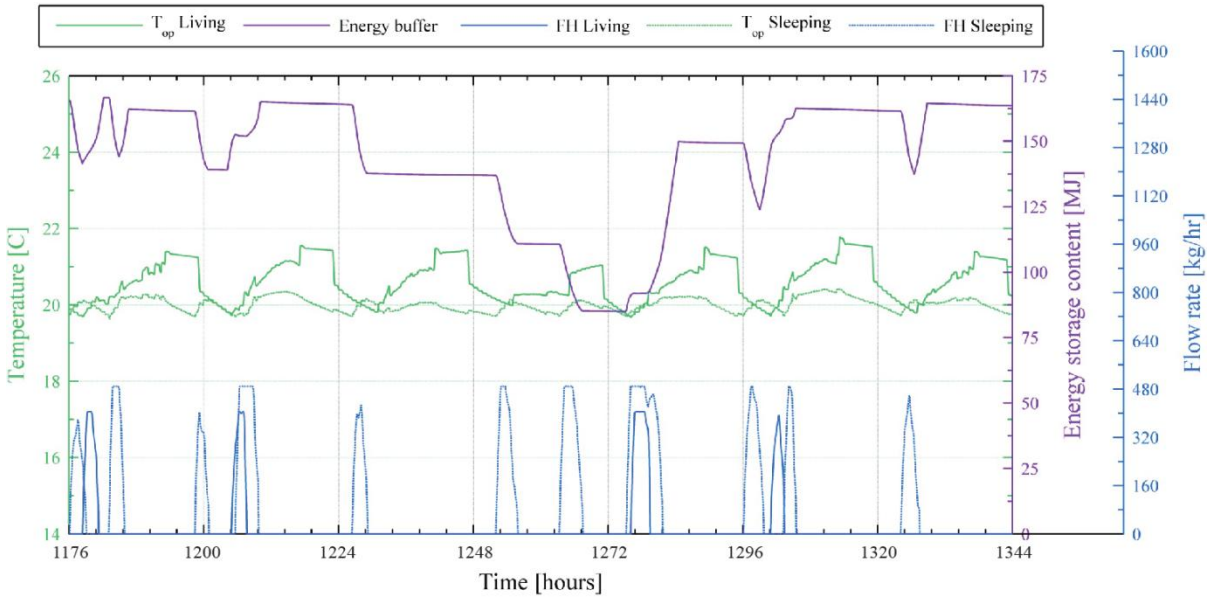

Figure 7-24: Energy content of the buffer and withdrawal flows to the Floor heating, Case C3 strategy A

Figure 7-25 shows the temperature levels in the buffer and the heat pump operation. The buffer is empty when T_{top} (at 80% tank height) drops more than 3˚C below the climatecurve. The heat pump stops recharging the buffer after T_{bottom} crosses $T_{climatecurve}$ + 1˚C. Figure 7-26 shows that strategy A results in very little on/off cycles. In terms of exergy/primary energy consumption, the strategy performs bad[6]. Almost every day, the buffer needs to be recharged during hours with unfavorable exergy factors (lowest ambient temperatures).

[6] Exergy factor calculated according to fex = 1-T0/T_{room}, where T_{room} is the average operative room temperature (actual operative room temperatures differ max. 0,3˚C).

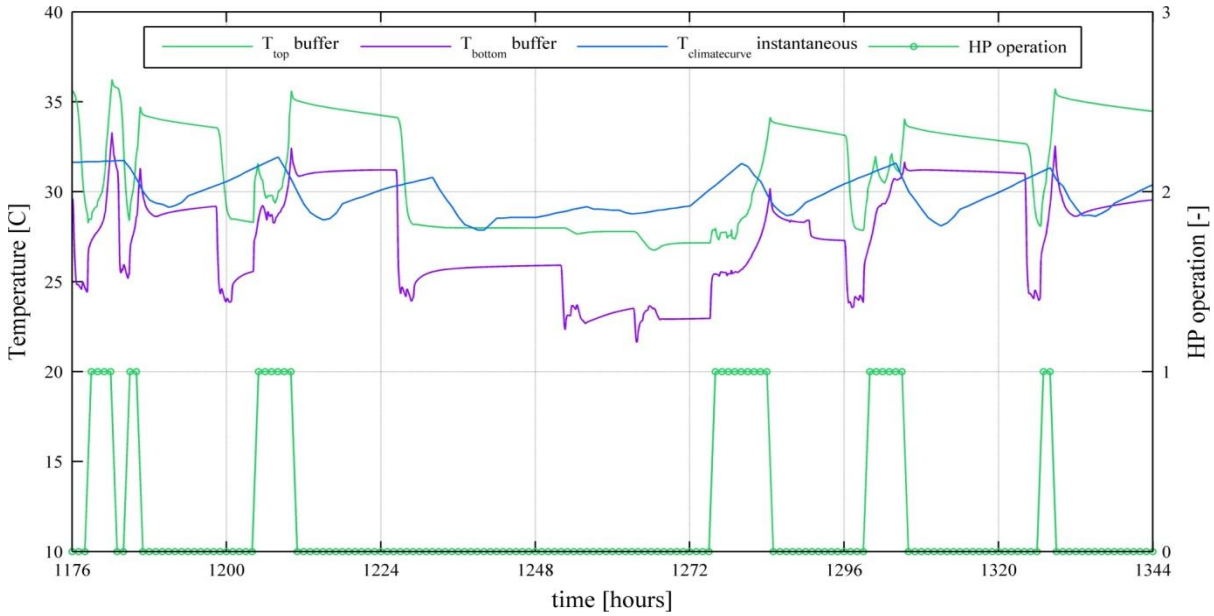

Figure 7-25: Temperatures in buffer (20 and 80% height) and heat pump operation, case C3 strategy A

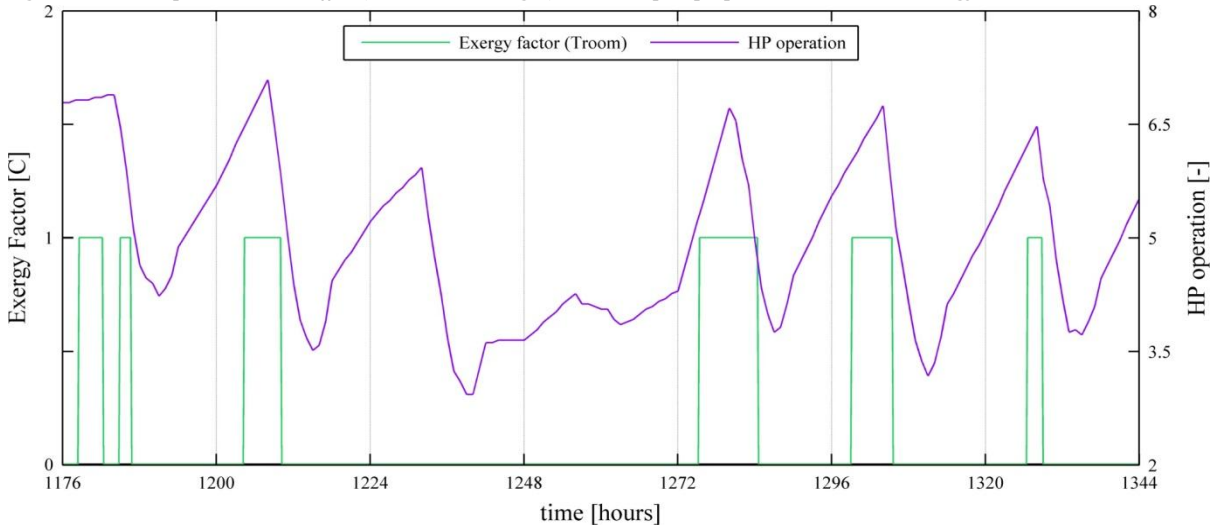

Figure 7-26: Exergy factor and operation pattern of the installation, case C3 strategy A

For strategy D (see Figure 7-27 to Figure 7-29), the temperatures of the storage are a few ˚C lower on average than for strategy A. This partly explains the small energy savings of the strategy (lower thermal losses, higher COP). Although the algorithm forces the heat pump to reheat the buffer, the supply water temperatures maintain below the climate curve. Therefore, the system's reaction time on disturbances in room temperature is more slow than for the strategy A system (compare flow rates of Figure 7-24 and Figure 7-27). This behavior is a direct consequence of the algorithm, which assumes the buffer to be empty when energy content is below 60 MJ (fixed lower limit). In a dynamic situation however, temperatures in the buffer in "empty" state will be too low to provide high discharge powers to the emission system during relatively cold days. The final system fulfils comfort criteria (room temperatures do never drop more than 0,3˚C below setpoint, and in worst case it takes one hour before temperature is above setpoint again which is reasonable for a floor heating emission system).

Despite the large storage capacity, the buffer is not always able to provide energy until the peak heat demand around 8 AM. After relatively cold nights, the heat pump needs to assist which causes the saw-tooth peaks in the top temperature of the tank (see Figure 7-28), because that is where the warm water enters the tank. On the first weekdays, the buffer is not completely recharged during the optimal hours of generation (note the small energy content in Figure 7-27). This seems to point at inaccurate prediction of the heat demand. This is reasonable, because prediction is based on monthly averages, and these very cold days do have a heat demand that is above average. During the other weekdays, the installation shows better anticipation. Combined with a smaller heat demand (midweek because of higher outside temperature, weekend because of more internal gains), this leads to an increase of heat pump operation during optimal conditions (Figure 7-29).

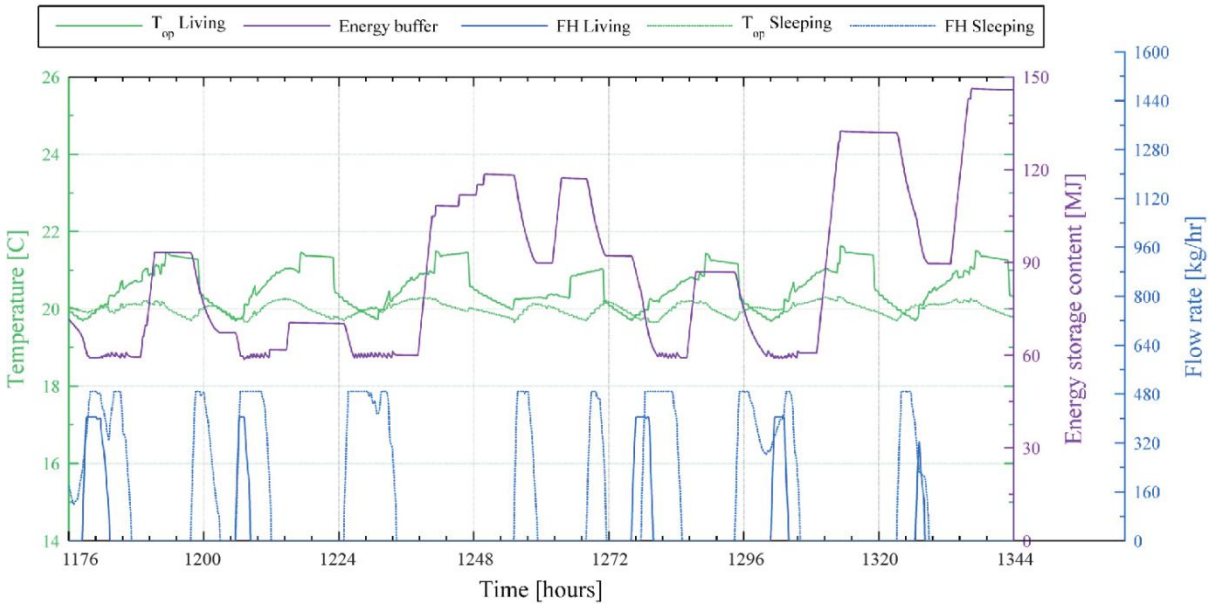

Figure 7-27: Energy content of the buffer and withdrawal flows to the Floor heating, Case C3 strategy D (24 hr)

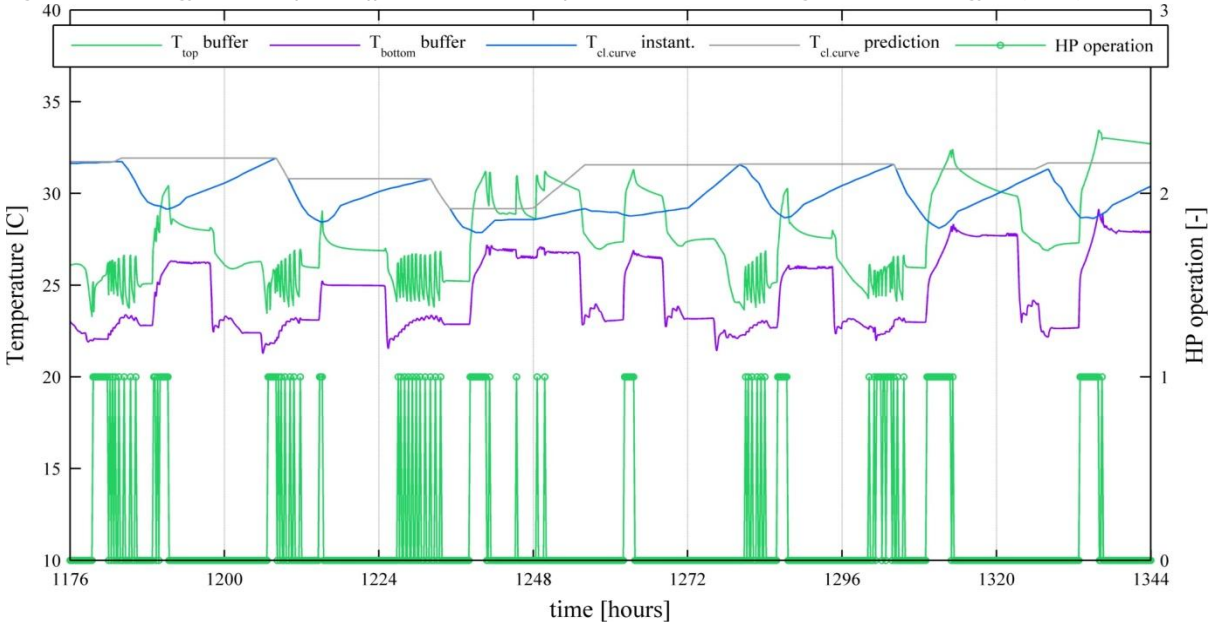

Figure 7-28: Temperatures in buffer (20 and 80% height) and heat pump operation, case C3 strategy D (24hr)

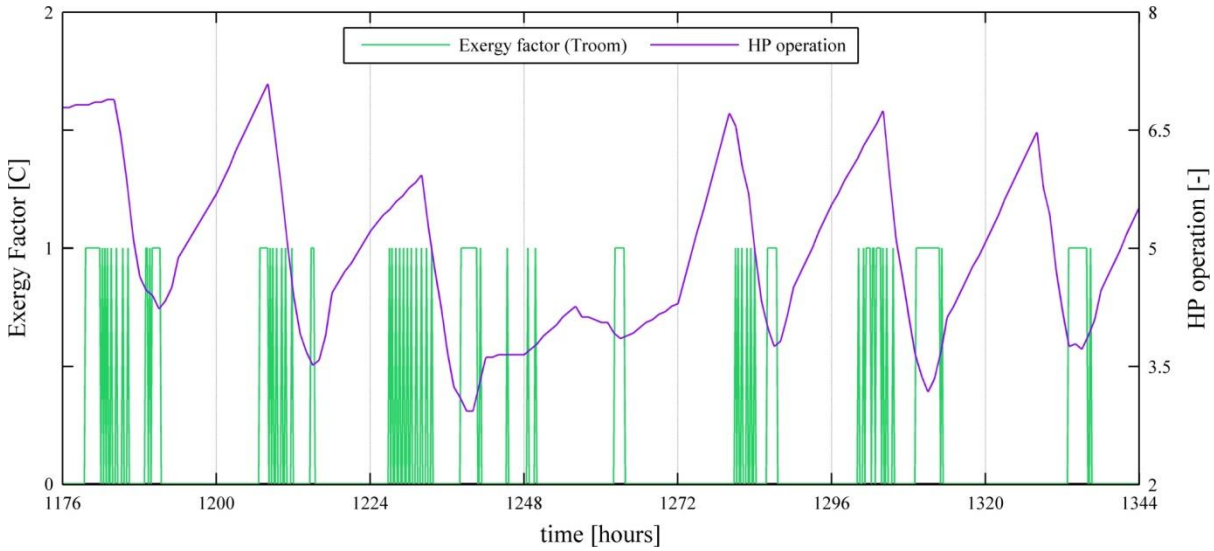

Figure 7-29: Exergy factor and operation pattern of the installation, case C3 strategy D (24 hr)

7.3.2 Comparison yearly outcomes of six use cases

Yearly dynamic simulations (0,1 hr time step) were performed for the six use cases that are summarized in Table 7-5. It is important to mention that only rough fine-tuning of some variables was possible (e.g. the buffer setpoint, temperature limits, prediction horizon), because yearly simulations were time-consuming. Table 7-6 summarizes the final input for these variables (PCM temperatures were only varied for C2 and C3). The resulting annual heating *energy* demands are comparable to the outcomes of the simplified calculation (see Appendix G - Detailed results TRNSYS for comparison). Outcomes will be compared using the input output approach which is described in (Torio & Schmidt, 2011). The energy and exergy in- and outputs were calculated for the components in Figure 7-30.

Table 7-6 Simulation input for important variables per case

Case-strategy	Main properties	Low temperature limit TES [C]	High temperature limit TES [C]	Bset [MJ]	Pr. horizon [hr]	Tsmelt PCM [C]
A1-A	200L	Ttop(80%) < $T_{climatecurve}$ – 3	Tbottom(20%) > $T_{climatecurve}$ +1	-	-	31
A1-D	15vol% PCM	Ttop(75%) < $T_{climatecurve}$ – 5	Tbottom(25%) > $T_{climatecurve\_prediction}$	9	24	31
A2-A	200L	Ttop(80%) < $T_{climatecurve}$ –3	Tbottom(20%) > $T_{climatecurve}$ +1	-	-	31
A2-D	30vol% PCM	Ttop(75%) < $T_{climatecurve}$ – 5	Tbottom(25%) > $T_{climatecurve\_prediction}$	12,5	24	31
B-A	Sensible	Ttop(80%) < $T_{climatecurve}$ – 3	Tbottom(20%) > $T_{climatecurve}$ +1	-	-	-
B-D		Ttop(75%) < $T_{climatecurve}$ – 5	Tbottom(25%) > $T_{climatecurve\_prediction}$	2,5	24	-
C1-A	600L	Ttop(80%) < $T_{climatecurve}$ – 3	Tbottom(20%) > $T_{climatecurve}$ +1	-	-	31
C1-D	15vol% PCM	Ttop(75%) < $T_{climatecurve}$ – 5	Tbottom(25%) > $T_{climatecurve\_prediction}$	2,5	24	31
C2-A	600L	Ttop(80%) < $T_{climatecurve}$ – 3	Tbottom(20%) > $T_{climatecurve}$ +1	-	-	29
C2-D	30vol% PCM	Ttop(75%) < $T_{climatecurve}$ – 5	Tbottom(25%) > $T_{climatecurve\_prediction}$	2,0	24	29
C3-A	600L	Ttop(80%) < $T_{climatecurve}$ – 3	Tbottom(20%) > $T_{climatecurve}$ +1	-	-	29
C3-D	50vol% PCM	Ttop(75%) < $T_{climatecurve}$ – 5	Tbottom(25%) > $T_{climatecurve\_prediction}$	9,0	24	29

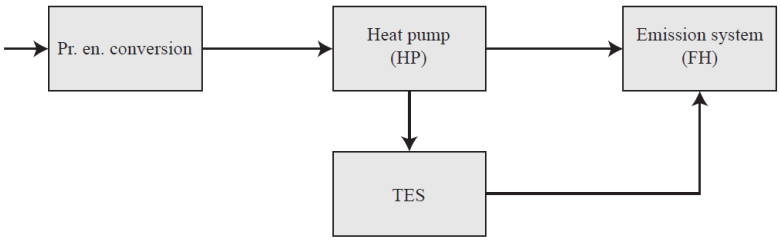

Figure 7-30: Analyzed components of the energy system.

The detailed simulations confirmed the MATLAB observation that increasing storage capacities do not result in primary energy and exergy reduction for control strategy A (due to increasing energy losses). Therefore, only one case (Case A1, smallest buffer content) is presented for strategy A in the following comparison. Case A1 has best energetic performance in combination with strategy A. Complete data for all cases can be found in subsection 16.1.3 of Appendix G.

For Case A1A and all cases with control strategy D, the resulting primary energy input (to heat pump) and the demand, or: systems energy output (i.e. energy supplied to the emission system resp. directly from the heat pump or via the buffer) is shown in Figure 7-31. Free input is energy extracted from outdoor air by the heat pump. The exergy inputs and outputs are presented in Figure 7-32, as well as the annual savings in energy and exergy for all components in Table 7-7.

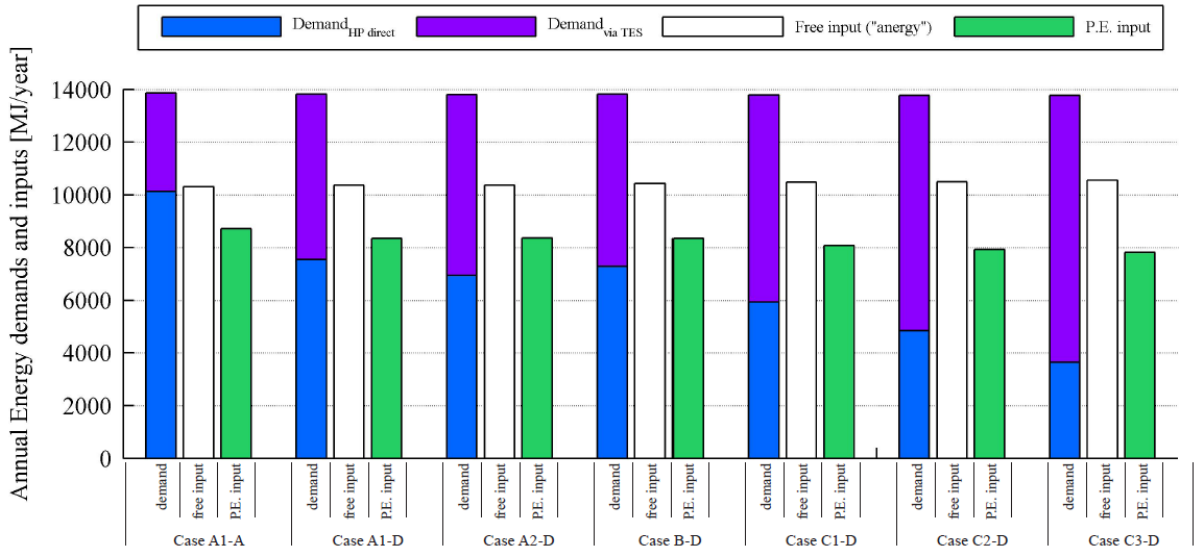

Figure 7-31: Annual energy demands and inputs for the considered cases (case A1 for strategy A, strategy D: all cases)

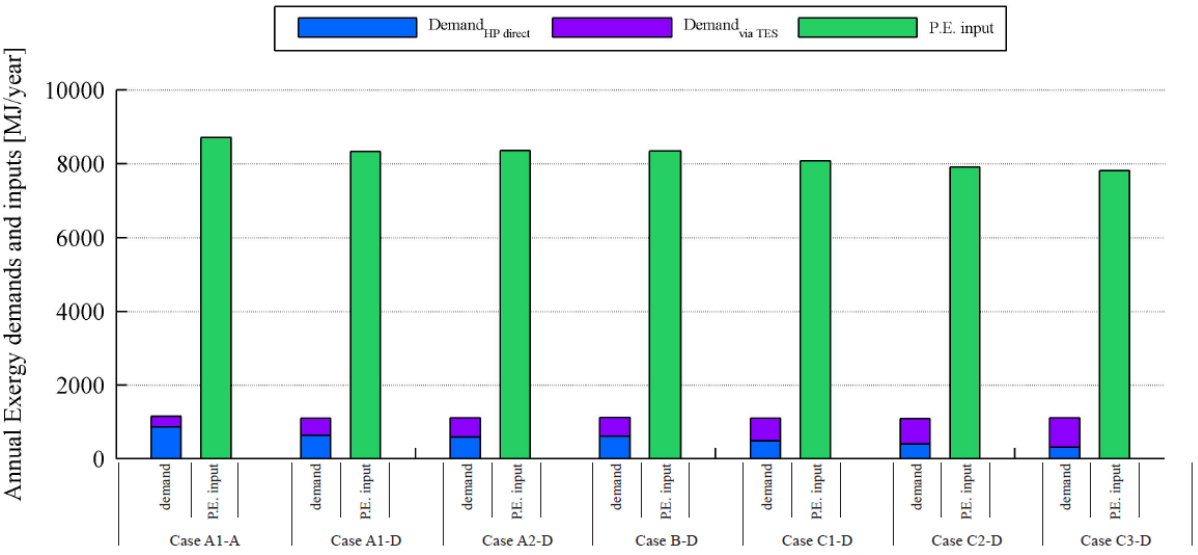

Figure 7-32: Annual exergy demands and inputs for the considered cases (case A1 for strategy A, strategy D: all cases)

The annual energy demands sum up to values similar for each Case (Figure 7-31). In every Case, the share of the heating energy delivered by via the buffer is increased for strategy D. This shows the degree in which the TES is able to decouple demand and generation. Cases with larger energy content do have a larger TES energy share, which means more energy could be generated by the heat pump during optimal hours in terms of exergy. Figure 7-32 shows that the annual reduction in primary energy input and associated exergy input are equal. This is because an exergy factor of 1 is assumed for primary energy in accordance with (Jansen, et al., 2010).

Table 7-7 Results energy and exergy reduction of strategy D compared to case A1A per system component, per case

	Q	Q	EX	Q	EX	Q	EX	Q	EX	Q	EX	Q	Q
Case	**P.E.**	**HP in**	**HP in**	**HP out**	**HP out**	**TES in**	**TES in**	**FH in HP**	**FH in HP**	**FH in TES**	**FH in TES**	**Sum FH_LZ**	**Sum FHSZ**
	[MJ]	[MJ]	[MJ]	[MJ]	[MJ]	[MJ]	[MJ]	[MJ]	[MJ]	[MJ]	[MJ]	[MJ]	[MJ]
A1-D	-4%	-4%	-4%	0%	-7%	84%	63%	-28%	-30%	88%	82%	0%	0%
A2-D	-4%	-4%	-4%	0%	-7%	80%	61%	-32%	-33%	84%	80%	0%	-1%
B-D	-4%	-4%	-4%	0%	-8%	73%	51%	-28%	-29%	75%	74%	0%	0%
C1-D	-7%	-7%	-7%	-1%	-11%	106%	75%	-41%	-44%	111%	107%	1%	-1%
C2-D	-9%	-9%	-9%	-1%	-13%	133%	96%	-52%	-54%	140%	134%	0%	-1%
C3-D	-10%	-10%	-10%	-1%	-13%	164%	120%	-64%	-64%	172%	170%	0%	-1%

Table 7-7 shows that control strategy D works better when applied to larger buffer volumes. The outcomes are all compared to Case A1-strategy A. Since minimization of the exergy of energy generation (i.e. *EX HP out* in the table above) forms the subject of optimization by the strategy D algorithm, this part of the system is responsible for the net total exergy savings (also decreasing *EX TES in*). The table also shows that the average quality of the energy supplied to the emission system (*FH in TES* and *FH in HP*) is more or less similar for case A1-A and cases with strategy D. This means thermal comfort is maintained. A detailed analysis of the losses of the components heat pump and TES is attached in appendix F. The yearly COP of the heat pump is presented below:

Table 7-8 Annual COP of the heat pump (energy output/electrical energy input) for all cases, strategy A and D

Strategy	Case A1	Case A2	Case B	Case C1	Case C2	Case C3
A	4,02	4,00	4,01	3,99	3,98	3,95
D	4,18	4,17	4,20	4,32	4,39	4,45

7.3.3 Accuracy of the heat demand prediction

The results for an exemplary week emphasized the impact of the heat demand prediction on the performance of the strategy D algorithm when applied to a dynamic system. A closer look to the accuracy of the prediction could give more insight in the influence of this. A detailed discussion is therefore included in Appendix G. The main conclusion is that the prediction shows good accuracy on a monthly basis, but that *daily* heat demand estimation can differ significantly from actual values (i.e. actual vs. predicted daily sums of heat demand). During days on which the actual demand turns out to be larger than predicted, the performance of the strategy D algorithm is deteriorated, resulting in a higher on/off frequency of the installation. Chapter 5.4 showed that this reduces compressor lifetime.

7.3.4 Economic feasibility

A short explorative economic feasibility study was performed, see Appendix G. Case A1-A functions as the reference system, since this case has the lowest investment costs and best energetic performance for control strategy A. A1-A is compared with case A1-D (contemporary heat pumps already include hardware like temperature sensors and internet connection, so only additional control software is required compared to A1-A) and case C3-D which has most energetic potential.

Table 7-9 – Payback time cases A1 and C3 for strategy D compared to case A1A

Case	A1-A	A1-D	C3-D
Total investment	€ 90,0 / m²	€ 91,7 / m²	€ 129,4 / m²
Extra investment strategy D	-	€ 200 (+)	€ 4.885 (+)
Operational cost (yearly)	€ 1,6 / m²	€ 1,5 / m²	€ 1,4 / m²
Annual savings in op. cost	-	€ 9 (-)	€ 21 (-)
Payback time [years]	-	22	232

Table 7-9 shows that additional investments that are required for strategy D to perform good, do dramatically increase the payback time. Savings in operational costs do not outweigh the investments because of the big difference between installation costs and energy costs. This makes it hard to interpret the resulting payback time; it takes over twenty years to regain an additional investment of only €200. It is important to state that the subject of the optimization in this research was minimal energy consumption, and not cost. Nevertheless, table 7-9 shows clearly that additional investments that are necessary for control strategy D to gain significant primary energy savings, won't be economically interesting (high PCM prices are the main hurdle).

Residential climate systems are known for higher investment costs per m^2 floor area than buildings with other uses. Annual energy costs for space heating in a well-insulated dwelling are relatively small compared to these installation costs. This reduces the impact of primary energy reduction on the payback time. Economic feasibility could be better in offices, which do typically have lower investment costs of ca. €40/m^2 and higher energy consumption –i.e. higher operational costs.

7.3.5 Different energy generator

Dynamic simulation of a different energy generator would be too complex for now. The potential savings of the heat pump system compared to a conventional gas boiler can however be roughly illustrated using annual efficiencies. The annual COP of the heat pump for case C3-D is 4,45, which means 0,22 MJ_{el} is necessary to generate 1 MJ_{th}. Calculating with efficiency ranges of 40-60% for typical power plants, the *annual primary energy efficiency (en. output/P.E. input) is in between 1,8 and 2,7*. Gas boilers are 100% energy efficient, meaning that 1 MJ gas is burned for generation of 1 MJ_{th}. The primary energy factor for gas is 1,0 (NEN 7120), so it's *annual P.E. efficiency is 1,0*. This gives an idea of the reduction of high quality energy input associated with the generation of a certain quantity of heat using a heat pump, compared to a gas boiler.

7.4 Conclusions

The six different use cases that derived from the MATLAB exploration have been further developed and were analyzed under dynamic conditions. A literature study on systems that actively use PCM for latent thermal energy storage has been performed in order to design an appropriate latent storage for the low temperature heat demand of the case study dwelling. Use cases A and C store latent thermal energy using the heat exchanger principle which is suitable for short term energy storage because high (dis)charge powers up can be obtained. Hydrated salt PCM were integrated in the TES using macro encapsulation in cylindrical modules. A low melting temperature of the PCM (29˚C) showed better results than 31˚C.

In accordance with the outcomes of the MATLAB model, control strategies A and D were further investigated in TRNSYS. Both reference strategy A and the optimization strategy D, were adjusted in order to be combined with the developed storage systems. The TRNSYS model can be considered as a first attempt to simulate the performance of the optimization strategy in terms of energy and exergy in a dynamic calculation including effects of storage medium, emission system and temperature control.

Major adjustments that had to be done for strategy D compared to the MATLAB model were: development of a dynamic heat demand prediction based on forcing functions (predictive control) and a lower temperature limit which varies dependant on the instantaneous required water supply temperature to the floor heating system. Inaccuracies in the prediction of the total daily heat demand during extreme cold days do influence the performance of the algorithm of control strategy D during the winter season. These inaccuracies lead to a higher number of yearly on/off cycles than for the reference control strategy (without prediction), which is reasonable since the algorithm defines control operations based on this prediction. Because it is hard to predict the precise heat demand pattern throughout the day, optimization for a short prediction horizon of 12 hours does not gain savings in the dynamic model (contrary to MATLAB). 24 hours is the optimal horizon.

Significant savings in yearly primary energy consumption can be concluded from the first dynamic calculations of the different cases using optimization strategy D, when compared to a reference control strategy A. An increasing storage capacity due to higher PCM densities does not result in additional energy or exergy savings when using the reference control strategy. In the optimized cases, an increased portion of the heat demand is delivered by the TES (15 to 25% higher than for reference strategy A) instead of direct generation by the heat pump. Larger buffer capacities thus allow for a higher share of energy supply via the buffer. The quality of the heat supplied from the TES to the floor heating system remains similar to the reference situation.

The successful decoupling of demand and generation allows more frequent utilization of free, low quality energy input which minimizes the amount of work (electrical input) that is required for the heat pump to provide the demanded heating energy. An economic feasibility study showed that the

reduction of operational costs by savings in electrical energy consumption, do not return on investments. The main reasons for this are first, that annual energy costs for space heating in residential buildings are relatively small compared to the installation costs, and second, that cost minimization was left outside the scope of this research.

The potential reduction of the quality of the generated energy was quantified using exergy analysis, which can also be used to illustrate the cause of the final exergy and primary energy reduction (see Figure 7-33; control strategy D allows for energy generation at lower exergy factors). Figure 7-31 already showed that the annual heating energy output of the system is approximately similar for all cases, for both the reference control strategy and strategy D, while the latter reduces the exergy output of the heat pump and thereby the primary energy input with 4-10%, compared to strategy A.

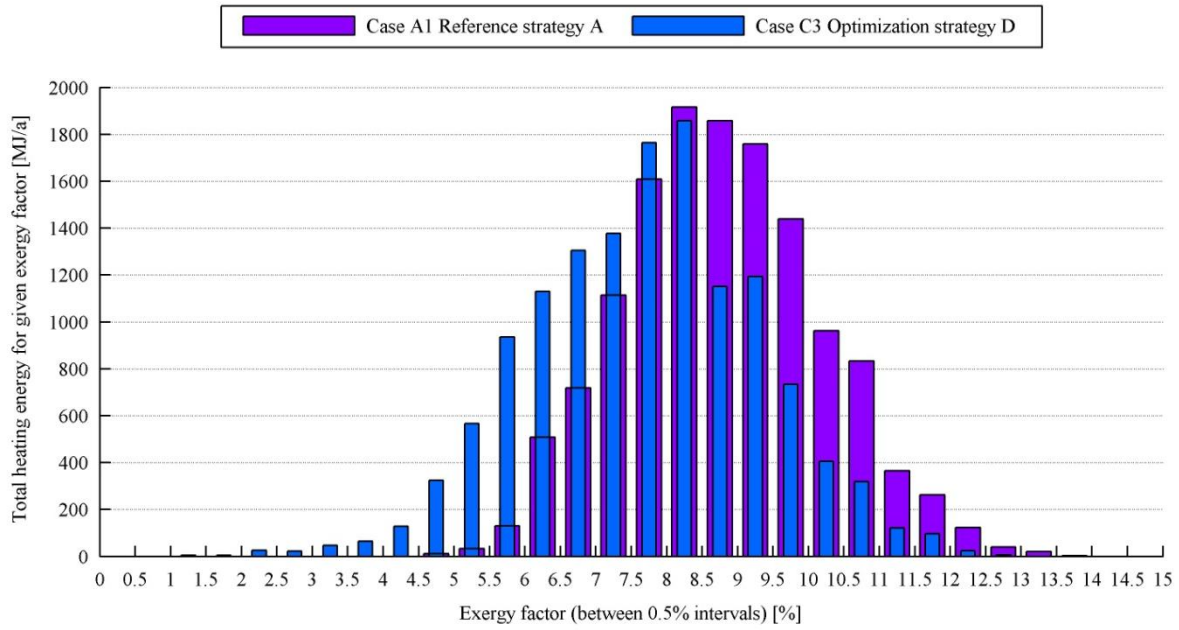

Figure 7-33: Distribution of yearly generated heating energy per exergy factor of this demand ($F_{ex} = EX_{HP\_OUT} / Q_{HP\_OUT}$)

8 Conclusions and recommendations

8.1 Conclusions

A literature study was performed in order to distinguish available energy storage technologies that could solve the mismatch between energy demand and generation. This is necessary for more advanced implementation of renewable energy resources. Particular interest was drawn by short term thermal energy storage as a method of solving the energy mismatch problem of low quality heat, which is relevant for water and space heating demand in industrial and domestic buildings. The potential of short term TES used as a heat sink in combination with an air-to-water heat pump with ambient air as (intermittent) heat source was further investigated, within residential buildings.

In conventional heat pump systems, the heat pump is operated without notion of exergetic optimal operation (translated into reference control strategy A in this study). An energy system was designed which decouples heating energy demand and generation in order to establish more frequent utilization of free, low quality energy input. More free input will minimize the amount of work (high quality input) that is additionally required for the heat pump to provide the heating energy. This results in minimum exergy factors of heat generation. Besides strategy A, three different storage strategies were developed that ensure optimal control of heat generation and active management of TES-capacities. These control strategies aim for minimization of the exergy of the energy generation. Strategy B operates the heat pump at fixed moments. Strategies C and D do select most optimal control operations of the installation dependent on estimates of future heat loads, using a Greedy optimization algorithm. Strategy C defines the optimal control sequence for a fixed horizon at the beginning of every day. Strategy D continuously decides optimal control using a receding horizon. The thermodynamic potential of each strategy was explored using a numerical MATLAB model.

Yearly calculations show that the control strategies can yield significant reduction of work and primary energy input, when applied to storage volumes larger than 250 liters. Strategy D leads to results that can be regarded with cautious optimism when applied to -large- buffer capacities that can be achieved with latent TES. Primary energy consumption was reduced with maximum 10% and the energy demand could be met when with 75% reduced installed system power. The best duration for low temperature heat storage (using the investigated capacities) turns out to be 24 hours.

Based on these outcomes, six different use cases were defined and used for further investigation of the most potential optimization strategy D using a TRNSYS simulation. This model can be considered as a first attempt of detailed calculation of the performance of strategy D in terms of energy and exergy, outcomes were compared to reference strategy A. Dynamic behavior of the storage medium, emission system and temperature control was included, as well as transient simulation of latent storage in salt hydrate PCM. The PCM was integrated in the TES tank using macroencapsulated modules, which

ensures good heat transfer. Energy densities were varied for different cases (15-50 Vol% PCM).

Significant savings in yearly primary energy consumption can be concluded from the dynamic calculations of the different cases using storage strategy D. In combination with TES with large energy storage capacities, optimization according to exergy principles could achieve up to 10% reduction of primary energy input compared to reference strategy A. Heating energy is generated at lower average exergy factors. This shift of energy generation is enabled by the fact that 15-25% more energy could be supplied to the emission system via the buffer. The quality of the supplied energy remains similar to the reference situation, meaning that the level of thermal comfort is maintained. Inaccuracies in the heat demand prediction in TRNSYS lower the performance of strategy D during extreme winter conditions. Maximum exergy reduction is achieved during in-between seasons. A reduction of primary energy consumption will reduce yearly energy costs for a household. Because operational costs for space heating in residential buildings are relatively small compared to the installation costs, large storage capacities are currently unfavorable from an economic point of view.

In conclusion, one could say that short term energy storage combined with a control strategy that aims to minimize the high quality energy input, can offer significant benefits to the energetic performance of an air-source heat pump. Benefits are a reduction in primary energy consumption and management of peak heat and electricity loads. Storage in the form of latent heat enables compact storage volumes.

8.2 Recommendations

Further investigation of the developed storage strategies in combination with the most potential use cases (30-50 Vol% PCM) is recommended. It is expected that with a more precise estimation of the future heat demand, energetic performance of the optimization algorithm at extreme conditions can be improved (reducing the heat pumps on/off frequency). This can be done by introduction of self-learning capacity which accounts for actual behavior of the emission system, or detailed analysis of the prediction model using statistical methods of estimation error minimization (e.g. the least squares method (Rao, et al., 1999)). Limitation of additional investment for installation components should however be taken into account in order to make it practically interesting.

Secondly, a comparison of optimized short term TES combined with a heat pump and competitive energy generators e.g. gas boilers or modulating heat pumps. would gain additional information on the feasibility and potential of the energy system that was investigated in this study.

Finally, it is recommended to further investigate application of the developed storage strategy to storage of low quality heat or cold from other resources, e.g. waste heat or cold, exhaust air or solar thermal. The developed strategies can be applied to TES systems of any size and could therefore improve storage for other time spans, storage mediums (ATES would be very interesting), and also for different final energy demands (heating or cooling, other cases studies).

9 Bibliography

Agyenim, F., 2009. Review of materials, heat transfer and phase change problem formulation for LHTESS. *Renewable and sustainable energy reviews.*

Ahmad, A., Yasin, N., Derek, C. & Kim, J., 2011. Microalgae as a sustainable energy source for biodiesel production: A review. *Renewable and Sustainable Energy Reviews,* Volume 15, pp. 584-593.

Albus, R., Burmeister, F. & Fischer, M., 2010. Bewertung und Perspektiven der Zukunftstechnologie KWK. *Energie / Wasser-praxis,* Volume 11, pp. 18-22.

Amaro, H., 2012. Microalgae: An alternative as sustainable source of biofuels?. *Energy,* Volume 44, pp. 158-166.

Amin, N., 2012. Effectiveness-NTU correlation for low temperature PCM encapsulated in spheres. *Applied Energy.*

Baetens, R., 2010. PCM for building applications: A state-of-the-art review. *Energy and Buildings,* Volume 42, pp. 1361-1368.

Beaudin, M., Zareipour, H., Schellenberglabe, A. & Rosehart, W., 2010. Energy storage for mitigating the variability of renewable electricity sources: An updated review. *Energy for Sustainable development,* Issue 14, pp. 302-314.

Bony, J., Ibanez, M. & Puschnig, P., 2005. *Three different approaches to simulate PCM bulk elements in a solar storage tank.* Switzerland, s.n.

Boulanger, P., 2003. Investigation on storage technologies for intermittent renewable energies. *Storage Technology report ST5: Electrolyser, hydrogen storage and Fuel Cell.*

Brown, D. & Chvala, W., 2005. Flywheel energy storage: An alternative to batteries for UPS Systems. *Energy Engineering,* Issue 102, pp. 7-26.

Cabeza, L., 2011. Materials used as PCM in TES in buildings: a review. *Renewable and Sustainable Energy Reviews,* Volume 15, pp. 1675-1695.

Cabeza, L., Ibanez, M., Sole, C. & Nogues, M., 2006. Experimentation with a water tank including a PCM module. *Solar Energy Materials and Solar Cells,* Volume 90, pp. 1273-1282.

Candanedo, J. & Athienitis, K., 2011. Predictive control of radiant floor heating and solar-source heat pump operation in a solar house. *HVAC&R Research,* 17(3), pp. 235-256.

Castell, A. & Margalef, P., 2010. Economic viability of a Molten Carbonate Fuel Cell working with

Biogas. *Journal of Fuel cell Science and Technology,* Volume 7, pp. 1-7.

Cavallo, A., 2007. Controllable and affordable utility-scale electricity from intermittent wind resources and compressed air energy storage. *Energy,* Issue 32, pp. 102-127.

Chen, H., Cong, T., Yang, W. & Tan, C., 2009. Progress in electrical energy storage systems: A critical review. *Progress in Natural Science,* Issue 19, pp. 291-312.

Cot-Gores, J., Castel, A. & Cabeza, L., 2012. Thermochemical energy storage and conversion: A-state-of-the-art review. *Renewable and Sustainable Energy Reviews,* Volume 16, pp. 5207-5224.

Daroch, M., Geng, S. & Wang, G., 2012. Recent advances in liquid biofuel production from algal feedstocks. *Applied Energy,* Volume 102, pp. 1371-1381.

de Gracia, A., 2010. Life Cycle Assessment of the inclusion of PCM in experimental buildings. *Energy and Buildings,* Volume 42, pp. 1517-1523.

Dickinson, J., Buik, N., Matthews, M. & Snijders, A., 2009. Aquifer thermal energy storage: theoretical and operational analysis. *Geotechnique,* 59(3), pp. 249-260.

Dincer, I. & Rosen, M., 2002. *Thermal energy storage - systems and applications.* Chichester: Wiley.

Drijver, B., 2012. *Meer met bodemenergie - Hogetemperatuuropslag.* [Online] Available at: http://www.meermetbodemenergie.nl [Accessed 15 12 2012].

Droste-Franke, B., Paal, B. & Rehtanz, C., 2012. *Balancing Renewable Electricity.* Berlin Heidelberg: Springerverlag.

Farret, F., 2006. *Integration of alternative sources of energy.* s.l.:IEEE Press.

Forsen, M., 2005. *Heat pumps - technology and environmental impact,* Sweden: SVEP.

Gommans, L., 2012. *Gebiedsgerichte Energetische Optimalisatie,* Delft: Delft University of Technology.

Gracia, A. d., 2011. Thermal analysis of including PCM in a domestic hot water cylinder. *Applied Thermal Engineering,* Volume 31, pp. 3938-3945.

Gunther, E., 2009. Enthalpy of Phase Change Materials as a Function of Temperature. *Int. Journal of Thermophysics,* 30(Spinger Science), pp. 1257-1269.

Gupta, K., Rehman, A. & Sarviya, R., 2010. Bio-fuels for the gas turbine: A review. *Renewable and Sustainable Energy Reviews,* Volume 14, pp. 2946-2955.

Gupta, R., 2011. Application of energy storage devices in power systems. *International Journal of Engineering, Science and Technology,* Issue 3, pp. 289-297.

Hadjipaschalis, I., 2009. Overview of current and future energy storage technologies for electric

power applications. *Renewable and Sustainable Energy Reviews,* Issue 13, pp. 1513-1522.

Haeseldonckx, D. & D'haeseleer, W., 2004. *Brandstofcellen voor stationaire toepassingen: Historiek, technische en economische haalbaarheid en trends,* s.l.: Katholieke Universiteit Leuven.

Hausladen, G., 2004. *Climate Design.* Munich: Birkhauser.

Hausladen, G. & Liedl, P., 2012. *Building to suit the climate.* s.l.:Birkhauser.

Heinz, A. & Schranzhofer, H., 2007. *Type 840 - Model for the transient simulation of water- or PCM slurry tanks with integrated PCM modules,* Graz: IWT.

Heinz, A. & Streicher, W., 2006. *Application of Phase change materials and PCM-slurries for thermal energy storage,* Graz: TU Graz.

Hensen, J., de Vaan, C. & Wiedenhoff, J., 2010. De mythe thermische massa. *TVVL,* Volume 39, pp. 28-31.

Hoogendoorn, A., Bierings, B. & van den Boom, R., 2008. *Centrale productie van bio-SNG via vergassing,* s.l.: SenterNovem.

Huggins, R., 2010. *Energy Storage.* Stanford: Springer Science.

Ibanez, M. et al., 2006. Modelization of a water tank including a PCM module. *Applied Thermal Engineering,* Volume 2006, pp. 1328-1333.

Ibanez, M. et al., 2006. Modelization of a water tank including a PCM module. *Applied Thermal Engineering,* Volume 26, pp. 1328-1333.

Ibrahim, H., Ilinca, A. & Perron, J., 2008. Energy Storage Systems - Characteristics and comparisons. *Renewable and Sustainable Energy Reviews,* Issue 12, pp. 1221-1250.

IEA, 2011. *Economical heating and cooling systems for low energy houses,* s.l.: s.n.

IEA, 2011. *Energy-efficient Buildings: Heating and Cooling Equipment,* s.l.: s.n.

IEA, 2011. Sustainable cooling with thermal energy storage. *IEA ECES Annex 20.*

IEC, 2010. *Coping with the Energy Challenge.* [Online] Available at: http://www.iec.ch/smartenergy/pdf/white_paper_lres.pdf[Accessed 5 12 2012].

IEC, 2011. *Electrical Energy Storage.* [Online] Available at: http://www.iec.ch/whitepaper/pdf/iecWP-energystorage-LR-en.pdf. [Accessed 2 12 2012].

IEC, 2012. *Grid integration of large-capacity Renewable Energy sources and use of large-capacity Electrical Energy Storage.* [Online] Available at: http://www.iec.ch/whitepaper/pdf/iecWP-gridintegrationlargecapacity-LR-en.pdf [Accessed 4 12 2012].

ISSO 32, 2011. *Uitgangspunten temperatuursimulatieberekeningen,* Rotterdam: ISSO.

ISSO 72, 2013. *ISSO publication 72 - Ontwerp van individuele en kleine elektrische warmtepompsystemen (to be published),* Rotterdam: ISSO.

ISSO 744, 2009. *ISSO-report 744 Lucht-waterwarmtepompen in woningen,* Rotterdam: ISSO.

Jansen, S., 2013. *Exergy in the built environment - The added value of exergy in analysis and assessment of energy systems for the built environment (doctoral thesis),* Delft: TU Delft (manuscript, to be published).

Jansen, S., Teres-Zubiaga, J. & Luscuere, P., 2010. The exergy approach for evaluating and developing an energy system for a social dwelling - Part 1.

Kammen, D., 2004. Renewable Energy, Taxonomic Overview. *Encyclopedia of Energy,* Volume 5, pp. 385-412.

Kilkis, S., 2011. *A rational Exergy Management to Curb CO2 emissions in the Exergy-Aware Built Environments of the Future, in School of Architecture and the built environment -Division of Building Technology,* Stockholm: KTH Royal Institute of Technology.

Klein, S. e. a., 2012. TRNSYS Reference manual. In: s.l.:Transsolar.

Klimrek, n.d. *Buffer oppervlaktewater.* [Online] Available at: http://www.klimrek.com/ [Accessed 15 12 2012].

Koenders, M., 2007. *Koude/Warmteopslag in de praktijk - Meetgegevens van 67 projecten,* s.l.: Senter Novem.

Koschenz, M. & Lehmann, B., 2000. *Handbuch thermoaktive Bauteilsysteme TABS,* Dubendorf: EMPA department Energy systems.

Krevel, A. v., 2000. Installatieconcepten warmtepompen: theorie en praktijk. *Verwarming en koeling,* 29(7/8).

Krevel, A. v., 2001. Warm tapwater met warmtepompen, een "hot item". *Verwarming en Ventilatie,* Issue 2.

Kummert, M., Andre, P. & Nicolas, J., 1996. *Development of simplified models for solar buildings optimal control.* Freiburg, s.n.

Lailler, P., 2003. Investigation on Storage Technologies for Intermittent Renewable Energies. *Storage Technology report ST1: Lead-acid systems.*

Lane, G., 1986. *Solar Heat Storage: latent heat materials.* s.l.:CRC Press.

Lang, R. & Marx, U., 2001. Das Zeolith-Wasser-Heitzgerat.

Lehmann, E. L. & Casella, G., 1998. *Theory of Point Estimation.* 2 ed. New York: Springer.

Medrano, M., 2009. Experimental evaluation of commercial heat exchanegrs for use as PCM thermal storage systems. *Applied Energy,* Volume 86, pp. 2047-2055.

Mehling, H., Cabeza, L., Hippeli, S. & Hiebler, S., 2003. PCM-module to improve hot water heat stores with stratification. *Renewable energy,* Volume 28, pp. 699-711.

Mehling, H. C. L., 2008. *Heat and Cold storage with PCM.* s.l.:Springer.

Moran, M. & Shapiro, H., 2006. *Fundamentals of Engineering Thermodynamics.* s.l.:John Wiley & Sons.

Nakken, T. et al., 2010. *The Utsira wind-hydrogen system,* s.l.: s.n.

Nath, K. & Das, D., 2003. Hydrogen from biomass.

Nomura, T., 2013. Heat storage in direct-contact heat exchangers with phase change material. *Applied thermal engineering,* Volume 50.

Novo, A. & Bayon, J., 2010. Review of seasonal heat storage in large basins: Water tanks and gravel–water pits. *Applied Energy,* Volume 87, pp. 390-397.

NVOE, 2012. *Werkingsprincipe bodemenergie.* [Online] Available at: www.bodemenergie.nl/bodemenergie/werkingsprincipe [Accessed 9 1 2013].

Pardo, N., Montero, A., Martos, J. & Urchueguia, J., 2010. Optimization of hybrid-ground coupled and air source - heat pump systems in combination with thermal storage. *Applied Thermal Egineering,* Volume 30, pp. 1073-1077.

Prodromidis, G. & Coutelieris, F., 2012. Simulations of economical and technical feasability of battery and flywheel hybrid energy storage systems in autonomous projects. *Renewable Energy,* Issue 39, pp. 149-153.

Puschnig, P., Heinz, A. & Streicher, W., 2005. *Trnsys simulation model for an energy storage for PCM slurries and/or PCM modules,* Graz: TU graz.

Rao, C. et al., 1999. *Linear Models: Least Squares and Alternatives.* s.l.:Springer Series.

Roijen, W. & Op 't Veld, P., 2010. Duurzame energie uit fossiele bron - voormalige steenkoolmijnen worden opnieuw benut. *VV+,* pp. 584-487.

Rosen, M., 2012. Geothermal heat pump systems: Status review and comparison with other heating options. *Applied Energy,* Volume 101, pp. 341-348.

Sauter, 2012. *Dankzij technologische samenwerking is de eensgezinswoning van de toekomst energieautonoom.* [Online] Available at: www.sauter-controls.com

Schranzhofer, H., Puschnig, P., Heinz, A. & Streicher, W., 2006. *Validation of a TRNSYS simulation model for PCM energy storages and PCM wall construction elements,* Graz: TU Graz.

Schrever, R., 2002. Betonkernactivering, een nieuwe manier van gebouwklimatisering. *VV.*

Semadeni, M., 2004. Storage of Energy, Overview. In: *Encyclopedia of Energy.* s.l.:Elsevier, pp. 719-739.

Sharma, A., Tyagi, V., Chen, C. & Buddhi, D., 2009. Review on TES with phase change materials and applications. *Renewable and Sustainable Energy Reviews,* Volume 13, pp. 318-345.

SKB, 2011. *Handreiking masterplannen bodemenergie.* [Online] Available at: http://www.meermetbodemenergie.nl/ [Accessed 15 12 2012].

Socaciu, L., 2011. Seasonal Sensible Thermal Energy Storage Solutions. *Journal of Practices and Technologies,* Issue 19, pp. 49-68.

Sorensen, B., 2007. *Renewable energy conversion, transmission, and storage.* s.l.:Academic Press.

Specht, M. et al., 2011. *Storing Renewable Energy in the Natural Gas Grid,* s.l.: ZSW & IWES.

Sterner, M., 2009. Bioenergy and renewable power methane in integrated 100% renewable energy systems. *Renewable energies and Energy Efficiency,* Volume 14.

Sterner, M., 2010. *Renewable (power to) methane: Storing renewables by linking power and gas grids.* [Online] Available at: http://www.iwes.fraunhofer.de/ [Accessed 8 12 2012].

Sterner, M., 2011. *Die Speicheroption Power-to-Gas.* s.l., Fraunhofer IWES.

Streicher, W., 2008. *Solar Heating and Cooling programme Task 32C: Phase Change Materials,* s.l.: IEA.

Stritih, U., 2003. Heat transfer enhancement in latent heat thermal storage system for buildings. *Energy and Buildings,* Volume 35.

Ter-Gazarian, A., 2011. *Energy storage for power systems.* 2nd ed. London: The Institution of Engineering and Technology.

Torio, H. & Schmidt, D., 2011. *Annex 49 - Low exergy systems for high-performance buildings and communities,* s.l.: I.E.A..

Traversari, A. & Oostendorp, P., 2000. Hydraulische schakelingen bepalend voor het rendement. *Intech (TNO and Novem),* pp. 10-12.

van der Hoeven, D., 2007. *Groenboek energietransitie.* s.l.:Platform Groene Grondstoffen.

van der Spoel, W., 2004. *Latente warmteopslag in constructies - consequenties voor energiegebruik en thermisch comfort,* s.l.: TU Delft.

Van Velzen, T., 2010. Reservewind - Turbinepark vereis megadepot. *Technisch Weekblad.*

Van Velzen, T., 2010. Reservewind - Turbinepark vereis megadepot. *Technisch Weekblad.*

van Voorden, A. et al., 2007. *The application of super capacitors to relieve battery-storage systems in autonomous renewable energy systems.* Lausanne, IEEE.

van Wijck, A., 2012. Bronproblemen - 70% van de WKO-systemen functioneert slecht. *De Ingenieur,* Volume 17, pp. 20-27.

Vizvari, B., 1987. On the greedy solution in integer linear programming. *Zeitschrift für Operations Research,* Volume 31, pp. 55-68.

Vollebrecht, R., 2012. Duurzame energie en spanningskwaliteit vragen om opslag. *VV+,* pp. 596-599.

Walls, G., 2009. *Exergetics.* s.l.:s.n.

Wang, X., 2008. Raising evaporative cooling potentials using combined cooled ceiling and MPCM slurry storage. *Energy and Buildings,* Volume 40.

Woudstra, N., 2012. *Sustainable Energy Systems - Limitations and challenges based on exergy analysis,* Delft: Delft University of Technology.

Yang, L. & Li, Y., 2008. Cooling load reduction by using thermal mass and night ventilation. *Energy and Buildings,* Volume 40, pp. 2052-2058.

Zalba, B., Marin, J., Cabeza, L. & Mehling, H., 2003. Review on TES with phase change, heat transfer analysis and applications. *Applied Thermal Engineering,* Volume 23, pp. 251-283.

Zhu, W. & Garett, D., 2012. *Overview of distributive Energy Storage for residential communities,* s.l.: s.n.

Zondag, H., 2010. *De ontwikkeling van thermochemische warmteopslag (intreerede),* s.l.: Eindhoven University of Technology.

10 Appendix A – Literature review

10.1 Chemical energy storage - Bio-fuels

10.1.1.1 Straight vegetable oils

Heating value	38-39 [MJ kg^{-1}]

The viscosity of straight vegetable oils is too high for direct combustion in a gas turbine, and needs modification first.

10.1.1.2 Biodiesel

Heating value	37-41 [MJ kg^{-1}]

The first and most well-known replacement of conventional fuels is bio-diesel. Biodiesels can be used in any gas turbine without modification. Bio-diesel characteristics are close to petroleum derived diesel (43 MJ kg-1), but it is less polluting, and has better biodegradability and a renewable nature. Some bio-oils are very viscous and require preheating. The bio-diesels and its blends used as fuel in micro-turbines for cogeneration led to no significant changes in the engine performance and behavior compared to diesel fuel. It can be produced from all from three generations feedstock, but at the moment, most biodiesel is made from first generation oil crops, e.g. palm, rapeseed or soybean (Amaro, 2012). Blended with diesel, it can reduce hazardous emissions over 20%.

10.1.1.3 Bio-ethanol

Heating value	25-26 [MJ kg^{-1}]

Other petroleum-like liquid fuels are biomass produced alcohols. The most widely used bio-alcohol is ethanol, which is derived from biomass via alcoholic fermentation (see **Fout! Verwijzingsbron niet evonden.**). In industrialized countries, corn is most used as feedstock, in developing countries sugarcane. Ethanol produced by fermentation of residues from sugar refining obtains circa 25% of the energy from the raw sugar input (Sorensen, 2007). Lignin vegetables like wood, straw or grasses are slowly replacing these feedstocks, using hydrolysis as conversion process. Ethanol is the most used liquid bio-fuel (Gupta, et al., 2010).

10.1.1.4 Bio-methanol

Heating value	20 [MJ kg^{-1}]

Methanol is derived from biomass via gasification, and can have woody feedstock or organic waste. Some fuel cell types can have methanol as fuel. Methanol can also be derived from coal gasification. Storage of methanol (and ethanol) has safety risk, due to the low flash point of alcohols. This is a disadvantage compared with diesel.

10.2 Chemical energy storage

10.2.1 Secondary batteries

Secondary batteries can be divided in two groups according to application. The power of batteries applied in electric power plants can be over 1 MW. Batteries applied at the customer side (electronics, cars) are in the order of 300-500 kW (Gupta, 2011). Small scale use is the main practice, the discharge period is usually not below 15 minutes. Advantages of batteries for electric energy storage are their high efficiencies, drawbacks are their high costs and scale limitations (Gommans, 2012).

10.2.1.1 Lead acid battery (LA)

Energy density	30-50 [Wh kg^{-1}]
Cycle lifetime	500-2.000
Maturity	Mature

The main advantages of lead-acid batteries are the mature, well investigated state of the technology and its low cost.. Cycle efficiencies are in the order of 80-90%, and self-discharge is no problem (2% per month). Usable capacity decreases when the batteries are discharged at high power. Its low cycle life (degraded by full discharges) and its low energy density make LA less attractive for energy management. Furthermore, lead is an environmentally hazardous material. Typical applications are emergency power supply, stand-alone systems with PV (applied in 75% of the PV systems in China (Beaudin, et al., 2010)), or leveling of output fluctuations from wind power (IEC, 2011).

10.2.1.2 Nickel cadmium (NiCd) and nickel metal hydride battery (NiMH)

Energy density	50-80 [Wh kg^{-1}]
Cycle lifetime	1.000-2.000
Maturity	Used

Has high mechanical robustness and best deep temperature performance of all rechargeable battery technologies. Since 2006, cadmium batteries are prohibited for consumer use, because of toxity. Therefore, NiMH batteries were developed with higher energy densities and comparable power densities. The NiMH have relatively low efficiencies of 65-70%, self-discharge is higher than that of lead-acid batteries (10% per month). Sealed NiMH batteries are mainly applied in hybrid vehicles.

10.2.1.3 Lithium ion battery (Li-ion)

Energy density	75-200 [Wh kg^{-1}]
Cycle lifetime	1.000-10.000
Maturity	Pre-commercial

Highest energy densities of batteries, efficiency of 90-100%. Nearly any discharge time in the range from seconds to weeks is feasible due to its relatively low self-discharge of 5% per month (Chen, et al., 2009). However, lifetime decreases at deep discharges, which make them unsuitable for back-up applications in which they are completely discharged (Hadjipaschalis, 2009). Currently only applied

in portable applications, batteries for grid load leveling and daily storage of renewable energy are being developed and its potential for residential scale energy storage is big (IEC, 2011). Up till now only competitive with lead-acid batteries for discharge times below 1h. Li-ion batteries are still too expensive for other (large scale) applications.

10.2.1.4 Metal air battery (Me-air)

Energy density	150-3.000 [Wh kg^{-1}]
Cycle lifetime	100-300
Maturity	Developing

In metal air batteries, the cathode is ventilated with air, whereas the oxygen is used in the electrochemical reaction. Currently, only the zinc air combination showed technical feasibility with an energy density of 1.350 Wh/kg and negligible self-discharge. Energy storage ranging from hours to months seems feasible. However, these batteries are not yet commercially available (IEC, 2011). Tests show a limited operating temperature range.

10.2.1.5 Sodium-based battery

Energy density	100-240 [Wh kg^{-1}]
Cycle lifetime	2.500-4.500
Maturity	Commercial

Sodium sulphur batteries (NaS) require a very high operating temperature of around 300℃ to keep the electrodes molten. No external heat source is required to maintain these temperatures, heat produced by the (dis-)charging process itself is sufficient. The cycle efficiency is about 75-90%, and the batteries combine a fast response with a typical discharge time of circa seven hours, which makes them interesting for application for power quality control and time shift applications.

With a lifetime up to 10.000 cycles and relatively high energy density, but also the high corrosion sensitivity of sodium, NaS batteries are most promising for large scale stationary applications. Especially for energy management and integration with variable renewable resources. The minimal commercial power and energy range of NaS batteries is 1 MW-7MWh, already applied in many countries, e.g. Japan (Van Velzen, 2010). The Sodium nickel chloride battery (NaNiCl) is another high-temperature sodium battery. These batteries are mainly applied in electric vehicles. Ideas for the connection of car batteries to the power grid, forming a virtual superbattery that can store large amounts of excess electricity, is an interesting for overproduction of renewable energy but does not provide a solution during periods of shortage (Van Velzen, 2010; Gommans, 2012).

10.2.2 Flow batteries

The technology is now in a developed stage and applied in some large scale projects (Beaudin, et al., 2010; IEC, 2011). The different electrolytes that have been developed, are discussed below.

10.2.2.1 Redox flow battery (RFB)

Energy density	10-30 [Wh kg^{-1}]
Cycle lifetime	12.000+
Maturity	Pre-commercial

The vanadium RFB is most far developed. Total charge-discharge efficiencies of 75-85%. Power and energy can be easily be scaled, independently from each other. The energy capacity can be scaled by changing the tank size. The power rating can be influenced by scaling the stack. A 500 kW-5MWh storage system was installed in Japan by SEI. The system can also be used as power quality device because it can be recharged fast by replacing the electrolyte. It can also be integrated with renewable energy generation in electricity utilities.

10.2.2.2 Hybrid flow battery (HFB)

Energy density	30-75 [Wh kg^{-1}]
Cycle lifetime	2.000+
Maturity	Pre-commercial

When one of the electrolytes is stored within the electrochemical reactor and one liquid electrolyte is stored externally, the system is called a hybrid flow battery. HFB are not suitable for discharge times more than several hours and small distributed energy storage (Droste-Franke, et al., 2012)(Beaudin, et al., 2010). Zinc-Bromide (Zi-Br) and Zn-Ce are two examples of a hybrid flow battery. Zi-Br achieve cycle efficiencies of 75%. A 5 kW-20 kWh Zn-Br battery is currently in development (IEC, 2011).

10.2.3 Availability of metals for Electric Energy Storage

Table 10-1: Metals availability (Beaudin 2010)

Metal	Used for EES	Reserves ktons	Use $year^{-1}$ ktons	Years left
Bismuth	SMES	320	5,8	55
Barium	SMES	190k	7770	25
Copper	SMES	550k	15,7k	35
Lead	LA, SMES	79k	3800	21
Lithium	Li-ion	4100	27,4	150
Magnsium	SMES, FC	N/A	808	>1000
Nickel	NiCd, FC	70k	1610	44
Palladium	FC	80	0,41	197
Sodium	NaS	3.300k	4000	825
Strontium	SMES	6800	512	13
Titanium	FES, FC	5280	166	32
Vanadium	VRB	13k	60	217
Yttrium	SMES	540	8,9	61
Zinc	Zi-Br	180k	11,3k	16
Zirconium	FC	51k	1360	38

11 Appendix B – Properties of Case study dwelling

11.1 Geometrical and constructional data

Table 11-1 Geometrical characteristics of reference dwelling

Characteristic		
Width	5.1 m	[m]
Depth	8.9 m	[m]
Floor height	2.6 m	[m]
Usable floor space Ag	124.3	[m^2]
Envelope area	156.9	[m^2]
Ratio floor space/envelope	0.8	[-]
Volume	306.5	[m^3]

Table 11-2 Characteristics reference dwelling

Characteristic		
Rc façade	3,5	[$m^2K\ W^{-1}$]
Rc roof	4,0	[$m^2K\ W^{-1}$]
Rc ground floor	3,5	[$m^2K\ W^{-1}$]
U-value windows	1,6 (U_f < 2,4, U_{HR++} < 1,0)	[$W\ m^{-2}K^{-1}$]
U-value front door	2,0	[$W\ m^{-2}K^{-1}$]
Sunshading on facades:	S	
Ventilation system	Balanced ventilation	
Efficiency heat recovery	95% + bypass	
Infiltration (50 Pa: 2,5)		[h^{-1}]
Extra	Shower-WTW	
Thermal mass	550 (traditional, mixed heavy)	[$kJ\ m^{-2}\ K^{-1}$]

In order to be able to simulate the effect of different occupation patterns and comfort requirements within the dwelling, a single zone model would not suffice. Therefore, two zones are distinguished:

Living zone

Including the living room, kitchen and bathroom. Total floor space: 51.6 m^2, volume:137.2 m^3.

Category	Wall name	Floor	Area m^2	Adjacent to
Boundary	GR_FLOOR_01A	BG	46.2	10˚C
	SEP_WALL	BG	48.0	Identical
	SEP_WALL	1	6.0	Identical
External	EXT_WALL_01	BG	8.6	North
	- WINDOW_01		2.9	
	DOOR	BG	2.4	North
	EXT_WALL_01	BG	4.2	South
	- WINDOW_01		9.7	
Adjacent	ADJ_WALL	1	22.4	ZONE_SLEEPING
	ADJ_FLOOR	1	40.8	ZONE_SLEEPING

	ADJ_FLOOR	2	5.4	ZONE_SLEEPING
Internal	INT_WALL	BG	33.6	
	INT_FLOOR_A*	1	5.4	

* both sides are calculated in TRNSYS

Sleeping zone

Including all other spaces like sleeping rooms and attic. Total floor space: 72.7 m^2, volume:169.3 m^3.

Category	Wall name	Floor	Area m²	Adjacent to
Boundary	SEP_WALL	1	42.0	Identical
	SEP_WALL	2	34.5	Identical
External	EXT_WALL_01	1	12.2	North
	- WINDOW_01		5.1	
	EXT_WALL_01	1	12.2	South
	- WINDOW_01		5.1	
	ROOF	2	31.1	North
	ROOF	2	29.7	South
	- WINDOW_01		1.4	
Adjacent	ADJ_WALL	1	22.4	ZONE_LIVING
	ADJ_FLOOR	1	40.8	ZONE_LIVING
	ADJ_FLOOR	2	5.4	ZONE_LIVING
Internal	INT_FLOOR_A*	2	40.1	
	INT_WALL	1	44.8	

* double input in TRNSYS (both sides)

The composition of the walls is very important since capacitance will influence the simulation outcomes significantly. Construction layers and materials are defined according to Dutch SBR referentie details, and shown in the overview on the next page.

In traditional dwellings, the SWM (specific thermal mass) is higher than 450 kJ m^{-2} K^{-1}, according to NEN-7120 [7]. The modeled construction has a SWM of 545 kJ m^{-2} K^{-1}, calculated in accordance with Appendix H of NEN-7120.

[7] NEN 7120 Energieprestatie van gebouwen

	Conductivity	Thickness	Resistance	Heat transfer Coef	Heat transfer	HTC demand	Spec. heat	Density	Area	Mass	Capacitance	Mass*	Capacitance* NEN7
	[W/mK]	[m]	[m2K/W]	[W/m2K]	[W/K]		[kJ/kgK]	[kg/m3]	[m2]	[kg]	[kJ/K]	[kg]	[kJ/K]
General													
SEP_WALL				2.705		-			130.5				
Concrete	1.70	0.120	0.07				0.84	2200		34452.0	28939.7	17226.0	14469.8
Cavity (air)			0.17										
INT_WALL				3.569		-			61.6				
Gypsum plaster	0.35	0.001	0.00				1.00	1200		73.9	73.9	-	-
Concrete	1.70	0.025	0.01				0.84	2200		3388.0	2845.9	-	-
Gypsum plaster	0.35	0.001	0.00				1.00	1200		73.9	73.9	-	-
INT_FLOOR_A				6.607		-			91.7				
Cement mortar	1.32	0.030	0.02				0.84	2000		5502.0	4621.7	5502.0	4621.7
Active layer													
Cement mortar	1.32	0.030	0.02				0.84	2000		5502.0	4621.7	5502.0	4621.7
Concrete	1.70	0.180	0.11				0.84	2200		36313.2	30503.1	36313.2	30503.1
Envelope EPC 0.6													
GR_FLOOR_01A				0.290	13.38	0.286			46.2				
Cement mortar	1.32	0.060	0.05				0.84	2000		5544.0	4657.0	5544.0	4657.0
Active layer													
Cement mortar	1.32	0.010	0.01				0.84	2000		924.0	776.2	924.0	776.2
Mineral wool	0.04	0.035	0.90				0.90	80		129.4	116.4	129.4	116.4
Concrete	1.70	0.180	0.11				0.84	2200		18295.2	15368.0	-	-
Mineral wool	0.04	0.080	2.06				0.90	80		295.7	266.1	-	-
Air layer (hor)		0.051	0.17									-	-
EXT_WALL_01				0.293	10.89	0.286			37.2				
Gypsum plaster	0.35	0.002	0.01				1.00	1200		89.3	89.3	89.3	89.3
Concrete	1.70	0.125	0.07				0.84	2200		10230.0	8593.2	8020.3	6737.1
Mineral wool	0.04	0.110	2.83				0.90	80		327.4	294.6	-	-
Cavity (air)		0.040	0.17									-	-
Brick	0.60	0.100	0.17				0.84	1600		5952.0		-	-
WINDOW_01				1.520	36.78	1.600			24.2				
Glazing	0.00			1.270								-	-
Frame	0.00			2.270								-	-
DOOR_01				1.974	4.74	2.000			2.4				
Wood	0.15	0.050	0.33				1.20	800		96.0	115.2	96.0	115.2
ROOF_01				0.204	12.38	0.200			60.8				
Gypsum plaster	0.35	0.015	0.04				1.00	1200		1094.4	1094.4	1094.4	1094.4
Mineral wool	0.04	0.170	4.37				0.90	80		826.9	744.2	48.6	43.8
Wood	0.15	0.020	0.13				1.20	800		972.8	1167.4	-	-
Cavity (air)			0.17									-	-
Rooftiles	0.66	0.015	0.02				0.84	1500		1368.0		-	-
				Heat transfer total envelope W/K:	78.17				ECP 0.6	Total capacitance	104961.8		67845.6
										SWM*	844.4		545.8

* NEN 7120 Append

11.2 Ventilation and air infiltration rates

The modeled ventilation and infiltration rates are defined in accordance with respectively NEN 7120 and NEN 8088[8]. Formulas that have been used are described in the next paragraphs.

11.2.1 Ventilation

Standard ventilation rates are calculated according to NEN 7120 as follows: qve;sys;reken = fkan × (freg × fsys) × fT × (qg;spec;functie g × Ag)

Where,

freg correction factor control system

1.00 [-] (heat exchanger without zoning)

fsys ventilation system based air flowrate factor

1.00 [-] (balanced ventilation, system D)

fT correction factor for occupancy

1.00 [-]

fkan correction factor leaks in air ducts

1.10 [-]

qg;spec;f function-specific ventilation rate

0.43 [$dm^3\ s^{-1}\ m^{-2}$]

Ag usable floorspace [m^2]

This means that the minimum ventilation rate should be:

qve;sys;reken = 0.473 x Ag [$dm^3\ s^{-1}\ m^{-2}$]

The supplied air temperature depends on the outside temperature and the efficiency of the Heat recovery unit following this formula:

$Ts = \eta_{HRU} * (Tr - Te) + Te$

where,

Ts Supply air temperature [C]

η_{HRU} Efficiency HRU [-], assumed 0.85

Tr Average retour air temperature rooms [C]

Te Temperature supply air to HRU [C]

[8] NEN-8088-1+C1 Ventilation and infiltration for buildings

Natural ventilation has been taken in account following dynamic simulation guidelines from ISSO 32[9]. When the windows can be opened, an additional ventilation flow of 3 dm^3 s^{-1} m^{-2} is modeled in for the ground and first floor. The decision making conditions are described below:

Windows open when:	Windows closed again when:
Toperative room > 24C AND	Toperative room < 20C OR
Air velocity lij < 6 m/s AND	Air velocity lij > 6 m/s OR
Air velocity loef < 3 m/s AND	Air velocity loef > 3 m/s
12C < Tambient < 26C	

11.2.2 Infiltration

In accordance with NEN 8088, the value for air permeability, $q_{v,10,kar}$, was defined: 0.7 dm^3 s^{-1} m^2 usable floor space. The resulting infiltration flow rate can be deducted from Figure 11-1, and is $14.8x10^{-5}$ m^3/s per m^2 envelope[10] (linear interpolation is allowed).

Ventilatiesysteem	$q_{v,10,kar}$				
	≤ 0,3	0,5	1,0	1,5	≥ 2,0
Systeem A Natuurlijke toevoer en natuurlijke afvoer ventilatie;			$17 \cdot 10^{-5}$	$26 \cdot 10^{-5}$	$39 \cdot 10^{-5}$
Systeem C Natuurlijke toevoer en centrale mechanische afvoer*) ventilatie;			$16 \cdot 10^{-5}$	$23 \cdot 10^{-5}$	$34 \cdot 10^{-5}$
Systeem C (variant) Natuurlijke toevoer van ventilatielucht en mechanische afvoer per vertrek	$10 \cdot 10^{-5}$	$12 \cdot 10^{-5}$	$19 \cdot 10^{-5}$	$30 \cdot 10^{-5}$	$42 \cdot 10^{-5}$
Systeem B Mechanische toevoer en natuurlijke afvoer ventilatie	$11 \cdot 10^{-5}$	$14 \cdot 10^{-5}$	$21 \cdot 10^{-5}$	$33 \cdot 10^{-5}$	$45 \cdot 10^{-5}$
Systeem D Mechanische toevoer en mechanische afvoer ventilatie (gebalanceerde ventilatie)	$10 \cdot 10^{-5}$	$12 \cdot 10^{-5}$	$19 \cdot 10^{-5}$		
*) centrale mechanische afvoer is mechanische afvoer uit alleen keuken, badkamer en toilet					
Niet toegestaan					

Figure 11-1: Infiltration flowrate (m^3/s per m^2 envelope) depending on $q_{v,10,kar}$ and ventilation system

The results that are used as input for the models are summarized in Table 11-3.

Table 11-3 Model input values for ventilation and infiltration rates for both building zones

Zone	Ag	Aenv	Volume	Ventilation		Natural ventilation		Infiltration	
	[m^2]	[m^2]	[m^3]	[m^3/h]	[V/h]	[m^3/h]	[V/h]	[m^3/h]	[V/h]
Living	51.6	27.8	137.2	87.86	0.64	498.96	4.07	14.81	0.11
Sleeping	72.7	96.8	169.3	123.79	0.73	785.16	4.64	51.58	0.30
Total	124.3	124.6	306.5	211.66	0.69	291.95	4.40	66.39	0.22

[9] ISSO 32 Uitgangspunten temperatuursimulatieberekeningen 2011

[10] ISSO Publicatie 51 Warmteverliesberekening voor woningen en woongebouwen

11.3 Heat gains

11.3.1 Internal gains

The internal gains are based on guidelines in NEN-ISO 13790[11] because, contrary to NEN-8088, internal gains are specified per hour of the day and per zone. It comprises heat gains by occupants and appliances:

Table 11-4 – Internal gains modelled per m^2

Days	Hours	Living zone		Sleeping zone	
	[h]	[W/m2]	[kJ/hm2]	[W/m2]	[kJ/hm2]
Mon-fri	00:00-07:00	2.0	7.20	6.0	21.60
	07:00-17:00	8.0	28.80	1.0	3.60
	17:00-23:00	20.0	72.00	1.0	3.60
	23:00-00:00	2.0	7.20	6.0	21.60
Sat+sun	00:00-07:00	2.0	7.20	6.0	21.60
	07:00-17:00	8.0	28.80	2.0	7.20
	17:00-23:00	20.0	72.00	4.0	14.40
	23:00-00:00	2.0	7.20	6.0	21.60
Average		9.0	32.40	3.0	10.80

The loads for the living zone are applied on 46.2 m^2, the loads for the sleeping zone on 45.5 m^2. The attic is assumed to be not occupied on regularly basis.

11.3.2 Solar gains - sunshading

Weather data within TRNSYS has been used as a basis for both the MATLAB and TRNSYS model. The weather data files available in TRNSYS derive from Meteonorm data for a typical meterorological year (TMY). Weather and radiation values are based on monthly data generated stochastically to hourly values by Meteonorm V 5.0.13[12]. NL-Amsterdam-Schiphol-62400.tm2 has been used.

Typical Dutch dwellings do have sunshading on the South façade (Senternovem). When shading is down, the ZTA of the windows as specified in TRNSYS changes from 0.6 (no shading) to 0.2 (in TRNSYS: shading factor 0.8). The sunshading is controlled using irradiation limits advised for simulations by ISSO 32:

Sunshading down when:	[W m^{-2}]	[kJ hr^{-1} m^2]
Total irradiation on South facade qz,s	> 300	> 1080

[11] NEN-ISO 13790 Energy performance of buildings

[12] TRNSYS 17 Documentation vol 08 Weather Data

11.4 DHW consumption

As stated in the main text, this study focused on the optimization of low temperature energy storage for space heating purposes. The optimization strategy is also applied to DHW generation and consumption, see Appendix C. Therefore, a daily pattern for DHW consumption was constructed in accordance with NEN 7120. NEN 7120 provides different DHW draw patterns that can be used for energy calculations. In this study, Class 3 has been used. It consists of a base water draw pattern shower excluded, and a separate pattern for the shower draws at 8 AM and 11PM. The pattern can be translated into dm^3 of water of 60C, and the energy required to heat up water of 10C to this required temperature. This sums up to a yearly energy demand for DHW of 16089 MJ.

Hour of the day	dm3/hr	Tgen [C]	kJ
1	0	0	0
2	0	0	0
3	0	0	0
4	0	0	0
5	0	0	0
6	0	0	0
1-7	0	0	0
8	78.2	60	16382.9
9	3.6	60	754.2
10	3.6	60	754.2
11	3.6	60	754.2
12	3.6	60	754.2
13	3.6	60	754.2
14	3.6	60	754.2
15	3.6	60	754.2
16	3.6	60	754.2
17	3.6	60	754.2
18	3.6	60	754.2
19	3.6	60	754.2
20	3.6	60	754.2
21	3.6	60	754.2
22	3.6	60	754.2
23	3.6	60	754.2
0	78.2	60	16382.9
Sum	210.4		44079

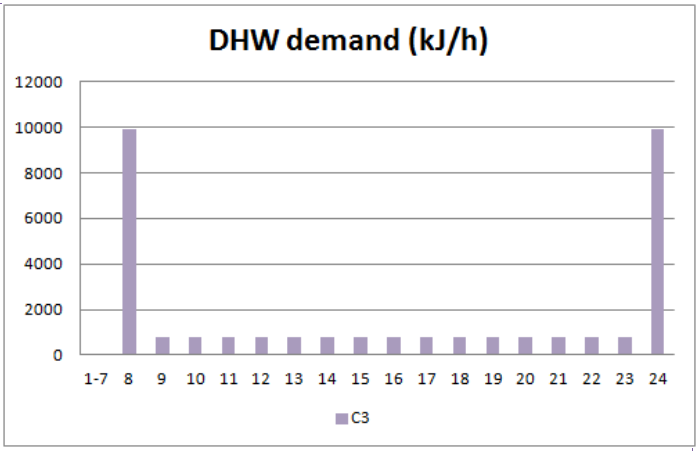

12 Appendix C – Detailed results MATLAB

12.1 Detailed data of results

12.1.1 Variable - buffer volumes

Variables	
P_{el} heat pump [kW]	1.0
Temperature limits [C]	23 – 25
Climatecurve (hrs ahead)	A(24),B(24),C(24/36/60) ,D(12/24/48)
Insulation tank [W/m2K]	0,35
Heating demand	Default (D=0.8)
Buffer height [m]	1
Factor work/electrical energy to primary energy	2.56 (39% generation efficiency, NEN 7120)

Operational cost (i.e. cost of electricity) is calculated using the contemporary price structure of day- and night electricity tariffs. Prices were obtained from a typical household consumer contract (1 jaar vast, including energy tax and BTW) at http://www.energiedirect.nl/energie/energietarieven :

Table 12-1 – Electricity prices day-night tariff

Period	Price [€/kWh]
Workdays 07-23h (day)	0,21802
Workdays 23-07h (night)	0,19802
Weekend	0,19802

Single tariff (used in the economic feasibility study) is: 0,20913 €/kWh.

12.1.1.1 Strategy A

Table 12-2 – yearly sums per buffer volume strategy A

Buffer volume [kg]	1e2	2e2	2.5e2	5e2	1e3	1.5e3	2e3
Energy demand [MJ]	14.488	14.488	14.488	14.488	14.488	14.488	14.488
Work [MJ]	3.982	3.982	3.996	4.025	4.072	4.079	4.061
Primary energy consumed [MJ]	10.193	10.193	10.230	10.303	10.423	10.442	10.396
Hours that installation is on [h]	1.106	1.106	1.110	1.118	1.131	1.133	1.128
Number of on/off cycles [-]	1.063	891	682	369	201	143	111
Operational cost (electricity) [€]	229	229	230	231	236	238	237

12.1.1.2 Strategy B (start installation at 14h)

Table 12-3 – yearly sums per buffer volume strategy B

Buffer volume [kg]	1e2	2e2	2.5e2	5e2	1e3	1.5e3	2e3
Energy demand [MJ]	14.488	14.488	14.488	14.488	14.488	14.488	14.488
Work [MJ]	3.935	3.884	3.863	3.794	3.744	3.733	3.722
Primary energy consumed [MJ]	10.073	9.944	9.889	9.714	9.585	9.557	9.529
Hours that installation is on [h]	1.093	1.079	1.073	1.054	1.040	1.037	1.034
Number of on/off cycles [-]	1.049	1.039	1.014	818	521	381	325
Operational cost (electricity) [€]	228	227	226	226	225	225	225

12.1.1.3 Strategy C (prediction 12 hrs)

Table 12-4 – yearly sums per buffer volume strategy C

Buffer volume [kg]	1e2	2e2	2.5e2	5e2	1e3	1.5e3	2e3
Energy demand [MJ]	14.488	14.488	14.488	14.488	14.488	14.488	14.488
Work [MJ]	3.953	3.910	3.892	3.823	3.737	3.708	3.697
Primary energy consumed [MJ]	10.119	10.009	9.962	9.787	9.566	9.492	9.465
Hours that installation is on [h]	1.093	1.081	1.076	1.057	1.033	1.025	1.022
Number of on/off cycles [-]	1.053	1.030	1.007	836	596	493	468
Operational cost (electricity) [€]	228	227	226	225	222	221	220

12.1.1.4 Strategy C (prediction 24 hrs)

Table 12-5 – yearly sums per buffer volume strategy C

Buffer volume [kg]	1e2	2e2	2.5e2	5e2	1e3	1.5e3	2e3
Energy demand [MJ]	14.488	14.488	14.488	14.488	14.488	14.488	14.488
Work [MJ]	3.992	3.953	3.938	3.881	3.798	3.766	3.744
Primary energy consumed [MJ]	10.221	10.119	10.082	9.935	9.723	9.640	9.585
Hours that installation is on [h]	1.104	1.093	1.089	1.073	1.050	1.041	1.035
Number of on/off cycles [-]	1.064	1.045	1.022	900	732	641	585
Operational cost (electricity) [€]	230	228	228	226	224	222	221

12.1.1.5 Strategy C (prediction 48 hrs)

Table 12-6 – yearly sums per buffer volume strategy C

Buffer volume [kg]	1e2	2e2	2.5e2	5e2	1e3	1.5e3	2e3
Energy demand [MJ]	14.488	14.488	14.488	14.488	14.488	14.488	14.488
Work [MJ]	4.014	3.974	3.967	3.924	3.848	3.812	3.791
Primary energy consumed [MJ]	10.276	10.174	10.156	10.045	9.852	9.760	9.704
Hours that installation is on [h]	1.110	1.099	1.097	1.085	1.064	1.054	1.048
Number of on/off cycles [-]	1.068	1.049	1.036	948	789	702	638
Operational cost (electricity) [€]	231	320	230	229	226	224	223

12.1.1.6 Strategy D (prediction 12 hrs)

Table 12-7 – yearly sums per buffer volume strategy D

Buffer volume [kg]	1e2	2e2	2.5e2	5e2	1e3	1.5e3	2e3
Energy demand [MJ]	14.488	14.488	14.488	14.488	14.488	14.488	14.488
Work [MJ]	3.906	3.845	3.830	3.748	3.76	3.665	3.668
Primary energy consumed [MJ]	9.999	9.843	9.806	9.594	9.410	9.382	9.391
Hours that installation is on [h]	1.085	1.068	1.064	1.041	1.021	1.018	1.019
Number of on/off cycles [-]	1.043	1.030	1.016	861	697	700	674
Operational cost (electricity) [€]	226	224	224	222	220	220	220
Optimal bset [MJ]	0,5	5	8	7	7	1	5

12.1.1.7 Strategy D (prediction 24 hrs)

Table 12-8 – yearly sums per buffer volume strategy D

Buffer volume [kg]	1e2	2e2	2.5e2	5e2	1e3	1.5e3	2e3
Energy demand [MJ]	14.488	14.488	14.488	14.488	14.488	14.488	14.488
Work [MJ]	3.953	3.912	3.892	3.816	3.715	3.668	3.647
Primary energy consumed [MJ]	10.119	10.018	9.962	9.769	9.511	9.391	9.336
Hours that installation is on [h]	1.098	1.087	1.081	1.060	1.032	1.019	1.013
Number of on/off cycles [-]	1.059	1.041	1.027	880	626	513	455
Operational cost (electricity) [€]	228	226	226	224	221	219	218
Optimal bset [MJ]	1	6	3	26	41	41	44

12.1.1.8 Strategy D (prediction 48 hrs)

Table 12-9 – yearly sums per buffer volume strategy D

Buffer volume [kg]	1e2	2e2	2.5e2	5e2	1e3	1.5e3	2e3
Work [MJ]	3.989	3.949	3.935	3.884	3.798	3.751	3.719
Primary energy consumed [MJ]	10.211	10.110	10.073	9.944	9.723	9.603	9.520
Hours that installation is on [h]	1.108	1.097	1.093	1.079	1.055	1.042	1.033
Number of on/off cycles [-]	1.067	1.052	1.042	931	770	658	607
Operational cost (electricity) [€]	230	229	228	227	224	222	220
Optimal bset [MJ]	5	8	1	25	15	30	30

12.1.2 Extreme winter week (hr 780-1008)

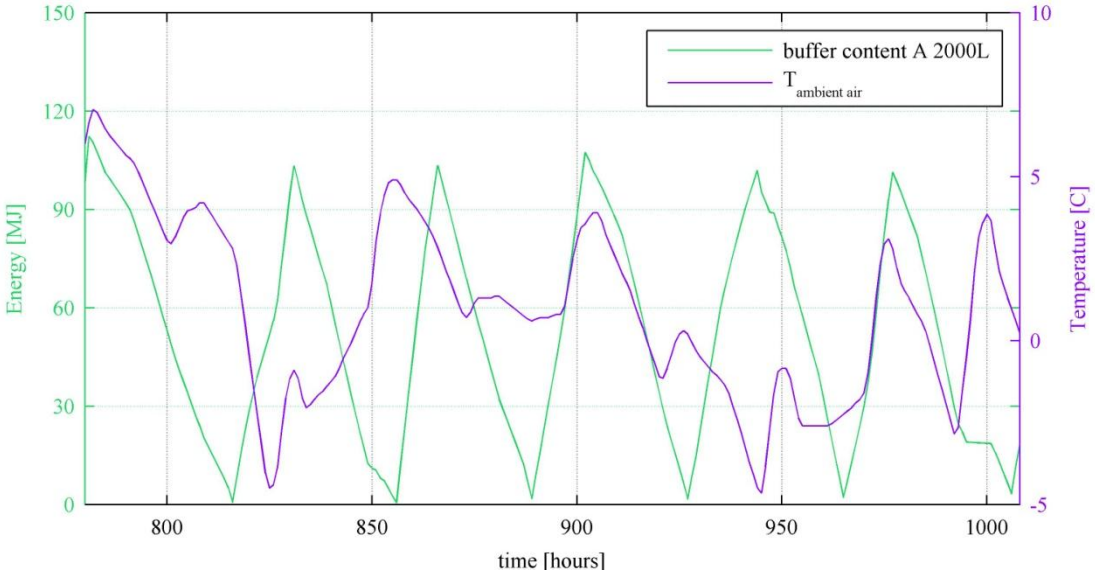

Figure 12-1: Energy content in buffer during winter week and outside temperature

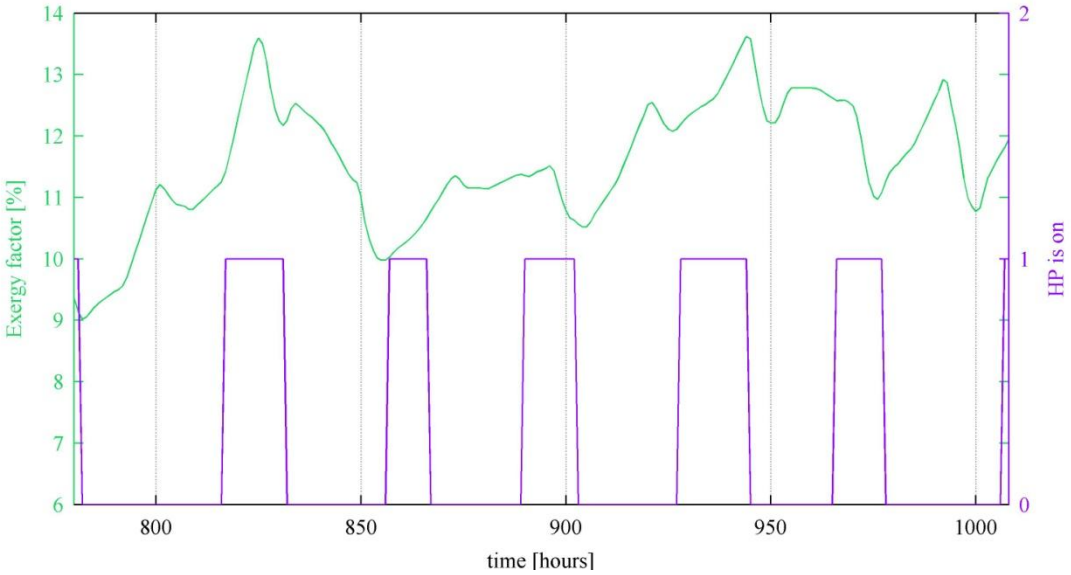

Figure 12-2: Installation operation pattern and exergy factor during winter week

During a winter week with more extreme outside temperatures, like the minima that occur around t=825 hr and t=950 hr, the buffer in strategy A is discharged faster because of high demands and it takes longer before the buffer is completely recharged due to bad outside conditions. Although

strategy D isn't able to cover a full days heat load anymore (resulting in a very high on/off frequency), still heat pump operation during maximum exergy factors (minimum temperatures) is avoided.

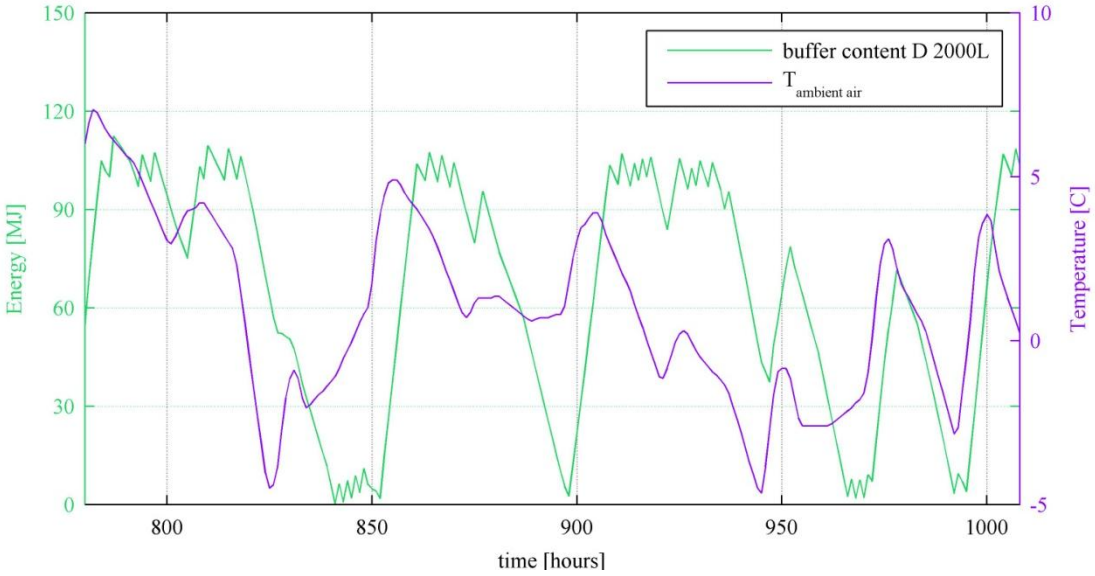

Figure 12-3: Energy content in buffer during winter week and outside temperature for strategy D (24 hrs horizon)

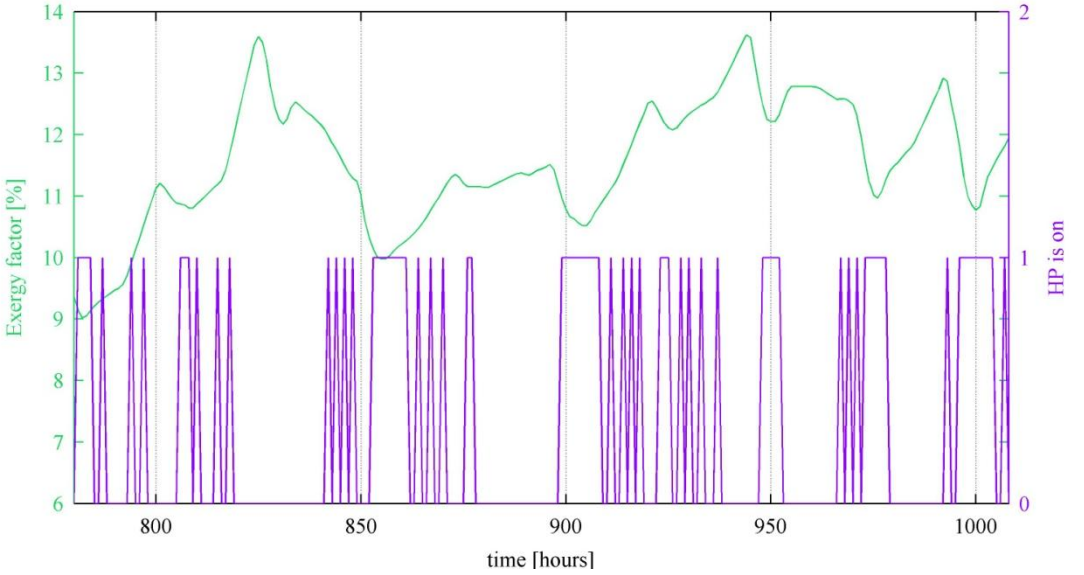

Figure 12-4: Installation operation pattern and exergy factor during winter week for strategy D (24 hrs horizon)

12.1.3 Variable - heat demand

Variables	
P_{el} heat pump [kW]	1.0
Temperature limits [C]	23 – 25
Insulation tank [W/m2K]	0,35
Buffer height [m]	1
Heat demand	100%, 75% and 50%

Besides the reference case (yearly heat demand 14.488 MJ, high), two other cases have been calculated. One associated with a heat demand of dwellings at current energy performance standards (10.866 MJ/a, or 24 kWh/m^2, 75% of the reference heat demand) and a demand of 7.244 MJ/a (or 50% of reference, 16 kWh/m^2), which corresponds with passive house demands.

At lower heat demands, the savings of strategy D increases (from max. 10% at high demand to 15% at low demand). This could be expected, since the same buffer volumes can now provide energy for longer periods, so more suboptimal hours of operation are prevented. At low heat demand, a prediction horizon of 24 hrs performs slightly better in combination with small volumes.

12.1.4 Variable - temperature difference in buffer tank

When temperature differences between a full and empty buffer are not allowed to be too large (e.g. in case of PCM storage or specific emission systems), the storage capacity of the buffer volumes is significantly reduced. Figure 12-6 shows that this results in smaller savings (max. 8 instead of 10%).

Variables	
Pel heat pump [kW]	1.0
Temperature limits [C]	23 – 25 (default), 29 - 36
Heat demand	100% (14.488 MJ/a)

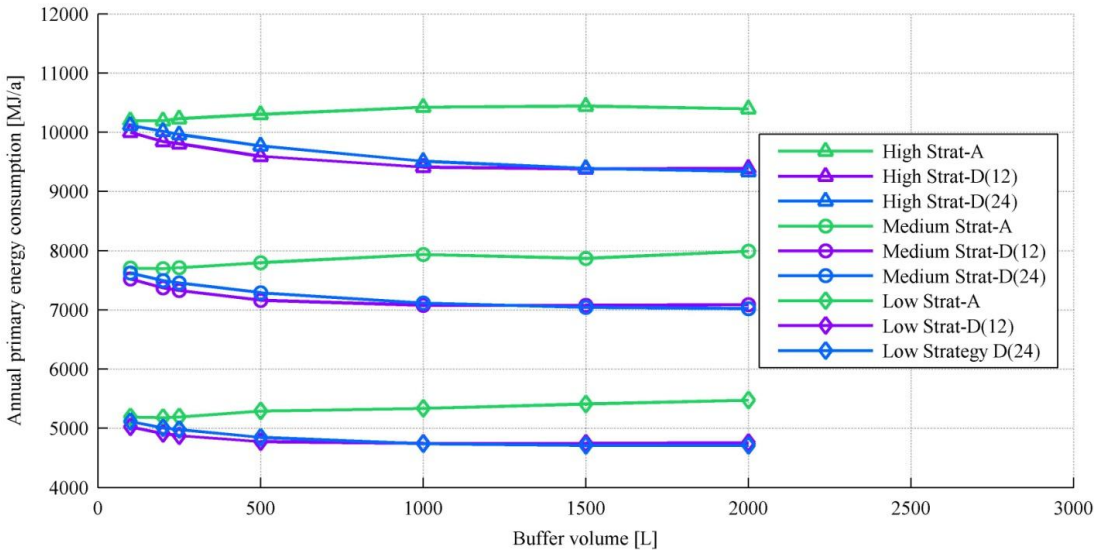

Figure 12-5: Yearly primary energy consumption for strategy A and D at high, medium and low yearly heat demand

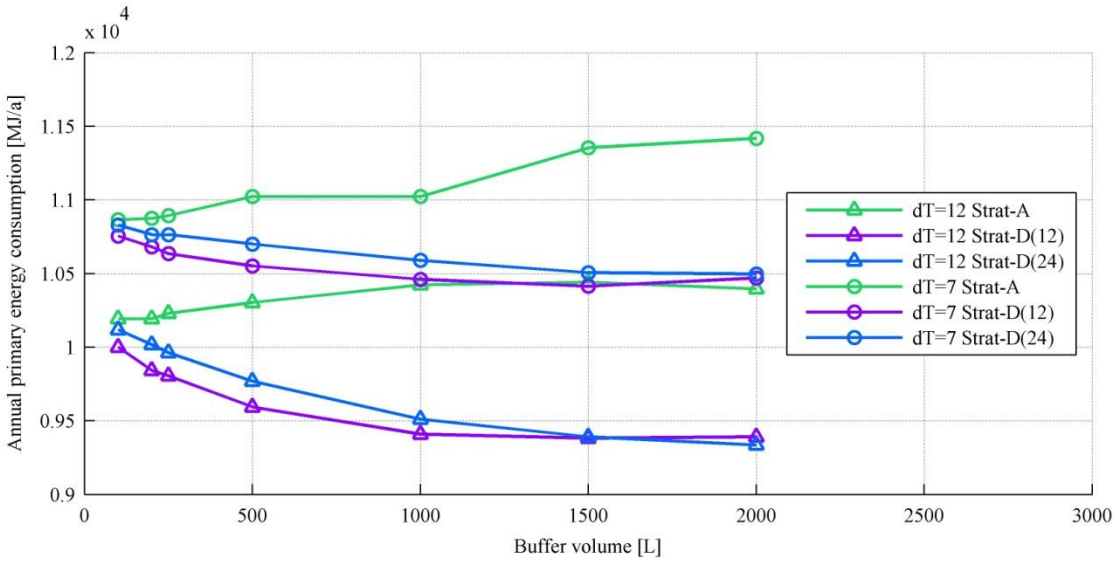

Figure 12-6: Yearly primary energy consumption for strategy A and D, differenent temperature differences buffer

12.1.5 Variable – installed electrical power heat pump

A smaller installed power does not significantly increase primary energy savings and on/off cycles (0,75kW returns maximum 1% difference with the reference power of 1kW$_{el}$). Still, heat demand is always met. The same goes for a larger installed power, which does only yield small additional savings (the buffer is recharged faster, so less operational hours are required, also during suboptimal conditions). What does change is the number of yearly operational hours, ± 33% compared to 1 kW$_{el}$.

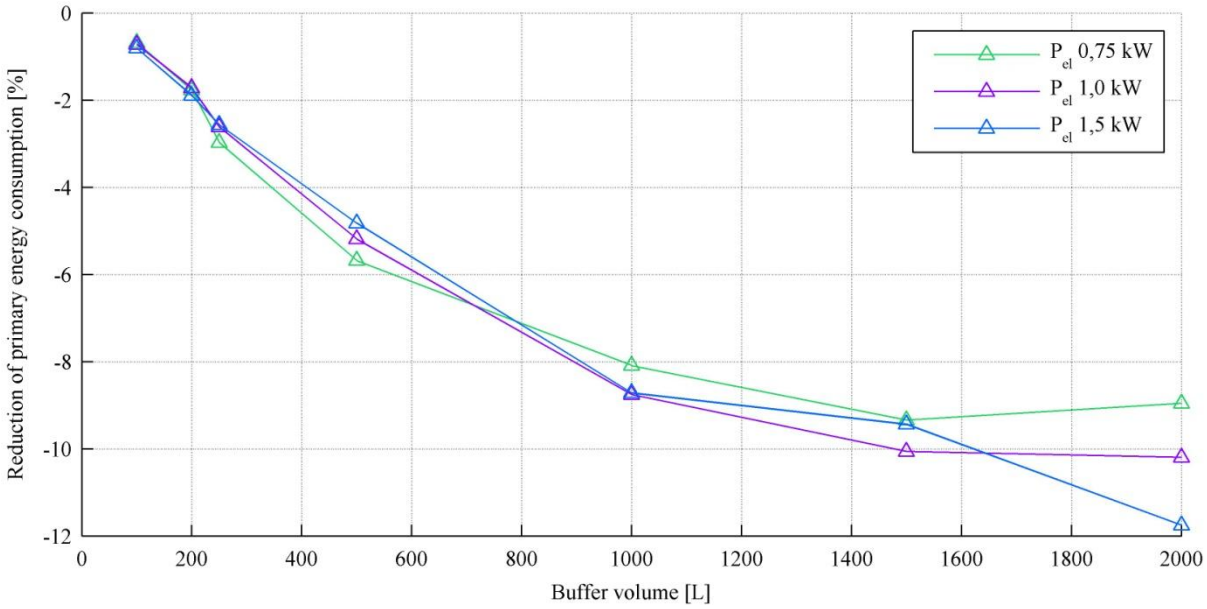

Figure 12-7: Annual savings of primary energy/work consumed (strategy D(24) compared to strategy A

12.2 Case Optimization DHW

What could the most potential strategy gain when applied to the DHW production, as explained in Appendix B? This was investigated for a 1,5 kW heat pump, heating up water from 10 to 60degrees C (condenser temperature 75 C, theoretical COP multiplied by 0,5 compressor efficiency).

Variables	
P_{el} heat pump [kW]	1.5
Temperature limits [C]	55 – 60
Insulation tank [W/m2K]	0,35
DHW demand [MJ/a]	16.089 (44 MJ/day), conform DHW class 3
Buffer height [m]	1
Optimal bset [MJ]	1 (for all volumes and strategies)

Although Figure 12-8 and Table 12-10 show that the algorithm results in smaller absolute and relative savings when applied to DHW demand (than space heating demand). Main reason is the increasing impact of thermal losses of the buffer (larger buffer volumes perform worse) because the buffer contains water at higher temperatures. Work savings resulting from generation at lower exergy factors are therefore in a small extent destroyed by thermal losses that accompany storage for several hours.

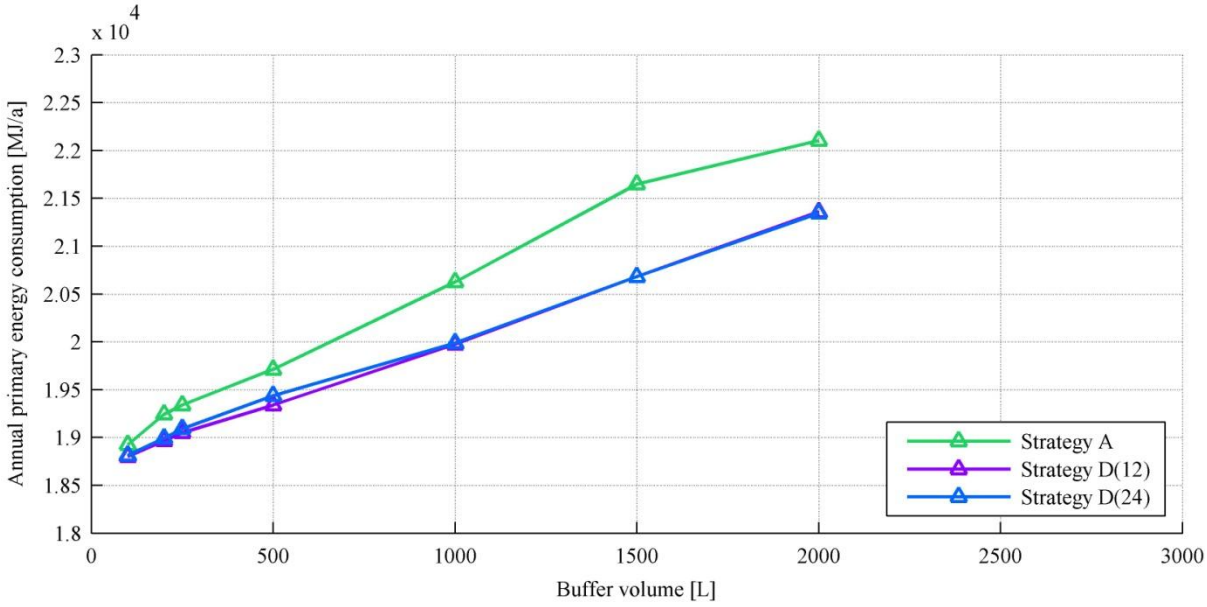

Figure 12-8: Yearly primary energy consumption for DHW production, strategies A and D

Most important output for a 1500L buffer is presented in the following table:

Table 12-10 – yearly sums for a 1500 L buffer, different strategies

	Strategy A	Strategy D (12 hrs)	Savings [abs (%)]	Strategy D (24 hrs)	Savings [abs (%)]
Work [MJ]	8.456	8.078	378 (4%)	8.078	378 (4%)
Primary energy consumed [MJ]	21.648	20.681	968 (4%)	20.681	968 (4%)
Hours that installation is on [h]	1.566	1.496	70 (4%)	1.496	70 (4%)
Number of on/off cycles [-]	242	989	+(309%)	837	+(246%)
Cost generation (electricity) [€]	488	488	-	482	-

13 Appendix D – Heat pump data

Table 13-1 - Data heat pump supplier (used in simulations)

Type	Reversible air to water heat pump	
Emplacement	Split/outside	
Heating power / COP at A7/W35	6,8 / 4,46	kW / -
Cooling power / EER at A35/W18	7,4 / 3,97	kW / -
Air flow rate	3.000	m^3/h
Refrigerant / quantity	R290 / 2,1	- / kg
Eff. consumed power / current at A7/W35	1,5 / 3,2	kW_{EL} / A

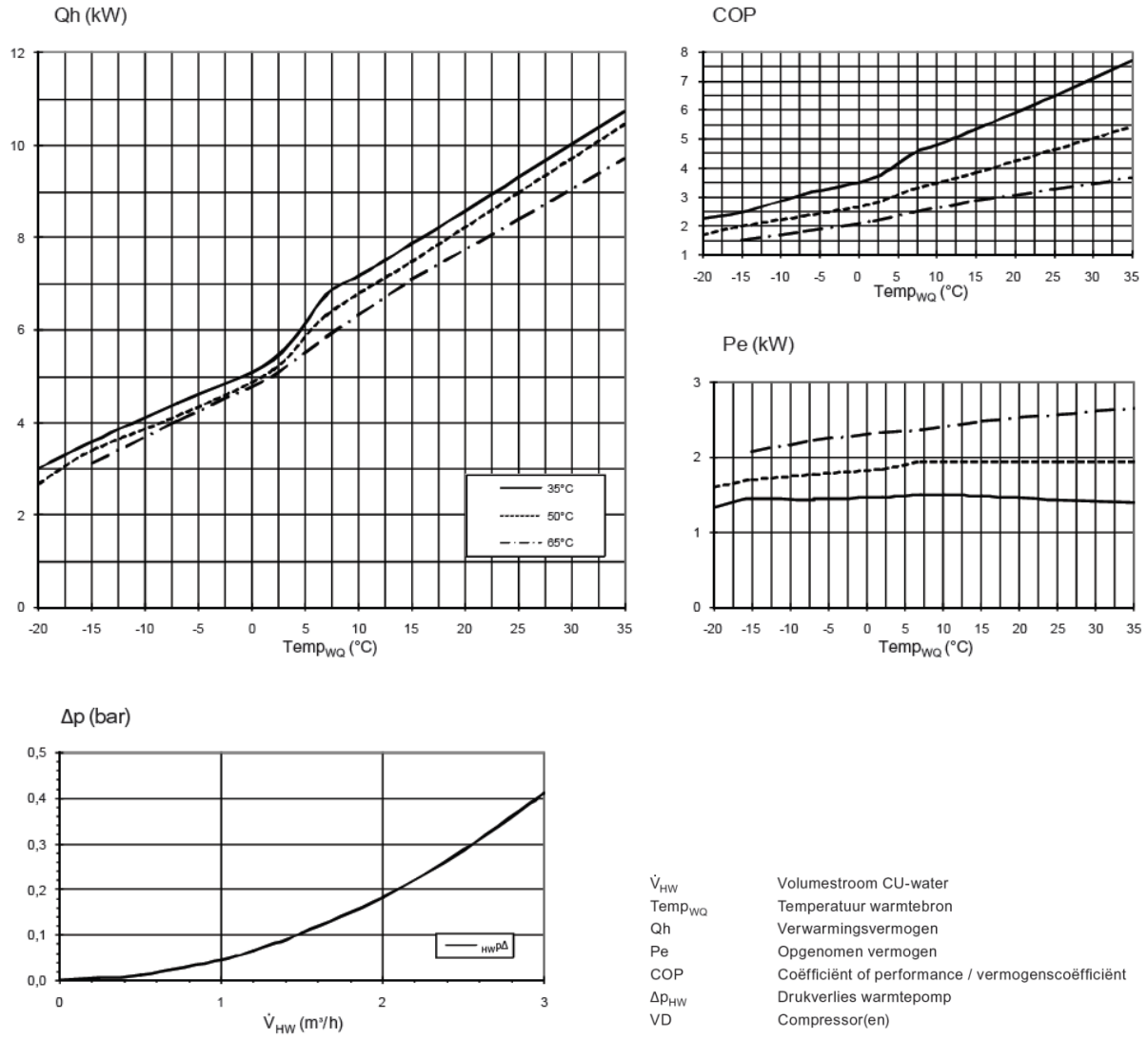

Figure 13-1: Performance curves heating mode

Tabular data were only available for three different entering water temperatures (see Figure 13-2), the other temperatures were interpolated by a linear fit, as shown in Figure 13-3 and Figure 13-4.

	Qh						Pe					
Tse	35°C	45°C	50°C	55°C	65°C	60°C	35°C	45°C	50°C	55°C	65°C	60°C
-20	2.96		2.77			2.71	1.37		1.63			1.86
-15												
-7	4.54		4.16		3.98		1.52		1.77		2.23	
2	5.47		5.24		5.11		1.48		1.85		2.34	
7	6.85		6.24		5.86		1.53		1.89		2.34	
10	7.04						1.48					
15	7.91		7.49		7.00		1.49		1.95		2.45	
25	9.63						1.41					
35	10.90		10.53		9.77		1.40		1.95		2.60	

	COP					
Tse	35°C	45°C	50°C	55°C	65°C	60°C
-20	2.15		1.70			1.46
-15						
-7	3.00		2.35		1.79	
2	3.68		2.84		2.19	
7	4.46		3.30		2.51	
10	4.76					
15	5.31		3.85		2.86	
25	6.81					
35	7.79		5.41		3.75	

Figure 13-2: Tabular performance data as provided by supplier d.d. june 2013

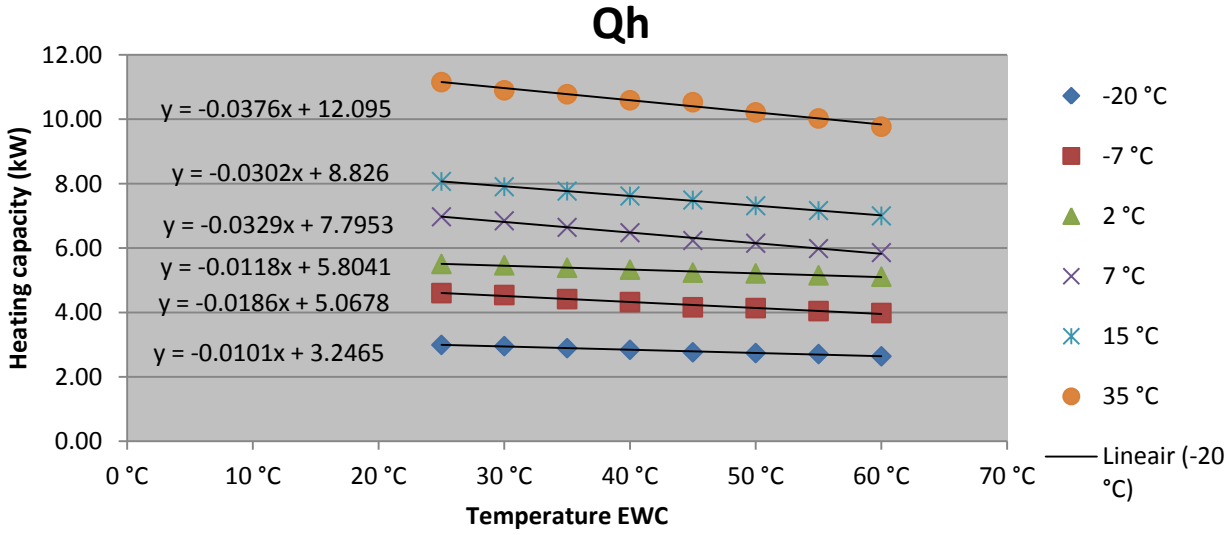

Figure 13-3: Heating capacity at different ambient air temperatures, as function of water temperature (linear fit)

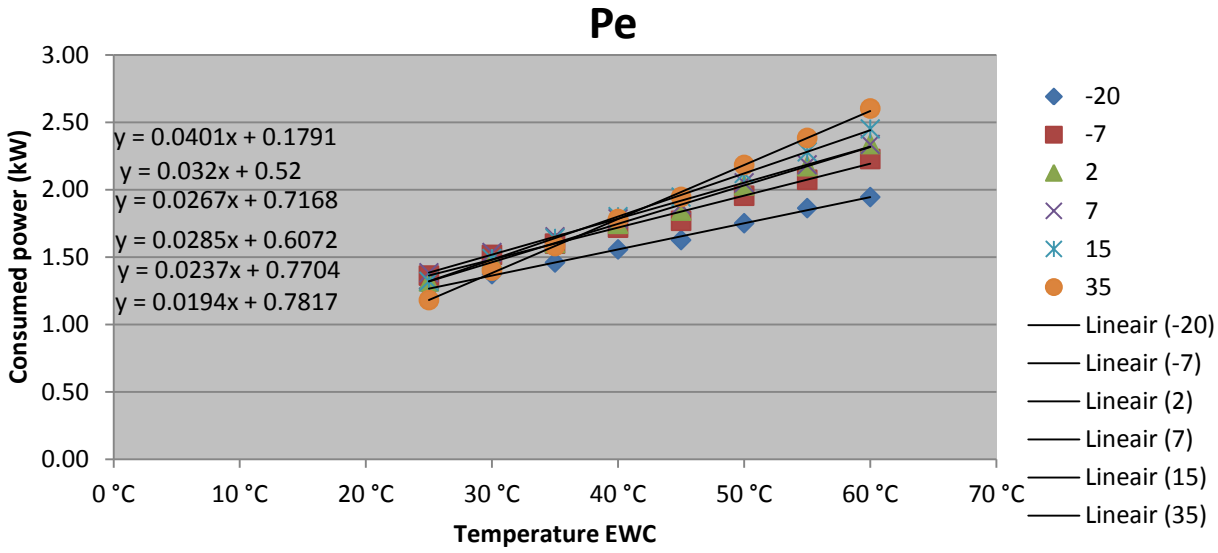

Figure 13-4: Consumed power at different ambient air temperatures, as function of water temperature (linear fit)

Table 13-2 – Input heating capacity as factor of rated cap (T_EWC = entering water temperature condenser)

T_EWC> T_air_in	***25 °C***	**30 °C**	***35 °C***	**40 °C**	***45 °C***	**50 °C**	**55 °C**
-20 °C	0.437	0.432	0.422	0.415	0.404	0.400	0.396
-10 °C	0.618	0.609	0.595	0.584	0.564	0.561	0.551
-7 °C	0.672	0.663	0.645	0.631	0.608	0.604	0.591
2 °C	0.805	0.798	0.787	0.779	0.765	0.761	0.753
7 °C	1.018	1.000	0.970	0.946	0.911	0.898	0.874
10 °C	1.060	1.027	1.022	1.003	0.985	0.965	0.946
15 °C	1.179	1.155	1.135	1.112	1.094	1.068	1.046
35 °C	1.629	1.592	1.574	1.547	1.538	1.492	1.464

Table 13-3 – Input consumed power as factor of rated power

T_EWC> T_air_in	***25 °C***	**30 °C**	***35 °C***	**40 °C**	***45 °C***	**50 °C**	**55 °C**
-20 °C	0.825	0.895	0.952	1.015	1.060	1.141	1.214
-10 °C	0.869	0.957	1.017	1.090	1.138	1.238	1.316
-7 °C	0.888	0.988	1.043	1.120	1.153	1.274	1.351
2 °C	0.860	0.967	1.045	1.138	1.202	1.324	1.417
7 °C	0.902	1.000	1.076	1.163	1.229	1.337	1.424
10 °C	0.845	0.964	1.042	1.140	1.215	1.336	1.436
15 °C	0.860	0.971	1.069	1.173	1.268	1.382	1.486
35 °C	0.770	0.912	1.031	1.162	1.268	1.423	1.554

TRNSYS Type 941 Air-source heat pump, requires an input file containing factors for the heating capacity as ratio of rated heating capacity at T entering condenser = 30°C and T air = 7°C. Similar input data is required to simulate the accompanied consumed electrical power. The factors are tabled in Table 13-2 and Table 13-3. The figure below shows the resulting COP (temperature exiting condenser is five degrees higher than T entering according to NEN-EN14511 and manufacturer).

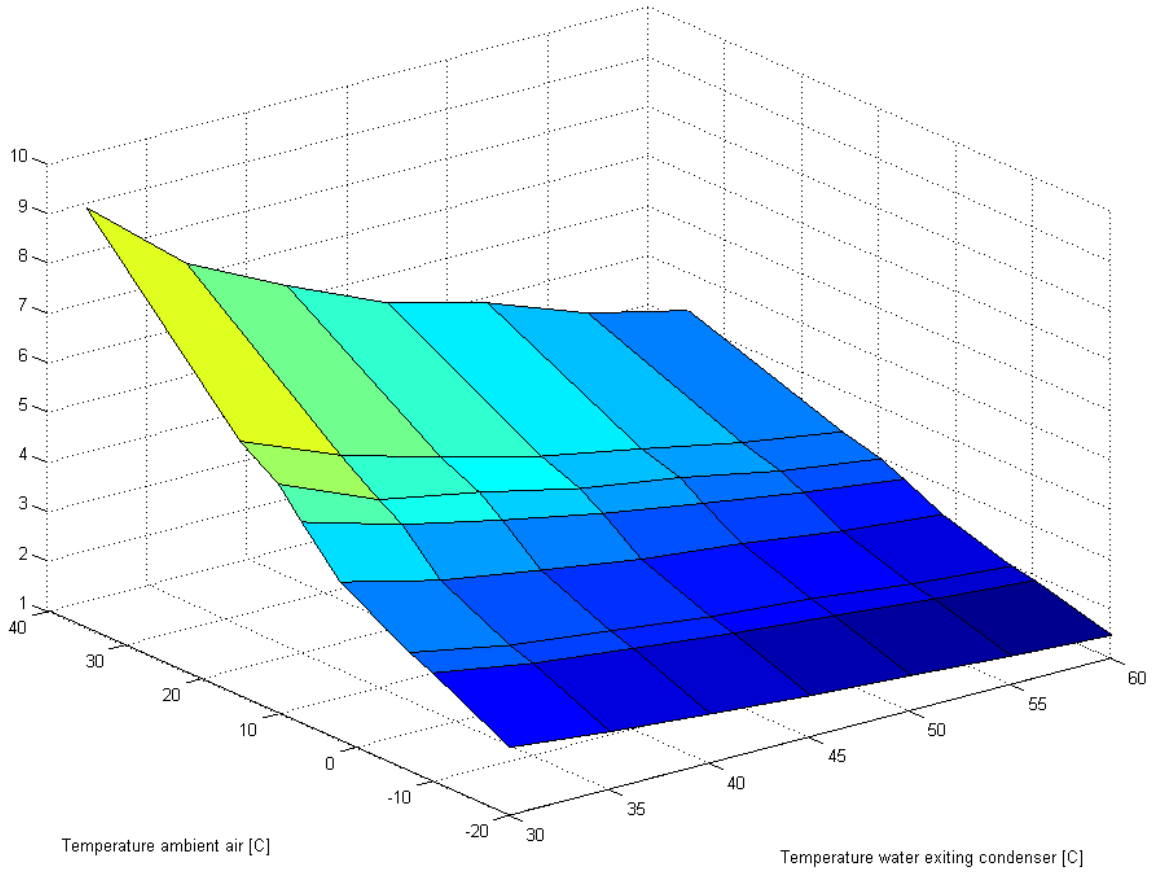

Figure 13-5: COP as function of exiting water temperature and ambient air temperature.

Dimensioning heating capacity

Preliminary TRNSYS calculations showed a peak instantaneous space heating demand of 2860 W_{th} (for the whole dwelling). This heat demand occurred at -7°C Tair. From here, we can select the rated heating capacity required at A7/W35 in order to deliver the peak heat demand at -7°C (including a safety margin): 3000*(1/0.663) = *4525* W_{th} (equals 16279 kJ/hr).

Using the manufacturers data gives us the accompanied rated electrical input: 4525/4.46 = *1.0* kW_{el} (equals 3649 kJ/hr).

14 Appendix E – LHS options

The design guidelines from literature were translated into several storage layouts that could be implemented in the basic circuit of the case study dwelling as follows:

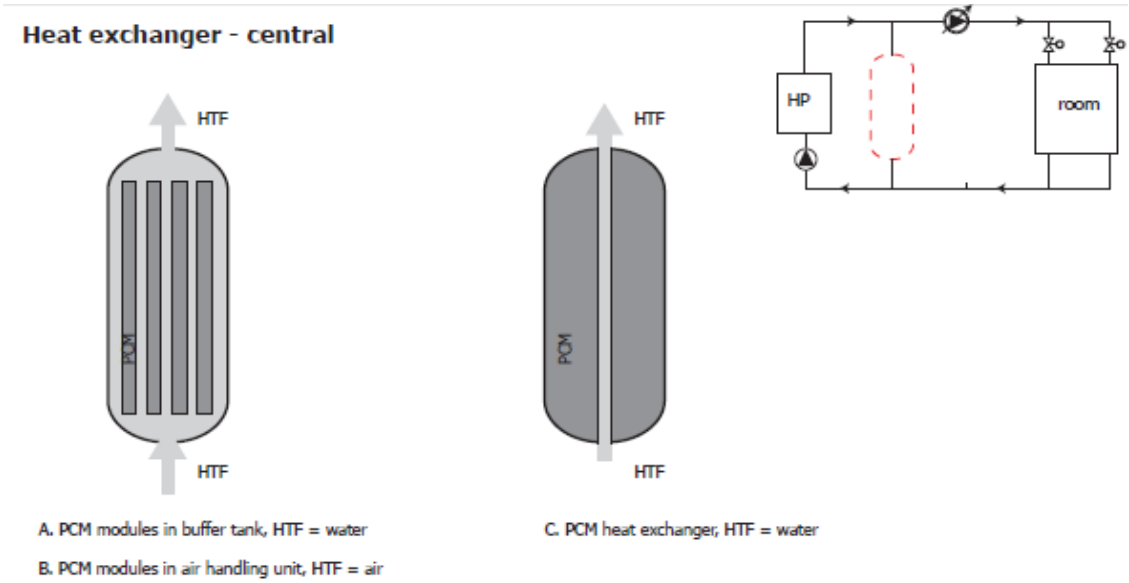

Figure 14-1: central buffer including PCM (heat exchanger types)

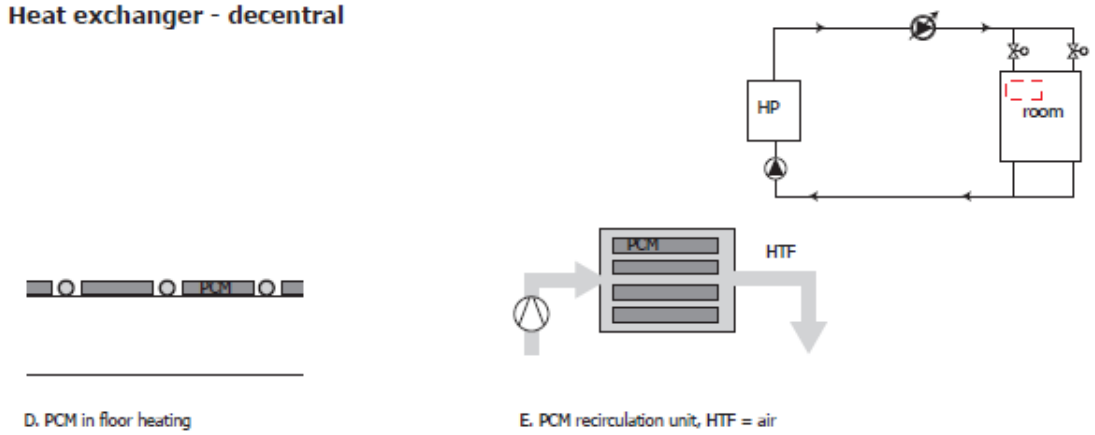

Figure 14-2: decentral latent buffer in floor heating or recirculation unit

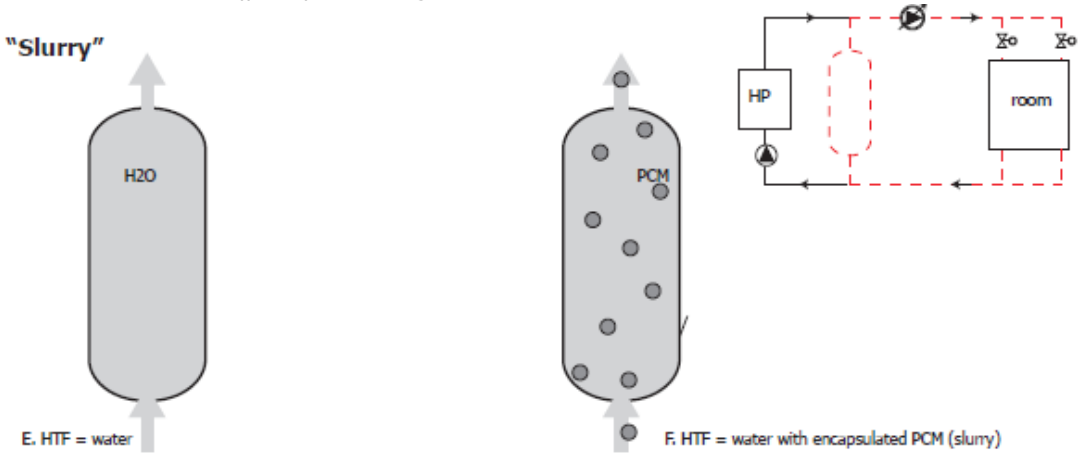

Figure 14-3: storage medium as heat transfer fluid: water and PCM

15 Appendix F – PCM study

Additional results for a 600L storage tank:

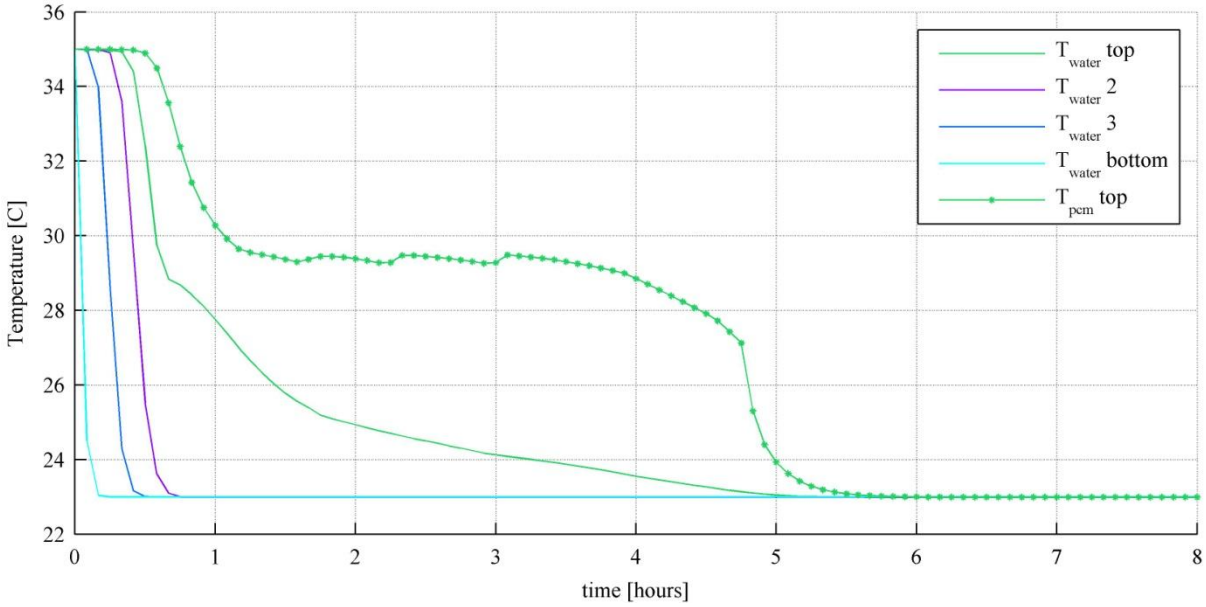

Figure 15-1: Temperatures of storage medium and PCM (core) during discharge, 600L case I, 53mm diameter, 15 Vol%

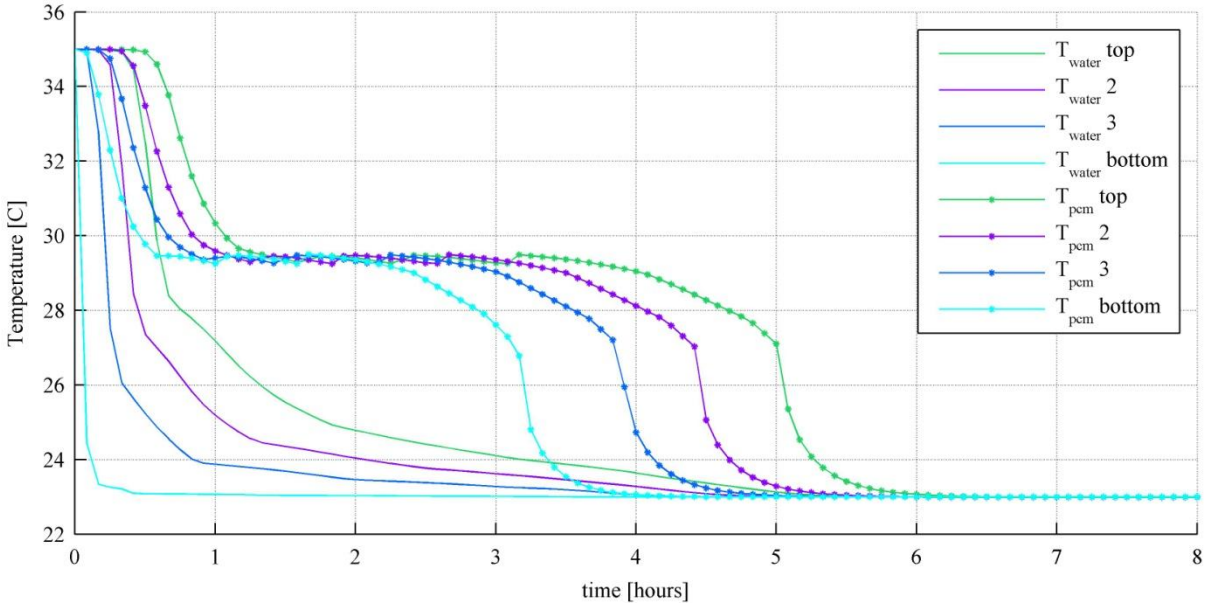

Figure 15-2: Temperatures of storage medium and PCM (core) during discharge, 600L case II, 53mm diameter, 15 Vol%

Results for a 200L storage tank:

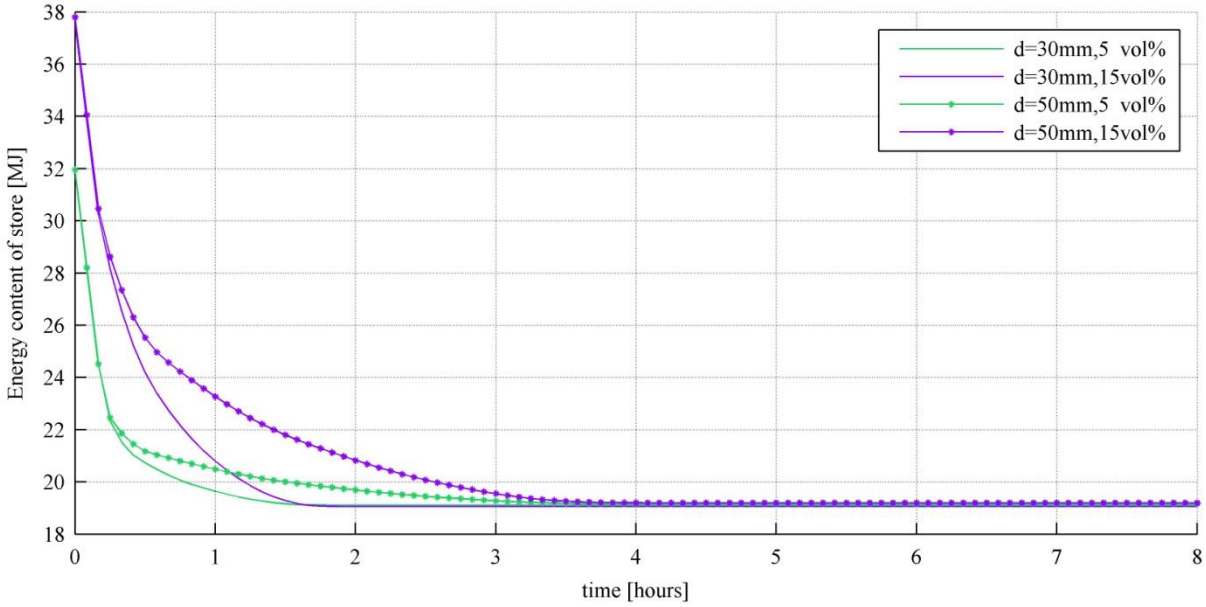

Figure 15-3: Energy content of the storage during discharge, 200L case I

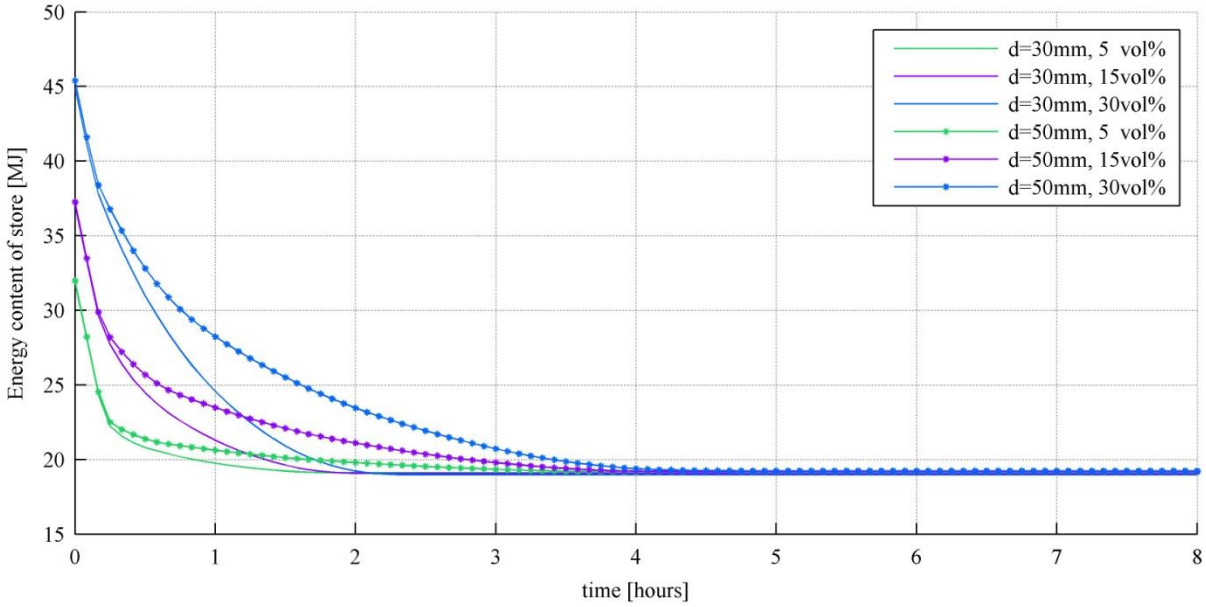

Figure 15-4: Discharge power of the storage, 200L case II

16 Appendix G - Detailed results TRNSYS

16.1 Yearly results

16.1.1 Comparison simplified and detailed TRNSYS calculation

Table 16-1 Annual heating energy and exergy demand simplified calculation

	Avg Te [C]	QHEAT living [MJ]	Exdem,Q_H living [MJ]	QHEAT sleeping [MJ]	Exdem,Q_H sleeping [MJ]	QHEAT total [MJ]	Exdem,Q_H total [MJ]	F_{EX} (Ex/En) [%]
Total [MJ/y]	9,5	4.261	271	9.869	584	14.129	855	6,1
Total [kWh/y]	-	1.184	75	2.741	162	3.925	237	6,1

Table 16-2 Annual heating energy and exergy demand[13] for most deviating case (Case C2 strategy D)

	Avg Te [C]	QHEAT living	Exdem,Q_H living	QHEAT sleeping	Exdem,Q_H sleeping	QHEAT total	Exdem,Q_H total	F_{EX} (Ex/En) [%]
Total [MJ/y]	9,5	3.269	N/A	10.557	N/A	13.781	1.085	7,8
Total [kWh/y]	-	908	N/A	2.932	N/A	3.828	301	7,8

When comparing the annual energy and exergy of the heat demand resulting from the simplified model (without building services) and the detailed cases, one can observe that almost no energy reduction occurs between both models (2% maximum). This could be expected, because the strategies aim for primary energy and exergy reduction on the generation side. This does not affect exergy of the heat demand.

16.1.2 Results per case

Table 16-3 – yearly sums per case, case A1A compared to cases with strategy D

Case-control strategy	A1-A	A1-D	A2-D	B-D	C1-D	C2-D	C3-D
Work [MJ]	3.405	3.258	3.267	3.261	3.157	3.094	3.055
Primary energy consumed [MJ]	8.716	8.340	8.363	8.348	8.082	7.922	7.820
Hours that installation is on [h]	1.023	990	982	999	956	939	925
Number of on/off cycles [-]	381	3.259	3.129	2.579	2.348	2.191	1.826
Operational cost (electricity) [€][14]	198	189	190	189	183	180	177

16.1.3 Detailed results for energy and exergy (input output) for all system components

Table 16-4 Results in out per component, energy and exergy and savings of strategy D compared to strategy A per case

	Q	Q	EX	Q	EX	Q	EX	Q	EX	Q	EX	Q	Q	Q
Case	**P.E.**	**HP in**	**HP in**	**HP out**	**HP out**	**TES in**	**TES in**	**FH in HP**	**FH in HP**	**FH in TES**	**FH in TES**	**FH_LZ**	**FH_SZ**	**loss TES**
	[MJ]	[MJ]	[MJ]	[MJ]	[MJ]	[MJ]	[MJ]	[MJ]	[MJ]	[MJ]	[MJ]	[MJ]	[MJ]	[MJ]

[13] Heating demand are values of energy and exergy *to* the emission system (FH in)

[14] Contemporary single-tariff electricity price of 0,20913 €/kWh assumed (energiedirect.nl)

A1A	**8716**	3405	3405	13703	1202	3883	340	10142	863	3728	292	3260	10650	-156
A1D	**8340**	3258	3258	13629	1107	6397	489	7547	627	6272	470	3264	10589	-143
D/A	-4%	-4%	-4%	-1%	-8%	65%	44%	-26%	-27%	68%	61%	0%	-1%	-9%
A2A	8759	3421	3421	13701	1216	4535	408	9483	812	4385	340	3269	10640	-158
A2D	**8363**	3267	3267	13635	1122	7005	550	6941	581	6869	526	3273	10570	-161
D/A	-5%	-5%	-5%	0%	-8%	54%	35%	-27%	-28%	57%	55%	0%	-1%	2%
BA	8839	3453	3453	13843	1220	6723	596	7438	638	6395	537	3243	10628	-324
BD	**8348**	3261	3261	13697	1111	6729	514	7281	610	6537	508	3254	10606	-206
D/A	-6%	-6%	-6%	-1%	-9%	0%	-14%	-2%	-4%	2%	-6%	0%	0%	-37%
C1A	8824	3447	3447	13750	1212	6456	578	7618	649	6212	488	3289	10584	-276
C1D	**8082**	3157	3157	13632	1068	8005	594	5935	487	7857	604	3302	10526	-203
D/A	-8%	-8%	-8%	-1%	-12%	24%	3%	-22%	-25%	26%	24%	0%	-1%	-26%
C2A	8858	3460	3460	13773	1227	6750	610	7349	632	6483	516	3301	10572	-293
C2D	**7922**	3094	3094	13587	1051	9050	667	4840	400	8941	685	3269	10557	-186
D/A	-11%	-11%	-11%	-1%	-14%	34%	9%	-34%	-37%	38%	33%	-1%	0%	-37%
C3A	8923	3486	3486	13781	1239	7315	661	6798	593	7035	554	3294	10582	-284
C3D	**7820**	3055	3055	13606	1045	10261	750	3645	309	10135	791	3266	10561	-225
D/A	-12%	-12%	-12%	-1%	-16%	40%	13%	-46%	-48%	44%	43%	-1%	0%	-21%

Table 16-4 shows that relative savings of strategy D within the cases increase at larger buffer capacities. This is reasonable, since strategy A performs worse at larger volumes, while strategy D on contrary performs more optimal at large energy contents. In case C3, strategy D saves more than 12% primary energy compared to strategy A.

This is not a realistic comparison though, because in reality, strategy A will be combined with the smallest buffer volume of 200L (case A1A), since this yields the best performance in combination with this strategy (and will cost less). This can be seen in Table 16-4, the bolt numbers in the first column. In Chapter 7 therefore compares the outcomes for strategy D (for all cases) to case A1A only. Thermal losses from the buffer are hard to interpret because they depend on the average temperature levels in the tank but also by the ratio of heat supplied via the TES/directly from the heat pump.

16.1.4 Calculation of energy and exergy losses per relevant component

Detailed losses the components heat pump and TES can be compared using the following parameters (Jansen, et al., 2010):

- energy efficiency η (used energy output/total energy input)

- energy losses L (total energy input – used energy output)

- exergy efficiency ψ (used exergy output/total exergy input)

- exergy losses D (tot exergy input – used exergy output)

Table 16-5 Yearly results for case A1

	Case A1 strategy A				Case A1 strategy D			
	η	L	ψ	D	η	L	ψ	D
	[-]	[MJ]	[-]	[MJ]	[-]	[MJ]	[-]	[MJ]
Heat Pump	4,02	-10299	0,35	2203	4,18	-10371	0,34	2151
TES	0,96	155	0,86	48	0,98	125	0,96	19

Table 16-6 Yearly results for case A2

	Case A2 strategy A				Case A2 strategy D			
	η	L	ψ	D	η	L	ψ	D
	[-]	[MJ]	[-]	[MJ]	[-]	[MJ]	[-]	[MJ]
Heat Pump	4,00	-10280	0,36	2205	4,17	-10368	0,34	2144
TES	0,97	150	0,83	69	0,98	136	0,96	23

Table 16-7 Yearly results for case B

	Case B strategy A				Case B strategy D			
	η	L	ψ	D	η	L	ψ	D
	[-]	[MJ]	[-]	[MJ]	[-]	[MJ]	[-]	[MJ]
Heat Pump	4,01	-10390	0,35	2232	4,20	-10436	0,34	2150
TES	0,95	328	0,90	59	0,97	191	0,99	6

Table 16-8 Yearly results for case C1

	Case C1 strategy A				Case C1 strategy D			
	η	L	ψ	D	η	L	ψ	D
	[-]	[MJ]	[-]	[MJ]	[-]	[MJ]	[-]	[MJ]
Heat Pump	3,99	-10303	0,35	2235	4,32	-10475	0,98	2089
TES	0,96	244	0,84	90	0,34	147	0,98	10

Table 16-9 Yearly results for case C2

	Case C2 strategy A				Case C2 strategy D			
	η	L	ψ	D	η	L	ψ	D
	[-]	[MJ]	[-]	[MJ]	[-]	[MJ]	[-]	[MJ]
Heat Pump	3,98	-10313	0,35	2234	4,39	-10492	0,34	2043
TES	0,96	267	0,85	94	0,99	109	0,97	18

Table 16-10 Yearly results for case C3

	Case C3 strategy A				Case C3 strategy D			
	η	L	ψ	D	η	L	ψ	D
	[-]	[MJ]	[-]	[MJ]	[-]	[MJ]	[-]	[MJ]
Heat Pump	3,95	-10296	0,36	2246	4,45	-10551	0,34	2010
TES	0,96	280	0,80	108	0,99	126	0,95	40

No big differences are found between the cases. There are big differences between strategy A and D though. First, in energy efficiency of the heat pump, which improves because the same energy is generated with less electrical energy input (see Table 16-4). Secondly, the exergy losses for the TES component are significantly reduced by strategy D, because this strategy results in more energy input from the heat pump at a lower quality (exergy output is comparable with the quality levels of strategy A, except for case A1D and C2D which do have a 5% reduction).

16.2 Accuracy of the heat demand prediction

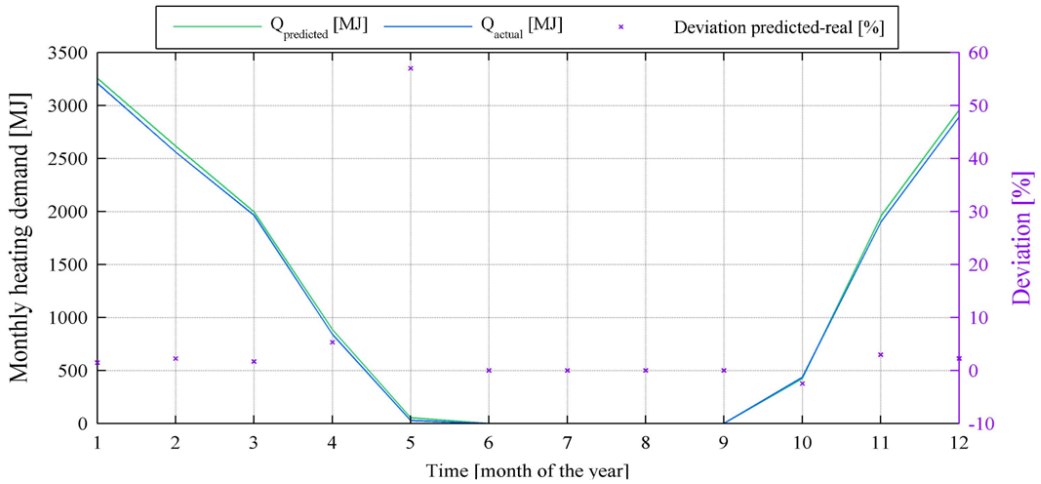

Figure 16-1: Deviation of estimated monthly heat demand from actual monthly heat demand, Case C3 strategy D

Since the predicted (hereafter: estimated) heating energy was derived a monthly assessment of the heat demand depending on a set of forcing functions, the monthly heat demand sums estimated should show good agreement with the totals obtained from the real dynamic calculation. Figure 16-1 depicts the estimation accuracy for case C3 (which may be assumed exemplary for other cases). In general, estimated monthly heat demand deviates less than 5% from the actual, although May shows an exceptional large deviation. The difference can be explained by the small number of data for May (only a few hours of heat demand present), so one large deviation can have big impact.

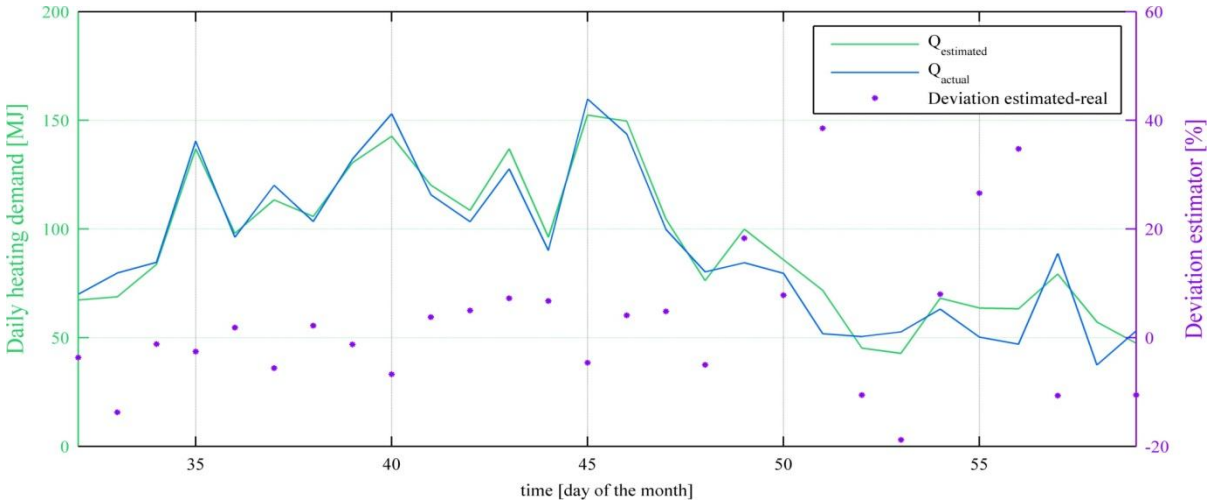

Figure 16-2: Deviation of estimated daily heat demand from actual daily heat demand for February, Case C3D

Although from Figure 16-1 could be concluded that the prediction achieves good accuracy on a monthly basis, daily heat demand estimations do differ significantly from actual values. This is illustrated by the daily heat demands estimated and actual for February (incl. the exemplary winter week) in Figure 16-2. One can see that during the last days of the month (which is the exemplary winter week used for presentation of the results in Chapter 7), the actual demand is higher than estimated (which caused minor performance of the algorithm).

Zoomed in to hourly values, the course of the pattern of the heating power differs within one day as well, due to the control of the emission system. Figure 16-3 shows a phenomenon that leads to a course of the energy content of the buffer that differs from estimation. As described before, one of the forcing functions the prediction is based on, was the sum of the internal gains from both thermal zones. The peak heat load that occurs in the sleeping zone around 22:00h is therefore not foreseen, because during these hours the algorithm assumes a relatively low energy demand because maximum internal gains in living zone are predicted. As long as the total daily energy demand estimated is still equal to the actual however, this does not have a major influence on the algorithms performance, but it does influence temperature levels in the buffer and thus the heating power that remains during the second heat demand peak around sunrise.

A proper reaction time of the system was assured by increasing the lower temperature limits (at which the buffer is assumed empty), see Table 7-6 for the final values. The lower temperature limit needs to be related to the instantaneous climate curve (instead of a fixed lower limit temperature) in order to force heat pump operation during peak required heating power, and this causes more on/off cycles of the heat pump. This hourly inaccuracy is the reason for the fact that TRNSYS results no savings for the algorithm when using a prediction horizon of 12 hours.

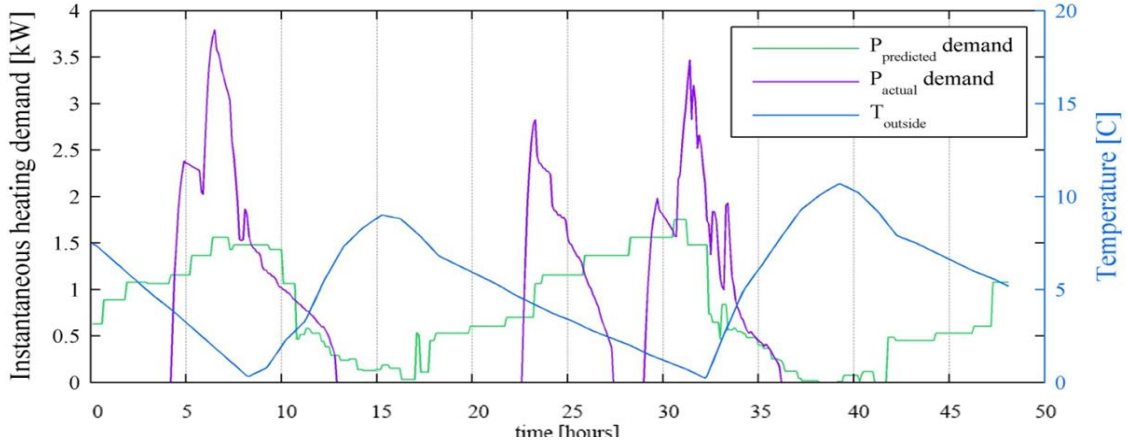

Figure 16-3: Estimated versus actual instantaneous heating power for two exemplary days, Case C3 strategy D

16.3 Costs and economic feasibility

For the calculation of initial investments (prices installation components), prices from the Technische Unie (wholesale of technical installation materials and components) were accessed (www.technischeunie.nl). A typical price was deduced from products from different suppliers for every main component of the modeled energy system.

Concerning the PCM, prices are obtained via communication with manufacturers. For commercial salt hydrates in the temperature range of this study (30-35C), only two manufacturers were known to the authors knowledge: Rubitherm and Salca. Important to mention is that the calculations use a retail

price, which can drop with more than 50% for bulk orders. Development and production from raw PCM material to a macroencapsulated module leads to an element price which is double or quadruple the raw material price (again highly dependent on batch size). The best scenario is calculated, since these modules could very well be produced in large quantities.

The payback time is calculated relative to case A1A which is most attractive from economic point of view (smallest buffer tank and minimal primary energy consumption in combination with reference control strategy A). Operational costs are already presented and discussed at the start of this appendix.

Table 16-11 – Investment cost reference case A1-A

	Sub	Total
Air/water Heatpump 1kW$_{el}$		€ 10.000,-
Buffer vessel		€ 725,- (200L)
PCM modules		€ 440
Salt hydrate	*€ 220 (44 kg a 5,0 €/kg)*	
Encapsulation	*€ 220*	

Table 16-12 – Investment cost case A1-D

	Sub	Total
Air/water Heatpump 1kW$_{el}$		€ 10.000,-
Buffer vessel		€ 725,- (200L)
PCM modules		€ 440
Salt hydrate	*€ 220 (44 kg a 5,0 €/kg)*	
Encapsulation	*€ 220*	
More advanced control unit		€ 200

Table 16-13 – Investment cost case C3-D

	Sub	Total
Air/water Heatpump 1kW$_{el}$		€ 10.000,-
Buffer vessel		€ 1.500,- (600L)
PCM modules		€ 4.350
Salt hydrate	*€ 2.175 (435 kg a 5,0 €/kg)*	
Encapsulation	*€ 2.175*	
More advanced control unit		€ 200

Table 16-14 – Payback time compared to case A1A

	A1A		A1D		C3D	
Total investment	€ 11.165	€ 90,0 / m^2	€ 11.365	€ 91,7 / m^2	€ 16.050	€ 129,4/ m^2
Extra investment str D	-	-	+ € 200	-	+ € 4.885	-
Operational cost (yearly)	€ 198	€ 1,6 / m^2	€ 189	€ 1,5 / m^2	€ 177	€ 1,4 / m^2
Annual savings in op. cost	-	-	- € 9	-	- € 21	-
Payback time [years]	-	-	22		232	

Table 16-14 clearly shows that the additional investments that are required for strategy D to perform well (mainly PCM and larger vessels), do dramatically increase the payback time. Savings in operational costs do not outweigh the investments because of the big difference between installation costs and energy costs.

17 Appendix H – Emission system

Dimensions emission system (floor heating) are based on:

- ISSO 49 Vloer en wandverwarmingssytemen
- NEN- 7730

Assumptions done:

- maximum surface temperature floor 29 C (verblijfsgebied)
- maximum allowed supply temperature to floor: 40C
- layer above piping >30mm
- in critical room: dT supply-retour <8K (smaller dT increases COP because lower Tsupply)
- other spaces: dT supply-retour <5-8K

The table below shows the final design parameters which are defined in accordance with design guidelines from ISSO and NEN:

Ontwerpovertemperatuur heating and piping distance	Living zone		Sleeping zone	
Specific heat demand	45.6	[W/m2]	69.8	[W/m2]
Design supply temperature	35	[C]	35	[C]
dT supply – retour	5	[K]	8	[K]
Setpointtemperature room	20	[C]	20	[C]
Thickness layer above piping	0.060	[m]	0.060	[m]
Pipe outside diameter	0.02	[m]	0.02	[m]
Design over temperature	12.5	[K]	12.5	[K]
Rc top layer (oak parquet)	0.05	[m2K/W]	0.05	[m2K/W]
Minimum piping distance	0.2	[m]	0.125	[m]
dT floor surface - room	4.4	[K]	5.2	[K]
Average floor temperature	24.4	[C]	25.2	[C]
Maximum flowrate to Floor heating	404,3	[kg/hr]	489,3	[kg/hr]

In TRNBuild, an insulation layer of 35mm is included in the floor composition. The layer is positioned on top of the structural layer (concrete) and below the finishing layer containing the floor heating piping. The total thickness of the finishing cement mortar is 60mm.

The ratio's of the minimum flowrate to the floor heating system is based on a preliminary static calculation of the required heating power per zone. For the floor heating system in the ground floor of the living zone, 15% system related heat losses to the outside (downwards) are assumed, in accordance with ISSO 49.